ANALYTICA CHIMICA ACTA

International monthly devoted to all branches of analytical chemistry
Revue mensuelle internationale consacrée à tous les domaines de la chimie analytique
Internationale Monatsschrift für alle Gebiete der analytischen Chemie

ELSEVIER PUBLISHING COMPANY
AMSTERDAM

Anal. Chim. Acta, Vol. 55, No. 2, 285–464, July 1971
Published monthly

Publication Schedule for 1971

In the interests of rapid publication it has been found necessary to schedule 5 volumes for appearance in 1971. Since monthly publication will be maintained, this implies that 2 of the volumes will each consist of three issues, while 3 of the volumes will each consist of only 2 issues. The following provisional schedule applies:

Vol. **53,** No. **1**	January 1971	
Vol. **53,** No. **2**	February 1971	**(completing Vol. 53)**
Vol. **54,** No. **1**	March 1971	
Vol. **54,** No. **2**	April 1971	
Vol. **54,** No. **3**	May 1971	**(completing Vol. 54)**
Vol. **55,** No. **1**	June 1971	
Vol. **55,** No. **2**	July 1971	**(completing Vol. 55)**
Vol. **56,** No. **1**	August 1971	
Vol. **56,** No. **2**	September 1971	
Vol. **56,** No. **3**	October 1971	**(completing Vol. 56)**
Vol. **57,** No. **1**	November 1971	
Vol. **57,** No. **2**	December 1971	**(completing Vol. 57)**

Subscription price: $17.50 or Dfl. 63.— per volume plus postage. Total subscription price for 1971: $87.50 or Dfl. 315.— plus postage. Additional cost for copies by airmail available on request. For subscribers in the U.S.A. and Canada, 2nd class postage paid at New York, N.Y. For advertising rates apply to the publishers.

Subscriptions should be sent to:

ELSEVIER PUBLISHING COMPANY P.O. Box 211, Amsterdam, The Netherlands

GENERAL INFORMATION

Languages

Papers will be published in English, French or German.

Submission of papers

Papers should be sent to:

Prof. Philip W. West,
Coates Chemical Laboratories,
College of Chemistry and Physics,
Louisiana State University,
Baton Rouge 3,
La. 70803 (U.S.A.)

or to:

Dr. A. M. G. Macdonald,
Department of Chemistry,
The University,
P.O. Box 363
Birmingham B15 2TT (Great Britain)

Reprints

Fifty reprints will be supplied free of charge. Additional reprints (minimum 100) can be ordered at quoted prices. They must be ordered on order forms which are sent together with the proofs.

Kodak

For a copy of the new Eastman Catalog (No. 46)

or for any of the 6,000 chemicals it contains, contact one of these laboratory supply houses. EASTMAN Organic Chemicals are stocked locally in the continental U.S.A. by:

B&A
CURTIN
FISHER
HOWE & FRENCH
NORTH-STRONG
PREISER
SARGENT-WELCH
WILL/VW&R

For EASTMAN Organic Chemicals service elsewhere:

ARGENTINA
Cientifica Comercial
Argentina S.A.C.I.
Buenos Aires

AUSTRALIA
H. B. Selby and Co., Pty., Ltd.
Adelaide Melbourne
Brisbane Perth
Hobart Sydney
Ramsay Surgical Limited
Victoria

BELGIUM
s. a. Belgolabo
Overijse

BRAZIL
Atlantida Representacoes
e Importacoes, Ltda.
Rio de Janeiro
Tennant Quimica S.A.
Sao Paulo

CANADA
Fisher Scientific Co., Ltd.
Edmonton Toronto
Montreal Vancouver
Ottawa
Sargent-Welch Scientific of
Canada, Ltd.
Vancouver Weston

DENMARK
H. Struers Chemiske
Laboratorium
Copenhagen K

FINLAND
Havulinna Oy
Helsinki

FRANCE
Touzart & Matignon
Paris

W. GERMANY
Serva International
Chemie-Handels GmbH & Co.
Heidelberg

GREECE
P. Bacacos S.A.
Athens

GUATEMALA
F. Krafka and Co., Ltd.
Emaoa

INDIA
Kodak Limited
Bombay

ISRAEL
Landseas Israel
Tel Aviv

ITALY
Prodotti Gianni, s.r.l.
Milan

JAPAN
Muromachi Kagaku Kogyo
Kaisha, Ltd.
Tokyo
Nagase and Co., Ltd.
Tokyo

KOREA
The Sang Chung
Commercial Co., Ltd.
Seoul

MEXICO
Alfonso Marhx, S.A.
Mexico 1, D. F.
Hoffmann-Pinther and
Bosworth, S.A.
Mexico 1, D. F.

NETHERLANDS
N. V. Holland-Indie
Agenturen Mij, HIAM
Amsterdam C

NEW ZEALAND
Kempthorne, Prosser & Co's.
New Zealand Drug Co., Ltd.
Wellington-Dunedin

NORWAY
Nerliens Kemisk Tekniske
Aktieselskap
Oslo

PORTUGAL
Soquimica, Sociedad de
Representacoes de Quimica
Lisbon

PUERTO RICO
Fisher Scientific Co.
Santurce

REPUBLIC OF CHINA
San Ho Instrument Co.
Taipei, Taiwan
Teh Ying Co., Ltd.
Taipei, Taiwan

REPUBLIC OF MALAWI
Baird and Tatlock
(International) Ltd.
Blantyre

REPUBLIC OF SOUTH AFRICA
Baird and Tatlock S.A., Pty.
Johannesburg

REPUBLIC OF ZAMBIA
Baird and Tatlock (Zambia) Ltd.
Ndola

SWEDEN
KEBO AB
Stockholm 6

SWITZERLAND
Dr. Bender and Dr. Hobein AG
Zurich 6

UNITED KINGDOM
Kodak Limited
Kirkby, Liverpool

VENEZUELA
Equipos Cientificos y
Educativos S.A.
Caracas

The catalog may also be obtained from:
Dept. 412L, Eastman Organic Chemicals,
Eastman Kodak Company, Rochester, N.Y. 14650, U.S.A.

ห้องสมุด กรมวิทยาศาสตร์
16 พ.ย. 2514

Comprehensive Biochemistry

edited by

MARCEL FLORKIN, *Professor of Biochemistry, University of Liège (Belgium) and*

ELMER H. STOTZ, *Professor of Biochemistry, University of Rochester, School of Medicine and Dentistry, Rochester, N.Y. (U.S.A.)*

Section I

PHYSICO-CHEMICAL AND ORGANIC ASPECTS OF BIOCHEMISTRY

This section is intended neither as a textbook of organic nor of physical chemistry, but rather as a collection of chapters which seem generally pertinent in the interpretation of biochemical techniques and in the understanding of the chemistry of biological compounds and reaction mechanisms.

Vol. 1. Atomic and Molecular Structure
Vol. 2. Organic and Physical Chemistry
Vol. 3. Methods for the Study of Molecules
Vol. 4. Separation Methods

Section II

CHEMISTRY OF BIOLOGICAL COMPOUNDS

Deals with the organic and physical chemistry of the major organic constituents of living material. This section includes a sound treatment of the important biological high polymers—their shape and physical properties. A number of substances peculiar to plants, certain isoprenoids, flavonoids, tannins, lignins, and plant hormones, often omitted from textbooks of biochemistry, are also covered.

Vol. 5. Carbohydrates
Vol. 6. Lipids—Amino Acids and Related Compounds
Vol. 7. Proteins (Part 1)
Vol. 8. Proteins (Part 2) und Nucleic Acids
Vol. 9. Pyrrole Pigments; Isoprenoid Compounds; Phenolic Plant Constituents
Vol. 10. Sterols, Bile Acids and Steroids
Vol. 11. Water-Soluble Vitamins, Hormones, Antibiotics

Section III

BIOCHEMICAL REACTION MECHANISMS

Section III is devoted primarily to Enzymes, focusing attention on the chemistry and function of the coenzymes. Other chapters treat thermodynamic and kinetic aspects of enzyme catalysis, hydrolytic enzymes displaying "active center" characteristics, and chelation and stereochemical considerations in enzyme catalysis. Much attention is given to biological oxidation mechanisms.

Vol. 12. Enzymes—General Considerations
Vol. 13. Enzyme Nomenclature (2nd revised edition)
Vol. 14. Biological Oxidations
Vol. 15. Group-Transfer Reactions
Vol. 16. Hydrolytic Reactions; Cobamide and Biotin Coenzymes

Subscribers who place a standing order for the whole series will be entitled to an overall 20% discount. Detailed brochure available on request.

Elsevier

Book Division, P.O. BOX 3489,
Amsterdam – The Netherlands

313E

Section IV

METABOLISM

This section concerns itself with the degradative and biosynthetic pathways of carbohydrates, lipids, amino acids, porphyrins, purines, pyrimidines, etc., with special emphasis on experimental data as evidence for the metabolic schemes now admitted. Not only mammalian metabolism, but also the related metabolism in other organisms is treated. Special sections are devoted to the metabolism of special organs in the mammal, and highly characteristic variations of metabolism occurring in non-mammals. Abnormal cellular metabolism and the resulting disease states are discussed in detail.

Vol. 17. Carbohydrate Metabolism
Vol. 18. Lipid Metabolism
Vol. 18S. Pyruvate and Fatty Acid Metabolism
Vol. 19. Metabolism of Amino Acids, Proteins, Purines, and Pyrimidines
Vol. 20. Metabolism of Cyclic Compounds
Vol. 21. Metabolism of Vitamins and Trace Elements

Section V

CHEMICAL BIOLOGY

Section V is devoted to a number of topics which, in an earlier state of development, were primarily descriptive and included in the field of biology, but which have been rapidly brought to study at the molecular level. Besides the chapters often grouped under 'molecular biology', Section V also deals with modern aspects of bioenergetics, immunochemistry, photobiology, and a consideration of the molecular phenomena that underlie the evolution of organisms.

Vol. 22. Bioenergetics
Vol. 23. Cytochemistry
Vol. 24. Biological Information Transfer. Immunochemistry
Vol. 25. Regulatory Functions, Membrane Phenomena
Vol. 26A. Extracellular and Supporting Structures
Vol. 26B. Extracellular and Supporting Structures (continued)
Vol. 26C. Extracellular and Supporting Structures (continued)
Vol. 27. Photobiology, Ionizing Radiations
Vol. 28. Morphogenesis, Differentiation and Development
Vol. 29. Comparative Biochemistry. Molecular Evolution

Further volumes in the series not related to Section V

Vol. 30. History of Biochemistry
Vol. 30A. (part I). Protobiochemistry
Vol. 30A. (part II). From Protobiochemistry to Biochemistry
Vol. 30B. The Unravelling of Metabolic Pathways
Vol. 30C. The Molecular Basis of Biological and Physiological Concepts
Vol. 31. General Index

Analytica Chimica Acta
Elsevier Publishing Company, Amsterdam
Printed in The Netherlands

ACID–BASE STRENGTHS IN PYRIDINE. PART II

M. BOS AND E. A. M. F. DAHMEN
Department of Chemical Technology, Twente University of Technology, Enschede (The Netherlands)

(Received 19th March 1971)

Weak acids can readily be titrated in pyridine media with quaternary ammonium bases[1]. In order to calculate these titrations, one should know the equilibrium constant in pyridine (K_{H_2O}) of the reaction

$$H_2O \rightleftharpoons H^+ + OH^- \qquad (1)$$

It is possible to determine K_{H_2O} from the curve of a titration of an acid of known dissociation constant in pyridine with a quaternary ammonium base.

With the K_{H_2O} determined in this way, the dissociation constants of acids can be calculated from the curves of the titrations of these acids with a quaternary ammonium base. The influence of water on other acid–base titrations in pyridine can also be calculated.

THEORY

It can be assumed that the following equilibria play a part in the titration of an acid HX with tetramethylammonium hydroxide (TMAOH) in pyridine:

$$HX \overset{K_{HX}}{\rightleftharpoons} H^+ + X^- \qquad (2)$$

$$TMAOH \overset{K_{TMAOH}}{\rightleftharpoons} TMA^+ + OH^- \qquad (3)$$

$$H^+ + OH^- \overset{1/K_{H_2O}}{\rightleftharpoons} H_2O \qquad (4)$$

$$TMA^+ + X^- \overset{1/K_{TMAX}}{\rightleftharpoons} TMA^+X^- \qquad (5)$$

With this set of equilibria, one can calculate K_{H_2O} from this titration carried out with a calibrated glass electrode if K_{HX}, K_{TMAOH} and K_{TMAX} are known. To do this, the titration curve is calculated with the known dissociation constants K_{HX}, K_{TMAOH}, K_{TMAX} and different estimated values for K_{H_2O} by the general methods of equilibria calculations[2]. The correct value of K_{H_2O} is the one that gives the best fit between the experimental and calculated titration curves. In the same way K_{HX} can be found from the titration of an acid, HX, with TMAOH if K_{H_2O} and K_{TMAX} are known. In the case of the carboxylic acids, there is some evidence for other than simple dissociation[3].

The carboxylic acids will most probably behave in one of the following ways in pyridine:

(*a*) Simple dissociation

$$\mathrm{HX} \overset{K_{\mathrm{HX}}}{\rightleftharpoons} \mathrm{H}^+ + \mathrm{X}^- \tag{2}$$

(*b*) Dissociation/dimerization

$$\mathrm{HX} \overset{K_{\mathrm{HX}}}{\rightleftharpoons} \mathrm{H}^+ + \mathrm{X}^- \tag{2}$$

$$2\mathrm{HX} \overset{K_{\mathrm{dimer}}}{\rightleftharpoons} (\mathrm{HX})_2 \tag{6}$$

(*c*) Dissociation/homoconjugation

$$\mathrm{HX} \overset{K_{\mathrm{HX}}}{\rightleftharpoons} \mathrm{H}^+ + \mathrm{X}^- \tag{2}$$

$$\mathrm{HX} + \mathrm{X}^- \overset{K_{\mathrm{HX}_2^-}}{\rightleftharpoons} \mathrm{HX}_2^- \tag{7}$$

Now the titration curves can be calculated for the types of behaviour *a*, *b* and *c* with the known values of K_{TMAOH}, $K_{\mathrm{H_2O}}$ and K_{TMAX} and estimated values of the constants of the equilibria (2), (6) or (7). For each type the estimated values of the unknown equilibrium constants can be changed and the calculation repeated until the calculated titration curve gives the best fit with the experimental one. Finally, the results for the three types of behaviour can be compared and from this conclusions can be drawn about which type describes the titration best.

EXPERIMENTAL

Chemicals

Tetramethylammonium hydroxide (*TMAOH*). The starting material was a solution of 0.1 *M* TMAOH in isopropanol–methanol (Merck). This solution was evaporated at 30° under reduced pressure to one quarter of the original volume. Then pyridine was added up to the original volume. Again the solution was evaporated to one quarter of the starting volume under the same conditions. After another addition of pyridine and evaporation, the strength of the solution was made about 0.1 *M* by addition of pyridine. This solution is not stable for more than one day. For this reason it was standardized against benzoic acid and used only on the day of preparation.

Tetramethylammonium acetate. Tetramethylammonium acetate was prepared by neutralizing 0.1 *M* TMAOH in isopropanol–methanol (Merck) with a solution of acetic acid in methanol. The resulting solution was evaporated and the salt was recrystallized from ether–ethanol. Finally the salt was dried *in vacuo* at 40°.

Tetramethylammonium benzoate. Tetramethylammonium benzoate was prepared from 0.1 *M* TMAOH and a solution of benzoic acid in methanol in the same way as tetramethylammonium acetate.

The other chemicals were used as described before[4].

Potentiometric titrations

The potentiometric titrations were carried out with a calibrated glass electrode as described previously[4].

Determination of salt dissociation constants

The dissociation constants in pyridine of the salts formed in the titrations were determined by the differential vapour pressure method[4] at 37°.

TABLE I

SALT DISSOCIATION CONSTANTS FROM DVP MEASUREMENTS

Mol. stoich. (*M*)	*Mol. dissoc.* (*M*)	*K*
TMA 2,4-dinitrophenolate		
$1.66\cdot10^{-2}$ m	$2.14\cdot10^{-2}$ m	$1.95\cdot10^{-3}$
$1.32\cdot10^{-2}$ m	$1.73\cdot10^{-2}$ m	$1.85\cdot10^{-3}$
$1.00\cdot10^{-2}$ m	$1.41\cdot10^{-2}$ m	$2.85\cdot10^{-3}$
TMA picrate		
$1.00\cdot10^{-2}$ m	$1.27\cdot10^{-2}$ m	$9.98\cdot10^{-4}$
$1.50\cdot10^{-2}$ m	$1.89\cdot10^{-2}$ m	$1.37\cdot10^{-3}$
$2.00\cdot10^{-2}$ m	$2.53\cdot10^{-2}$ m	$1.91\cdot10^{-3}$
$3.00\cdot10^{-2}$ m	$3.91\cdot10^{-2}$ m	$3.96\cdot10^{-3}$
$4.00\cdot10^{-2}$ m	$5.05\cdot10^{-2}$ m	$3.73\cdot10^{-3}$
$5.00\cdot10^{-2}$ m	$6.13\cdot10^{-2}$ m	$3.29\cdot10^{-3}$
TMA 2,5-dinitrophenolate		
$2.92\cdot10^{-3}$ m	$4.08\cdot10^{-3}$ m	$7.64\cdot10^{-4}$
$2.34\cdot10^{-3}$ m	$3.72\cdot10^{-3}$ m	$1.97\cdot10^{-3}$
$1.76\cdot10^{-3}$ m	$2.38\cdot10^{-3}$ m	$3.37\cdot10^{-4}$
TMA acetate		
$1.35\cdot10^{-3}$ m	$2.23\cdot10^{-3}$ m	$1.64\cdot10^{-3}$
$2.02\cdot10^{-3}$ m	$3.44\cdot10^{-3}$ m	$3.36\cdot10^{-3}$
$2.70\cdot10^{-3}$ m	$4.78\cdot10^{-3}$ m	$6.97\cdot10^{-3}$
$4.05\cdot10^{-3}$ m	$6.41\cdot10^{-3}$ m	$3.28\cdot10^{-3}$
$5.40\cdot10^{-3}$ m	$8.64\cdot10^{-3}$ m	$4.85\cdot10^{-3}$
$6.75\cdot10^{-3}$ m	$10.48\cdot10^{-3}$ m	$4.60\cdot10^{-3}$
TMA benzoate		
$2.91\cdot10^{-3}$ m	$3.12\cdot10^{-3}$ m	$1.48\cdot10^{-5}$
$3.88\cdot10^{-3}$ m	$4.17\cdot10^{-3}$ m	$2.20\cdot10^{-5}$
$4.68\cdot10^{-3}$ m	$5.35\cdot10^{-3}$ m	$1.09\cdot10^{-4}$

RESULTS

Salt dissociation constants

The dissociation constants of the salts formed in the titrations, that are needed in the calculations of the titration curves were determined from differential vapour pressure (DVP) measurements. These DVP measurements were carried out as before[4].

The results are summarized in Tables I and II.

Determination of K_{H_2O}

The determination of the dissociation constant of water in pyridine was carried out with the aid of potentiometric titrations of 2,5-dinitrophenol and picric acid with tetramethylammonium hydroxide. For the pK values of 2,5-dinitrophenol and picric acid the values 6.5 and 3.0 were used in the calculations[4]. In the case of 2,5-dinitrophenol, a homoconjugation constant of 100 was taken into account, the following set of equilibria being used.

TABLE II

MEAN SALT DISSOCIATION CONSTANTS FROM DVP MEASUREMENTS

Compound	*K*
TMA 2,4-dinitrophenolate	$2.3\cdot10^{-3}$
TMA picrate	$2.5\cdot10^{-3}$
TMA 2,5-dinitrophenolate	$1.0\cdot10^{-3}$
TMA acetate	$4.1\cdot10^{-3}$
TMA benzoate	$3.1\cdot10^{-5}$

$$HX \xrightleftharpoons{K_{HX}} H^+ + X^-$$

$$HX + X^- \xrightleftharpoons{K_{HX_2^-}} HX_2^-$$

$$TMAOH \xrightleftharpoons{K_{TMAOH}} TMA^+ + OH^-$$

$$H^+ + OH^- \xrightleftharpoons{1/K_{H_2O}} H_2O$$

$$TMA^+ + X^- \xrightleftharpoons{1/K_{TMAX}} TMAX$$

With regard to the dissociation constant of tetramethylammonium hydroxide in pyridine, changing its value from 1 to 10^{-5} did not change the calculated titration curve.

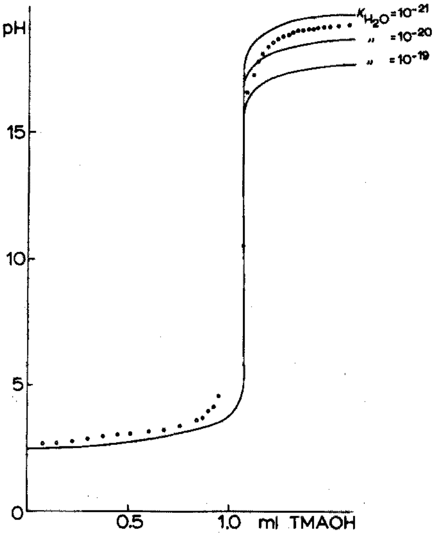

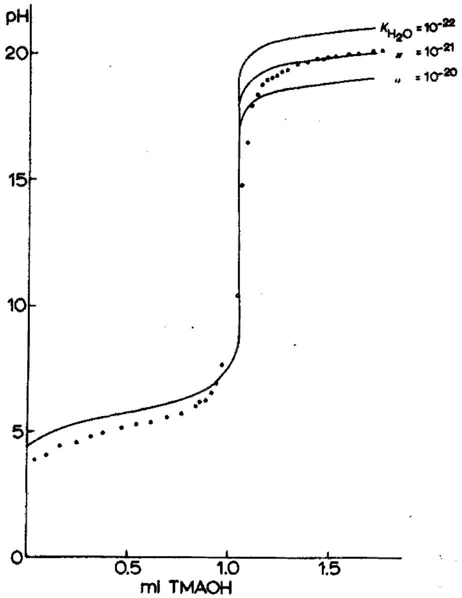

Fig. 1. Titration of 0.100 meq of picric acid with 0.0939 *M* TMAOH. Starting volume = 5 ml. (——) Calculated curve; (......) experimental curve.

Fig. 2. Titration of 0.100 meq of 2,5-dinitrophenol with 0.0939 *M* TMAOH. Starting volume = 5 ml. (——) Calculated curve; (......) experimental curve.

TABLE III

K_{H_2O} FROM DIFFERENT TITRATIONS WITH TMAOH

Titrated compound	K_{H_2O}
2,5-Dinitrophenol	10^{-21}
Picric acid	10^{-20}

The calculated and experimental titration curves for 2,5-dinitrophenol and picric acid are represented in Figs. 1 and 2.

A comparison of the values of K_{H_2O} found from the different titrations is given in Table III.

The determination of the dissociation constants of benzoic acid and acetic acid

The dissociation constants of acetic and benzoic acid were determined from the curves of potentiometric titrations of these compounds with tetramethylammonium hydroxide.

In the calculations the value 10^{-21} was used for K_{H_2O}. For the dissociation constants of the TMA salts of acetic acid and benzoic acid, the DVP results were used.

With benzoic acid simple dissociation (type *a*) described the titration best.

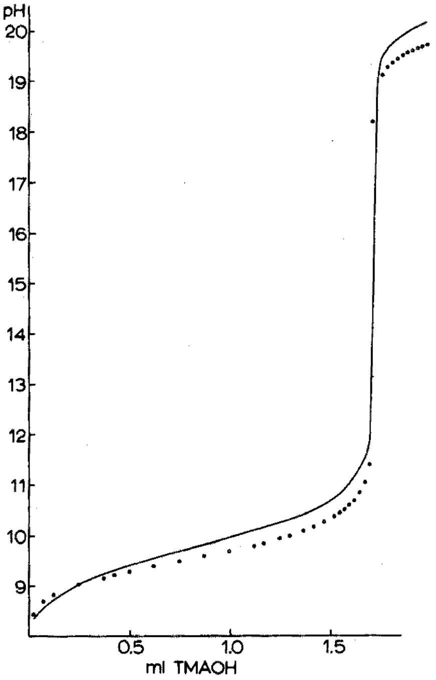

Fig. 3. Titration of 0.210 meq of benzoic acid with 0.122 *M* TMAOH. Starting volume = 4 ml. (——) Experimental curve; (......) calculated curve.

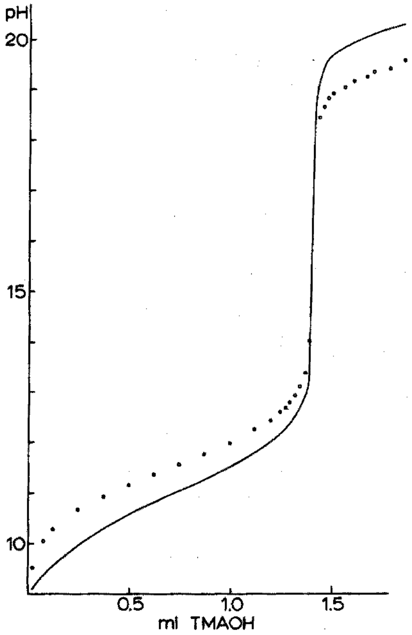

Fig. 4. Titration of 0.172 meq of acetic acid with 0.122 *M* TMAOH. Starting volume = 4 ml. (——) Experimental curve; (......) calculated curve.

TABLE IV

DISSOCIATION CONSTANTS OF BENZOIC ACID AND ACETIC ACID IN PYRIDINE AND IN WATER

	pK (pyr)	pK (H_2O)	ΔpK
Acetic acid	12	5	7
Benzoic acid	11	4	7

The dissociation constant of benzoic acid in pyridine was found to be 10^{-11}. The titration curves are represented in Fig. 3.

The titration of acetic acid with TMAOH could be described best by homoconjugation (type *c*). The dissociation constant of acetic acid in pyridine was found to be 10^{-12}. The homoconjugation constant $K_{HX_2^-}$ was 10^2. Titration curves for acetic acid are represented in Fig. 4.

A comparison of the pK values of acetic acid and benzoic acid in water and pyridine is given in Table IV.

DISCUSSION

The differences in the values of pK (pyr) and pK (water) found for acetic acid and benzoic acid are considerably greater than one would expect from the results with phenols[4]. However, this is in agreement with the conclusions based on the polarographic half-wave potentials of Tsuji and Elving[5] and with the results of the titrations of Streuli[6].

The authors wish to thank Mrs. M. Heidemans for carrying out some of the titrations and Miss A. L. Dekkers for preparing the manuscript.

SUMMARY

The dissociation constant of water in pyridine was determined from the titration of some acids with known dissociation constants with tetramethylammonium hydroxide; a value of 10^{-21} was found. This dissociation constant was used in determining the dissociation constants of acetic acid and benzoic acid in pyridine; the pK values found were 12 and 11, respectively.

RÉSUMÉ

La constante de dissociation de l'eau dans la pyridine a été déterminée par titrage de quelques acides à constantes de dissociation connues, à l'aide d'hydroxyde de tétraméthylammonium. On arrive à une valeur de 10^{-21}. Cette constante de dissociation a été utilisée pour déterminer les constantes de l'acide acétique et de l'acide benzoïque dans la pyridine. Les valeurs pK ainsi trouvées sont respectivement 12 et 11.

ZUSAMMENFASSUNG

Die Dissoziationskonstante von Wasser in Pyridin wurde durch Titration

einiger Säuren mit bekannten Dissoziationskonstanten mit Tetramethylammoniumhydroxid bestimmt; es wurde der Wert 10^{-21} gefunden. Diese Dissoziationskonstante wurde für die Bestimmung der Dissoziationskonstanten von Essigsäure und Benzoesäure in Pyridin verwendet; die gefundenen p*K*-Werte waren 12 bzw. 11.

REFERENCES

1 C. A. Streuli and R. R. Miron, *Anal. Chem.*, 30 (1958) 1978.
2 D. F. Detar, *Computer Programs for Chemistry, Vol. II*, 1969, p. 65–67.
3 H. B. van der Heijde, *Anal. Chim. Acta*, 16 (1957) 392.
4 M. Bos and E. A. M. F. Dahmen, *Anal. Chim. Acta*, 53 (1971) 39.
5 K. Tsuji and P. J. Elving, *Anal. Chem.*, 41 (1969) 286.
6 C. A. Streuli, *Anal. Chem.*, 32 (1960) 407.

Analytica Chimica Acta
Elsevier Publishing Company, Amsterdam
Printed in The Netherlands

ELECTROCHEMICAL REDUCTION OF CHLORDIAZEPOXIDE AT MERCURY ELECTRODES

EINAR JACOBSEN AND TROND V. JACOBSEN
Department of Chemistry, University of Oslo, Blindern, Oslo 3 (Norway)

(Received 16th March 1971)

Chlordiazepoxide (Librium, Clopoxide) is the first member of a new class of chemical compounds showing powerful antianxiety effects[1,2]. Because of its frequent clinical use the need arose for sensitive and specific methods for its determination in tablets, blood, urine, etc. In the last decade this drug has been determined by colorimetry following diazotization and coupling of its hydrolysis product[3,4], by spectrofluorimetry after hydrolysis to a lactane derivative which is converted to a compound exhibiting a characteristic fluorescence[5], and by gas–liquid chromatography[6]. Very few data for the polarographic determination of chlordiazepoxide are reported in the literature. Oelschläger[7] observed that in Britton–Robinson buffers the drug is reduced in three steps. Below pH 4 only the two first waves are observed and he claims that the height of these waves is proportional to the concentration in the range 0.1–1 m*M*. According to Senkowski *et al.*[8] well-defined waves are obtained from mixtures of alcohol and water and they recommend 0.1 *M* hydrochloric acid containing 20% methanol as supporting electrolyte for the polarographic determination of chlordiazepoxide. Cimbura and Gupta[9] claim that the drug can be extracted from alkaline biological media by ether and determined polarographically after stripping with 1 *M* hydrochloric acid. The over-all recovery is about 90%.

The polarographic method is very sensitive, selective and it is less time-consuming than other methods recommended for the determination of chlordiazepoxide. The objective of the present work was to study the electroreduction of chlordiazepoxide in detail and to investigate the application of polarography to rapid analysis of the drug in tablets and biological materials.

EXPERIMENTAL

Polarograms were recorded with a Metrohm E 261 R Polarecord connected to a Metrohm E 393 a.c. modulator. An Ag/AgCl/saturated KCl electrode served as reference electrode and a tungsten electrode was employed as auxiliary electrode. All a.c. polarograms were obtained with an amplitude of 10 mV r.m.s. The capillary characteristics of the dropping mercury electrode, measured in 0.1 *M* potassium nitrate (open circuit) at a mercury height of 59.5 cm, were $m = 2.104$ mg sec^{-1} and $t =$ 3.82 sec. All experiments were performed at 25±0.1°. Dissolved air was removed from the solutions by bubbling oxygen-free nitrogen through the cell for 10 min and passing it over the solution during the electrolysis.

Cyclic voltammetric and coulometric experiments were performed with a versatile solid-state instrument constructed in this laboratory following the design of Goolsby and Sawyer[10]. A Mosely 7030 AM X-Y recorder and a Honeywell Electronic 194 strip-chart recorder were used in conjunction with the instrument. A three-electrode assembly was used for all measurements. A Metrohm E410 hanging mercury drop was used as working electrode for the cyclic voltammetric experiments and a mercury pool was employed for the controlled-potential coulometric measurements. The reference electrode was an aqueous Ag/AgCl wire and a platinum coil served as auxiliary electrode. These electrodes were isolated in glass tubes with fine-porosity fritted-glass discs. The shield tubes were filled with the supporting electrolyte used in the sample solution. The solution was stirred with a magnetic stirrer and a Teflon-covered stirring bar.

Chlordiazepoxide hydrochloride (99% pure) was obtained from Apothekernes Laboratorium, Oslo, Norway. A 1 m*M* stock solution was prepared by dissolving the appropriate amount of the commercial product "Clopoxide" in 0.1 *M* sulphuric acid. All other chemicals were reagent grade and were used without further purification. The pH of the solutions was determined with a Beckman Zeromatic pH meter.

RESULTS

Preliminary experiments showed that chlordiazepoxide is easily reduced at the dropping mercury electrode. In agreement with earlier data[7] a maximum was observed on polarograms recorded from 1 *M* hydrochloric acid. Moreover, the dissolution wave of mercury interfered with the first polarographic step of the drug. The maximum also occurred when nitric acid was used as supporting electrolyte. How-

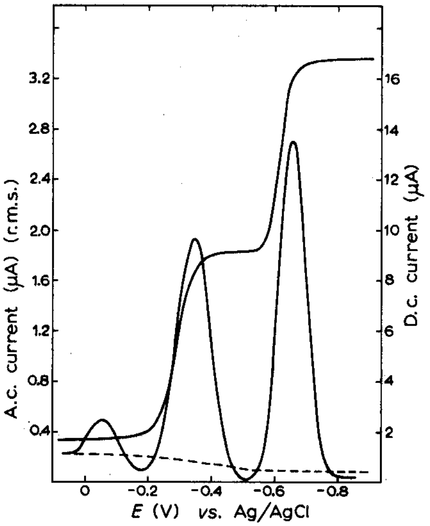

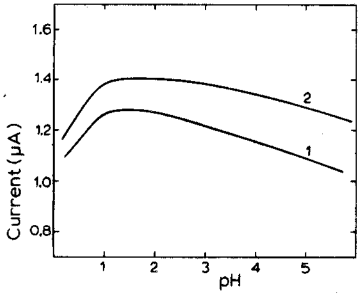

Fig. 1. A.c. and d.c. polarograms of $1.1 \cdot 10^{-3}$ *M* chlordiazepoxide in 0.1 *M* sulphuric acid. Dashed line represents the a.c. base current.

Fig. 2. Limiting current of the first (curve 1) and second (curve 2) polarographic wave of $2 \cdot 10^{-4}$ *M* chlordiazepoxide at various pH values.

ever, polarograms recorded from sulphuric acid solutions exhibited no maximum at any pH value or concentration of the depolarizer (Fig. 1). Hence, dilute sulphuric acid was used as supporting electrolyte in the following experiments.

Strongly acidic solutions of chlordiazepoxide acquire a yellow colour on standing, probably as a result of hydrolysis. In order to test the effect of hydrolysis on the current–voltage curves, polarograms of a stock solution (10^{-3} M chlordiazepoxide in 0.01 M sulphuric acid) were recorded each day for three weeks. The limiting current decreased gradually with time and after three weeks the current was only 85% of its original value. Moreover, the half-wave potentials shifted about 25 mV to more negative values. Consequently, a fresh solution of the drug was prepared just before all of the following experiments. Provided that the concentration of the sulphuric acid was 0.1 M or less, no shift in potentials or decrease in limiting current was observed the first day after mixing the solution.

Polarography

The effect of pH on the current–voltage curves was investigated by recording polarograms of $2 \cdot 10^{-4}$ M chlordiazepoxide in phthalate buffers. The pH of each solution was adjusted to the desired value by addition of sulphuric acid or sodium hydroxide and measured with a pH meter. The reversibility of the electrode reaction was tested by determining the value $E_{\frac{3}{4}} - E_{\frac{1}{4}}$ of each polarogram. The results are given in Table I and indicate that the electrode reaction becomes increasingly more irreversible with increasing pH. The half-wave potential of both waves is shifted linearly to more negative values, indicating that hydrogen ions are consumed in the reduction. In the pH range 0–6 the half-wave potentials may be expressed by the equations:

$$E_{\frac{1}{2}} = -0.15 - 0.076 \cdot \text{pH}$$

and

$$E_{\frac{1}{2}} = -0.51 - 0.064 \cdot \text{pH}$$

The third polarographic wave of chlordiazepoxide previously reported[7] was not observed in strongly acidic medium.

The limiting currents of both waves are also very dependent on the pH of the electrolyte (Fig. 2). However, the heights of the waves are almost independent of pH in the range 1–2, and because more reversible waves are obtained at low pH values (Table I), 0.1 M sulphuric acid (pH = 1.1) was used as supporting electrolyte subsequently.

The d.c. polarographic steps are followed by a.c. polarographic waves and the summit potentials, E_s, are slightly more negative than the half-wave potentials. The a.c. polarograms exhibit a positive tensammetric wave at $E_{T+} = -0.05$ V. Moreover, the base current is much lower than in the absence of the depolarizer (Fig. 1), which implies that both chlordiazepoxide and its reduction products are adsorbed at the electrode surface[11]. Electrocapillary curves of the drug (Fig. 3) show a large decrease in droptime over a considerable potential range, confirming a strong adsorption at the electrode.

The effect of drop time was investigated by recording polarograms of 10^{-5} M chlordiazepoxide in 0.1 M sulphuric acid at various heights of the mercury column. The value $ih^{-\frac{1}{2}}$, where h is the height of the column after correction for the "back pressure", was constant, indicating that the current is diffusion-controlled. Exactly the

TABLE I

EFFECT OF pH ON POLAROGRAMS OF $2 \cdot 10^{-4}$ *M* CHLORDIAZEPOXIDE

First wave			*Second wave*	
pH	$-E_{\frac{1}{2}}$ (*V*)	$-(E_{\frac{3}{4}}-E_{\frac{1}{4}})$ (*mV*)	$-E_{\frac{1}{2}}$ (*V*)	$-(E_{\frac{3}{4}}-E_{\frac{1}{4}})$ (*mV*)
0.25	0.17	38	0.53	34
0.40	0.18	42	0.54	35
0.60	0.19	43	0.55	36
0.90	0.20	44	0.56	36
1.10	0.22	48	0.57	36
1.35	0.24	52	0.59	36
1.65	0.26	58	0.60	37
2.10	0.31	64	0.66	38
2.40	0.34	70	0.68	40
3.00	0.37	76	0.72	42
3.40	0.39	76	0.74	44
5.00	0.53	77	0.83	45
5.70	0.60	78	0.88	46
6.10	0.62	79	0.90	47

same result was obtained by repeating the experiment with a solution containing 10^{-3} *M* chlordiazepoxide; this implies that the adsorption must be fast and that diffusion is the rate-controlling step in the overall electrode reaction. The height of the a.c. waves increases linearly with increasing height of the mercury column (Table II). This is a characteristic feature of "penetration waves" and indicates that the a.c. current is partly controlled by the rate of adsorption[12].

The temperature coefficient (determined in the range 18–45°) of each of the d.c. waves is +1.48% per degree, and that of the a.c. waves, +0.86% per degree; this again implies that the current is controlled essentially by diffusion. The temperature coefficients of the half-wave potentials (and of the summit potentials), +2 mV/degree and +0.03 mV/degree, for the first and second wave, respectively, indicate that the

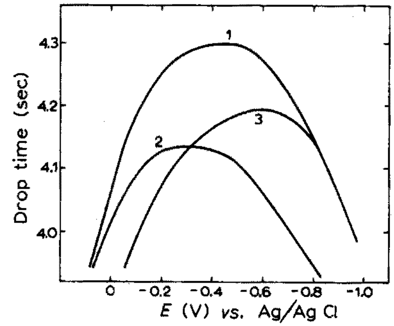

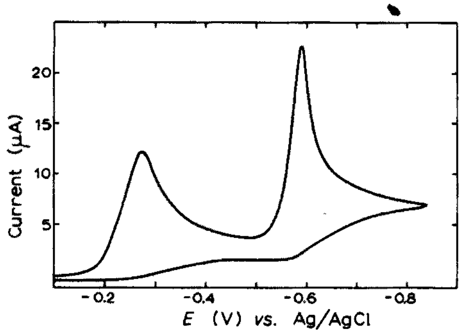

Fig. 3. Electrocapillary curves of 0.1 *M* sulphuric acid (curve 1), $8 \cdot 10^{-4}$ *M* chlordiazepoxide in 0.1 *M* sulphuric acid (curve 2) and 20% serum in 0.1 *M* sulphuric acid (curve 3).

Fig. 4. Cyclic voltammogram of $5 \cdot 10^{-4}$ *M* chlordiazepoxide in 0.1 *M* sulphuric acid. Scan rate 0.1 V sec^{-1}.

TABLE II

EFFECT OF PRESSURE OF MERCURY ON THE HEIGHT OF THE a.c. WAVES OF $5 \cdot 10^{-4}$ *M* CHLORDIAZEPOXIDE IN 0.1 *M* SULPHURIC ACID

h_{corr} *(cm)*	*First wave* *μA (r.m.s.)*	*Second wave* *μA (r.m.s.)*
37.9	0.85	1.21
47.9	0.93	1.33
57.9	1.02	1.45
62.9	1.05	1.51
67.9	1.08	1.56

second electrode reaction is less irreversible than the first one.

Polarograms recorded from 0.1 *M* sulphuric acid with various amounts of chlordiazepoxide present, showed that the d.c. current increases linearly with concentration (Table III). Below 10^{-4}. *M* the half-wave potentials are constant and the heights of the two waves are equal. At higher concentrations the value i_d/C for the first wave decreases and both waves are shifted to more negative potentials with increasing concentration of chlordiazepoxide. Apparently, when the concentration of the depolarizer is increased above 10^{-4} *M*, the electrode is probably completely covered with a monomolecular layer of the adsorbed material and a further increase in the concentration of the surface-active depolarizer results in a slight distortion of the waves. However, the data in Table III are perfectly reproducible, and imply that chlordiazepoxide can be determined by polarography in the entire concentration range $2.5 \cdot 10^{-6}$–10^{-3} *M*, which corresponds to 0.8–336 μg ml^{-1}.

The diffusion current constant, $I = i_d/C\ m^{\frac{2}{3}}\ t^{\frac{1}{6}}$, calculated from the data in Table III (at concentrations below 10^{-4} *M*) is $I = 3.12$ for each of the two waves.

The height of the a.c. polarographic waves of chlordiazepoxide is not proportional to the concentration. Moreover, the a.c. current is much lower than the corresponding d.c. current (Fig. 1), and below 10^{-5} *M*, no a.c. wave is observed on the polarograms. Hence, a.c. polarography has no advantage over conventional d.c. polarography for quantitative determinations of chlordiazepoxide.

Cyclic voltammetry

Voltammetric experiments were performed at a hanging mercury drop electrode. A typical voltammogram is shown in Fig. 4. When the potential sweep was repeated at the same mercury drop, the peak heights decreased and the peak potentials were shifted to more negative values, even when the solution was well stirred between each cyclic sweep. This is probably the result of the adsorption of chlordiazepoxide and its reduction product at the electrode. However, reproducible waves were obtained for the first potential sweep on each mercury drop. Hence, in the following experiments the mercury drop was changed between each experiment and just before the next potential sweep.

A few voltammetric data are given in Table IV. No anodic peak resulting from reoxidation of the reduction product was observed at any scan rate. The current function, $i_p/Cv^{\frac{1}{2}}$, was fairly constant and independent of the scan rate, which implies

TABLE III

POLAROGRAPHIC DATA FOR THE REDUCTION OF VARIOUS AMOUNTS OF CHLORDIAZEPOXIDE IN 0.1 *M* SULPHURIC ACID

Concn. (*mM*)	*First wave*			*Second wave*		
	$-E_{\frac{1}{2}}$ (*V*)	i_d (*μA*)	i_d/C (*μA/mM*)	$-E_{\frac{1}{2}}$ (*V*)	i_d (*μA*)	i_d/C (*μA/mM*)
1.000	0.27	6.40	6.40	0.61	6.85	6.85
0.750	0.26	4.80	6.40	0.60	5.20	6.93
0.500	0.24	3.22	6.44	0.60	3.38	6.95
0.250	0.22	1.62	6.47	0.57	1.76	7.03
0.100	0.21	0.65	6.50	0.56	0.70	7.00
0.075	0.21	0.51	6.79	0.55	0.52	6.94
0.050	0.21	0.34	6.80	0.56	0.34	6.80
0.025	0.21	0.17	6.80	0.56	0.17	6.80
0.010	0.21	0.068	6.80	0.56	0.068	6.80
0.0075	0.21	0.051	6.80	0.56	0.051	6.80
0.0050	0.21	0.034	6.80	0.56	0.034	6.80
0.0025				0.56	0.016	6.40

TABLE IV

VOLTAMMETRIC DATA FOR THE REDUCTION OF $5 \cdot 10^{-4}$ *M* CHLORDIAZEPOXIDE IN 0.1 *M* SULPHURIC ACID

Scan rate $v_1(V\ sec^{-1})$	$(i_p)_1$ (*μA*)	$(i_p)_2$ (*μA*)	$(i_p)_1/Cv^{\frac{1}{2}}$	$(i_p)_2/Cv^{\frac{1}{2}}$
0.2000	17.4	27.0	77	120
0.1000	12.4	18.5	78	116
0.0333	6.9	10.6	76	116
0.0167	4.9	7.2	76	111

that the electrode reaction is a simple irreversible electron-transfer and that it is neither preceded nor followed by a slow chemical reaction[13].

Coulometry

Coulometric reductions at controlled potential were performed to determine the number of electrons involved in each of the two electron-transfer reactions. The experiments were carried out in the absence of air in a small electrolysis cell with a mercury pool as the cathode.

The potential of the working electrode was first controlled at -0.45 V. In this case 4.75 coulombs were consumed in the reduction of $2.5 \cdot 10^{-5}$ mol chlordiazepoxide, which yields the value $n = 1.97$ for the first electrode reaction. The experiment was repeated with a new solution containing $2.5 \cdot 10^{-5}$ mol chlordiazepoxide and with the potential of the cathode controlled at -0.90 V; 9.80 coulombs were consumed in this reduction, corresponding to a value of $n = 4.06$. These experiments clearly demonstrate that two electrons are involved in each of the two polarographic steps.

DISCUSSION

It is evident from the experimental results that chlordiazepoxide is adsorbed at the electrode. The adsorption is fast and each of the two polarographic steps is due to a diffusion-controlled, irreversible 2-electron reduction. The half-wave potentials are shifted −76 and −64 mV per pH unit, respectively, to more negative values with increasing pH. The number of hydrogen ions, Z, taking part in the electrode reaction is given by

$$\Delta E_{\frac{1}{2}}/\Delta \mathrm{pH} = -0.059\,(Z/\alpha n)$$

where α is the transfer coefficient. The value αn, calculated from the equation

$$E_{\frac{3}{4}} - E_{\frac{1}{4}} = -0.052\,(\alpha n^{-1})$$

in strongly acidic medium is 1.37 (first wave) and 1.53 (second wave), which gives the values $Z = 1.76$ and $Z = 1.66$ for the first and the second wave, respectively. Consequently, two hydrogen ions are probably taking part in each of the two electrode reactions.

In acidic medium the following electrode reactions may then be postulated:
First wave:

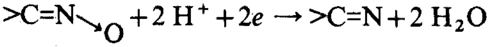

$$>\!C{=}N{\searrow}O + 2\,H^+ + 2e \rightarrow\, >\!C{=}N + 2\,H_2O$$

Second wave:

$$>\!C{=}N + 2\,H^+ + 2e \rightarrow\, >\!CH{-}NH$$

The third wave previously reported[7] occurs only on polarograms recorded at higher pH values and is probably attributable to reduction of the $-N{=}C\!<$ group in 1,2-position of the diazepine ring.

Analytical applications

Polarographic determinations in biological materials like serum are usually not possible because the waves are greatly distorted by the adsorbed film of proteins present in such materials. However, chlordiazepoxide is surface-active and, as indicated in Fig. 3, it is more strongly adsorbed at the electrode than the proteins in sera when the applied potential is more negative than −0.3 V. Hence, it should be possible to determine chlordiazepoxide in serum without any preceding and time-consuming separation.

Various amounts of chlordiazepoxide were added to 10 ml of serum and diluted to 50 ml with 0.1 M sulphuric acid; 25 ml was transferred to a polarographic cell, dissolved air was removed with nitrogen, and the polarogram was recorded. Well-defined waves were observed in the concentration range 10^{-5}–$5 \cdot 10^{-4}$ M. At lower concentrations the polarographic waves were masked by the adsorbed proteins. The experiment was repeated by mixing equal amounts of serum and sulphuric acid. In this case the lower limit of detection was $2 \cdot 10^{-5}$ M chlordiazepoxide which corresponds to $4 \cdot 10^{-5}$ M (13 μg ml^{-1}) in the serum.

The polarographic method is very rapid (15 min) and selective and gives very reproducible results. Unfortunately, it is not as sensitive as the gas chromatographic method[6] and it is probably not sufficiently sensitive for practical serum analysis. However, the proposed polarographic method should be very suitable for the analysis

TABLE V

POLAROGRAPHIC DETERMINATION OF CHLORDIAZEPOXIDE IN TABLETS

Tablet no.	*Compound*	*Current (μA)*	*mg found*
1	"Alpoxide"	1.95	4.69
2	"Alpoxide"	2.02	4.83
3	"Alpoxide"	1.98	4.75
4	"Alpoxide"	2.02	4.83
5	"Alpoxide"	1.96	4.71
6	"Alpoxide"	2.00	4.80
7	"Alpoxide"	1.95	4.69
8	"Prodixamon"	1.85	4.45
9	"Prodixamon"	1.86	4.47
10	"Prodixamon"	1.86	4.47

of other biological materials (*e.g.* urine) in which chlordiazepoxide occurs in higher concentrations. Moreover, the above experiments indicate that drugs which are more strongly adsorbed than chlordiazepoxide and which are reduced at more negative potentials can be determined in serum by polarography at very low concentrations and without any previous separation.

Chlordiazepoxide in tablets is usually determined by u.v. spectrophotometry after extraction of the drug with an organic solvent and removal of the insoluble material. The extraction is time-consuming and, moreover, the method cannot be used for tablets also containing propantheline bromide, because both drugs absorb light at the same wavelengths. Preliminary experiments showed that propantheline is polarographically inactive in acidic solutions and hence, a polarographic method was outlined for the determination of chlordiazepoxide in tablets.

The tablet was mixed with 10 ml of 0.5 *M* sulphuric acid and diluted with 10–15 ml of distilled water. After a few minutes of shaking, the mixture was diluted to 50 ml with water and transferred to a polarographic cell. Dissolved air was removed with nitrogen, a polarogram was recorded and the height of the second wave was measured.

The experiments showed that chlordiazepoxide was completely dissolved after shaking for 2–3 min. Moreover, the insoluble constituents in the tablets did not cause any interference and need not be removed before the polarogram was recorded. Hence, the proposed method is not only very accurate and selective, but it is also less time-consuming than earlier methods.

The results of a few determinations of the drug in "Alpoxide" tablets (containing about 5 mg of chlordiazepoxide) and in "Prodixamon comp." (containing about 5 mg of chlordiazepoxide and 15 mg of propantheline bromide) are given in Table V.

The authors wish to thank Apothekernes Laboratorium, Oslo, Norway, for the "Clopoxide" compound and the tablets used in this investigation.

SUMMARY

The electroreduction of chlordiazepoxide has been investigated by polarography, cyclic voltammetry and coulometry at controlled potential. In 0.1 *M* sulphuric acid the drug is reduced in two steps. The first step is a 2-electron reduction of the N-oxide group and the second step a 2-electron reduction of the C=N group. Two hydrogen ions are consumed in each step. The current is diffusion-controlled and proportional to the concentration in the range $2.5 \cdot 10^{-6}$–10^{-3} *M*. The drug is strongly adsorbed at the electrode, so that it can be determined in biological materials without prior separation. A rapid polarographic method for the determination of chlordiazepoxide in tablets is described.

RÉSUMÉ

Une étude est effectuée sur l'électroréduction de "chlordiazepoxide" par polarographie, voltammétrie cyclique et coulométrie à potential contrôlé. En milieu acide sulfurique 0.1 *M*, la drogue est réduite en deux stades: le premier correspond à une réduction à 2 électrons du groupe N-oxyde, le second à une réduction à 2 électrons du groupe C=N. Deux ions hydrogène sont consommés dans chaque cas. Le courant de diffusion est proportionnel à la concentration de $2.5 \cdot 10^{-6}$ à 10^{-3} *M*. Cette drogue est fortement adsorbée à l'électrode, ce qui permet de la doser dans des substances biologiques, sans séparation préalable. Une méthode polarographique rapide est décrite pour l'analyse de tablettes.

ZUSAMMENFASSUNG

Die elektrochemische Reduktion von Chlordiazepoxid wurde durch Polarographie, cyclische Voltammetrie und Coulometrie bei kontrolliertem Potential untersucht. In 0.1 *M* Schwefelsäure wird das Arzneimittel in zwei Stufen reduziert. Die erste Stufe ist eine 2-Elektronenreduktion der N-oxid-Gruppe und die zweite Stufe eine 2-Elektronenreduktion der C=N-Gruppe. Bei jeder Stufe werden zwei Wasserstoffionen verbraucht. Der Strom wird durch die Diffusion bestimmt und ist der Konzentration im Bereich $2.5 \cdot 10^{-6}$ – 10^{-3} *M* proportional. Das Arzneimittel wird an der Elektrode fest adsorbiert, so dass eine Bestimmung in biologischen Stoffen ohne vorhergehende Abtrennung möglich ist. Eine schnelle polarographische Methode für die Bestimmung von Chlordiazepoxid in Tabletten wird beschrieben.

REFERENCES

1 T. Harris, *J. Amer. Med. Assoc.*, 172 (1960) 1162.
2 J. M. Tobin and N. D. C. Lewis, *J. Amer. Med. Assoc.*, 174 (1960) 96.
3 L. O. Randall, *Diseases of the Nervous System*, 22, Suppl. No. 7 (1961) 1.
4 J. Bäumler and S. Rippstein, *Helv. Chim. Acta*, 44 (1961) 2208.
5 B. A. Koechlin and L. D'Arconte, *Anal. Biochem.*, 5 (1963) 195.
6 J. A. F. DeSilva, M. A. Schwartz, V. Stefanovic, J. Kaplan and L. D'Arconte, *Anal. Chem.*, 36 (1964) 2099.
7 H. Oelschläger, *Arch. Pharm.*, 296 (1963) 396.
8 B. Z. Senkowski, M. S. Levin, J. R. Urbigkit and E. G. Wollish, *Anal. Chem.*, 36 (1964) 1991.
9 G. Cimbura and R. C. Gupta, *J. Forensic Sci.*, 10 (1965) 282.
10 A. D. Goolsby and D. T. Sawyer, *Anal. Chem.*, 39 (1967) 411.
11 B. Breyer and H. H. Bauer, *Alternating Current Polarography and Tensammetry*, Interscience, New York, 1963, p. 268.
12 E. Jacobsen, *Anal. Chim. Acta*, 35 (1966) 447.
13 R. S. Nicholson and I. Shain, *Anal. Chem.*, 36 (1964) 706.

Analytica Chimica Acta
Elsevier Publishing Company, Amsterdam
Printed in The Netherlands

EINE KINETISCHE DIFFERENZMETHODE UNTER VERWENDUNG KATALYSIERTER REAKTIONEN

H. WEISZ UND H. LUDWIG

Lehrstuhl für Analytische Chemie, Chemisches Laboratorium, Universität Freiburg i.Br. (Deutschland)

(Eingegangen den 27. März 1971)

Katalysierte Reaktionen finden infolge ihrer Empfindlichkeit und ihrer oftmals ausgeprägten Selektivität—es sei hier an enzymatische Systeme erinnert—in steigendem Masse Anwendung in der analytischen Chemie. So lassen sich mit Hilfe derartiger Reaktionen Bestimmungen von Katalysatormengen im Mikrogramm- und Nanogrammbereich mit befriedigender Genauigkeit durchführen.

Verschiedene kinetische Methoden wurden zur Bestimmung der Katalysatorkonzentration entwickelt[1-3]. Bei der von Bognar[4] beschriebenen Methode der "Simultankomparation" wird die der unbekannten Katalysatorkonzentration entsprechende Reaktionsgeschwindigkeit verglichen mit den Geschwindigkeiten einer Reihe von "Standardreaktionen" mit bekannten Katalysatorgehalten, die unter denselben Bedingungen gleichzeitig mit der "Probereaktion" gestartet werden. Gleichen Veränderungen des Systems nach Ablauf einer bestimmten Zeit entsprechen gleiche Reaktionsgeschwindigkeiten und damit auch gleiche Katalysatorkonzentrationen. Yatsimirskii[5] beschreibt eine Methode, bei welcher eine katalysierte Reaktion unter identischen Reaktionsbedingungen (gleiche Katalysatorkonzentration) in zwei Ansätzen abläuft, wobei die Reaktion in dem einen Ansatz um eine vorgegebene Zeit früher gestartet wird als im anderen Ansatz. Bei photometrischer Verfolgung des Reaktionsablaufs ist die gemessene Differenz der Extinktion ein Mass für die Katalysatorkonzentration.

Wir haben ein Verfahren entwickelt, das im Gegensatz dazu auf der Verschiedenheit der Reaktionsgeschwindigkeiten einer gleichzeitig in zwei Ansätzen ablaufenden, katalysierten Reaktion beruht.

Die durch den Katalysator K beschleunigte Reaktion zwischen den Stoffen A und B läuft in zwei Ansätzen durch gleichzeitigen Start simultan ab. Beim Start unterscheiden sich die beiden Ansätze nur in der Katalysatorkonzentration. Die Katalysatorkonzentration in Gefäss I hat bei jeder Bestimmung denselben Wert ($[K]_v$ = Konzentration im Vergleichsansatz). Die Katalysatorkonzentration in Gefäss II stellt die zu bestimmende Konzentration dar ($[K]_p$ = Konzentration im Probeansatz).

Reaktion in Gefäss I: $A+B \xrightarrow{K_v} C+D$

Reaktion in Gefäss II: $A+B \xrightarrow{K_p} C+D$

Der Ablauf der Reaktion lässt sich in beiden Fällen anhand der Abnahme eines Partners, z.B. A, mit der Zeit verfolgen. Zum Zeitpunkt des Starts der Reaktion ist die

Konzentration von A in Gefäss I ($[A]_v$) gleich der Konzentration von A in Gefäss II ($[A]_p$). Nach dem Start tritt zunächst eine zunehmende Differenz zwischen $[A]_v$ und $[A]_p$ auf, die schliesslich ein Maximum erreicht. Nach vollständigem Ablauf der katalysierten Reaktion in beiden Gefässen (Gleichgewichtseinstellung) ist wieder $[A]_v = [A]_p$. Eine Kurve, welche Werte für $\Delta[A] = [A]_v - [A]_p$ in Abhängigkeit von der Zeit wiedergibt, beginnt daher zur Zeit $t=0$ bei $\Delta[A]=0$, durchläuft ein Maximum und endet wiederum bei $\Delta[A]=0$. Wenn $[K]_v$ bei jeder Bestimmung denselben Wert hat, hängen Grösse und Vorzeichen des Maximums der Konzentrationsdifferenz von A ($\Delta[A]_{max}$) von $[K]_p$ ab. Für $[K]_p > [K]_v$ nimmt $\Delta[A]_{max}$ einen positiven Wert und für $[K]_p < [K]_v$ einen negativen Wert an. Für $[K]_p = [K]_v$ gilt: $\Delta[A]_{max} = 0$. Anstelle von $\Delta[A]_{max}$ kann auch die Fläche unter einer Kurve, welche $\Delta[A]$ in Abhängigkeit von der Zeit wiedergibt, als Mass für $[K]_p$ verwendet werden. Für ein bestimmtes Zeitintervall ist weiterhin die Steigung dieser Kurve ein Mass für $[K]_p$. Zur Messung der Konzentration von A kann jede geeignete, physikalisch-chemische Messmethode verwendet werden.

Wir haben Kupfer aufgrund seiner katalytischen Wirkung auf die Reaktion von Eisen(III) mit Thiosulfat bestimmt. Die Reaktion wurde photometrisch verfolgt, wobei das gemessene Maximum der Extinktionsdifferenz ausgewertet wurde. Bei der Bestimmung von L-Cystin aufgrund seiner katalytischen Wirkung auf die Reaktion von Jod mit Azid wurde der Reaktionsablauf potentiometrisch verfolgt. Hierbei gelangte die Steigung der während des Reaktionsablaufs registrierten Kurve zur Auswertung.

BESTIMMUNG VON KUPFER MIT EINER KINETISCH-PHOTOMETRISCHEN DIFFERENZMETHODE

Bereits 1867 beschrieb Oudemans[6] die beschleunigende Wirkung von Kupfer(II) auf die Reaktion von Eisen(III) mit Thiosulfat.

$$2\,Fe^{3+} + 2\,S_2O_3^{2-} \rightarrow 2\,Fe^{2+} + S_4O_6^{2-}$$

Verschiedene Autoren haben dieses System zur kinetischen Bestimmung von Kupfer herangezogen. Dabei wurde der Reaktionsablauf visuell[7-10], photometrisch[11] und mit Hilfe der "dead-stop"-Methode[12] verfolgt. Bei den optischen Methoden lässt sich der Reaktionsablauf mit Hilfe des stark rot gefärbten Eisen(III)-Thiocyanatkomplexes indizieren, wobei allerdings die Reaktionsgeschwindigkeit der katalysierten Reaktion verringert wird[7]. Die Kinetik der katalysierten Reaktion wird von Yatsimirskii beschrieben[11]. Hinsichtlich der Kinetik der unkatalysierten Reaktion lassen sich unterschiedliche Angaben finden[11,13].

Experimentelles

Unter Verwendung einer Startpipette (Abb. 4) wird die durch Kupfer katalysierte Reaktion von Eisen(III) mit Thiosulfat in zwei Reaktionsgefässen gleichzeitig gestartet. Hierbei werden zu zwei Lösungen, welche gleiche Mengen Eisen(III) und unterschiedliche Kupfermengen enthalten, jeweils gleiche Mengen Thiosulfat gegeben. Zur photometrischen Verfolgung des Reaktionsablaufs haben wir das "Universal Kolorimeter Modell J" der Fa. Lange, Berlin, verwendet.

Während der Bestimmungen soll die Schwankung der Raumtemperatur nicht mehr als ±1.5° betragen. Es ist fernerhin darauf zu achten, dass alle verwendeten

Gefässe und Pipetten in gleicher Weise behandelt werden und keine Temperaturunterschiede zur Raumtemperatur aufweisen.

Lösungen. Eisen(III)-chlorid, 1 mg Fe^{3+} ml^{-1} (+10 ml konz. HCl ad 1000 ml) ($FeCl_3 \cdot 6\,H_2O$, Fa. Merck, Darmstadt, "Cu höchstens 0.004%").

Ammoniumeisen(II)-sulfat, 10 mg Fe^{2+} ml^{-1} (+2 ml 0.1 *N* H_2SO_4 ad 100 ml) ($(NH_4)_2Fe(SO_4)_2 \cdot 6\,H_2O$, Fa. Merck, "Cu höchstens 0.002%").

Kupferstammlösung. 100 μg Cu ml^{-1}.

Kupferstandardlösungen. 1, 2, 3, 4, 5, 7, 10, 15, 20 und 25 μg Cu ml^{-1}.

Durchführung. An das Verteilerstück der Startpipette (Abb. 4) werden zwei Vollpipetten (3 ml) angesetzt und mit 0.1 *M* Natriumthiosulfat gefüllt. Anschliessend werden in zwei Bechergläser (25 ml) unter Rühren jeweils 2.5 ml Eisen(III)-chloridlösung, 2.5 ml Ammoniumeisen(II)-sulfatlösung und 1.0 ml 1.0 *M* Kaliumthiocyanat einpipettiert. Danach werden in Becherglas I 1.0 ml Kupfervergleichslösung (5 μg Cu ml^{-1}) gegeben. In Becherglas II wird 1.0 ml Probelösung gegeben. Durch Zugabe von 0.1 *M* Natriumthiosulfat wird die Reaktion in beiden Gefässen gestartet (Startpipette). Das Gesamtvolumen in beiden Ansätzen beträgt 10 ml. Nach kräftigem Rühren werden die Ansätze getrennt in zwei Küvetten (Schichtdicke 10 mm) überführt. 90 Sekunden nach dem Start der katalysierten Reaktion wird die Küvette mit dem Vergleichsansatz in den rechten Strahlengang, die Küvette mit dem Probeansatz in den linken Strahlengang des Kolorimeters gebracht, und die Extinktionsdifferenz unter Verwendung zweier Grünfilter (max. *ca.* 525 nm) sofort abgelesen. Wenn die Kupferkonzentration im Probeansatz ($[Cu]_p$) kleiner als die Kupferkonzentration im Vergleichsansatz ($[Cu]_v$) ist, bleibt der Zeiger des Messinstruments unter null (entsprechend einer "negativen" Extinktionsdifferenz). In diesem Falle werden beide Küvetten gegenseitig ausgetauscht. Die nach etwa zwei bis sieben Minuten auftretende, maximale Extinktionsdifferenz (ΔE_{max}) wird abgelesen. Die Messung wird

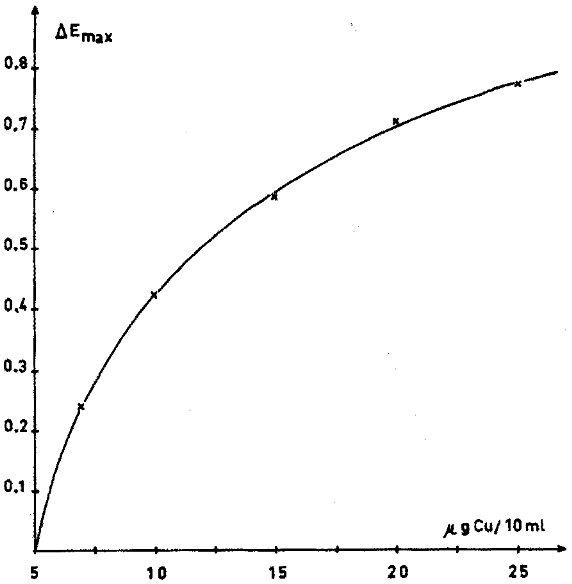

Abb. 1. Eichkurve für den Fall $[Cu]_p > [Cu]_v$. $[Cu]_v = 5$ μg Cu pro 10 ml.

abgebrochen, sobald ΔE_{max} erreicht worden ist. Dadurch wird verhindert, dass die Küvetten durch elementaren Schwefel, der nach vollständigem Ablauf der katalysierten Reaktion abgeschieden wird[8], verunreinigt werden. Die gesuchte Kupferkonzentration $[Cu]_p$ wird unter Verwendung von Eichkurven ermittelt.

Um Störungen zu vermeiden, welche durch am Glas haftende Kupferspuren auftreten können, werden die Reaktionsgefässe nach jeder Bestimmung kurz mit warmem Köningswasser behandelt.

Zur Herstellung der Eichkurve für den Fall $[Cu]_p > [Cu]_v$ werden die ΔE_{max}-Werte für 7, 10, 15, 20 und 25 µg Cu pro 10 ml gemessen (Abb. 1). Hierbei befindet sich der Vergleichsansatz ($[Cu]_v = 5$ µg Cu pro 10 ml) jedesmal im rechten Strahlengang des Kolorimeters. Die Eichkurve für den Fall $[Cu]_p < [Cu]_v$ wird mit den ΔE_{max}-Werten für 1, 2, 3 und 4 µg Cu pro 10 ml erstellt (Abb. 2), wobei der Vergleichsansatz ($[Cu]_v = 5$ µg Cu pro 10 ml) sich jedesmal im linken Strahlengang des Kolorimeters befindet. Die gesuchte Kupferkonzentration wird aus der entsprechenden Eichkurve graphisch extrapoliert.

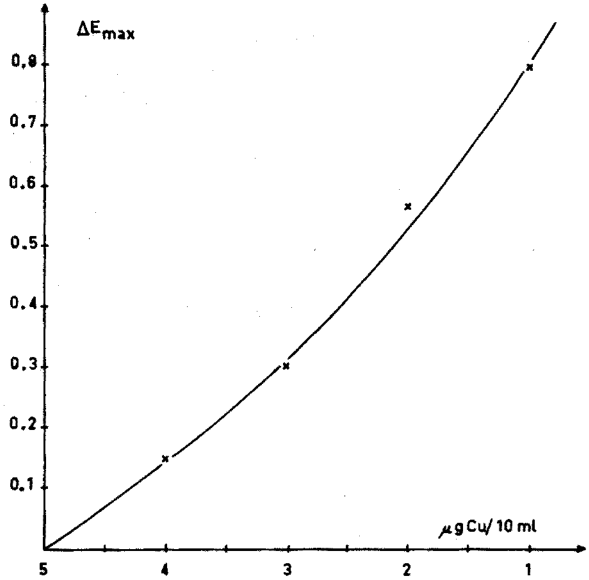

Abb. 2. Eichkurve für den Fall $[Cu]_p < [Cu]_v$. $[Cu]_v = 5$ µg Cu pro 10 ml.

Ergebnisse

In Abbildung 3 ist der typische, gesamte Verlauf einer Kurve dargestellt, welche die Abhängigkeit der Extinktionsdifferenz von der Zeit wiedergibt. Der letzte Teil der Kurve wurde strichliniert gezeichnet, da die Messung der Extinktion zu diesem Zeitpunkt durch Abscheidung von Schwefel gestört wird. Da zur Auswertung der Messung, wie bereits erwähnt, das Maximum der Extinktionsdifferenz verwendet wird, ist es nicht erforderlich, den gesamten Kurvenverlauf aufzunehmen.

Nach dem geschilderten Verfahren wurden zahlreiche Bestimmungen im Bereich von 1–25 µg Cu pro 10 ml durchgeführt. In Tabelle I sind einige Ergebnisse aufgeführt. Die bei dieser Differenzmethode gemessenen ΔE_{max}-Werte lagen zwischen 0 und 0.82 für Kupferkonzentrationen zwischen 1 und 25 µg Cu pro 10 ml. Die Zeit,

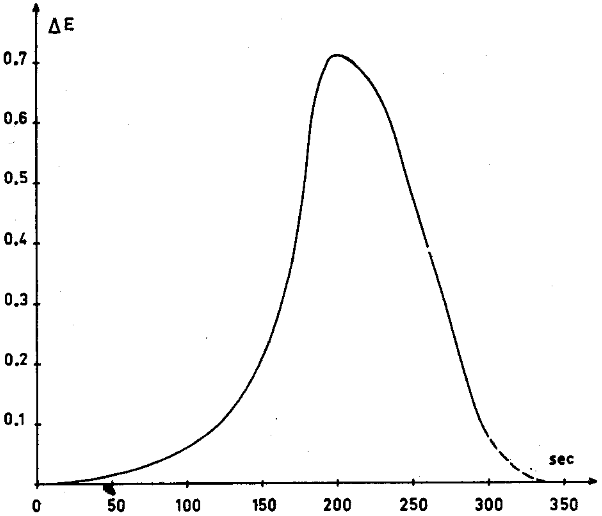

Abb. 3. Abhängigkeit der Extinktionsdifferenz von der Zeit für $[\mathrm{Cu}]_p = 20$ μg Cu pro 10 ml und $[\mathrm{Cu}]_v = 5$ μg Cu pro 10 ml.

TABELLE I

BESTIMMUNG VON KUPFER

μg Cu pro 10 ml		*Relativer Fehler* (%)
Gegeben	*Gefunden*	
0.95	0.88	−7.4
1.53	1.57	+2.6
3.20	3.48	+8.8
4.51	4.62	+2.5
8.00	7.87	−1.6
16.20	17.25	+6.5
21.20	20.00	−5.7
24.30	23.00	−5.4

welche bis zum Auftreten von $\Delta E_{\max}$ verstreicht, ist von den entsprechenden Kupferkonzentrationen und von der herrschenden Versuchstemperatur abhängig. Sie beträgt, wie bereits erwähnt, zwei bis sieben Minuten.

Natürlich kann auch eine andere Kupferkonzentration im Vergleichsansatz als $[\mathrm{Cu}]_v = 5$ μg Cu pro 10 ml verwendet werden. Unter den beschriebenen, experimentellen Bedingungen wurde gefunden, dass das Verhältnis $[\mathrm{Cu}]_p : [\mathrm{Cu}]_v = 5:1$ beziehungsweise $[\mathrm{Cu}]_v : [\mathrm{Cu}]_p = 5:1$ nicht überschritten werden darf; ausserdem soll die Konzentration im Probeansatz im Bereich von 1–25 μg Cu pro 10 ml liegen.

BESTIMMUNG VON L-CYSTIN MIT EINER KINETISCH-POTENTIOMETRISCHEN DIFFERENZMETHODE

Über die katalytische Wirkung von L-Cystin auf die Reaktion von Jod mit Azid

$$J_2 + 2\,N_3^- \rightarrow 2\,J^- + 3\,N_2$$

wurde von Friedmann[14] berichtet. Die Kinetik dieser Reaktion wurde eingehend von Dahl und Pardue[15] untersucht. Unter bestimmten Reaktionsbedingungen ($[N_3^-] \gg [J_2]$) entspricht die Reaktionsgeschwindigkeit der folgenden Gleichung[16]:

$$-d[J_2]/dt = k^* \cdot [J_2] \cdot [Cy] \tag{1}$$

$[J_2]$ = Jodkonzentration, $[Cy]$ = L-Cystinkonzentration, k^* = Geschwindigkeitskonstante.

Die kinetische Differenzbestimmung von L-Cystin unter Verwendung der Reaktion von Jod mit Azid stellt bei potentiometrischer Verfolgung des Reaktionsablaufs eine neue, methodische Variante zu dem bisher geschilderten Verfahren dar.

Läuft die katalysierte Reaktion wiederum in zwei getrennten Ansätzen ab, die sich zu Beginn der Reaktion nur in der L-Cystinkonzentration unterscheiden, so ergibt sich während des Reaktionsablaufs zunächst eine lineare Abhängigkeit des zwischen beiden Halbzellen herrschenden Potentials von der Zeit. Wenn die L-Cystinkonzentration im Vergleichsansatz ($[Cy]_v$) bei jeder Bestimmung denselben Wert hat, so ist die Steigung der Geraden, welche die Abhängigkeit des gemessenen Potentials von der Zeit wiedergibt, ein Mass für die L-Cystinkonzentration im Probeansatz ($[Cy]_p$).

Aus Gleichung (1) ist zu ersehen, dass die durch L-Cystin katalysierte Reaktion von Jod mit Azid erster Ordnung in Bezug auf Jod ist. Die integrierte Form von Gleichung (1) lautet:

$$\ln [J_2] = \ln [J_2]_0 - k^* \cdot [Cy] \cdot t \tag{2}$$

wobei $[J_2]_0$ die Jodkonzentration zur Zeit $t = 0$ ist. Wenn die katalysierte Reaktion gleichzeitig in zwei getrennten Ansätzen abläuft, die sich zu Beginn nur in den L-Cystinkonzentrationen $[Cy]_p$ und $[Cy]_v$ unterscheiden, so gilt für die zur Zeit t herrschende Differenz der Logarithmen der Jodkonzentrationen:

$$\ln [J_2]_v - \ln [J_2]_p = ([Cy]_p - [Cy]_v) \cdot k^* \cdot t \tag{3}$$

Hierin sind $[J_2]_v$ und $[J_2]_p$ die Jodkonzentrationen im Vergleichsansatz bzw. im Probeansatz zur Zeit t. Bei Anwendung der Nernstschen Gleichung ergibt sich durch einfache Rechenoperationen für das zwischen zwei Jod–Jodid-Halbzellen herrschende Potential:

$$e = e_v - e_p = (RT/2F)[\ln (a^2_{J^-})_p/(a^2_{J^-})_v + \ln (f_{J_2})_v/(f_{J_2})_p + \ln [J_2]_v - \ln [J_2]_p] \tag{4}$$

$(a_{J^-})_v$, $(a_{J^-})_p$ = Jodidaktivität im Vergleichsansatz bzw. im Probeansatz.
$(f_{J_2})_v$, $(f_{J_2})_p$ = Aktivitätskoeffizient von Jod für den Vergleichsansatz bzw. für den Probeansatz.

Wenn in beiden Lösungen die Jodidaktivität denselben Wert hat und sich während des Reaktionsablaufs nur in vernachlässigbarem Ausmasse ändert, wird der erste Ausdruck in eckiger Klammer in Gleichung (4) gleich null. Bei einer hohen ionalen Konzentration, die in beiden Lösungen denselben Wert hat und sich während des Reaktionsablaufs nur in vernachlässigbarem Ausmasse ändert, haben die beiden Aktivitätskoeffizienten $(f_{J_2})_v$ und $(f_{J_2})_p$ denselben konstanten Wert. Dadurch wird auch der zweite Ausdruck in eckiger Klammer in Gleichung (4) gleich null und diese vereinfacht sich zu:

$$e = K^*(\ln[\mathrm{J}_2]_v - \ln[\mathrm{J}_2]_p) \qquad (5)$$

wobei $K^* = RT/2F$ ist.

Unter Einführen der neuen Konstante $K = K^* \cdot k^*$ ergibt die Kombination von Gleichung (3) mit Gleichung (5):

$$e = K \cdot t \cdot [\mathrm{Cy}]_p - K \cdot t \cdot [\mathrm{Cy}]_v = K \cdot t \cdot ([\mathrm{Cy}]_p - [\mathrm{Cy}]_v) \qquad (6)$$

Bei unterschiedlichen L-Cystinkonzentrationen in beiden Ansätzen ($[\mathrm{Cy}]_p \neq [\mathrm{Cy}]_v$) besteht nach Gleichung (6) eine lineare Beziehung zwischen dem gemessenen Potential e und der Zeit t. Wenn $[\mathrm{Cy}]_v$ bei jeder Messung denselben Wert hat und wenn die Messzeit (t^*) ebenfalls einen vorgegebenen, konstanten Wert besitzt, besteht nach Gleichung (6) weiterhin eine lineare Beziehung zwischen der Potentialänderung, welche im Zeitintervall t^* auftritt, und der L-Cystinkonzentration im Probeansatz ($[\mathrm{Cy}]_p$). Wenn $[\mathrm{Cy}]_p$ grösser als $[\mathrm{Cy})_v$ ist, nimmt das für das Zeitintervall t^* gemessene Potential einen positiven Wert, im umgekehrten Falle einen negativen Wert an.

Experimentelles

Die bei der potentiometrischen Verfolgung des Reaktionsablaufs verwendete Versuchsanordnung ist in Abb. 4 wiedergegeben. Die Potentialmessung erfolgte mit zwei Platinelektroden (4 mm × 4 mm) und dem Präzisions-pH-Meter "pH 35" der Fa. Knick, Berlin. Die leitende Verbindung zwischen beiden Halbzellen wurde durch eine Elektrolytbrücke (0.6% Agar; 0.2 M KCl) hergestellt. Die Elektroden wurden

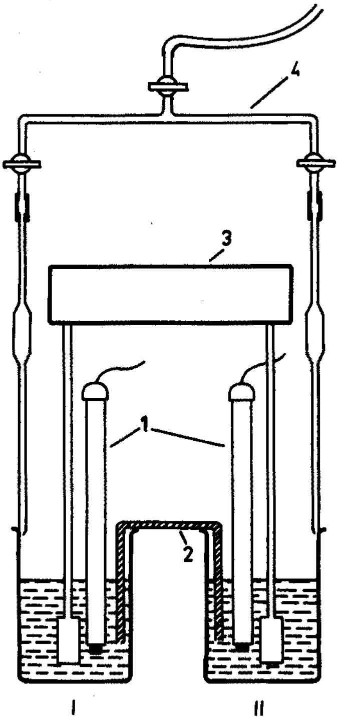

Abb. 4. Versuchsanordnung. (I), (II) Reaktionsgefässe; (1) Elektroden, (2) Elektrolytbrücke, (3) Rührer, (4) Startpipette mit auswechselbaren Vollpipetten.

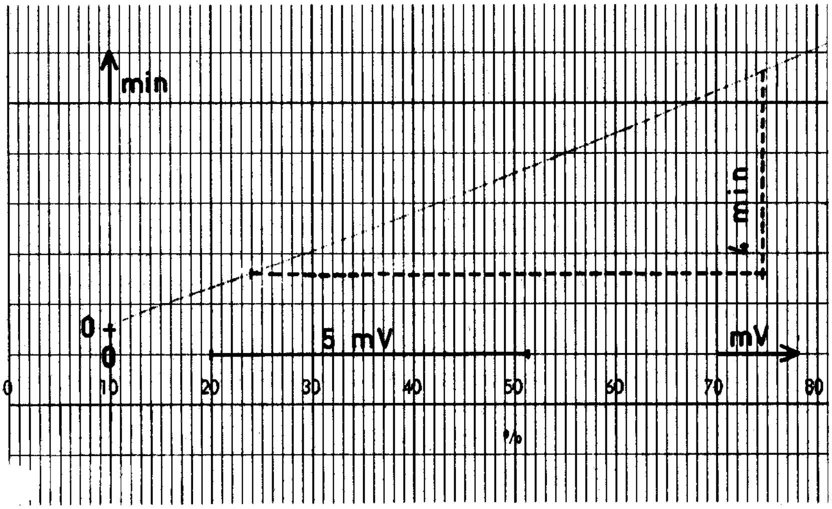

Abb. 5. Registrierung des Reaktionsablaufs durch den Schreiber. $[\mathrm{Cy}]_p = 50$ μg L-Cystin pro 10 ml und $[\mathrm{Cy}]_v = 20$ μg L-Cystin pro 10 ml.

in der Weise an das pH-Meter angeschlossen, dass das gemessene Potential für $[\mathrm{Cy}]_p > [\mathrm{Cy}]_v$ einen positiven Wert und für $[\mathrm{Cy}]_p < [\mathrm{Cy}]_v$ einen negativen Wert hatte. Diese Anordnung gestattet Richtung und Grösse des während des Reaktionsablaufs auftretenden Potentials zwischen dem Vergleichsansatz und dem Probeansatz direkt zu messen. Zur Registrierung diente der Kompensations-Linienschreiber "Servogor" der Fa. Metrawatt, Nürnberg. Die beiden Lösungen wurden von zwei Rührern durchmischt, welche von einem Motor über eine Transmission (1 : 1) angetrieben wurden.

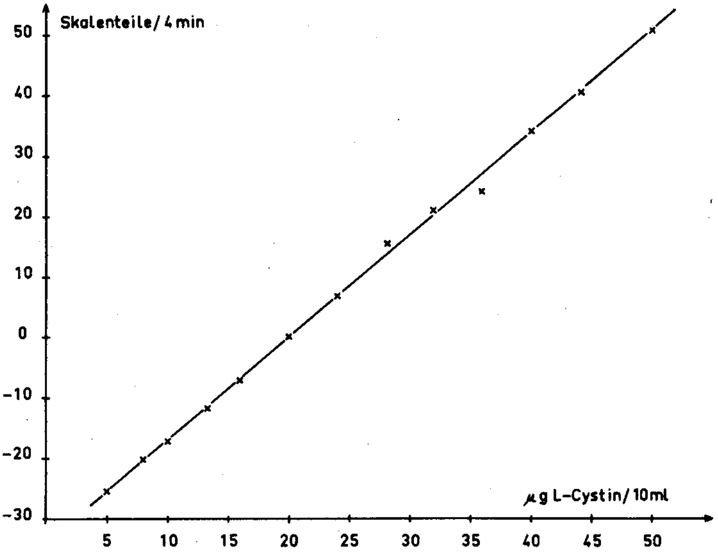

Abb. 6. Abhängigkeit der gemessenen $e_{4\,\mathrm{min}}$-Werte (ausgedrückt in Skalenteilen pro 4 min) von der L-Cystinkonzentration. $[\mathrm{Cy}]_v = 20$ μg L-Cystin pro 10 ml.

Lösungen. Jod/Jodidlösung. $2.5 \cdot 10^{-3}$ *M* J_2/$2.5 \cdot 10^{-2}$ *M* KJ.

L-Cystin-Stammlösung. 50 μg L-Cystin ml^{-1}.

L-Cystin-Standardlösungen. 5, 20 und 50 μg L-Cystin ml^{-1}.

Durchführung. An den Verteiler der Startpipette werden zwei Vollpipetten (1 ml) angesetzt. Die linke Pipette wird mit der L-Cystin-Vergleichslösung (20 μg L-Cystin ml^{-1}) und die rechte Pipette mit der Probelösung gefüllt. Anschliessend werden in zwei Bechergläser (25 ml) jeweils 2.0 ml 4.6 *M* Natriumazidlösung, 5.0 ml Chlorwasserstoffsäure 0.09 *M* und 2.0 ml Jod/Jodidlösung einpipettiert. Dabei wird die Lösung kräftig gerührt. Danach werden die beiden Platinelektroden und die Elektrolytbrücke eingeführt. Eine Minute nach Beginn der Potentialmessung wird die katalysierte Reaktion durch Zugabe der L-Cystinlösungen gestartet (Start der Reaktion: $t=0$). Richtung und Grösse der zeitlichen Potentialänderung können der vom Schreiber registrierten Kurve entnommen werden.

Zwischen den Messungen werden die Platinelektroden in Jod/Jodidlösung und die Elektrolytbrücke in einer 0.2 *M* Kaliumchloridlösung aufbewahrt.

Auswertung und Ergebnisse

Zur Auswertung werden Vorzeichen und Grösse der Potentialänderung, welche im Verlauf der Reaktion innerhalb von 4 Minuten auftritt ($e_{4\text{min}}$), aus der vom Schreiber registrierten Kurve ermittelt. Hierzu wird die Potentialänderung für die Zeit von $t=1$ min bis $t=5$ min aus der vom Schreiber registrierten Kurve graphisch extrapoliert (Abb. 5). Die gesuchte L-Cystinkonzentration erhält man unter Verwendung einer Eichkurve, welche mit den $e_{4\text{min}}$-Werten für $[\text{Cy}]_p=5$ μg L-Cystin pro 10 ml und $[\text{Cy}]_p=50$ μg L-Cystin pro 10 ml bei einer L-Cystinkonzentration im Vergleichsansatz von $[\text{Cy}]_v=20$ μg L-Cystin pro 10 ml aufgenommen wird. Der $e_{4\text{min}}$-Wert für $[\text{Cy}]_p=20$ μg L-Cystin pro 10 ml ist natürlich vorgegeben ($e_{4\text{min}}=0$). In Abb. 6 wird die Abhängigkeit der gemessenen $e_{4\text{min}}$-Werte (ausgedrückt in Skalenteilen pro 4 min) von der L-Cystinkonzentration wiedergegeben.

Nach dem geschilderten Verfahren wurden zahlreiche Bestimmungen durchgeführt. Tabelle II gibt einige Ergebnisse wieder. Der relative Fehler einer Einzelbestimmung ist kleiner als ±5%.

Es wurde untersucht, ob bei der kinetischen Differenzbestimmung auch ein auftretendes Potentialmaximum zur Auswertung herangezogen werden kann. Dies

TABELLE II

BESTIMMUNG VON L-CYSTIN

μg L-Cystin pro 10 ml		*Relativer Fehler* (%)
Gegeben	*Gefunden*	
5.00	5.00	±0
6.67	6.40	−4.0
9.18	9.00	−2.0
12.75	12.75	±0
24.00	23.75	−1.0
28.00	29.10	+4.0
36.70	36.25	−1.2
50.00	50.40	+0.8

ist im vorliegenden Fall weniger vorteilhaft, da unter den gegebenen experimentellen Bedingungen die Zeit, welche bis zum Auftreten des Potentialmaximums verstreicht, für den untersuchten Konzentrationsbereich ($[Cy]_p < 50$ μg L-Cystin pro 10 ml, $[Cy]_v = 20$ μg L-Cystin pro 10 ml) mindestens 45 Minuten betrug. Erst hohe L-Cystinkonzentrationen im Probeansatz und im Vergleichsansatz ergeben kürzere, für quantitative Bestimmungen vertretbare Messzeiten.

Selbstverständlich können bei der L-Cystinbestimmung auch andere L-Cystinkonzentrationen im Vergleichsansatz als 20 μg L-Cystin pro 10 ml verwendet werden. In diesen Fällen müssen natürlich die entsprechenden Eichkurven hergestellt werden.

ZUSAMMENFASSUNG

Es wird eine kinetische Differenzmethode beschrieben. Das Prinzip besteht darin, dass eine katalysierte Reaktion in zwei Ansätzen gleichzeitig abläuft. Unter sonst identischen Bedingungen enthält ein Ansatz eine bekannte, jeweils gleiche Katalysatormenge und der andere eine unbekannte Katalysatormenge. Die unbekannte Katalysatormenge wird aus der während des simultanen Reaktionsablaufs auftretenden Differenz der einzelnen Messgrössen ermittelt. Kupfer wurde aufgrund seiner beschleunigenden Wirkung auf die Reaktion von Eisen(III) mit Thiosulfat im Bereich von 1–25 μg pro 10 ml bestimmt, wobei der Reaktionsablauf photometrisch verfolgt wurde. Die durch L-Cystin katalysierte Reaktion von Jod mit Azid wurde potentiometrisch verfolgt. Es wurden L-Cystinkonzentrationen im Konzentrationsbereich von 5–50 μg pro 10 ml bestimmt.

SUMMARY

A kinetic difference method is described. The method is based on a catalytic reaction proceeding simultaneously in two mixtures, one of which contains a known constant amount of the catalyst and the other the unknown amount. The unknown concentration can be established from the difference of separate measurements during the simultaneous reaction processes. Copper can be determined spectrophotometrically in the range 1–25 μg per 10 ml by means of its accelerating action on the reaction of iron(III) with thiosulphate. L-Cystine can be determined potentiometrically in the range 5–50 μg per 10 ml, based on its catalytic action on the iodine–azide reaction.

RÉSUMÉ

On décrit une méthode cinétique par différence, basée sur une réaction catalytique se produisant simultanément dans deux mélanges, l'un contenant une quantité constante connue du catalyseur, l'autre la quantité inconnue. Le cuivre peut être dosé (1 à 25 μg/10 ml) spectrophotométriquement, grâce à son action catalytique sur la réaction fer(III)–thiosulfate; on peut également doser la L-cystine, par potentiométrie (5 à 50 μg/10 ml), en se basant sur son action catalytique dans la réaction iode-azoture.

LITERATUR

1 K. B. Yatsimirskii, *Kinetic Methods of Analysis*, Pergamon Press, Oxford, 1966.
2 H. B. Mark und G. A. Rechnitz, *Kinetics in Analytical Chemistry*, Interscience, New York, 1968.

3 H. U. Bergmeyer, *Methoden der enzymatischen Analyse*, Verlag Chemie, Weinheim, 1970.
4 J. Bognar, *Mikrochim. Acta*, (1963) 397.
5 K. B. Yatsimirskii, *Kinetic Methods of Analysis*, Pergamon Press, Oxford, 1966, S. 41.
6 A. C. Oudemans, *Z. Anal. Chem.*, 6 (1867) 129.
7 F. L. Hahn und G. Leimbach, *Ber.*, 55 (1922) 3070.
8 J. Bognar und O. Jellinek, *Anal. Chim. Acta*, 29 (1963) 395.
9 H. Hesselbarth, *Z. Anal. Chem.*, 248 (1969) 163.
10 K. Khalifa, H. Doss und R. Awadallah, *Analyst*, 95 (1970) 207.
11 K. B. Yatsimirskii, *Kinetic Methods of Analysis*, Pergamon Press, Oxford, 1966, S. 120.
12 K. Czarnecki, *Chem. Anal. (Warsaw)*, 5 (1960) 377; vgl. *Z. Anal. Chem.*, 182 (1961) 113.
13 J. Holluta und A. Martini, *Z. Anorg. Chem.*, 140 (1924) 206; 141 (1924) 23; 144 (1925) 321.
14 E. Friedmann, *J. Prakt. Chem.*, 146 (1936) 179.
15 W. E. Dahl und H. L. Pardue, *Anal. Chem.*, 37 (1965) 1382.
16 H. L. Pardue und S. Shepherd, *Anal. Chem.*, 35 (1963) 21.

Analytica Chimica Acta
Elsevier Publishing Company, Amsterdam
Printed in The Netherlands

STERIC HINDRANCE TO THE FORMATION OF METAL COMPLEXES OF 2-CHLORO-1,10-PHENANTHROLINE*

H. M. N. H. IRVING AND P. J. GEE

Department of Inorganic and Structural Chemistry, The University of Leeds, and the Inorganic Chemistry Laboratory, South Parks Road, Oxford (England)

(Received 18th March 1971)

The steric effect of substituents *ortho* to a donor nitrogen atom upon the stability of metal complexes has been studied quantitatively for pyridine and its derivatives[1], for 8-hydroxyquinoline and sundry aza-derivatives[2] and for 1,10-phenanthroline[3,4] and various derivatives of cinnoline[5]. The present paper reports a comparison between the behaviour of 2-methyl-1,10-phenanthroline and 2-chloro-1,10-phenanthroline where the group expected to cause steric hindrance to coordination to a metal atom has an "interference volume" not much smaller than that of a methyl group.

The absorption spectrum of 2-chlorophenanthroline (L) in aqueous buffers of pH 6.6 and upwards is identical with that in 0.01 *M* sodium hydroxide and the neutral species, L, has maxima at 227.3 nm (ε_{max} 45,500) and 270.3 nm (ε_{max} 30,900) with a shoulder at 290 nm. In organic solvents the spectra are comparatively simple. For chloroform $\lambda_{max} = 270$ nm ($\varepsilon_{max} = 31{,}860$) and the corresponding results for carbon tetrachloride 269 (31,030) and *n*-hexane 231 (54,130) and 267 (30,720) are very similar. Beer's law was shown to hold in each solvent up to at least $4 \cdot 10^{-4}$ *M*.

In aqueous acid (pH 1) there is a bathochromic shift at the longer wavelength to 280.9 nm ($\varepsilon_{max} = 34{,}880$) with a shoulder at 303.0 nm (ε_{max} 7,690), whereas the peak at the shortest wavelength is displaced hypsochromically to 222.2 nm (41,380).

The absorbances of a series of solutions containing the same concentration of 2-chlorophenanthroline in buffers of pH 1–9 and constant ionic strength 0.1 *M* (KCl) were measured at a series of wavelengths (Fig. 1). Although constant absorbance, due to the neutral ligand, L, is achieved above pH 7 in every case, the curves never become horizontal in the more acidic media corresponding to complete protonation to HL^+ and the general indication is that while an approximate value $\log (K_1^H = [H^+][L]/[HL^+]) = -4.2^5 \pm 0.1$ can be estimated, there is evidence of the addition of a second proton to give the species H_2L^{2+} for which $K_2^H = [H^+][HL^+]/[H_2L^{2+}]$.

If *A* is the measured absorbance (calculated for a 1-cm path length) of a solution containing a total concentration, L_T, of ligand we have

$$A = L_T \frac{\{\varepsilon_L + (\varepsilon_{HL}[H^+]/K_1^H) + (\varepsilon_{H_2L}[H^+]^2/K_1^H K_2^H)\}}{\{1 + ([H^+]/K_1^H) + ([H^+]^2/K_1^H K_2^H)\}} \tag{1}$$

---

* This paper, regarded as Part VIII of the series "Steric Hindrance in Analytical Chemistry", is immediately preceded by *Analytical Chemistry 1962* (*Proc. Feigl Symp.*), Elsevier, Amsterdam, 1962, p. 122.

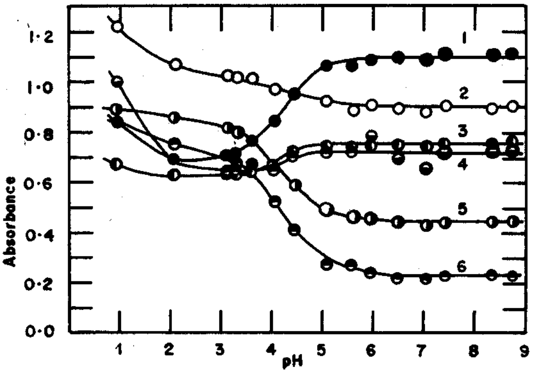

Fig. 1. The absorbance of a 2.4494 · 10^{-5} M solution of 2-chloro-1,10-phenanthroline in buffers of various pH and ionic strength $I = 0.1$ M (KCl). (1, 2, 3 and 5) Measurements at 227.3, 222.2, 270.3 and 280.9 nm (1-cm cell); (4 and 6) measurements at 243.9 and 303.0 nm (4-cm cell).

which on rearrangement gives

$$\frac{\{(A/L_T)-\varepsilon_{HL}\}}{\{\varepsilon_L-(A/L_T)\}} = \frac{K_1^H}{[H^+]} + \frac{\{\varepsilon_{H_2L}+(A/L_T)\}}{\{\varepsilon_L-(A/L_T)\}}\cdot\frac{[H^+]}{K_2^H} \qquad (2)$$

where ε_L, ε_{HL} and ε_{H_2L} are the molar absorptivities for the species L, HL^+ and H_2L^{2+} respectively. On taking decadic logarithms

$$\begin{aligned} pH &= pK_1 + \log[\{(A/L_T)-\varepsilon_{HL}\} - \{\varepsilon_{H_2L}+(A/L_T)\}[H^+]/K_2^H]/\{\varepsilon_L-(A/L_T)\} \\ &= pK_1 + \log(B-C) \qquad (3) \end{aligned}$$

where the values of B and C can be calculated from experimental data for pH, A and L_T, provided that values of ε_L, ε_{HL} and ε_{H_2L} are available. That of ε_L is provided from experiments at pH 7. By assuming that $\varepsilon_{H_2L} \cong \varepsilon_{HL}$ and adopting the value $\log K_2^H = 0.22$ derived from partition measurements (q.v.), values of B and C were calculated and pK_1 was obtained as the intercept of the best straight line obtained by plotting pH against $\log(B-C)$. Values of C were always found to be less than 5% of those of B for $pH > 3$. Values of ε_{HL} were sought to give values of pK_1^H for each wavelength that had the lowest standard deviation. Final estimates were

nm	ε_{HL}	pK_1^H	
227.3	27,500	4.19	
280.9	34,875	4.16	Average $4.16^5 \pm 0.02$
303.0	7,690	4.15	

Since the contribution of the species H_2L^{2+} is less than 1% of L_T at $pH > 3$, eqn. (1) reduces to

$$A = L_T\{\varepsilon_L + \varepsilon_{HL}([H^+]/K_1^H)\}/\{1+([H^+]/K_1^H)\} \qquad (4)$$

whence on differentiation

$$A' = dA/dpH = 2.303\ K_1^H L_T(\varepsilon_L-\varepsilon_{HL})/[H^+]\{1+(K_1^H/[H^+])\}^2 \qquad (5)$$

By eliminating K_1^H from eqns. (4) and (5) we arrive at $\varepsilon_L A' L_T + 2.303A(A-\varepsilon_L L_T) =$

$\varepsilon_{HL}\{A'L_T+2.303L_T(A-\varepsilon_L L_T)\}$ which is of the form

$$Y=\varepsilon_{HL}\cdot X \tag{6}$$

Values of A' were obtained from the experimental data (A, pH) and A, ε_L and L_T are known. Plots of calculated values of X against Y gave excellent straight lines (not reproduced) of slope ε_{HL}. Least squares treatment gave the following results:

nm	ε_{HL}	pK_1^H	
227.3	27,710	4.21	
280.9	34,850	4.15	Average 4.17±0.03
303.0	7,670	4.15	

If $p=[L]_{org}/[L]$ is the stoicheiometric partition coefficient and q the measured distribution for 2-chloro-1,10-phenanthroline between organic solvent and an aqueous buffer, then

$$p=q\{1+([H^+]/K_1^H)+([H^+]^2/K_1^H K_2^H)\} \tag{7}$$

Measurements were carried out at 25° as previously described[3,4,6] and led to $p=0.679\pm0.003$ for n-hexane, 12.30 ± 0.01 for carbon tetrachloride and $4{,}024\pm49$ for chloroform.

Similar measurements were carried out in which the aqueous phase contained different total concentrations of ligand, C_L, and metal cation, C_M, in aqueous buffers of constant ionic strength 0.1 M (KCl).

Values of the formation constant, $\bar{n}$, and the free ligand concentration in the aqueous phase, [L], were calculated from the equations

$$\bar{n}=(C_L-\{1+([H^+]/K_1^H)+([H^+]^2/K_1^H K_2^H)+p\}[L]_{org}/p)/C_M \tag{8}$$

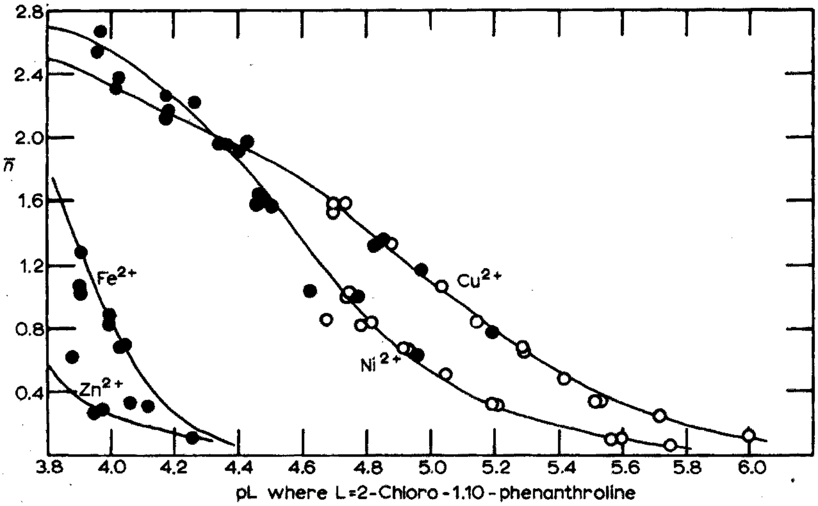

Fig. 2. Formation curves of complexes of divalent copper, nickel, iron and zinc with 2-chloro-1,10-phenanthroline calculated from the stability constants given in Table II. The organic solvents used in the partition measurements were carbon tetrachloride (○) or n-hexane (●).

TABLE I

EXPERIMENTAL AND CALCULATED VALUES OF FORMATION CONSTANTS ($\bar{n}$) OF DIFFERENT COMPLEXES

$10^4 C_L$	$10^4 C_M$	*pH*	*pL*	$\bar{n}$ *found*	$\bar{n}$ *calc.*
(*i*) *Nickel(II) and 2-chlorophenanthroline. With carbon tetrachloride as organic solvent*					
4.0545	54.392	3.77	5.744	0.070	0.075
4.0545	54.392	3.765	5.759	0.070	0.072
6.7575	54.392	3.755	5.568	0.117	0.118
6.7575	54.392	3.755	5.562	0.117	0.120
2.7030	5.3888	3.765	5.193	0.334	0.300
2.7030	5.3888	3.77	5.182	0.300	0.308
4.0545	5.3888	3.76	5.056	0.510	0.422
4.0545	5.3888	3.755	5.052	0.507	0.424
5.4060	5.3888	3.76	4.925	0.675	0.574
5.4060	5.3888	3.755	4.931	0.670	0.569
6.7575	5.3888	3.78	4.820	0.840	0.856
6.7575	5.3888	3.78	4.792	0.812	0.960
5.4060	2.6944	3.77	4.746	1.02	1.02
5.4060	2.6944	3.755	4.750	1.02	1.02
5.4060	2.6944	3.76	4.743	1.01	1.03
With n-*hexane as organic solvent*					
2.2584	2.6944	3.79	4.959	0.672	0.601
2.2584	2.6944	3.79	4.956	0.671	0.606
3.3876	2.6944	3.79	4.780	1.00	0.942
3.3876	2.6944	3.79	4.776	1.00	0.950
4.5168	2.6944	3.795	4.628	1.32	1.31
4.5168	2.6944	3.795	4.617	1.31	1.33
3.3876	1.3472	3.78	4.507	1.56	1.61
3.3876	1.3472	3.78	4.506	1.56	1.62
2.2584	0.5389	3.79	4.463	1.59	1.72
2.2584	0.5389	3.79	4.471	1.63	1.70
5.6460	2.6944	3.795	4.496	1.62	1.59
5.6460	2.6944	3.795	4.486	1.60	1.67
4.5168	1.3472	3.795	4.339	1.98	1.93
4.5168	1.3472	3.795	4.336	1.97	1.93
3.3876	0.5389	3.795	4.267	2.22	2.15
3.3876	0.5389	3.795	4.267	2.22	2.15
5.6460	1.3472	3.81	4.174	2.22	2.31
5.6460	1.3472	3.81	4.181	2.25	2.32
5.6460	0.5389	3.815	3.964	2.53	2.58
5.6460	0.5389	3.815	3.972	2.68	2.57
(*ii*) *Copper(II) and 2-chlorophenanthroline. With carbon tetrachloride as organic solvent*					
2.7030	10.049	3.64	5.717	0.239	0.258
2.7030	10.049	3.65	5.718	0.239	0.258
4.0545	10.049	3.645	5.556	0.360	0.363
4.0545	10.049	3.635	5.540	0.358	0.375
5.4060	10.049	3.735	5.420	0.481	0.494
5.4060	10.049	3.735	5.418	0.481	0.494
4.0540	5.0246	3.70	5.310	0.658	0.626
4.0540	5.0246	3.70	5.341	0.659	0.664
5.4060	5.0246	3.715	5.128	0.851	0.891
5.4060	5.0246	3.715	5.135	0.855	0.881

TABLE I (*continued*)

EXPERIMENTAL AND CALCULATED VALUES OF FORMATION CONSTANTS ($\bar{n}$) OF DIFFERENT COMPLEXES

$10^4 C_L$	$10^4 C_M$	pH	pL	$\bar{n}$ found	$\bar{n}$ calc.
6.7575	5.0246	3.72	5.043	1.07	1.03
6.7575	5.0246	3.71	5.039	1.07	1.00
5.4060	2.5123	3.705	4.877	1.35	1.30
5.4060	2.5123	3.70	4.875	1.34	1.31
6.7575	2.5123	3.71	4.713	1.52	1.56
6.7575	2.5123	3.71	4.737	1.58	1.52
With n-*hexane as organic solvent*					
2.2584	2.5123	3.70	5.192	0.781	0.793
2.2584	2.5123	3.695	5.178	0.776	0.814
3.3876	2.5123	3.71	4.985	1.16	1.13
3.3876	2.5123	3.695	4.983	1.16	1.13
4.0545	2.5123	3.72	4.840	1.36	1.36
4.0545	2.5123	3.71	4.826	1.34	1.39
4.0545	2.5123	3.715	4.861	1.37	1.33
4.0545	2.5123	3.71	4.848	1.36	1.35
5.4060	2.5123	3.72	4.592	1.69	1.73
5.4060	2.5123	3.76	4.586	1.69	1.73
5.4060	2.5123	3.74	4.597	1.71	1.72
5.4060	2.5123	3.725	4.599	1.70	1.72
4.0545	1.2561	3.765	4.427	1.97	1.93
4.0545	1.2561	3.765	4.414	1.92	1.93
6.7575	2.5123	3.735	4.373	1.95	1.98
6.7575	2.5123	3.735	4.378	1.96	1.98
5.4060	1.2561	3.775	4.182	2.12	2.17
5.4060	1.2561	3.78	4.193	2.19	2.16
6.7575	1.2561	3.795	4.030	2.31	2.31
6.7575	1.2561	3.79	4.025	2.31	2.31
(*iii*) *Zinc*(*II*) *and 2-chlorophenanthroline. With* n-*hexane as organic solvent*					
3.3876	10.863	3.805	4.262	0.111	0.119
3.3876	10.863	3.805	4.252	0.106	0.121
5.6460	5.4315	3.82	3.978	0.282	0.238
5.6460	5.4315	3.84	3.950	0.258	0.252
5.6460	1.0863	3.845	3.881	0.602	0.302
(*iv*) *Iron*(*II*) *and 2-chlorophenanthroline*					
8.4690	0.8772	3.555	3.907	1.53	1.29
8.4690	0.8772	3.56	3.909	1.50	1.28
8.0674	1.2927	3.565	3.949	1.28	1.08
8.0674	1.2927	3.55	3.954	1.14	1.06
7.6704	1.7082	3.515	4.003	0.885	0.842
7.6616	1.7082	3.52	3.993	0.827	0.884
7.2588	2.1237	3.49	4.047	0.688	0.670
7.2514	2.1237	3.515	4.028	0.676	0.741
6.8050	2.5392	3.425	4.083	0.325	0.550
6.3514	2.9547	3.425	4.122	0.298	0.439

$$\text{pL} = \log p - \log [\text{L}]_{\text{org}} \tag{9}$$

and

$$[\text{L}]_{\text{org}} = A/\varepsilon_{\text{L}} \tag{10}$$

where ε_L is the molar absorptivity of the base in the organic solvent used. Each measurement was carried out at least in duplicate and conditions were chosen such that the numerator of eqn. (8) was always less than 30% of C_L since otherwise small errors in A (and thus in $[L]_{org}$) produce disproportionately large errors in pL. Typical results are shown in Fig. 2 where the solid lines are formation curves calculated from the experimental data using a computer programme written by Dr. M. H. Stacey.

Difficulties were experienced with iron(II) where, because of the low stability of the complexes, it was necessary to use values of pL < 4 despite the limited solubility of 2-chlorophenanthroline. Attempts were made to overcome this by starting with a very concentrated aqueous solution of the ligand already containing some metal salt (*ca.* 10^{-4} *M*). This gave a solution of high $\bar{n}$ and after equilibration with an equal volume of *n*-hexane aliquot portions of each phase were removed for the determination of the ligand content.

EXPERIMENTAL

2-Chloro-1,10-phenanthroline was prepared from the methiodide of 1,10-phenanthroline by oxidation with alkaline hexacyanoferrate(III) to the corresponding phenanthroline and treatment of this with phosphorus pentachloride under reflux. Recrystallization from aqueous ethanol (1:1, v/v) in the presence of active charcoal that had been freed from traces of iron by prior digestion with hydrofluoric acid, gave pure white needles m.p. 128–9° (lit.[9] 129°). (Found: C, 67.2; H, 3.35; N, 12.85. Calc. for $C_{12}H_7N_2Cl$: C, 67.1; H, 3.3; N, 13.05, and for $C_{12}H_7N_2Cl \cdot \frac{1}{2}H_2O$: C, 64.4; H, 3.6; N, 12.5%.) Clearly, unlike 1,10-phenanthroline itself, the compound is anhydrous when dried *in vacuo*.

Measurements of absorption spectra were made on a Unicam SP500 spectrophotometer with matched silica cells. Distribution coefficients in the presence and absence of AnalaR samples of transition metal nitrates were carried out as previously described[4,6]. Potassium chloride was present in all buffers (prepared from sodium formate–hydrochloric acid, sodium acetate–hydrochloric acid, phosphoric and boric acids with alkali) to maintain a constant ionic strength $I = 0.1$ *M*.

The experimental results (Table I) were obtained in measurements with total concentrations C_M and C_L of metal ion and ligand respectively. Calculated values of the formation constant, $\bar{n}$, were obtained from the experimental values of pL in conjunction with the stability constants listed in Table II.

DISCUSSION

A comparison of the values of pK_1 for phenanthroline (4.95) and 2-chloro-1,10-phenanthroline (4.17) with that of pyridine (5.2) and 2-chloropyridine (0.7) suggests that the first proton becomes attached to the nitrogen of 2-chloro-1,10-phenanthroline in the 10-position, *i.e.* the nitrogen furthest from the chlorine atom.

TABLE II

STABILITY CONSTANTS VALID FOR 25° AND $I=0.1$ *M* (KCl)

Ligand	*pK_1^H*		*log K_1*	*log K_2*	*log K_3*	*log β_3*
1,10-Phenanthroline[a]	4.95	Fe	5.85	5.25	10.0	21.2
		Ni	8.6	8.15	7.6	24.3
		Cu	9.05	6.7	5.0	20.8
		Zn	6.45	5.65	5.0	17.1
2-Methyl-1,10-phenanthroline[b]	5.42	Fe	4.2	3.6	3.0	10.8
		Ni	5.95	5.85	4.9	16.7
		Cu	7.40	6.45	—	—
		Zn	4.96	4.40	3.35	12.7
2-Chloro-1,10-phenanthroline[c]	4.17	Fe	—	—	—	11.6
		Ni	4.58	4.68	4.34	13.60
		Cu	5.07	5.00	3.86	13.93
		Zn	3.3	3.3	—	—
5-Chloro-1,10-phenanthroline[d]	4.18	Fe	—	—	—	19.7
		Zn	5.85	—	—	—

[a] Values from Ref. 3.
[b] Values from Ref. 4.
[c] Present work.
[d] Values from Ref. 7.

pK_2 thus refers to protonation of the weakly basic 1-nitrogen atom.

Stability constants for the various metal complexes are given in Table II, together with values for the isomeric 5-chloro-1,10-phenanthroline[7] and those reported for 1,10-phenanthroline itself[3] and its 2-methyl homologue[4].

Calculation of values of K_1, K_2 and K_3 for the copper and nickel complexes presented no difficulty and the agreement between the calculated and experimental formation curves (Fig. 2) is good. The close similarity in the magnitude of the successive stepwise stability constants is noteworthy. For K_1 and K_2 the copper complex is the more stable but the reluctance of copper to assume 6-fold coordination is reflected in the lower value of K_3 relative to that of the nickel complex.

Few data were obtained for the zinc system owing to its weakness and the experimental impossibility of obtaining a sufficiently high concentration of free ligand. The results could best be interpreted with two formation constants of equal value $K_1 = K_2 = 3.3$ but the fit remains poor and the occurrence of hydroxylated or polymerised species may be the reason. The situation with the iron system proved difficult to handle, for the formation curve was exceptionally steep and it was immediately obvious that values of K_1 and K_2 were small compared to that of K_3 and changes in their magnitude had little effect on calculated values of $\bar{n}$.

It has been pointed out[10] that a graph of $\bar{n}/[L]$ against $[L]$ will normally decrease monotonically from the limiting value of β_1 when $[L] \rightarrow 0$. In the present case (as with the system iron(II)–1,10-phenanthroline), $\bar{n}/[L]$ *increases* with $[L]$, from which it must be concluded that $2K_2 > K_1$ or that $K_3 > K_1$ or K_2. An estimate, $\beta_3 = 10^{11.6}$, results if β_1 and β_2 are neglected in comparison. The paucity and probably low precision of the results does not justify a closer analysis but the fact that this value suggests a slightly greater stability than that of the complex with 2-methylphenanthroline is interesting.

The effect of substitution in 1,10-phenanthroline will be twofold. There will be a change in the basicity of the donor nitrogen atoms and a concomitant change in the strength of a metal–ligand bond. There will also be steric effects if the substituent is in the 2- or/and 9-position[4] and these may dominate the situation. Since both 2- and 5-chloro-1,10-phenanthroline are less basic than the parent phenanthroline it is natural that there should be a decrease in the corresponding values of $K_1 = [ML]/[M][L]$ for all the metals studied. Indeed, a decrease of 4.95—4.17 = 0.8 log units would be predicted in each case, for it has been shown that the relationship

$$\log K_{MP} = \log K_{MQ} + (pK_{HP} - pK_{HQ}) \tag{11}$$

predicted on thermodynamic grounds for two very similar ligands P and Q holds very well provided that there are no conflicting steric factors and the type of bonding remains the same for different metals[8]. For example, there is an excellent straight-line relationship for P = phenanthroline and Q = 5-methylphenanthroline[6]. Effects of steric hindrance can be demonstrated by plotting a line of the theoretical unit slope through the points for $\log K_{HP}$ ($= pK_{HP^+}$) and $\log K_{HQ}$ ($= pK_{HQ^+}$) and noting to what extent the experimental results fall below those predicted. Thus in Fig. 3 the solid line is that predicted for phenanthroline ($\log K_{HP} = 4.95$) and 5-chlorophenanthroline ($\log K_{HQ} = 4.18$) and the only available result (that for the zinc complex) almost lies on it. The same line applies to 2-chlorophenanthroline since $\log K_{HQ} = 4.17$, but now the points for the metal complexes (open circles) all lie below the line indicating destabilisation to the extent of 3.25, 3.21 and 2.38 log units for Ni, Cu and Zn respectively (1 log unit is equivalent to 5.703 kJ). The broken straight line and blackened circles show similar data for 1,10-phenanthroline and its 2-methyl homologue and the extent of the steric hindrance to coordination now amounts to 2.12, 3.12, 2.12 and 1.96 log units. If the assumptions made in deducing and applying eqn. (11) are accepted, it follows that steric hindrance is greater for a 2-chloro than a 2-methyl substituent.

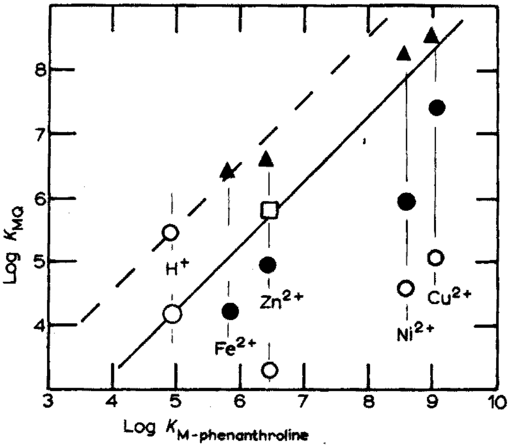

Fig. 3. Comparisons of experimental and predicted stability constants. The continuous line applies to 1,10-phenanthroline and 5-chloro- (or 2-chloro-) phenanthroline. (○) Values of $\log \beta_1$ for metal complexes; (- - -) 1,10-phenanthroline and 2-methylphenanthroline where stability constants for metal complexes appear as blackened circles; (▲) values of $\log \beta_1$ for 5-methylphenanthroline.

SUMMARY

2-Chloro-1,10-phenanthroline (L) readily accepts one proton on the 10-nitrogen atom and in strongly acidic media a second proton on the 1-nitrogen atom. Stoicheiometric acid dissociation constants $pK_1^H = 4.17$ and $pK_2^H = 0.22$ for the species HL^+ and H_2L^{2+} were obtained from spectrophotometric measurements in aqueous buffers at 25° and $I = 0.1$ M(KCl). Partition coefficients were determined for the uncharged base between water and *n*-hexane, carbon tetrachloride, and chloroform, and the stepwise formation constants of metal complexes were obtained from similar measurements with salt solutions. Stabilities increased in the order $Fe < Co < Cu > Zn$ and, when due account is given to differences in ligand basicities, steric hindrance to complex-formation is about the same as that due to a 2-methyl substituent. In the iron(II) complex, $K_3 > K_1$, K_2, an anomaly previously found only with 2,2′-bipyridine and 1,10-phenanthroline.

RÉSUMÉ

La 2-chloro-1,10-phénanthroline accepte facilement un proton sur l'atome d'azote-10 et un second proton sur l'azote-1 en milieu fortement acide. Les constantes de dissociation acide sont, respectivement pour HL^+ et H_2L^{2+}, $pK_1^H = 4.17$ et $pK_2^H = 0.22$; elles ont été déterminées par mesures spectrophotométriques en milieu tampon aqueux à 25° et $I = 0.1$ M (KCl). Les coefficients de partage sont calculés pour la base non chargée entre eau et *n*-hexane, tétrachlorure de carbone et chloroforme. Les constantes de formation des complexes métalliques sont obtenues de la même façon avec des solutions de sel. Les stabilités augmentent dans l'ordre: $Fe < Co < Cu > Zn$. Dans le cas du complexe fer(II), nous avons $K_3 > K_1$, K_2, une anomalie déjà observée avec la 2,2′-bipyridine et la 1,10-phénanthroline.

ZUSAMMENFASSUNG

2-Chlor-1,10-phenanthrolin (L) nimmt leicht ein Proton am 10-ständigen Stickstoffatom auf und in stark sauren Medien ein zweites Proton am 1-ständigen Stickstoffatom. Für die Spezies HL^+ und H_2L^{2+} wurden aus spektrophotometrischen Messungen in wässrigen Pufferlösungen bei 25° und $I = 0.1$ M (KCl) die stöchiometrischen Säuredissoziationskonstanten $pK_1^H = 4.17$ und $pK_2^H = 0.22$ erhalten. Für die ungeladene Base wurden die Verteilungskoeffizienten zwischen Wasser und *n*-Hexan, Tetrachlorkohlenstoff und Chloroform ermittelt; aus ähnlichen Messungen mit Salzlösungen wurden die stufenweisen Bildungskonstanten von Metallkomplexen erhalten. Die Beständigkeit nahm in der Reihenfolge $Fe < Co < Cu > Zn$ zu, und die sterische Hinderung bei der Komplexbildung ist unter Berücksichtigung der Unterschiede in den Ligandbasizitäten etwa dieselbe wie bei einem 2-Methylsubstituenten. Beim Eisen(II)-Komplex ist $K_3 > K_1$, K_2, eine Anomalie, die bisher nur bei 2,2′-Bipyridin und 1,10-Phenanthrolin gefunden worden ist.

REFERENCES

1 Stability Constants of Metal-Ion Complexes, *Chem. Soc. Special Publ.*, No. 17 (1964).
2 H. IRVING AND H. S. ROSSOTTI, *J. Chem. Soc.*, (1954) 2910.

3 H. Irving and D. H. Mellor, *J. Chem. Soc.*, (1962) 5222.
4 H. Irving and D. H. Mellor, *J. Chem. Soc.*, (1962) 5237.
5 E. A. Hobday, M. Tomlinson and H. Irving, *J. Chem. Soc.*, (1962) 4914.
6 W. A. E. McBryde, D. A. Brisbin and H. Irving, *J. Chem. Soc.*, (1962) 5245.
7 C. V. Banks and R. C. Bystroff, *J. Amer. Chem. Soc.*, 81 (1959) 6153.
8 H. Irving and H. S. Rossotti, *Acta Chem. Scand.*, 10 (1956) 72.
9 B. E. Halcrow and W. O. Kermack, *J. Chem. Soc.*, (1946) 155.
10 H. Irving, *J. Chem. Soc.*, (1962) 4056.

Anal. Chim. Acta, 55 (1971) 315–324

Analytica Chimica Acta
Elsevier Publishing Company, Amsterdam
Printed in The Netherlands

NOUVELLE METHODE DE SEPARATION CALCIUM–STRONTIUM APPLIQUEE A LA PREPARATION D'UN SEL DE CALCIUM DE TRES FAIBLE TENEUR EN STRONTIUM

F. PATTI ET J. A. HERNANDEZ*

Commissariat à l'Energie Atomique, Département de la Protection Sanitaire, Section de Contrôle Sanitaire, B.P. No. 6, 92-Fontenay-aux-Roses (France)

(Reçu le 12 mars 1971)

Les échantillons biologiques renferment généralement des teneurs en strontium assez faibles qui se trouvent en présence de quantités relativement importantes de calcium. Le dosage du strontium par fluorescence-X ou par photométrie de flamme nécessite la construction de courbes d'étalonnages réalisées au moyen d'étalons devant avoir une composition chimique très voisine de celle des échantillons à mesurer; pour la confection de ces étalons, le produit de base auquel on ajoutera des surchages en strontium doit être un sel de calcium dont la concentration en strontium est inférieure à la limite de détection de la méthode analytique utilisée. Pour obtenir un tel produit, une séparation calcium–strontium s'avère indispensable du fait que les sels de calcium de qualité analytique: chlorure, nitrate, phosphate tricalcique, renferment des concentrations de strontium comprises entre 100 et 200 p.p.m.

Nous avons voulu éviter l'emploi de l'acide nitrique fumant et l'échange ionique sur résine, méthodes assez fastidieuses en particulier pour le traitement de quantités relativement importantes de calcium, et avons envisagé une nouvelle méthode de séparation basée sur la différence de solubilité de l'hydroxyde de calcium et de strontium en milieu sodique; les valeurs publiées indiquent que dans l'eau à 20° l'hydroxyde de strontium est sept fois plus soluble que l'hydroxyde de calcium[1-3] et bien que la solubilité diminue de manière importante en milieu sodique, elle devrait cependant permettre une séparation convenable de ces deux éléments; différentes valeurs ont été publiées sur la solubilité de l'hydroxyde de calcium en solution de soude diluée[1], mais nous n'avons trouvé aucune indication concernant l'hydroxyde de strontium.

Le but de ce travail est donc de définir le degré de spécificité de la séparation calcium–strontium en déterminant d'une part les quantités de strontium présentes dans la fraction calcium, et, d'autre part, les quantités de calcium présentes dans la fraction strontium, en fonction de la concentration en strontium et en soude de la solution.

CONDITIONS EXPÉRIMENTALES

Nous avons opéré sur 2.5 g de calcium et précipité l'hydroxyde par 10 g et 20 g de soude, soit un excès suffisant pour une précipitation quantitative, la quantité stoechiométrique étant de 5 g.

---

* Adresse actuelle: Institut des Affaires Nucléaires, Bogota, Colombie.

Les solutions sodiques obtenues après centrifugation titrent respectivement 0.53 *M* et 1.6 *M*, dans les conditions définies ci-dessous. Les séparations ont été effectuées à température ambiante soit environ 24°.

Dosage du strontium

Nous avons utilisé le ^{85}Sr comme indicateur radioactif et mesuré le rayonnement-γ de 0.51 MeV à l'aide d'un spectromètre multicanaux Intertechnique type SA 40 B à cristal de INa(Tl).

Les mesures sur les surnageants ont été effectués sur des prélèvements de 100 cm^3 ; l'activité de l'hydroxyde de calcium a été déterminée après dissolution de celui-ci dans 50 cm^3 d'une solution chlorhydrique 6 *M*.

Nous avons également effectué les dosages par fluorescence-X, au moyen d'une installation Philips fonctionnant sous 54 kV et 28 mA avec un tube générateur de rayons X à anticathode de molybdène; le strontium stable a été dosé dans les hydroxydes de calcium après transformation sous forme d'oxalate[4].

La première de ces deux méthodes nous a permis, en opérant avec une activité suffisante, 10 nCi par échantillon, d'atteindre une limite de détection de 0.5 p.p.m.; par fluorescence-X la limite de détection est de 3 p.p.m. (par rapport à l'oxalate).

Dosage du calcium

Les mesures ont été effectuées par compleximétrie au moyen d'une solution 0.01 *M* de E.G.T.A. (acide éthylèneglicol-bis-aminoéthyléther tétracétique) avec la calcéine comme indicateur coloré, au moyen du spectrophotomètre enregistreur de M. Jean et R. Constant.

Pour les surnageants titrant 1. 6 *M* en soude, il est nécessaire, pour obtenir une courbe de titrage correcte, de neutraliser une partie de la soude en excès par une solution chlorhydrique 6 *M*; pour une prise de 25 cm^3, nous avons ajouté 5 cm^3 de solution chlorhydrique.

Dans le calcul des concentrations, nous avons tenu compte de la présence du strontium en considérant que 1 cm^3 de E.G.T.A. 0.01 $M = 0.876$ mg de strontium.

Les réactifs utilisés sont des produits Prolabo: nitrate de calcium pur sec (contenant 120 p.p.m. de Sr), soude en pastilles (non carbonatée) etc.; le E.G.T.A. est un produit Eastman Kodak; le ^{85}Sr est fourni par le Centre Nucléaire de Saclay, référence: Sr-85-S-1.

Mode opératoire

Introduire 10.28 g de nitrate de calcium anhydre dans un tube à centrifuger de 250 cm^3 et effectuer la dissolution par 100 cm^3 d'eau distillée; ajouter 10 g (ou 20 g) de soude préalablement dissoute dans de l'eau distillée de façon à obtenir 75 cm^3 de solution; rincer le bécher par 25 cm^3 d'eau distillée.

Agiter 15 min puis centrifuger 8 min à 3,000 tours min^{-1}; écarter soigneusement le surnageant.

Pour une double précipitation, nous avons poursuivi de la façon suivante: dissoudre l'hydroxyde dans le minimum d'HCl 6 *M*; neutraliser par une solution de soude diluée et effectuer une seconde précipitation. Centrifuger, écarter le surnageant.

Dissoudre l'hydroxyde de calcium et réaliser un précipité d'oxalate (ou d'un autre sel insoluble) lequel est utilisé pour le dosage du strontium par fluorescence-X.

ESSAIS RELATIFS À L'ÉTUDE DE LA SÉPARATION CALCIUM–STRONTIUM

Influence de la concentration en strontium

Nous avons effectué une première série d'essais dans les conditions opératoires ci-dessus précissées en effectuant une seule précipitation de l'hydroxyde de calcium et nous avons déterminé la variation du rendement de séparation du strontium en fonction de sa concentration en milieu de soude 0.53 *M* (10 g de soude); la courbe de la Fig. 1 représente cette variation. On constate que le rendement diminue progressivement et atteint 80% pour un rapport Sr/Ca = 0.2; la variation décroît ensuite plus rapidement et correspond très probablement à la précipitation de l'hydroxyde de strontium.

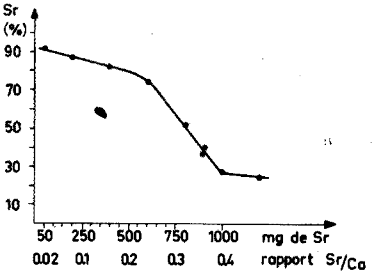

Fig. 1. Variation du rendement de séparation du strontium en fonction de sa concentration en solution de soude 0.53 *M*, pour une précipitation de l'hydroxyde de calcium.

Solubilité des faibles concentrations de strontium et du calcium

Une seconde série d'essais a été réalisée en milieu de soude 1.6 *M* (20 g de soude); pour des rapports Sr/Ca compris entre $8 \cdot 10^{-4}$ et $2 \cdot 10^{-2}$ (1.2 à 50 mg de Sr) la variation du rendement est représentée Tableau I. Ce Tableau permet de comparer les résultats

TABLEAU I

RENDEMENT DE SÉPARATION DU STRONTIUM ET QUANTITÉS DE CALCIUM

(Ce Tableau permet de comparer les rendements de séparation du strontium et les quantités de calcium présentes dans la fraction strontium en fonction de la quantité de strontium et de la concentration en soude de la solution; une seule précipitation de l'hydroxyde de calcium ayant été effectuée. Les chiffres entre parenthèses indiquent le nombre d'essais effectués; milieu 0.53 *M* moyenne du calcium = 5.2 mg et milieu 1.6 *M* moyenne du calcium = 1.9 mg)

Concentration NaOH solution	*Quantité de strontium (mg)*	*Surnageant*	
		Ca (mg)	*%^{85}Sr*
0.53 *M*	1.2	5	94 ± 1.9 (5)
	10	4.9	94 ± 1.9 (2)
	25	5.7	93 ± 1.9 (2)
	50	5.4	91 ± 1.8 (2)
1.6 *M*	1.2	1.8	93 ± 1.9 (5)
	10	1.9	90 ± 1.8 (2)
	25	1.8	86 ± 1.7 (2)
	50	2.2	82 ± 1.7 (2)

obtenus en milieu de soude 0.53 *M* et 1.6 *M*; on remarque qu'en milieu 1.6 *M* les rendements de séparation du strontium sont inférieurs à ceux obtenus en milieu 0.53 *M*; entre 1.2 et 10 mg les valeurs sont assez voisines et dans les deux cas supérieures à 90 %; la différence s'accentue avec l'augmentation de la quantité de strontium.

Ces résultats montrent que le rendement de séparation du strontium est lié à la quantité de strontium contenue dans la solution ainsi qu'à la concentration en soude.

En ce qui concerne le calcium, les quantités solubles en milieu 1.6 *M* sont 2.7 fois plus faibles que celles observées en milieu 0.53 *M*, soit respectivement: 1.9 et 5.2 mg (valeurs moyennes).

De ces résultats il ressort qu'en une seule précipitation on réalise une séparation quantitative du calcium; il ne reste en effet en solution, en milieu de soude 0.53 *M*, que 0.2 % du calcium initial. En ce qui concerne le strontium, on remarque qu'en présence de 1.2 mg de cet élément, quantité normalement contenue dans les 2.5 g de calcium traités, on obtient un hydroxyde de calcium ne refermant que 6 % de la quantité initiale de strontium; dans ces conditions, on peut admettre qu'après une double précipitation on obtiendra un hydroxyde de calcium ne renfermant que 0.4 % du strontium initial.

Cette méthode permet donc très commodément de séparer de petites quantités de strontium dans des quantités relativement importantes de calcium.

PRÉPARATION D'UN SEL DE CALCIUM DE TRÈS FAIBLE TENEUR EN STRONTIUM

Sur la base des résultats ci-dessus exposés, nous avons, dans les conditions opératoires précisées, effectué sur six échantillons de 10.28 g de nitrate de calcium, équivalent à 2.5 g de calcium, une double précipitation de l'hydroxyde de calcium en utilisant 10 g de soude.

Les valeurs des teneurs en strontium des différents hydroxydes obtenus par mesure de ^{85}Sr sont représentées en Tableau II; on constate que la teneur moyenne représente les 0.6 % de la teneur initiale. Cette valeur est sensiblement plus élevée que celle estimée par le calcul (soit 0.4 %, § précédent), mais reste très satisfaisante, du

TABLEAU II

TENEURS EN STRONTIUM DES DIFFÉRENTS HYDROXYDES

(Les chiffres de ce Tableau indiquent les concentrations de strontium présentes dans la fraction calcium et les quantités de calcium dans la fraction strontium en milieu sodique 0.53 *M*)

Essais no.	*Hydroxyde de Ca Activité (%^{85}Sr)*		*Oxalate de Ca p.p.m. Sr calculées*	*Surnageant Ca (mg)*
1	0.7 ± 0.1	→	0.9	10.3
2	0.6 ± 0.1	→	0.8	8.5
3	0.7 ± 0.1	→	0.9	9.8
4	0.5 ± 0.08	→	0.7	13.0
5	0.5 ± 0.08	→	0.7	7.0
6	0.8 ± 0.1	→	1	10.0
Moyenne	0.6 ± 0.04	→	0.8	9.8

fait que l'on obtient un oxalate de calcium renfermant en moyenne 0.8 p.p.m. de strontium soit une concentration plus de trois fois inférieure à la limite de détection possible par fluorescence-X qui est de 3 p.p.m.

Les Figs. 2 et 3 représentent les enregistrements des dosages effectués par

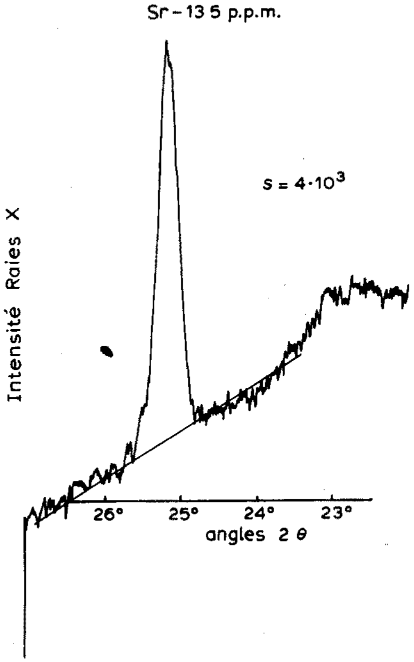

Fig. 2. Dosage du strontium dans le nitrate de calcium. Enregistrement représentant les raies Kα_1 et Kα_2 (composante à 25.1°) obtenu sur un oxalate de calcium. S indique la sensibilité de l'enregistrement.

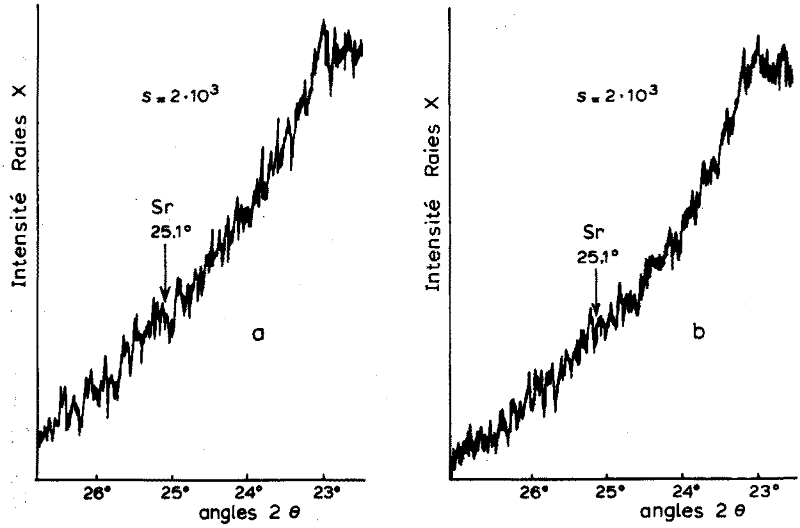

Fig. 3. Recherche du strontium après séparation chimique sur : (a) un oxalate de calcium après traitement de 2.5 g de calcium; (b) oxalate de calcium après traitement de 250 g de calcium. Dans les deux cas le pic à 25.1° est inexistant.

fluorescence-X respectivement sur:

1. un oxalate de calcium précipité d'une solution de nitrate de calcium non traité,
2. un oxalate de calcium après séparation chimique (Fig. 3a).

On constate que dans ce dernier cas le pic caractéristique des raies Kα_1 et Kα_2 du strontium, à la position angulaire $2\theta = 25.1°$ est inexistant, la concentration en strontium étant inférieure à la limite de détection.

Par ailleurs le Tableau II indique également les quantités de calcium présentes dans le surnageant (0.53 M en soude); les valeurs sont environ deux fois plus grandes que celles figurant au Tableau I, soit, respectivement, en considérant les moyennes: 9.8 et 5.2 mg, ceci du fait que les deux surnageants provenant de la double précipitation ont été réunis.

Dans le but de préparer un sel de calcium utilisable comme "blanc" en analyse radiochimique, nous avons appliqué cette méthode à 250 g de calcium; pour de telles quantités, nous avons opéré dans une cuve de polyéthylène d'une contenance de 30 dm^3 dans laquelle nous avons introduit:

1.028 kg de nitrate de calcium anhydre, 20 dm^3 d'eau distillée, 1 kg de soude. Le mode opératoire est le suivant:

Agiter vigoureusement pendant environ une heure, laisser déposer le précipité pendant quelques heures puis séparer l'hydroxyde par filtration sur entonnoir à plaque filtrante de porosité no. 4. Rincer le précipité par 800 cm^3 d'une solution de soude 0.2 M; dissoudre l'hydroxyde par une solution chlorhydrique 6 M (environ 3.5 dm^3), agiter et neutraliser par une solution de soude; effectuer une seconde précipitation, filtrer, rincer; dissoudre l'hydroxyde comme précédemment et après neutralisation de la solution précipiter le calcium sous forme de carbonate par addition de 800 g de Na_2CO_3 en poudre.

L'enregistrement de l'intensité des raies X du strontium par fluorescence-X, représenté Fig. 3b, indique que la concentration est inférieure à la limite de détection, ce qui signifie qu'au moins 98% du strontium a été éliminé.

DISCUSSION

Cette méthode nous paraît intéressante du fait qu'en une seule précipitation elle permet de séparer des quantités importantes de calcium avec une séparation du strontium, variant de 80 à 94%, selon les quantités présentes en solution (500 à 1.2 mg), soit des rapports Sr/Ca compris entre 1/5 et 1/2000. Ce rendement peut être amélioré en effectuant plusieurs précipitations de l'hydroxyde de calcium.

Le fait de pouvoir séparer de très petites quantités de strontium constitue un avantage sur la méthode utilisant la précipitation du nitrate de strontium par l'acide nitrique fumant[5] qui devient particulièrement fastidieuse lorsque les rapports strontium/calcium sont petits, car une partie importante du calcium précipite avec le strontium et de nombreuses précipitations sont nécessaires pour déplacer la totalité du calcium.

D'autre part, les résultats montrent que de petites quantités de calcium se trouvent dans la fraction strontium, ceci du fait de la solubilité de l'hydroxyde de calcium (2 mg en milieu de soude 1.6 M et 5 mg en milieu 0.53 M, après une précipitation); ces petites quantités peuvent très facilement être éliminées par extraction du nitrate de calcium au moyen d'un solvant organique tel que l'acétone[6,7], ce qui permet le dosage du strontium par gravimétrie.

Des essais sont actuellement en cours pour réduire la quantité de calcium restant en solution, en effectuant la séparation à température plus élevée.

Les différentes valeurs obtenues et figurant Tableau I et II montrent que cette méthode permet d'obtenir une bonne reproductibilité des résultats, même lorsque les quantités de strontium à séparer sont de l'ordre du milligramme et que l'on peut très facilement préparer un sel de calcium de très faible teneur en strontium (stable ou radioactif). Dans ce cas il est préférable d'opérer en présence d'un très faible excès de soude, un excès trop important favorisant la précipitation du strontium. Des quantités de 250 grammes de calcium ont été traitées de manière satisfaisante.

Nous envisageons d'appliquer cette méthode au dosage de ^{90}Sr dans les échantillons biologiques.

Nous remercions Melle Astrain et Mme Dubuc de leur collaboration technique pour l'exécution de ce travail.

RÉSUMÉ

Une nouvelle méthode de séparation calcium–strontium, basée sur la différence de solubilité des hydroxydes est exposée dans ce travail. Par précipitation de l'hydroxyde de calcium en milieu de soude diluée, elle permet la séparation de petites quantités de strontium (1 à 500 mg) en présence de quantités importantes de calcium; les rendements de séparation ont été déterminés en fonction des quantités de strontium présentes et de la concentration en soude de la solution; le degré de spécificité de la séparation calcium–strontium a été étudié. La méthode a été appliquée à la préparation de sels de calcium de très faible teneur en strontium stable (2.9 p.p.m. par rapport au calcium) ou radioactif, utilisables soit pour la confection d'étalons nécessaires au dosage du strontium stable par fluorescence-X ou par photométrie de flamme, soit pour l'obtention d'un "blanc" utilisé en analyse radiochimique.

SUMMARY

A new separation of calcium and strontium based on the different solubilities of their hydroxides has been developed. By precipitation of calcium hydroxide in a dilute sodium hydroxide solution, small amounts of strontium (1–500 mg) can be separated from large amounts of calcium; the separation yields have been determined as a function of the amounts of available strontium and the concentration of the sodium hydroxide solution. The degree of selectivity of the separation has also been studied. The method is applied to the preparation of calcium salts with a very low content of stable (2.9 p.p.m. in relation to calcium) or radioactive strontium, which can be used either for the preparation of standards for the determination of stable strontium by X-ray fluorescence or flame photometry, or to obtain a "blank" for radiochemical analysis.

ZUSAMMENFASSUNG

Es wurde eine neue Trennungsmethode für Calcium und Strontium entwickelt, die auf den unterschiedlichen Löslichkeiten der Hydroxide beruht. Durch Fällung von Calciumhydroxid in einer verdünnten Natronlauge können kleine Mengen Strontium (1–500 mg) von grossen Mengen Calcium abgetrennt werden; die Trennausbeuten wurden als Funktion der vorliegenden Strontiummengen und der Konzentration der Natronlauge bestimmt. Der Selektivitätsgrad der Trennung wurde ebenfalls untersucht. Die Methode wird auf die Herstellung von Calciumsalzen mit sehr geringem Gehalt an stabilem (2.9 p.p.m. in bezug auf Calcium) oder radioaktivem Strontium angewendet, welche für Vergleichsproben bei der Bestimmung von stabilem Strontium durch Röntgenfluoreszenz oder Flammenphotometrie oder als "Blindprobe" für die radiochemische Analyse benutzt werden können.

BIBLIOGRAPHIE

1 P. Pascal (Ed.), *Nouveau Traité de Chimie Minérale*, Tome IV, Masson, Paris, 1958, pp. 393, 610.
2 H. Stephen et T. Stephen (Editeurs), *Solubility of Inorganic and Organic Compounds, Vol. 1*, Part 1, Pergamon Press, Oxford, 1963.
3 A. Seidell, *Solubility of Inorganic and Metal Organic Compounds, Vol. 1*, Van Nostrand, New-York, 1953.
4 F. Patti, *Bull. Soc. Chim. France*, (1970) 4145.
5 H. H. Willard et E. W. Goodspeed, *Ind. Eng. Chem.*, 9 (1936) 414.
6 G. Charlot, *Les Méthodes de la Chimie Analytique. Analyse Quantitative Minérale*, Masson, Paris, 1966, p. 655.
7 A. N. Shreve, C. H. Watkins et J. C. Browning, *Ind. Eng. Chem., Anal. Ed.*, 11 (1939) 215.

Analytica Chimica Acta
Elsevier Publishing Company, Amsterdam
Printed in The Netherlands

RADIOCHEMICAL STUDIES ON THE SOLVENT EXTRACTION OF SEVERAL ELEMENTS IN $Mn(NO_3)_2 \cdot 6\ H_2O$–AND $CaCl_2 \cdot 6\ H_2O$–Tri-*n*-BUTYL PHOSPHATE SYSTEMS

EIKO AKATSU AND MASAHARU ASANO

Japan Atomic Energy Research Institute, Tokai Research Establishment, Tokai-Mura, Ibaraki-ken (Japan)

(Received 26th January 1971)

The solvent extraction of molten salt–organic extractant systems has been investigated by Gruen *et al.*[1] and other investigators[2,3]. They used eutectics of $LiNO_3$–KNO_3[1,3], CuCl–KCl[2] and others[4] above 150°. Some metal ions show high distribution ratios in molten salt systems. However, the use of these systems is limited by the fact that eutectics have to be kept anhydrous, a temperature above 150° is necessary and that organic extractants are usually unstable at high temperatures.

On the other hand, salting-out in solvent extraction has widely been studied, and practically utilized in thorex and redox processes[5–7]. In these methods, it is rather difficult to satisfy some requirements. One is that a larger salting-out effect is obtained with lower acidity and with cations of higher valency, and another that aqueous phases become acid-deficient by hydrolysis of the salt at low acidity, and metal ions, which are to be extracted into the organic phase, may be hydrolyzed and not salted out.

Angell[8,9] and other investigators[10–12] have studied calcium nitrate hydrates from several points of view, and showed that water exists at 25–100° in the form of $Ca(H_2O)_n^{2+}$ ($n \leqq 6$) in the fused calcium nitrate hydrates. They concluded that systems of salts hydrates with fixed melting point like $Ca(NO_3)_2 \cdot 6\ H_2O$ are similar to the usual anhydrous molten salts, and called them "hydrate melts". It is, therefore, expected that water in a hydrate melt would not cause hydrolysis of other cations added.

In this work, $Mn(NO_3)_2 \cdot 6\ H_2O$ (m.p. 25.8°) and $CaCl_2 \cdot 6\ H_2O$ (m.p. 29.9°) were used at 30° as inorganic phases in solvent extraction. Although the former has not been ascertained yet to form a hydrate melt, it was expected to be similar to the hydrate melt. Organic phases were considered stable enough at the temperature. Solvent extraction with TBP from inorganic phases was studied by radioactive tracer techniques.

EXPERIMENTAL

Reagents

Manganese nitrate hexahydrate was prepared from manganese carbonate and nitric acid, and recrystallized. Calcium chloride hexahydrate (JIS special grade) was used as received. Commercial tri-*n*-butyl phosphate (TBP) was purified by washing with sodium hydrogencarbonate solution, hydrochloric acid and water. Diluents were used as received: Progil pure (90–95% 2,4,5,7-tetramethyloctane) in the manganese nitrate system and *n*-paraffin (a mixture of n-$C_{12}H_{26}$ and n-$C_{13}H_{28}$; Maruzen Oil Co.) in the calcium chloride system. There was no appreciable difference between them in a preliminary test of determination of distribution ratios. The organic phases were used after pre-equilibration, when increase of the volume of the organic phase was about 10% with a pure TBP–$Mn(NO_3)_2 \cdot 6\ H_2O$ system.

Most radioactive tracers were imported or obtained from Radioisotope Center, JAERI. Uranium-237 and thorium-234 were prepared as reported[13]. Mixtures of fission products were obtained by neutron irradiation of natural or enriched uranium (93%) in JRR-2. All tracers were used after conversion into nitrate. Cerium(III), neptunium (IV) and plutonium(IV) were prepared by treatment with hydroxylamine, ascorbic acid and sodium nitrite, respectively. Neptunium(V) was obtained by warming in 1 *M* perchloric acid, and the inorganic phase was scrubbed with fresh pre-equilibrated TBP.

Determination of distribution ratios

Distribution ratios, K_d, were determined by three methods.

Method I. A solution of radioactive tracer was evaporated to dryness, the residue was dissolved in $Mn(NO_3)_2 \cdot 6\ H_2O$ or $CaCl_2 \cdot 6\ H_2O$ melt by warming, and the mixture was used as an inorganic phase. After both phases had been kept at 30 ± 1° for at least 30 min, they were mixed for 1 min and centrifuged for phase separation. Scrubbing techniques were used in cases of K_d values above 5. The radioactivity of both phases was measured by a conventional scintillation counter. The radioisotopes used were ^{85}Sr, ^{90}Y, ^{99m}Tc, ^{106}Ru, ^{137}Cs, ^{141}Ce, $^{152,154}Eu$, ^{170}Tm, ^{234}Th, ^{233}Pa, ^{237}U and ^{239}Np.

Distribution ratios of manganese in the manganese nitrate system were also measured by Method I with ^{56}Mn, and the K_d value was 0.24 with pure TBP (Fig. 2). Specific gravities of $Mn(NO_3)_2 \cdot 6\ H_2O$ and $CaCl_2 \cdot 6\ H_2O$ melts were 1.72 and 1.50 g ml^{-1} at 30 ± 1°. Molar concentrations of manganese and calcium were computed as 6.05 and 6.84 *M* by using the above values. From these results the concentration of manganese nitrate in the organic phase was calculated to be 1.45 *M*. In the case of calcium chloride system, the K_d values were determined by EDTA titration (Fig. 4). The K_d value 0.15 with 75% TBP corresponds to 1.03 *M* calcium chloride in the TBP phase.

Ratio of counting rates of ^{85}Sr, ^{95}Zr, ^{137}Cs, ^{141}Ce and ^{170}Tm in manganese nitrate melt to the counting rates in water was 0.97 ± 0.0 . In the subsequent measurements, no correction was applied for this ratio.

Method II. After the irradiated uranium oxide had been converted into nitrate and dissolved in $Mn(NO_3)_2 \cdot 6\ H_2O$ on a water bath, extraction experiments were performed in the same way as described in Method I. Gamma-ray spectra of both phases were measured by using a 30-ml Ge(Li) detector with nuclear data pulse-height analyzer for samples with cooling times of 1–13 days and a NaI(Tl) (3″ × 3″) detector for samples cooled for over one month. The area of photopeaks was determined by summing the numerical data. K_d values of ^{99}Mo, ^{103}Ru, ^{132}Te, ^{137}Cs, ^{140}Ba, ^{141}Ce, ^{143}Ce, ^{147}Nd and ^{239}Np were measured by this method.

Method III. The radioactive tracers of α-emitting ^{241}Am and ^{239}Pu, were used in the determination of distribution ratios of americium(III) and plutonium(IV). The radioactivities of inorganic phases could not be directly measured, but that of the organic phases could with a 2π gas-flow counter at dilute TBP regions; therefore, K_d values were obtained by the following calculation:

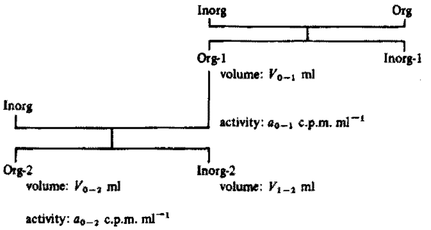

$K_d = (V_{1-2}/V_{0-2})[a_{0-1} - a_{0-2})]$
where V_{0-1} was equal to V_{0-2} in the experiments.

RESULTS

Pure TBP was so viscous after contacting with $Mn(NO_3)_2 \cdot 6\,H_2O$ or $CaCl_2 \cdot 6\,H_2O$ melt that most solvent extraction experiments were performed with solutions below 75% of TBP.

Solubilities of $UO_2(NO_3)_2 \cdot 6\,H_2O$ and $CsNO_3$ in $Mn(NO_3)_2 \cdot 6\,H_2O$ at 30° were about 0.8 and 0.6 wt.% on a preliminary test. It was not ascertained whether other nitrates were soluble or not, but the radioactive tracers dried in a beaker were transferred into melt phases by warming.

TABLE I

VARIATION OF K_d VALUES ON SCRUBBING

Element	*% TBP*	*Distribution ratio*		
		1st contact	*1st scrubbing*	*2nd scrubbing*
^{141}Ce	4.0	1.2	1.0	—
	10	4.5	4.5	4.3
$^{152,154}Eu$	4.0	35	33	—

Table I shows variation of K_d values of ^{141}Ce and $^{152,154}Eu$ on scrubbing. The results show that the K_d values did not change much and it was considered that the chemical species in the first contact were practically the same as those during the scrubbings.

Distribution ratios of $^{152,154}Eu$ were measured at 26 and 30±1°, and agreed with each other within experimental error, as seen in Table II.

The results obtained in $Mn(NO_3)_2 \cdot 6\,H_2O$ system are shown in Figs. 1–3, where the abscissa shows initial TBP concentration. K_d values of cesium, cerium and ruthenium determined by Method II agreed with those measured by Method I, but those of neptunium were higher than those of neptunium(V) by Method I. This fact was considered to show that neptunium was a mixture of tetra-, penta- and hexa-valent states in nitric acid solutions of irradiated uranium.

TABLE II

K_d VALUES OF ^{152,154}Eu AT 26 AND 30±1°

% *TBP*	*Distribution ratio at*	
	26°	30°
1.0	4.1	6.1
2.0	16	19
4.0	45	43
10	130	130
20	310	190
40	670	620
75	1100	1300

TABLE III

COMPARISON OF K_d VALUES IN ACID AND SALT HYDRATE SYSTEMS

Element	*Distribution ratios in the system of*		*Element*	*Distribution ratios in the system of*	
	19% TBP in kerosene $-14\,M\,HNO_3$ (25°)	*20% TBP in dodecane* $-Mn(NO_3)_2 \cdot 6\,H_2O$ (30°)		*10% TBP in toluene – concd. HCl (room temp.)*	*10% TBP in dodecane* $-CaCl_2 \cdot 6\,H_2O$ (30°)
U(VI)	6.0	10^5[b]	U(VI)	3.0	1500
Th	6.0	10^4[b]	Pa	54	0.24
Pu(IV)	2.7	10^4[b]	Th	0.69	900
Y	1.05	510	Eu	0.009	0.16
Ce(III)	0.060[a]	9.7	Ru	0.01	5.5
La	0.025[a]	3.3	Tc(VII)	1.8	270
Eu	3.0[a]	200	Y	0.011	0.21

[a] 48%.

[b] Estimated values.

TABLE IV

COMPARISON OF K_d VALUES IN SALT HYDRATE AND MOLTEN SALT SYSTEMS

Element	*Distribution ratios in the system of*		*Element*	*Distribution ratios in the system of*	
	4% TBP in polyphenyl $-LiNO_3+KNO_3$ (150°)	*4% TBP in dodecane* $-Mn(NO_3)_2 \cdot 6\,H_2O$ (30°)		*5% TBP in diphenyl* $-KCl+CuCl$ (180°)	*5% TBP in dodecane* $-CaCl_2 \cdot 6\,H_2O$ (30°)
U(VI)	14	64000	Am	0.050	0.073
Eu	5.9	35	U(IV)	5.0	—
Am	1.4	9	Th	—	300
			Cs	—	<0.004
			K	0.0002	—

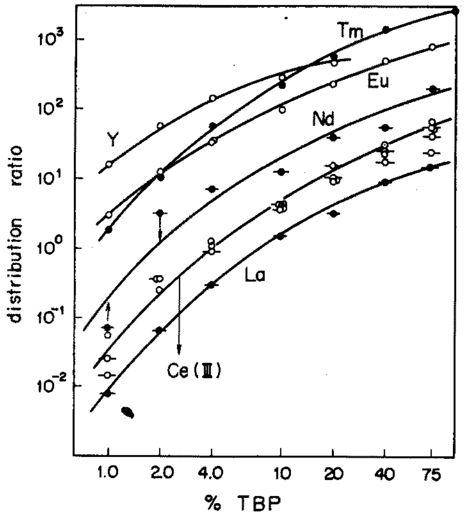

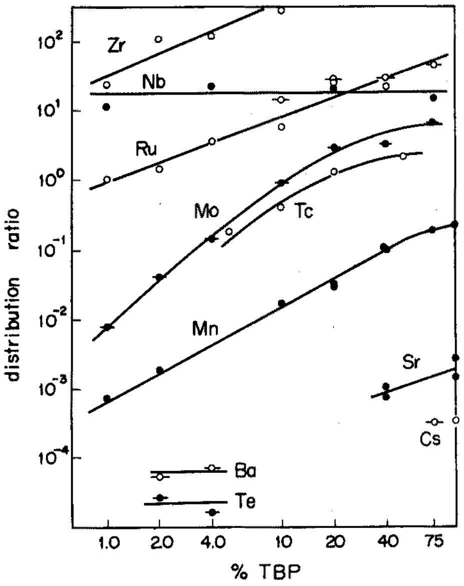

Fig. 1. The K_d values of rare earth elements in $Mn(NO_3)_2 \cdot 6\ H_2O$ system at 30°: (●, ○) by Method I, (-●-, -⊖-) by Method II.

Fig. 2. The K_d values of manganese and fission products in $Mn(NO_3)_2 \cdot 6\ H_2O$ system at 30°: (●, ○) by Method I, (-●-, -⊖-) by Method II.

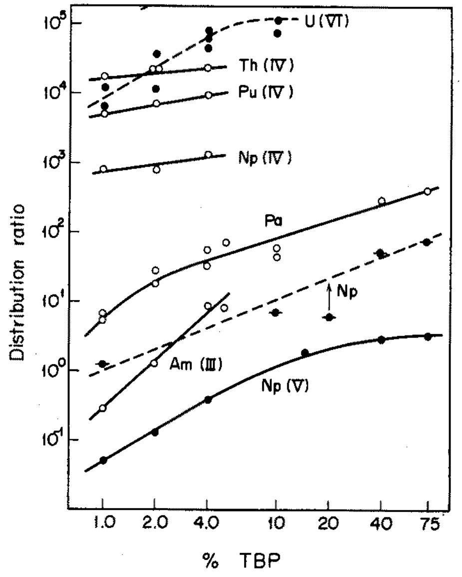

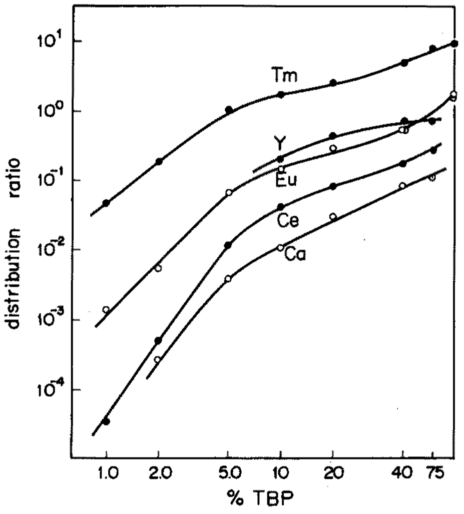

Fig. 3. The K_d values of actinide elements in $Mn(NO_3)_2 \cdot 6\ H_2O$ system at 30°: (●, ○) by Method I, (-●-, -⊖-) by Method II; Am and Pu by Method III.

Fig. 4. The K_d values of calcium and rare earth elements in $CaCl_2 \cdot 6\ H_2O$ system at 30°.

K_d values of cesium, strontium, barium and tellurium were below 10^{-3} whereas those of the other elements were greater than unity at certain TBP concentrations. As Fig. 1 shows, distribution ratios of lanthanum and some lanthanide elements increased with the increasing atomic number. A similar phenomenon was reported in nitric acid–TBP system[14]. Figure 3 shows also that actinide elements in the tetravalent state showed high K_d values. On the whole the distribution ratios in $Mn(NO_3)_2 \cdot 6\ H_2O$ system were higher than those in nitric acid system[15,16]. This is seen in Table III, where K_d values of several elements in the $Mn(NO_3)_2 \cdot 6\ H_2O$ system are compared with those in 14 M nitric acid at 25°. It is noticed that lanthanum and several lanthanide elements, which are nonextractable in the aqueous system, were extractable in the manganese nitrate hydrate system.

The results obtained on the $CaCl_2 \cdot 6\ H_2O$ system are shown in Figs. 4–6. The distribution ratios were high in comparison with those in hydrochloric acid systems[13,17] except for protactinium, as Table IV shows. Though the chemical species of protactinium was not made clear, the difference of acid and salt phase might have affected the extractability.

Nitrate and chloride concentrations in the inorganic phase were computed as 12.20 and 13.68 M, respectively, by using the specific gravities of $Mn(NO_3)_2 \cdot 6\ H_2O$ and $CaCl_2 \cdot 6\ H_2O$. The published values of nitrate and chloride concentrations are 22.4 M in KNO_3–$LiNO_3$ eutectic[3] and 27.7 M in CuCl–KCl[2], respectively. Although there are few data to be compared (Table III) the distribution ratios were comparable in molten salt hydrate and in fused salt systems[2,3]. Roughly speaking, it could be considered that manganese or calcium had some effect together with high anion concentration on increasing K_d values.

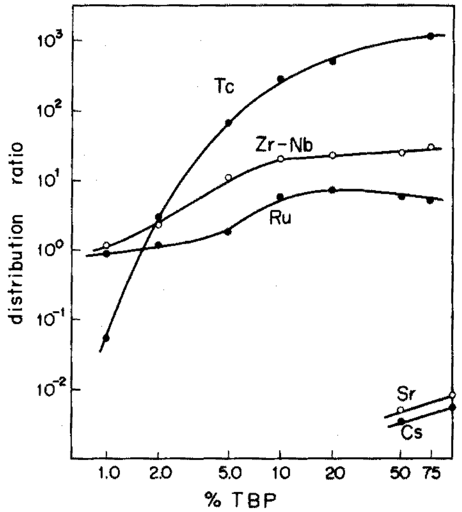

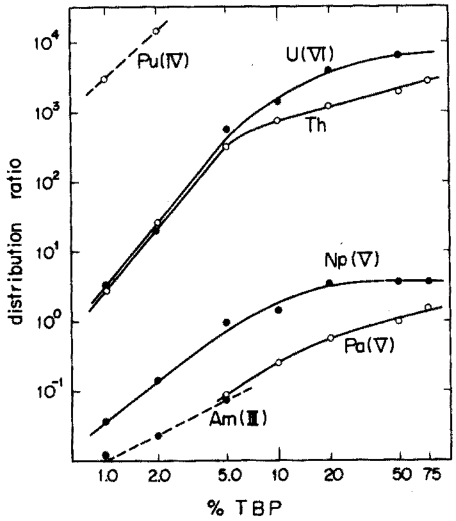

Fig. 5. The K_d values of some fission products in $CaCl_2 \cdot 6H_2O$ system at 30°.

Fig. 6. The K_d values of actinide elements in $CaCl_2 \cdot 6\ H_2O$ system at 30°; Am and Pu by Method III, the others by Method I.

The authors thank Drs. T. Ishimori and K. Ueno, JAERI, for their useful discussion, Mr. T. Tojo for his contribution to γ-spectrometry with Ge(Li) detector and Mr. K. Endo for his experimental assistance. This work was partly supported by a grant from the Ministry of Education.

SUMMARY

A solvent extraction study was carried out at 30° with organic phases of tri-*n*-butyl phosphate (TBP) in dodecane and inorganic phases of molten manganese nitrate hexahydrate (m.p. 25.8°). Distribution ratios of several rare earth and actinide elements and fission products were determined with TBP solutions of various concentration. The values obtained were higher than those in TBP–nitric acid system. Calcium chloride hexahydrate (m.p. 29.9°) was also used in a similar way.

RÉSUMÉ

Une étude est effectuée sur l'extraction dans un solvant à 30° avec phases organiques de TBP dans dodécane et phases inorganiques, nitrate de manganèse hexahydrate fondu (p.f. 25.8°). Les coefficients de partage de divers éléments de terres rares, actinides et produits de fission sont déterminés pour des solutions de TBP à diverses concentrations. Ces valeurs sont plus élevées que celles obtenues dans le système TBP–acide nitrique. Le chlorure de calcium hexahydrate (p.f. 29.9°) a été utilisé de la même façon.

ZUSAMMENFASSUNG

Es wurde die Solventextraktion mit organischen Phasen von TBP in Dodekan und anorganischen Phasen von geschmolzenem Mangannitrathexahydrat (Fp. 25.8°) bei 30° untersucht. Die Verteilungsverhältnisse einiger Elemente von Seltenen Erden, Actiniden und Spaltprodukten wurden mit TBP-Lösungen verschiedener Konzentration bestimmt. Die erhaltenen Werte waren grösser als die im TBP–Salpetersäure-System. Auch Calciumchloridhexahydrat (Fp. 29.9°) wurde in ähnlicher Weise verwendet.

REFERENCES

1 D. M. Gruen, R. L. McBeth, P. Graf and S. Fried, *Proc. Intern. Conf. Peaceful Uses At. Energy, 2nd, 1958, Vol. 28*, United Nations, New York, 1959, p. 112.
2 Z. Borkowska, M. Mielcarski and M. Taube, *J. Inorg. Nucl. Chem.*, 26 (1964) 359.
3 N. M. Isaac, P. R. Fields and D. M. Gruen, *J. Inorg. Nucl. Chem.*, 21 (1961) 152.
4 Y. Marcus, *Solvent Extraction Chemistry*, North-Holland, Amsterdam, 1967, p. 555.
5 J. F. Flagg, *Nuclear Science and Technology, 1; Chemical Processing of Reactor Fuels*, Academic Press, New York, 1961, p. 249; J. H. Siddall, p. 199.
6 F. L. Culler, *Progress in Nuclear Energy. Series III. Process Chemistry, Vol. 1*, Pergamon Press, London, 1956, p. 172.
7 R. C. Cairns, M. G. Baillie, B. J. Fox and R. K. Ryan, *Ind. Eng. Chem., Process Des. Develop.*, 7 (1968) 177.
8 C. A. Angell, *J. Phys. Chem.*, 68 (1964) 1917.
9 C. A. Angell, *J. Electrochem. Soc.*, 112 (1965) 1224.

10 C. T. Moynihan and A. Fratiello, *J. Amer. Chem. Soc.*, 89 (1967) 5546.
11 J. Braunstein and H. Braunstein, *Inorg. Chem.*, 8 (1969) 1528.
12 J. Braunstein, L. Orr and W. Macdonald, *J. Chem. Eng. Data*, 12 (1967) 415.
13 T. Ishimori and E. Nakamura, *JAERI-1047*, (1963).
14 D. F. Peppard, W. J. Driscoll, R. J. Sironen and S. McCarty, *J. Inorg. Nucl. Chem.*, 4 (1957) 326.
15 H. A. C. McKay and T. V. Healy, *Progress in Nuclear Energy. Series III. Process Chemistry, Vol. 2*, Pergamon Press, London, 1958, p. 546.
16 D. Scargil, K. Alcock, J. M. Fletcher, E. Hesford and H. A. C. McKay, *J. Inorg. Nucl. Chem.*, 4 (1957) 304.
17 T. Ishimori, E. Akatsu, K. Tsukuechi, T. Kobune, Y. Usuba, K. Kimura, G. Onawa and H. Uchiyama, *JAERI-1106*, 1966.

Analytica Chimica Acta
Elsevier Publishing Company, Amsterdam
Printed in The Netherlands

ETUDE DE L'EXTRACTION LIQUIDE–LIQUIDE DU ZINC(II) ET DU CADMIUM(II) PAR L'OXYDE DE (CARBOXY-2-ETHYL)DIPHENYLPHOSPHINE EN SOLUTION DANS LE CHLOROFORME

J. L. ROCCA ET M. PORTHAULT

Centre de Chimie Analytique, Faculté des Sciences de Lyon, 43, boulevard du 11 Novembre 1918, 69-Villeurbanne (France)

(Reçu le 11 mars 1971)

Dans de précédentes publications[1-3] nous avons traité l'étude de l'oxyde de (carboxy-2-éthyl)diphénylphosphine (HA) et de son comportement dans l'extraction liquide–liquide de cations métalliques tels que le fer(III) et le cuivre(II). Dans ce présent travail, nous nous sommes intéressé à l'extraction de zinc(II) et de cadmium(II) dans le chloroforme. Nous avons montré que ces deux cations sont extraits dans la phase organique, sous la forme $MA_2(HA)_2$. Une telle structure a déjà été obtenue avec des acides carboxyliques aliphatiques[4], ou l'oxime[5], comme agents d'extraction. Ces deux cations passent en phase organique pour des pH compris entre 5 et 6, alors que la concentration de HA en phase aqueuse (sous les formes HA et A^-) devient relativement importante. Nous avons montré que cet agent d'extraction pouvait alors complexer le zinc(II) et le cadmium(II) en phase aqueuse sous la forme MA_4^{2-}.

Nous avons ainsi déterminé, par des méthodes d'extraction liquide–liquide, les constantes d'équilibre de partage du zinc(II) et du cadmium(II) entre une phase aqueuse et le chloroforme, ainsi que les constantes d'équilibre de formation des complexes en phase aqueuse de force ionique 1.

ÉTUDE THÉORIQUE DE L'EXTRACTION

L'étude[1] de l'oxyde de (carboxy-2-éthyl)diphénylphosphine (HA) a montré que cet agent existait principalement sous forme de dimère dans le chloroforme, et nous ne ferons intervenir que cette forme en phase organique. Si o et a sont respectivement les indices des phases organique et aqueuse, nous écrivons l'extraction en phase organique du cation M^{2+} suivant l'équilibre:

$$jM_a^{2+} + j \times \tfrac{1}{2}n(H_2A_2)_o \rightleftarrows (MA_2 \cdot (n-2)HA)_{j,o} + 2jH_a^+$$

et la constante d'équilibre d'extraction:

$$K_M = [MA_2 \cdot (n-2)HA]_{j,o}\, [H^+]_a^{2j} / [M^{2+}]_a^j\, [H_2A_2]_o^{j \times \frac{1}{2}n}$$

Aux pH de travail, les complexes hydroxylés du zinc et du cadmium sont à des concentrations négligeables en phase aqueuse[6].

Par ailleurs, nous faisons l'hypothèse qu'une seule espèce est extraite et qu'elle est monomère, d'après les résultats obtenus à l'aide d'acides carboxyliques aliphatiques[4] avec de tels cations. Cette hypothèse s'est révélée conforme à les résultats expérimentaux. Ainsi le coefficient de partage D s'écrit alors:

$$D = [\text{métal}]_o/[\text{métal}]_a = [\mathrm{MA_2}\cdot(n-2)\mathrm{HA}]_o/[\mathrm{M}^{2+}]_a = K_\mathrm{M} \times [\mathrm{H_2A_2}]_o^{\frac{1}{2}n}[\mathrm{H}^+]_a^{-2}$$

et $\log D - 2\ \mathrm{pH} = \log K_\mathrm{M} + \frac{1}{2}n \log [\mathrm{H_2A_2}]_o$.

En fait, l'expérience montre que $\log D - 2$ pH n'est pas toujours une fonction linéaire de $\log [\mathrm{H_2A_2}]_o$, et que le coefficient de partage D expérimental peut être inférieur au coefficient théorique ainsi défini. Nous avons attribué ce phénomène à une complexation du cation M^{2+} en phase aqueuse suivant l'équilibre:

$$\mathrm{M}_a^{2+} + x\mathrm{A}_a^- \rightleftarrows \mathrm{MA}_x{}^{(x-2)-}{}_a$$

La constante d'équilibre β_{MA_x} de formation du complexe $\mathrm{MA}_x{}^{(x-2)-}$ étant:

$$\beta_{\mathrm{MA}_x} = [\mathrm{MA}_x{}^{(x-2)-}]_a/[\mathrm{M}^{2+}]_a [\mathrm{A}^-]_a^x$$

Ainsi $[\text{métal}]_a = [\mathrm{M}^{2+}]_a + [\mathrm{MA}_x{}^{(x-2)-}]_a = [\mathrm{M}^{2+}]_a (1 + \beta_{\mathrm{MA}_x}[\mathrm{A}^-]_a^x)$

Si K_a est le coefficient de dissociation de l'agent d'extraction HA, nous pouvons écrire:

$$[\text{métal}]_a = [\mathrm{M}^{2+}]_a (1 + \beta_{\mathrm{MA}_x} K_a{}^x [\mathrm{HA}]_a^x [\mathrm{H}^+]_a^{-x})$$

Ainsi, si

$$\alpha_{\mathrm{MA}_x} = 1 + \beta_{\mathrm{MA}_x} K_a{}^x [\mathrm{HA}]_a^x [\mathrm{H}^+]_a^{-x}$$

le coefficient de partage D devient:

$$D = [\mathrm{MA_2}\cdot(n-2)\mathrm{HA}]_o/[\mathrm{M}^{2+}]_a\, \alpha_{\mathrm{MA}_x} = K_\mathrm{M}[\mathrm{H_2A_2}]_o{}^{\frac{1}{2}n} [\mathrm{H}^+]_a^{-2}\, \alpha_{\mathrm{MA}_x}^{-1}$$

Soit alors les deux expressions

$$\log D - 2\mathrm{pH} = \log K_\mathrm{M} + \tfrac{1}{2}n \log [\mathrm{H_2A_2}]_o - \log \alpha_{\mathrm{MA}_x} \tag{1}$$

$$\log \alpha_{\mathrm{MA}_x} = \log (1 + \beta_{\mathrm{MA}_x} K_a{}^x [\mathrm{HA}]_a^x [\mathrm{H}^+]_a^{-x}) \tag{2}$$

Nous voyons que pour une valeur constante de $\log \alpha_{\mathrm{MA}_x}$, $\log D - 2\mathrm{pH}$ est une fonction linéaire de $\log [\mathrm{H_2A_2}]_o$. La pente de la droite obtenue nous permet de calculer la valeur de n. Nous pouvons rendre $\log \alpha_{\mathrm{MA}_x}$ constant lorsque $\log [\mathrm{HA}]_a + \mathrm{pH}$ reste constant. La valeur de n étant connue, nous pouvons ensuite tracer la courbe:

$$\log \alpha_{\mathrm{MA}_x} - \log K_\mathrm{M} = \tfrac{1}{2}n \log [\mathrm{H_2A_2}]_o - \log D + 2\mathrm{pH} = \mathrm{f}(\log[\mathrm{HA}]_a + \mathrm{pH})$$

Cette courbe est une courbe normalisée du type $\log \gamma = \log(1 + X^x) = \mathrm{f}(\log X)$ admettant deux asymptotes: l'une horizontale dont l'ordonnée à l'origine donne la valeur $-\log K_\mathrm{M}$, l'autre de pente x, permettant de connaître les valeurs de x et de β_{MA_x}.

PARTIE EXPÉRIMENTALE

Technique de partage

L'extraction est étudiée à 25°. L'ensemble thermostaté et la technique de partage ont déjà été décrits dans de précédentes publications[1-3].

La concentration de l'oxyde de (carboxy-2-éthyl)diphénylphosphine dans le chloroforme a varié de $1 \cdot 10^{-1}\ M$ à $3 \cdot 10^{-1}\ M$. Les concentrations initiales de zinc et de cadmium ont varié respectivement de $7.83 \cdot 10^{-4}\ M$ à $9.79 \cdot 10^{-4}\ M$ et de $5.60 \cdot 10^{-4}\ M$

à $6.80 \cdot 10^{-4}$ *M*. Les solutions sont préparées par dissolution d'aiguilles de zinc dans l'acide chlorhydrique puis dilution convenable, et, par mise en solution de sulfate de cadmium ($3\ CdSO_4 \cdot 8\ H_2O$) puis dilution convenable. Les produits utilisés sont des produits Prolabo RP.

L'étude cinétique de l'extraction a montré que 3 h d'agitation étaient suffisantes pour atteindre l'équilibre. Nous laissons décanter pendant 30 min pour séparer ces deux phases. Nous déterminons alors le pH et la concentration en cation métallique de la phase aqueuse. La concentration du métal en phase organique est déterminée après réextraction quantitative dans une solution d'acide chlorhydrique normale, par 3 h d'agitation à 25°. Les dosages des phases aqueuse et organique ont toujours été tels que nous avons retrouvé à 3 % près la concentration initiale en zinc ou cadmium.

Mesure du pH et dosages du zinc et cadmium

Après l'équilibre d'extraction, le pH de la phase aqueuse est déterminé à l'aide d'un compensateur Metrohm E 388[3].

Les dosages du zinc et du cadmium sont faits par spectrométrie d'absorption atomique sur un appareil Techtron type AA 4.

Détermination de $log[H_2A_2]_o$ *et* $log[HA]_a$

La connaissance des différentes constantes d'équilibre de HA dans le système eau–chloroforme[1], nous permet de tracer les courbes de la Fig. 1 représentant log $[H_2A_2]_0 = f([HA]_T)$ pour différents pH, nous pouvons connaître la concentration correspondante en forme dimère $[H_2A_2]_o$. Par les constantes d'équilibre de partage et de dimérisation, nous pouvons aussi déterminer la concentration $[HA]_a$ correspondante.

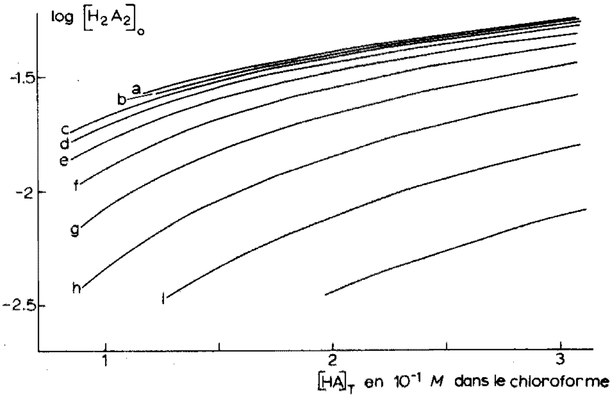

Fig. 1. Evolution de la forme dimère $[H_2A_2]_o$ en fonction du pH et de la concentration totale initiale $[HA]_T$ mise en solution dans la chloroforme. pH : (a) 4.60; (b) 4.80; (c) 5; (d) 5.20; (e) 5.40; (f) 5.60; (g) 5.80; (h) 6; (i) 6.20; (j) 6.40.

RÉSULTATS

Nous avons étudié l'extraction du zinc et du cadmium en fonction du pH, pour des concentrations initiales $[HA]_T$ de 10^{-1} *M*, $1.5 \cdot 10^{-1}$ *M*, $2 \cdot 10^{-1}$ *M*, $2.5 \cdot 10^{-1}$ *M* et $3 \cdot 10^{-1}$ *M*.

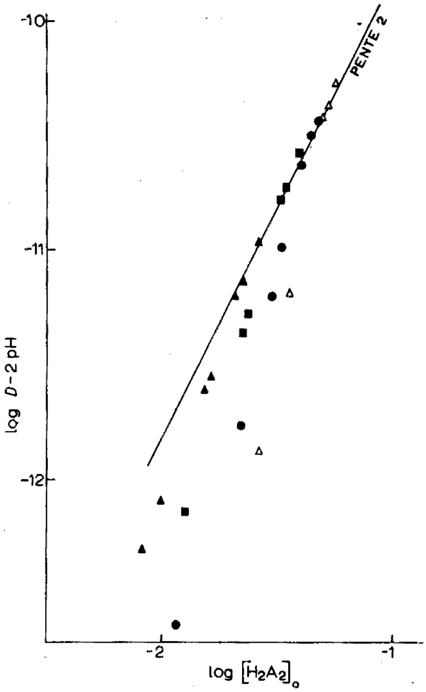

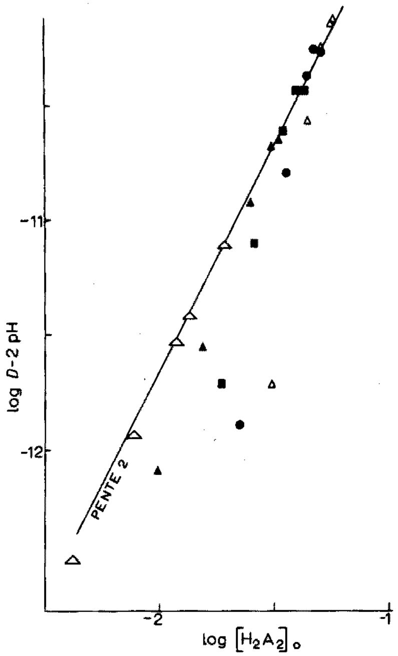

Fig. 2. Extraction de zinc pour différentes concentrations initiales en HA. (▲) $1.5\cdot10^{-1}$ *M*; (■) $2\cdot10^{-1}$ *M*; (●) $2.5\cdot10^{-1}$ *M*; (△) $3\cdot10^{-1}$ *M*.

Fig. 3. Extraction de cadmium pour différentes concentrations initiales en HA. (△) $1\cdot10^{-1}$ *M*; (▲) $1.5\cdot10^{-1}$ *M*; (■) $2\cdot10^{-1}$ *M*; (●) $2.5\cdot10^{-1}$ *M*; (△) $3\cdot10^{-1}$ *M*.

Détermination du degré de solvatation n

Sans tenir compte de la complexation du cation métallique en phase aqueuse, nous avons porté log $D-2$pH en fonction de log $[H_2A_2]_o$ (Figs. 2 et 3). Nous constatons que log $D-2$ pH n'est pas une fonction linéaire de log $[H_2A_2]_o$ pour l'ensemble des points expérimentaux. En effet, si une série de points s'alignent sur une droite de pente 2, un certain nombre s'en écartent et ceci d'autant plus que le pH augmente, pour une concentration initiale $[HA]_T$ donnée. Nous pouvons constater de plus que ces écarts sont toujours tels que le coefficient de partage *D* expérimental est inférieur au coefficient théorique attendu. Aussi nous supposons que le zinc et le cadmium sont complexés en phase aqueuse, ce qui limite leur extraction en phase organique. Nous devons alors tenir compte, dans la variation de log $D-2$ pH, de celle du terme log α_{MA_x}, qui dépend de la valeur de log $[HA]_a$ + pH.

Pour le zinc, nous constatons (Fig. 4) que lorsque log $[HA]_a$ + pH est inférieur à 2.97, la courbe log $D-2$ pH = f(log $[H_2A_2]_o$), est une droite unique de pente 2, pente que nous retrouvons pour d'autres droites correspondant à des valeurs de log $[HA]_a$ + pH bien déterminées mais plus élevées.

Pour le cadmium (Fig. 5) nous obtenons le même phénomène, des points alignés sur une seule droite de pente 2 pour des valeurs de log $[HA]_a$ + pH inférieures à 2.70. Pour des valeurs supérieures mais bien définies de log $[HA]_a$ + pH les points expéri-

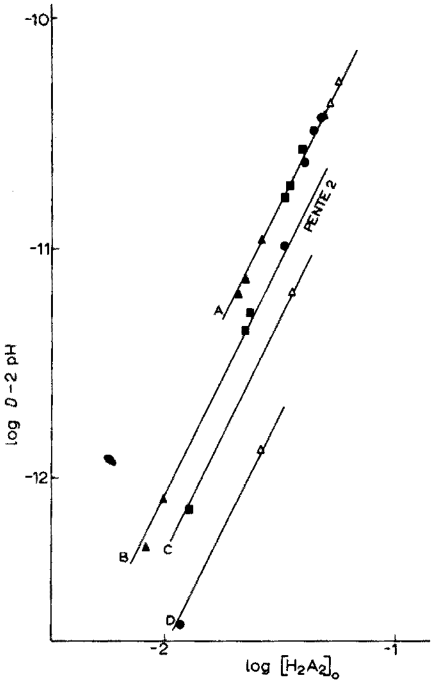

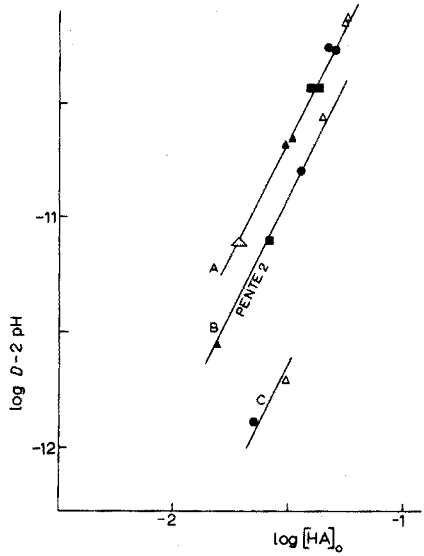

Fig. 4. Extraction de zinc; détermination de n pour différentes valeurs de log $[HA]_a$ + pH. (A) Inférieures à 2.97; (B) 3.14–3.18; (C) 3.28; (D) 3.40.

Fig. 5. Extraction de cadmium; détermination de n pour différentes valeurs de log $[HA]_a$ + pH. (A) Inférieures à 2.70; (B) 3.08–3.10; (C) 3.32–3.35.

mentaux se situent sur des droites également de pente de 2.

Ces résultats pour le zinc et le cadmium permettent de conclure que les relations (1) et (2) sont vérifiées et que $n=2$. Le complexe extrait en phase organique est donc unique et du type $(MA_2 \cdot (HA)_2)_o$.

Le fait que pour log $[HA]_a$+pH inférieur à 2.97 pour le zinc et à 2.70 pour le cadmium les points expérimentaux se situent sur une seule droite, laisse supposer que dans ces conditions log α_{MA_x} devient pratiquement nul.

Détermination du complexe en phase aqueuse

Nous avons établi précédemment les deux relations:

$$\log\alpha_{MA_x} - \log K_M = -\log D + 2\,\mathrm{pH} + \tfrac{1}{2}n\log\,[H_2A_2]_o \qquad (1)$$

$$\log\alpha_{MA_x} = \log(1 + \beta_{MA_x} K_a^{\,x}\,[HA]_a^x\,[H^+]_a^{-x}) \qquad (2)$$

Nour portons alors $-\log D + 2\,\mathrm{pH} + 2\log\,[H_2A_2]_o$ en fonction de log $[HA]_a$ + pH pour le zinc et le cadmium (Figs. 6 et 7). A ces courbes expérimentales, nous pouvons adapter une courbe normalisée du type $\log y = \log(1+X^4) = f(\log X)$, admettant une asymptote horizontale et une asymptote oblique de pente 4. Nous pouvons en conclure que dans nos extractions, le complexe formé en phase aqueuse est pratiquement unique et du type MA_4^{2-} pour le zinc et le cadmium. Nous retrouvons en phase aqueuse la

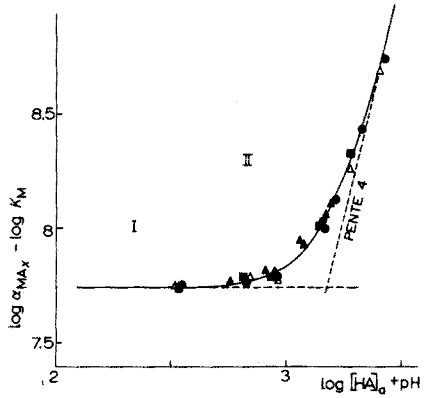

Fig. 6. Extraction de zinc; identification de la forme complexée en phase aqueuse.

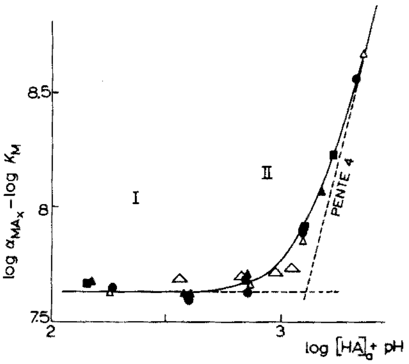

Fig. 7. Extraction de cadmium; identification de la forme complexée en phase aqueuse.

même solvatation que celle en phase organique. L'ordonnée à l'origine de l'asymptote horizontale donne alors la valeur de $-\log K_M$ et l'intersection des deux asymptotes permet d'atteindre la valeur de $\log \beta_{MA_x}$.

Nous dégageons ainsi les constantes:

pour le zinc $\log K_{Zn} = -7.80 \pm 0.1$

$\log \beta_{ZnA_4} = +3.70 \pm 0.1$

et pour le cadmium $\log K_{Cd} = -7.60 \pm 0.1$

$\log \beta_{CdA_4} = +3.90 \pm 0.1$

Nous constatons que les courbes précédentes peuvent être séparées en deux régions: région I — pas de complexation en phase aqueuse et extraction en phase organique de l'espèce $MA_2(HA)_2$ (cas où $\log [HA]_a + pH < 2.97$ pour le zinc et < 2.70 pour le cadmium) et région II—complexation en phase aqueuse sous forme de MA_4^{2-} et extraction en phase organique de l'espèce $MA_2(HA)_2$ (cas où $\log [HA]_a + pH > 2.97$ pour le zinc et > 2.70 pour le cadmium).

Courbes d'extraction du zinc et du cadmium

Nous avons représenté (Figs. 8 et 9) l'extraction respectivement de zinc et de cadmium en fonction du pH, pour différentes concentrations initiales $[HA]_T$. Nous constatons que le pourcentage d'extraction augmente avec le pH, passe par un maximum puis décroit du fait que d'une part la complexation en phase aqueuse devient de plus en plus importante, et que d'autre part pour une valeur $[HA]_T$ donnée, $\log [H_2A_2]_o$ diminue lorsque le pH augmente. Cependant pour la concentration $[HA]_T = 3 \cdot 10^{-1}$ *M*, le zinc et le cadmium peuvent être extraits jusqu'à environ 75%.

RÉSUMÉ

Les auteurs ont montré par des méthodes d'extraction liquide–liquide que le zinc et le cadmium sont extraits dans le chloroforme sous la forme $MA_2(HA)_2$ par l'oxyde de (carboxy-2-éthyl)diphénylphosphine, et qu'ils peuvent être complexés en

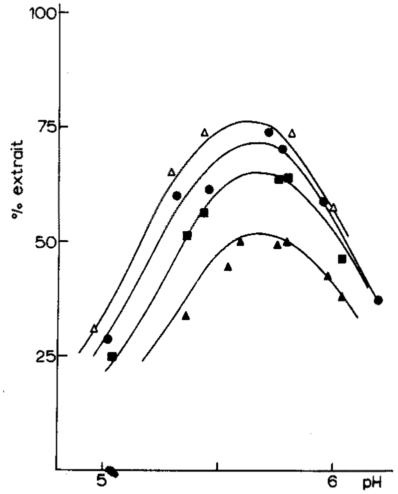

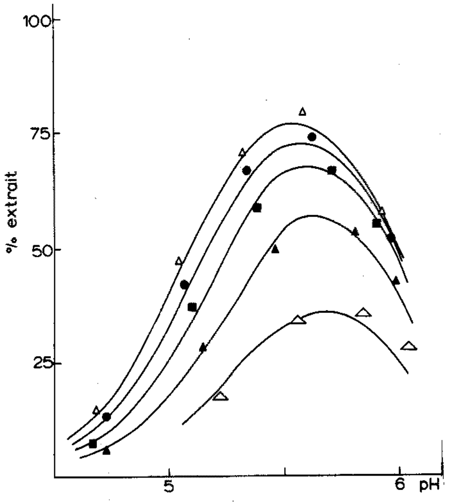

Fig. 8. Extraction de zinc en fonction du pH pour différentes concentrations initiales en HA. (▲) $1.5\cdot10^{-1}$ *M*; (■) $2\cdot10^{-1}$ *M*; (●) $2.5\cdot10^{-1}$ *M*; (△) $3\cdot10^{-1}$ *M*. Courbe théorique d'extraction calculée à l'aide des constantes K_{Zn} et β_{ZnA_4}.

Fig. 9. Extraction de cadmium en fonction du pH pour différentes concentrations initiales en HA. (△) $1\cdot10^{-1}$ *M*; (▲) $1.5\cdot10^{-1}$ *M*; (■) $2\cdot10^{-1}$ *M*; (●) $2.5\cdot10^{-1}$ *M*; (△) $3\cdot10^{-1}$ *M*. Courbe théorique d'extraction calculée à l'aide des constantes K_{Cd} et β_{CdA_4}.

phase aqueuse pour donner l'espèce MA_4^{2-} Ils ont donné les différentes constantes relatives aux équilibres d'extraction et de complexation. Le pourcentage d'extraction peut atteindre des valeurs relativement importantes. Cependant l'extraction, après être passée par un maximum, diminue lorsque le pH augmente, la complexation en phase aqueuse devenant de plus en plus importante.

SUMMARY

Zinc and cadmium can be extracted in the form $MA_2(HA)_2$ by (carboxy-2-ethyl)diphenylphosphine oxide in chloroform. Complex formation in the aqueous phase involves the species MA_4^{2-}. The extraction constants and dissociation constants are given. At the $3\cdot10^{-1}$ *M* level of metal ion, percentage extraction is *ca.* 75%. Extraction reaches a maximum as the pH is increased, and then decreases as complex formation in the aqueous phase becomes significant.

ZUSAMMENFASSUNG

Zink und Cadmium können als $MA_2(HA)_2$ mit (Carboxy-2-äthyl)diphenylphosphinoxid in Chloroform extrahiert werden. In der wässrigen Phase sind MA_4^{2-}-Spezies enthalten. Die Extraktionskonstanten und Dissoziationskonstanten werden angegeben. Im Bereich $3\cdot10^{-1}$ *M* Metallion ist die prozentuale Extraktion *ca.* 75%. Bei steigendem pH-Wert erreicht die Extraktion ein Maximum und wird dann geringer, wenn die Komplexbildung in der wässrigen Phase Bedeutung gewinnt.

BIBLIOGRAPHIE

1 J. L. Rocca et M. Porthault, *Bull. Soc. Chim. France*, 5 (1970) 2036.
2 J. L. Rocca et M. Porthault, *Bull. Soc. Chim. France*, 11 (1970) 4152.
3 J. L. Rocca et M. Porthault, *Anal. Chim. Acta*, 53 (1971) 55.
4 G. K. Schweitzer and F. C. Clifford, *Anal. Chim. Acta*, 45 (1969) 57.
5 J. Starý, *Anal. Chim. Acta*, 28 (1963) 132.
6 A. Ringbom, *Les Complexes en Chimie Analytique*, Dunod, Paris, 1967, pp. 331–336.

Analytica Chimica Acta
Elsevier Publishing Company, Amsterdam
Printed in The Netherlands

ATOMIC ABSORPTION AND FLUORESCENCE SPECTROSCOPY WITH A CARBON FILAMENT ATOM RESERVOIR

PART IV. THE DETERMINATION OF GOLD BY ATOMIC FLUORESCENCE AND ATOMIC ABSORPTION SPECTROSCOPY WITH AN UNENCLOSED ATOM RESERVOIR

J. AGGETT* AND T. S. WEST
Chemistry Department, Imperial College, London, S.W.7 (England)

(Received 21st January 1971)

Previous papers in this series[1-3] have described the development of a carbon filament atom reservoir as an alternative to flame and other non-flame methods of atomisation in atomic absorption and fluorescence spectroscopy and its use for the determination of several elements. The success of the technique has been clearly demonstrated for elements of relatively high volatility (*e.g.* silver, cadmium, lead) and current studies are concerned with extension of its use to the atomisation of less volatile elements. In this paper are reported the results of its application to the determination of gold (m.p. 1063°, b.p. 2600°) which is considerably less volatile than elements previously studied. As an atom reservoir for atomic fluorescence and atomic absorption spectroscopy[1-4] the carbon filament has been found to possess the following advantages

1. ability to handle micro samples,
2. high sensitivity,
3. low background signal.

However, in the only study of matrix effects so far reported[3] a disconcerting number of interferences was observed. The major cause of these was tentatively ascribed to the relatively cool atmosphere above the filament which permitted condensation of the atoms under examination with interfering species. A more detailed examination of matrix effects has been made on the gold system in an attempt to obtain greater understanding of the phenomenon and to limit its occurrence as effectively as possible.

EXPERIMENTAL

Apparatus

Atomic fluorescence and atomic absorption measurements were made with a Jobin-Yvon Model "Delta" spectrophotometer coupled to a Scripto III recorder. The carbon filament assembly, similar to that used by Alder and West[3], was mounted on the base-plate which in the commercial equipment normally holds the burner. In this position it was possible to utilise the burner-height adjustment control for positioning the filament relative to the monochromator slit. Normally the filament

---

* Present address: Chemistry Department, University of Auckland, Auckland, New Zealand.

was mounted longitudinally relative to the optical axis of the monochromator, but in experiments where it was necessary to observe signals close to the filament it was mounted at right angles to the monochromator axis.

The centre of the carbon filament (2 mm diam.) was filed to produce a flat surface 5 mm wide in which samples were placed. The depth of the recess so-formed was 1 mm. This modification was chosen because the reproducibility of sample geometry, which has an important effect on precision, was considerably improved; and because the hot-spot formed on application of power was largely confined to this central region which not only resulted in reduction of background radiation, but also prolonged filament life.

In order to limit radiation from the filament reaching the photodetector, a collimator was placed between the rod and the monochromator slit. The diameter of this collimator was relatively large (8 mm) to ensure that fluorescence signal loss was minimal.

A high-intensity gold hollow-cathode lamp (ASL) was used as source. It was normally operated at the highest currents recommended by the manufacturer. It was mounted above the carbon filament, the light being focussed on the filament with a quartz lens. This arrangement was chosen from spatial considerations. It was found that there was little difference in performance when the source was mounted in front of the sample compartment, but this latter arrangement was less convenient.

The collimator used for atomic absorption measurements was much smaller than that used for atomic fluorescence. Light entered this collimator through a slit 0.5 mm × 2.5 mm placed as close to the filament as practicable and 2 mm above the filament.

Measurement technique

From the results of preliminary experiments the following technique was found to be most suitable for the determination of gold. With argon flowing through the cell at $2\ \mathrm{l\ min^{-1}}$, aqueous samples (1 or 5 μl) were placed in the recess of the filament and dehydrated slowly by operating the filament at low power (*ca.* 1.5 V) for about 10 sec. Heating was discontinued immediately the last trace of moisture had disappeared. At this stage the filament was allowed to cool for 30 sec before atomisation was effected at high power (5–8 V). Unless this cooling period was observed lower signals were obtained.

The procedure for samples in methyl isobutyl ketone was essentially the same as that outlined above except that the initial evaporation did not normally require application of heat.

Reagents

All reagents were of analytical-reagent grade and the distilled water was checked for contamination before use.

Aqueous hydrochloric acid was chosen as the medium for this work and all elements were used as their chloride salts unless otherwise specified.

Samples were transferred to the filament with Drummond micro-pipettes which had been pre-treated with "Repelcote" to minimise surface adsorption.

Extracts of gold(III) in methyl isobutyl ketone were prepared by equilibrating aqueous phases 1 *M* in hydrochloric acid with equal volumes of methyl isobutyl ketone.

RESULTS AND DISCUSSION

Effect of hydrochloric acid concentration on signal

The results of measurements made at different hydrochloric acid concentrations showed that the intensity of the atomic fluorescence signal was not affected by hydrochloric acid at concentrations below 1 M. At higher acidities a slight decrease in intensity was observed. Subsequent data were obtained on solutions which were 10^{-2} M in hydrochloric acid, except for those in interference studies with iron(III) and aluminium(III), where 10^{-1} M acid was used to limit the hydrolysis of these cations. Similar results were found for atomic absorption measurements.

Effect of filament height on signal

It was found that for atomic fluorescence measurements on pure gold(III) solutions, optimal signal–background readings were obtained when the centre of the collimator was 6 mm above the filament. This arrangement was generally used. In the later examination of matrix effects the variation of signal with height was investigated in greater detail with the collimator designed for atomic absorption measurements.

Effect of filament voltage on signal

The manner in which the signal strength, as measured by peak height, varies with the applied filament voltage is illustrated in Fig. 1. The lowest voltage used was the minimum required to vaporise the gold quantitatively. That the gold was completely removed from the filament was demonstrated by the lack of memory effects observed when samples of different concentration were vaporised in turn, and the absence of signals when the filament was heated a second time for a given sample. Minor differences were observed in the behaviour of individual filaments and it is, therefore, necessary to determine the optimal power for each filament before routine use. It can be seen from Fig. 1 that maximum signal is obtained only over a relatively narrow range of applied voltage.

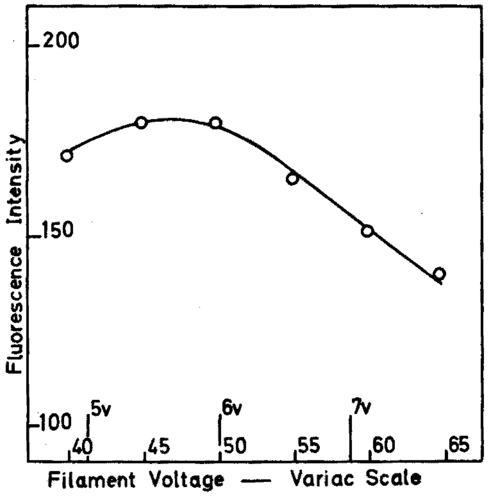

Fig. 1. Fluorescence intensity *vs.* filament voltage.

Detection limits and calibration curves

Under optimal conditions detection limits were determined at 242.8 nm and 267.5 nm (Table I). The data are shown as p.p.m. for 5-μl samples to enable comparison with those of Matousek and Sychra[5] which were obtained with an argon-separated oxy–hydrogen flame. In terms of weight of material detectable, the detection limit is $4 \cdot 10^{-12}$ g at 267.5 nm. Comparison of the two sets of results suggests that, for aqueous solutions, the carbon filament technique is more sensitive than the separated flame in atomic fluorescence although there is little difference in atomic absorption. However, it must be mentioned that quantitative comparison of the fluorescence results is not possible since the present data were obtained with different and probably more sensitive apparatus. There does appear to be one significant difference between our data and that of Matousek and Sychra, *viz.* the difference in sensitivity at 267.5 nm. The lower quantum efficiency which they observed for the 267.5-nm line was attributed to the large (0.47 eV) separation of the two components of the $\sigma_p^2 P^0$ term of gold. The present results do not appear to support this.

TABLE I

DETECTION LIMITS FOR GOLD[a]

Wavelength (nm)	*Carbon filament*[b] *(p.p.m.)*		*H_2–O_2–Ar flame*[5] *(p.p.m.)*
	Aqueous solution	*MIBK extract*	
Atomic fluorescence			
242.8	0.001 ($5 \cdot 10^{-12}$ g)	0.002	0.005
267.5	0.0008 ($4 \cdot 10^{-12}$ g)	0.002	0.02
302.9	20	—	—
Atomic absorption			
242.8	0.04 ($2 \cdot 10^{-10}$ g)	—	0.06

[a] For signal : noise = 2.

[b] 5-μl samples, argon flow 2 l min^{-1}, filament power 6 V.

Typical calibration curves are shown in Fig. 2. All curves showed negative deviations from linearity at higher signal strengths. This is believed to be due to the slowness of the recorder response (about 1-sec full scale deflection). Reproducibility was good provided that the heating cycle was observed strictly. A standard deviation of 1 % was obtained for a series of fifteen 5-μl samples of a 0.1-p.p.m. gold (III) solution delivered with the same pipette.

The poorer detection limits obtained for methyl isobutyl ketone extracts are the result of higher background signals rather than weaker fluorescence signals. At higher concentrations the signals are comparable with those of aqueous solutions.

Origin of the signals

The possibility that the signals arose from scatter was examined by using the platinum line at 265.9 nm and the palladium line at 247.6 nm as sources. No signals were observed for 1-p.p.m. solutions of gold(III) with the detector set at maximal sensitivity and the lamps at maximal currents, which indicates that the signals observed at 267.5 and 242.8 nm originate from atomic fluorescence of gold.

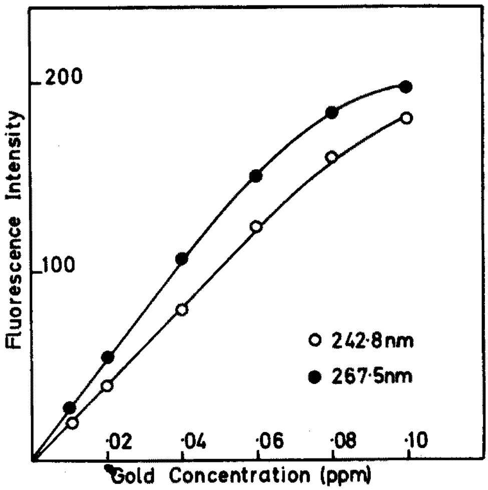

Fig. 2. Calibration curves for aqueous gold(III) solutions.

INTERFERENCE STUDIES

Preliminary interference studies were carried out on solutions of 0.1 p.p.m. gold(III) containing 1000-fold amounts of potential interfering ions. The conditions were identical to those used for experiments on pure gold(III) solutions. The results are listed in Table II. It can be seen that the extent of interference was often less when smaller samples were used. Although most interference data were obtained at 242.8 nm, it was shown for a few ions that the extent of interference at 267.5 nm was very similar.

For those elements which were found to cause interference, plots of interference

TABLE II

INTERFERENCES IN THE a.f.s. DETERMINATION OF GOLD AT 242.8 nm

Element	*% Change of signal*		*Element*	*% Change of signal*	
	5-µl samples	*1-µl samples*		*5-µl samples*	*1-µl samples*
Al	−20	0	Mg	0	0
Ba	0	0	Mn	−20	− 5
Ca	0	0	Mo (MoO_4^{2-})	−30	−15
Cd	0	0	Na	0	0
Ce	−20	− 5	NH_4^+	0	0
Co	−15	0	Ni	−20	− 5
Cr	−40	−15	Pd	−40	−25
Cs	0	0	Pb	−10	0
Cu	−20	− 8	Pt	0	0
Fe	−30	−24	Sr	0	0
Hg	0	0	Tl	0	0
K	0	0	W (WO_4^{2-})	−30	−20
Li	+10	0	Zn	0	0

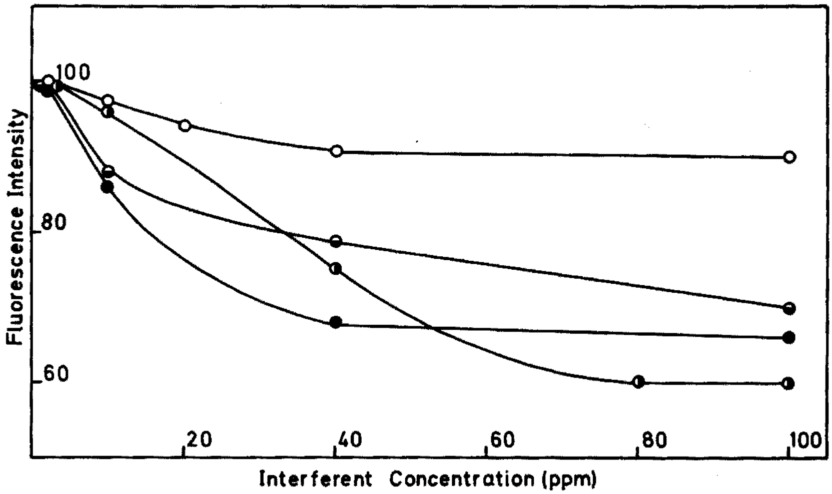

Fig. 3. Degree of interference as function of interfering ion concentration. A 0.1-p.p.m. gold solution was used. (○) Pb; (◐) Cr; (◒) Mo; (●) Fe. Lower sensitivity was used in obtaining these results.

against interfering ion concentration were also prepared. Generally these were of similar form, and a number are shown in Fig. 3.

All the non-interfering elements with the exception of platinum are more volatile than lead, as indicated by their vapour pressures at elevated temperatures[6]. This suggested that interferences occur through loss of atomic population in the vapour phase rather than as a result of a reaction on the filament itself. This idea was supported by the results of the following experiment in which the gold(III) solution and the interfering ion were vaporized from separate filaments.

A sample of gold(III) (5 μl of 0.1-p.p.m. solution) was placed on the upper filament and the interfering ion (5 μl of 100-p.p.m. solution) on the lower filament of the double-filament arrangement shown in Fig. 4, and the two filaments were heated simultaneously. As the data in Table III indicate, interference was still observed despite the fact that the two species were not mixed before vaporization.

Since it had been established that the interferences occur in the vapour phase, the variation in interference with height above the filament was examined. In these

TABLE III

EFFECT OF INTERFERING IONS ON SEPARATE FILAMENT

Interfering element	*Percentage loss of fluorescence signal*	
	Gold and interfering ion on upper filament	*Gold on upper filament. Interfering ion on lower filament*
Co[a]	30	26
Cu[a]	32	22
Pd[b]	24	18

[a] Filament 7 mm below collimator slit.
[b] Filament 5 mm below collimator slit.

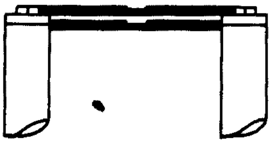

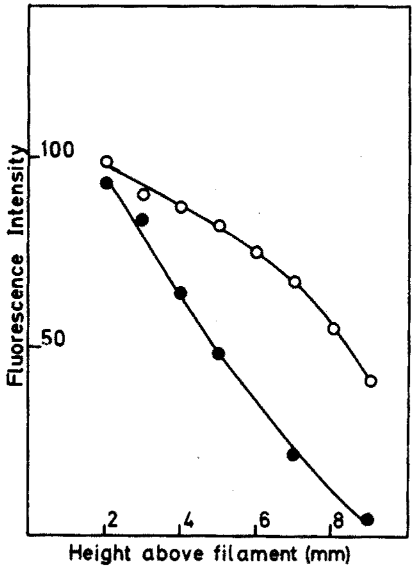

Fig. 4. Double filament arrangement.

Fig. 5. Variation of fluorescence intensity with height above the filament. (○) 0.1 p.p.m. Au; (●) 0.1 p.p.m. Au + 100 p.p.m. W.

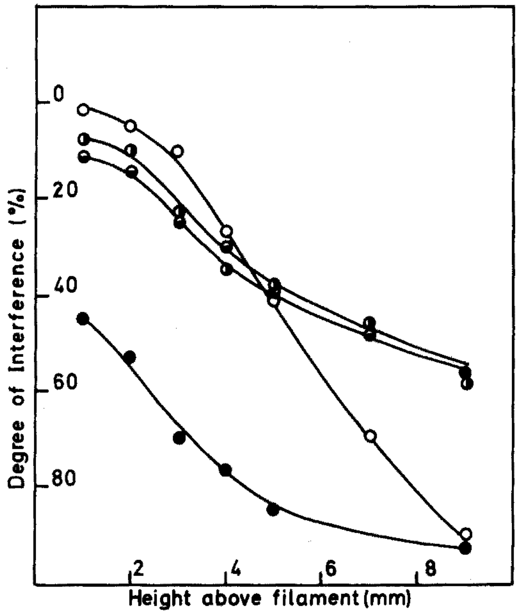

Fig. 6. Variation of degree of interference with height above the filament. (○) 0.1 p.p.m. Au + 100 p.p.m. W; (◑) 0.1 p.p.m. Au + 100 p.p.m. Cu; (◒) 0.1 p.p.m. Au + 100 p.p.m. Co; (●) 0.1 p.p.m. Au + 100 p.p.m. Cr.

experiments the atomic absorption collimator with 0.5 × 2.5 mm slit was used to facilitate a more precise examination, and the filament was mounted at right angles to the monochromator slit to permit measurements immediately above the filament. Typical data from these experiments are shown in Figs. 5 and 6.

In all systems examined, the extent of the interference increased with increasing height, which is consistent with the hypothesis that as the vapour cools the interfering species react with the gold atoms in some way to remove their ability to absorb or emit atomic radiation. That similar interferences occur in atomic absorption suggests that it is the absorption process which is affected. While the exact nature of the process is not known at present, it is possible that the gold atoms might react chemically in the vapour phase to form intermetallic species or simply condense from the atomic state as suggested previously[3]. However, it seems that if intermetallic compound formation were to be involved, a certain chemical affinity among the interferences would be expected and this is not yet apparent. It seems more likely that the gold atoms are simply physically occluded in a host of condensing interferent atoms in much the same manner as occurs in aqueous coprecipitation processes.

From a practical viewpoint it is clear that interferences may be minimised by arranging the light path as close to the filament as is practicable. However, in atomic fluorescence the loss of signal intensity which results from collimation must be balanced against the benefits of lower interference. One of the major factors which influences this compromise is the effective height of observation of the fluorescence signal. In the case of gold it can be seen from Fig. 5 that strong fluorescence is observed several mm above the filament, so that collimation will greatly reduce the observed signal. On the other hand since the atomic fluorescence signal from copper decreases much more rapidly with height, collimation should have less effect on the signal strength for an element such as copper.

Since in atomic absorption it is the ratio of signals which is measured, it should be possible to minimise interferences without loss of sensitivity by using a collimator and slit arrangement with the light path as close as possible to the filament.

Another approach to the problem of interferences was also examined. In this, the argon was preheated in an attempt to raise the temperature of the vapour phase above the filament. For this purpose the double filament arrangement (Fig. 4) was used, the upper filament containing the sample and the lower one supplying the extra heat. With this arrangement a general decrease in the extent of interference was observed. However, this device does not appear as promising in this respect as that recently reported by Amos[4] in which a hydrogen diffusion flame is used to maintain the temperature above the filament.

We are grateful to Jobin-Yvon S. A. for the loan of the spectrophotometer and the Nuffield Foundation for the award of a Travelling Fellowship in Science to J. A.

SUMMARY

The atomic absorption and fluorescence characteristics of gold generated in an argon atmosphere by a carbon filament atom reservoir and a high-intensity hollow-cathode lamp are examined. Strong fluorescence signals at 242.8 and 267.5 nm were observed which yielded detection limits of $5 \cdot 10^{-12}$ and $4 \cdot 10^{-12}$ g (0.001 and 0.0008 p.p.m.), respectively. Much weaker fluorescence was also observed at 302.9 nm. Absorption signals occurred at 242.8 nm with a detection limit of $2 \cdot 10^{-10}$ g (0.04 p.p.m.). The fluorescence sensitivity is better than the best previously reported for an argon-separated oxy–hydrogen flame. Condensation reactions occur in the gas phase and lead to abnormal loss of atomic gold when 1000-fold concentrations of elements such as Ce, Cr, Cu, Fe, Mn, Mo, Ni, Pd and W are present in the gold solution. When, however, the fluorescence signals are measured immediately above the surface of the filament, with restricted field viewing, virtually all these interferences disappear.

RÉSUMÉ

On examine les caractéristiques de fluorescence et d'absorption atomique de l'or, avec réservoir à filament de carbone et une lampe à cathode creuse de forte intensité. On observe de forts signaux de fluorescence à 242.8 et 267.5 nm permettant d'atteindre des limites de détection de $5 \cdot 10^{-12}$ et $4 \cdot 10^{-12}$ g respectivement (0.001 et 0.0008 p.p.m.). On observe également une fluorescence beaucoup plus faible à 302.9 nm. Les signaux d'absorption se trouvent à 242.8 nm avec une limite de détection de $2 \cdot 10^{-10}$ g (0.04 p.p.m.). La sensibilité de fluorescence est supérieure à celle signalée précédemment pour une flamme argon/oxy–hydrogène. Des réactions de condensation se produisent dans la phase gazeuse et conduisent à des pertes anormales d'or atomique, en présence des éléments Ce, Cr, Cu, Fe, Mn, Mo, Ni, Pd et W en concentrations 1000 fois supérieures. Toutes ces interférences peuvent disparaître lorsque la fluorescence est mesurée immédiatement audessus de la surface du filament.

ZUSAMMENFASSUNG

Es wurde das Verhalten von Gold bei der Atomabsorption und -fluoreszenz in einer Argonatmosphäre untersucht. Hierbei wurden eine hochintensive Hohlkathodenlampe und zur Atomisierung eine Kohlenstoffglühfaden-Anordnung eingesetzt. Starke Fluoreszenzsignale wurden bei 242.8 und 267.5 nm beobachtet; sie ergaben Nachweisgrenzen von $5 \cdot 10^{-12}$ bzw. $4 \cdot 10^{-12}$ g (0.001 bzw. 0.0008 p.p.m.). Eine viel schwächere Fluoreszenz wurde bei 302.9 nm festgestellt. Die Absorptionssignale bei 242.8 nm hatten eine Nachweisgrenze von $2 \cdot 10^{-10}$ g (0.04 p.p.m.). Die Fluoreszenzempfindlichkeit ist besser als die beste bisher für eine argongetrennte Sauerstoff–Wasserstoff-Flamme angegebene Empfindlichkeit. Kondensationsreaktionen treten in der Gasphase auf und führen zu einem abnormen Verlust an atomarem Gold, wenn 1000-fache Konzentrationen von Elementen wie Ce, Cr, Cu, Fe, Mn, Mo, Ni, Pd und W in der Goldlösung vorliegen. Wenn jedoch die Fluoreszenzsignale unmittelbar oberhalb der Oberfläche des Glühfadens unter Einschränkung des Beobachtungsfeldes gemessen werden, verschwinden alle diese Störungen.

REFERENCES

1 T. S. West and X. K. Williams, *Anal. Chim. Acta*, 45 (1969) 27.
2 R. G. Anderson, I. S. Maines and T. S. West, *Anal. Chim. Acta*, 51 (1970) 355.
3 J. F. Alder and T. S. West, *Anal. Chim. Acta*, 51 (1970) 365.
4 M. D. Amos, *American Laboratory*, Aug. 1970, p. 33.
5 J. Matousek and V. Sychra, *Anal. Chim. Acta*, 50 (1970) 175.
6 R. H. Perry, C. H. Chilton and S. D. Kirkpatrick, *Chemical Engineers Handbook*, 4th Edn., McGraw Hill, 1963.

Analytica Chimica Acta
Elsevier Publishing Company, Amsterdam
Printed in The Netherlands

MULTI-ELEMENT ATOMIC FLUORESCENCE SPECTROSCOPY

PART IV. THE DETERMINATION OF COBALT AND NICKEL IN STEELS BY ATOMIC FLUORESCENCE SPECTROSCOPY IN A SEPARATED AIR-ACETYLENE FLAME WITH A DUAL-ELEMENT ELECTRODELESS DISCHARGE LAMP*

J. D. NORRIS AND T. S. WEST
Department of Chemistry, Imperial College of Science and Technology, London, S.W.7 (England)

(Received 15th March 1971)

The high sensitivity and selectivity of atomic fluorescence spectroscopy for the determination of traces of a considerable number of metal ions in solution have been illustrated in several publications[1-4]. However, only a very few instances of the application of atomic fluorescence spectroscopy to the analysis of technical materials have been reported[5-11]. In this contribution, the application of the technique to the analysis of a variety of steels for cobalt and nickel with a dual-element excitation source is described.

The atomic fluorescence characteristics of both cobalt[12,13] and nickel [12,14] have been investigated. Fleet, Liberty and West[13] studied cobalt, using a high-intensity hollow-cathode lamp and a cobalt chloride electrodeless discharge lamp as sources. Armentrout[14] has examined nickel using a high-intensity hollow-cathode lamp, and Matousek and Sychra[12] have examined both elements using high-intensity hollow-cathode lamps.

The advantages to be found in the use of multi-element microwave-excited electrodeless discharge lamps as spectral sources for atomic fluorescence spectroscopy have been previously discussed by Marshall and West[15], who prepared Se–Te–Hg–I_2, Cd–Zn and Ga–In sources, and by Fulton, Thompson and West[16], who prepared As–Sb sources. These studies have shown that the combination of two or more elements, or their salts, in the same lamp does not cause more interferences that are found with the corresponding single-element lamps, and that there is no decrease in the line intensity of the source or in the fluorescence intensity obtained upon irradiation of an atomic population of the appropriate species in a flame.

In this paper, the preparation and operation of cobalt–nickel dual-element electrodeless discharge lamps is reported. Their application to the sequential atomic fluorescence determination of cobalt and nickel in steels, with an argon-separated air–acetylene flame is described, and results are given for the analysis of several types of standard steel by this method.

EXPERIMENTAL

Apparatus

A modified "Southern Analytical" A1740 grating flame spectrophotometer,

---

* Part III: *Anal. Chim. Acta*, 51 (1970) 530.

coupled to a "Servoscribe" chart recorder was employed[17]. This instrument is equipped for 20-sec integration and d.c. flame background correction.

An argon-separated air–acetylene flame was used throughout this work. Since the burner supplied with the A1740 spectrophotometer is too large to be converted for flame separation, the burner and burner housing were removed. A Unicam SP 900 air–acetylene burner head and stem were adapted for use with a separated flame, as described elsewhere[18]. The nebuliser unit from a Unicam SP 900 flame spectrophotometer was used in conjunction with the Unicam burner.

The electrodeless discharge lamps were operated at 2450±25 MHz with a "Microtron 200" microwave generator, and a three-quarter wave (Broida type) resonant cavity (Electro-medical Supplies, Ltd., Wantage, Model 210L). Discharge was initiated with a high-frequency Tesla vacuum tester.

Preparation of electrodeless discharge lamps

The general preparation of electrodeless discharge lamps and the equipment required have already been described[19]. The cobalt–nickel dual-element electrodeless discharge lamps were prepared by the following method. A blank tube, *ca.* 40 mm long, was prepared from 8-mm internal bore quartz tubing, and degassed in the usual manner. Cobalt chloride hexahydrate (*ca.* 1 mg; A.R. grade) and nickel chloride hexahydrate (*ca.* 1 mg; A.R. grade) were introduced. The tube was reconnected to the vacuum line, evacuated to *ca.* 0.1 Torr, and heated gently for 5 min, with several flushings of argon to dehydrate the metal chlorides. The dehydrated metal chlorides were sublimed under vacuum *ca.* 20 mm up the walls of the tube. The tube was then pressurised with argon at 4–5 Torr, and sealed. This lamp was conditioned in the microwave cavity for 1 h before use.

Instrumental parameters

The electrodeless discharge lamp was placed as near as possible to the flame (*ca.* 35 mm from the centre of the flame). An asbestos screen, with a slit 30 × 15 mm was placed between the resonant cavity and the flame. It was so arranged that this screen could be moved backwards and forwards to act as a shutter to eliminate irradiation of the flame by the source. The centre of the flame was situated *ca.* 50 mm from the entrance slit of the monochromator.

A slit width of 0.5 mm, corresponding to a band-pass of 3 nm was used. Use was made of the facilities for 20-sec integration.

Both cobalt and nickel emit by thermal processes in the flame at the same wavelengths at which the atomic fluorescence occurs, although in both cases the atomic fluorescence signal is about 100 times greater than the thermal emission signal. In addition to this and the flame background emission, various species present in the steels produce continuum radiation over these wavelengths. Since the A1740 spectrophotometer has a d.c. recording system, the above emission had to be subtracted arithmetically from the sum total of the thermal and fluorescence emissions to obtain the atomic fluorescence signal. By use of the d.c. background correction the thermal emissions could be backed off, thus almost the full scale of the recording potentiometer could be used for the fluorescence signal, and high gains could be used.

A fuel-lean argon-separated air–acetylene flame was used. Optimal gas flow rates were 10 $dm^3\ min^{-1}$ argon, 7 $dm^3\ min^{-1}$ air and 1.1. $dm^3\ min^{-1}$ acetylene. Atomic fluorescence readings were taken between 15 and 35 mm above the burner head.

Reagents

Cobalt stock solution (100 *p.p.m.*). Dissolve 0.4037 g of A.R. grade cobalt chloride hexahydrate in distilled water and dilute to 1 dm^3.

Nickel stock solution (100 *p.p.m.*). Dissolve 0.4049 g of A.R. grade nickel chloride hexahydrate in distilled water and dilute to 1 dm^3.

The acids used were of A.R. grade.

Procedure for the analysis of steel samples

For steels containing *ca.* 0.01% cobalt and/or nickel, weigh out 1.0–1.5 g of the steel into a 100-cm^3 beaker. Add 15 cm^3 of concentrated hydrochloric acid and 7.5 cm^3 of concentrated nitric acid, cover with a watch glass and heat to dissolve in the usual way. When all of the steel has dissolved, dilute to *ca.* 50 cm^3 and filter through a filter paper, collecting the filtrate in a 100-cm^3 volumetric flask. Wash the beaker and filter paper thoroughly and dilute the filtrate and washings to volume with distilled water. For steels of different cobalt and/or nickel concentrations take proportionate weights of sample, or carry out dilutions, so that the final solution contains *ca.* 1 p.p.m. of cobalt or nickel. In certain cases, different quantities of acid will be required to dissolve the steel, depending on the major constituents of the steel.

To prepare the calibration solutions transfer 10 cm^3 of the stock solution to a 100-cm^3 volumetric flask and dilute to volume with distilled water. Transfer 0-, 5-, 10-, 15- and 20-cm^3 aliquots of this solution to a series of 100-cm^3 volumetric flasks. Add 15 cm^3 of hydrochloric acid and 7.5 cm^3 of nitric acid to each flask and dilute to volume with distilled water. If the quantities of the acid used to dissolve the steel samples are different from those stated, the standard solutions should be prepared to contain corresponding amounts of acid.

Initiate the electrodeless discharge lamp and allow it to stabilise for 10 min at 60-W incident power. Nebulise the standard and sample solutions into the argon-separated air–acetylene flame as required. With the asbestos screen placed to prevent irradiation of the flame by the source, adjust the d.c. background correction control to reduce the integrated background signal to a low value. Note this reading, move the asbestos screen to allow irradiation of the flame and measure the combined integrated fluorescence and background signal. Subtract the background reading from the combined signals to obtain the fluorescence of cobalt at 240.7 nm and nickel at 232.0 nm.

As in all emission methods, standards should be run alongside unknown solutions periodically. The calibration curves obtained as described above are linear over the range up to 2 p.p.m. and pass through the origin.

RESULTS AND DISCUSSION

Operation of electrodeless discharge lamps

The electrodeless discharge lamps were an intense blue in colour, and showed the main spectral lines of cobalt and nickel. The cobalt 240.7-nm and nickel 232.0-nm resonance lines were of approximately equal intensity. In certain tubes, OH bands between 305 and 315 nm were observed. Their presence was probably due to failure to obtain complete dehydration of the metal chlorides used in the preparation of the tubes. The presence of the OH bands did not interfere with the efficiency of these lamps.

The operating characteristics of the dual-element lamps (power and intensity plots, power and fluorescence plots, stabilities and limits of detection, for the cobalt 240.7-nm resonance line and the nickel 232.0-nm resonance line) were compared with those of single-element cobalt and nickel electrodeless discharge lamps, prepared in a similar manner from the hydrated metal chlorides. No significant differences were observed in the operation of dual-element and single-element electrodeless discharge lamps.

The optimal incident power for the operation of the cobalt–nickel dual-element electrodeless discharge lamps was 60 W. At this power, the stabilities over a period of 1 h were within ±3% for all of the lamps used in this work, at both 240.7 nm and 232.0 nm. After the initial running-in period, a warm-up time of *ca.* 10 min was required when the discharge was initiated from the cold.

Calibration data and detection limits

Calibration curves for cobalt at 240.7 nm and for nickel at 232.0 nm are given in Fig. 1. Limits of detection were 0.01 p.p.m. for cobalt and 0.02 p.p.m. for nickel. Because of the use of integration, the limit of detection was defined as the concentration of cobalt or nickel in aqueous solution which produced a signal equivalent to twice the standard deviation in signal near the lower limit of the calibration curve.

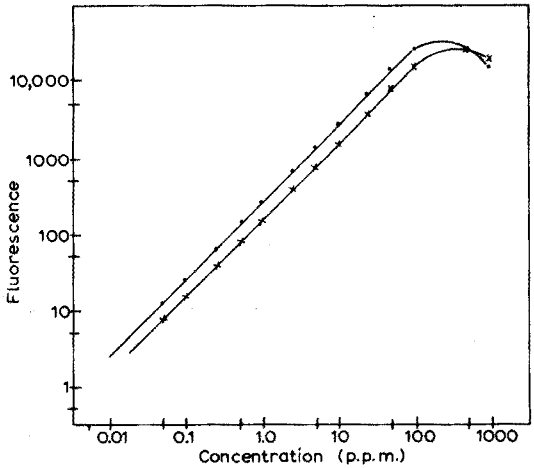

Fig. 1. Atomic fluorescence calibration for cobalt (●) at 240.7 nm and nickel (×) at 232.0 nm (p.p.m. refers to the measured solution).

Interferences and matrix effects

No interference (*i.e.* less than ±1% deviation in signal) was observed in the atomic fluorescence of 5 p.p.m. of cobalt from a 100-fold (weight) amount of nickel, and in the atomic fluorescence of 5 p.p.m. of nickel from a 100-fold (weight) amount of cobalt.

The effects on the atomic fluorescence of 5 p.p.m. of cobalt and 5 p.p.m. of nickel produced by the presence of 100-fold (weight) amounts of twenty-four elements commonly found in steels (*viz.* Al, As, B, Bi, Ca, Cd, Cr, Cu, Mg, Mn, Mo, Nb, P, Pb, S, Sb, Si, Sn, Ta, Ti, V, W, Zn, Zr) were examined. No interference (*i.e.* less than ±3%

deviation in signal) was observed with any of these elements.

The effects of a 10,000-fold (weight) amount of iron on the atomic fluorescence of 2 p.p.m. of cobalt and 2 p.p.m. of nickel were investigated. In both cases there was a decrease in the atomic fluorescence signal of less than 2%. This was not considered sufficiently significant to warrant further investigation of the effect of iron on the atomic fluorescence of cobalt and nickel. However, in the case of steels containing less than 0.01% of either nickel or cobalt a larger sample would be dissolved and it would be advisable to remove most of the iron, by a preliminary solvent extraction with amyl acetate or isobutyl acetate from strong hydrochloric acid solutions before carrying out the determination.

The effect of the acids used in the dissolution of the steel samples was also examined. Cobalt and nickel standards (5 p.p.m. of each metal) were prepared in 10% (v/v) nitric acid and 20% (v/v) hydrochloric acid solution. (This was the highest acid concentration necessary to dissolve any of the steel samples used in this work.) The atomic fluorescence signals obtained from these solutions were compared with those of normal aqueous solutions containing 5 p.p.m. of cobalt and 5 p.p.m. of nickel. The atomic fluorescence of the acid solutions was *ca.* 5% less than that of the aqueous solutions at both 240.7 nm and 232.0 nm. This effect was attributed to the higher surface tension and viscosity of the acid solutions reducing the efficiency of nebulisation compared to normal aqueous solutions. This showed the need for preparing the standard solutions with approximately the same acid concentration as the sample solutions.

Analysis of steel samples

The results obtained for the determination of cobalt and nickel in a variety of different types of standard steel, mostly from the B.C.S. range (Bureau of Analysed Samples Ltd., Middlesborough), are given in Table I, together with the certificate values. One sample of each steel was weighed and dissolved and four atomic fluorescence readings were taken and averaged to obtain these results.

The precision of the method was investigated for one of the standard steels (B.C.S. 277 Mild steel). Seven samples of this steel were weighed and dissolved. Four atomic fluorescence readings were taken and averaged for each of these samples, to obtain the results from which the ranges and standard deviations were calculated. These data are given in Table II.

These results show that atomic fluorescence spectroscopy, particularly with a dual-element source, has considerable merit as a means of analysing steels for their cobalt and nickel content. The procedure is extremely simple, consisting of sample dissolution, dilution and direct aspiration into the flame. A separated flame was used since this considerably lowers the background emission from the flame and allows higher instrumental gains to be used. Argon was preferred to nitrogen as the separating gas because of its lower quenching cross-section. It is not necessary to use large amounts of the separating gas since it is only turned on during actual measurements. At all other times the flame may be burned normally.

The cobalt–nickel dual-element electrodeless discharge lamp is not difficult to construct and is stable in operation if it is not over-run. After dissolution of the sample, an analysis only requires *ca.* 3 min to complete and the results obtained are precise and accurate.

TABLE I

DETERMINATION OF COBALT AND NICKEL IN STEELS

Sample	*Cobalt*		*Nickel*	
	Standard analysis[a]	*A.F.S.*	*Standard analysis*[a]	*A.F.S.*
B.C.S. 277 Mild steel	0.125	0.127	0.233	0.233
B.C.S. 273 Mild steel	0.021	0.020	0.031	0.030
B.C.S. 271 Mild steel	0.012	0.010	0.013	0.014
B.C.S. 225 Ni–Cr–Mo steel	0.01	0.010	1.67	1.64
B.C.S. 225/2 Ni–Cr–Mo steel			1.43	1.43
B.C.S. 406 Low-alloy steel			1.69	1.67
B.C.S. 407 Low-alloy steel			0.61	0.60
B.C.S. 328 Mild steel	0.17	0.168		
B.C.S. 260/3 High-purity iron	0.010	0.011	0.004	0.005
B.C.S. 334 Austenitic stainless steel	0.052	0.052	20.6	20.5
B.C.S. 341 Ferritic stainless steel			0.56	0.56
B.C.S. 483 High-speed steel	1.94	1.93		
3857y Stainless steel	0.66	0.67	2.07	2.08
3924y Stainless steel	0.36	0.38	0.82	0.84
7120 (08891) Stainless steel	0.027	0.027	0.24	0.237

[a] B.C.S. certificate value for B.C.S. samples. The remaining three samples had been analysed by "Quantovac" emission spectrography.

TABLE II

RANGES AND STANDARD DEVIATIONS FOR THE ATOMIC FLUORESCENCE DETERMINATION OF COBALT AND NICKEL IN STEEL (B.C.S. 277)

	Cobalt	*Nickel*
Certificate value	0.12 (5)	0.23 (3)
Mean value of atomic fluorescence analysis	0.127	0.233
Range in certificate values	0.119–0.137	0.227–0.242
Range by A.F.S.	0.120–0.133	0.225–0.237
Standard deviation (%) by A.F.S.	3.5	2.0

We are grateful to the S.R.C. for the award of a grant to one of us (J.D.N.) and to Mr. B. Bagshawe of Firth Brown Research Laboratories, Sheffield, for providing several of the steel samples and for the analysis of others. We also thank Southern Analytical Ltd. for the loan of the A1740 flame spectrophotometer.

SUMMARY

The atomic fluorescence determination of cobalt and nickel in a variety of mild, alloy, high-speed and stainless steels is described. The fluorescence of cobalt and nickel at 240.7 and 232.0 nm, respectively, is excited by a dual-element electrodeless discharge lamp, the construction of which is described. An argon-separated air–acetylene flame is used. The dissolved steel sample is aspirated directly into the flame and the cobalt and nickel are read sequentially from calibration curves prepared from pure cobalt and nickel solutions containing approximately the same concentration of acids. The method is rapid, precise and accurate. Over 20 other common trace and minor metal constituents of steels do not interfere with the procedure nor does the matrix element (iron).

RÉSUMÉ

On décrit une méthode de dosage du cobalt et du nickel par fluorescence atomique, dans divers types d'acier. La fluorescence du cobalt et du nickel, respectivement à 240.7 et 232.0 nm, est excitée par une lampe à décharge, à double élément, dont on décrit la construction. On utilise une flamme argon/air–acétylène. L'échantillon d'acier, mis en solution, est aspiré directement dans la flamme. La méthode est rapide, précise et exacte. Plus de 20 autres constituants métalliques des aciers ne gênent pas, de même que le métal de base (fer).

ZUSAMMENFASSUNG

Es wird die Bestimmung von Kobalt und Nickel in weichen, legierten, Schnelldreh- und Edelstählen durch Atomfluoreszenz beschrieben. Die Fluoreszenz von Kobalt und Nickel bei 240.7 bzw. 232.0 nm wird mit einer elektrodenlosen Zweielement-Entladungslampe angeregt; deren Aufbau wird beschrieben. Es wird eine argongetrennte Luft–Acetylen-Flamme verwendet. Die aufgelöste Stahlprobe wird direkt in die Flamme gesprüht und der Gehalt an Kobalt und Nickel nacheinander an Hand von Eichkurven ermittelt, die mit reinen Kobalt- und Nickellösungen mit annähernd denselben Säurekonzentrationen erstellt worden sind. Die Methode ist schnell, reproduzierbar und genau. Über 20 andere der üblichen Spuren- und Nebenbestandteile von Stählen und auch das Matrixelement (Eisen) stören nicht.

REFERENCES

1 J. D. Winefordner and T. J. Vickers, *Anal. Chem.*, 36 (1964) 161.
2 J. D. Winefordner and R. A. Staab, *Anal. Chem.*, 36 (1964) 165.
3 R. M. Dagnall, K. C. Thompson and T. S. West, *Anal. Chim. Acta*, 36 (1966) 269.
4 R. M. Dagnall, K. C. Thompson and T. S. West, *Talanta*, 14 (1967) 557.
5 R. Klaus, *Z. Klin. Chem.*, 4 (1966) 299.
6 T. J. Vickers and S. P. Merrick, *Talanta*, 15 (1968) 873.
7 R. Smith, C. M. Stafford and J. D. Winefordner, *Can. Spectrosc.*, 14 (1969) 38.
8 J. Matousek and V. Sychra, *Anal. Chim. Acta*, 49 (1970) 175.
9 G. F. Kirkbright, P. Rao and T. S. West, *Anal. Lett.*, 2 (1969) 465.
10 V. Sychra and J. Matousek, *Anal. Chim. Acta*, 52 (1970) 376.
11 D. H. Cotton and D. R. Jenkins, *Spectrochim. Acta*, 25B (1970) 283.
12 J. Matousek and V. Sychra, *Anal. Chem.*, 41 (1969) 518.
13 B. Fleet, K. V. Liberty and T. S. West, *Anal. Chim. Acta*, 45 (1969) 205.
14 D. N. Armentrout, *Anal. Chem.*, 38 (1966) 1235.
15 G. B. Marshall and T. S. West, *Anal. Chim. Acta*, 51 (1970) 179.
16 H. A. Fulton, K. C. Thompson and T. S. West, *Anal. Chim. Acta*, 51 (1970) 373.
17 M. S. Cresser and T. S. West, *Spectrochim. Acta*, 25B (1970) 61.
18 R. S. Hobbs, G. F. Kirkbright, M. Sargent and T. S. West, *Talanta*, 15 (1968) 997.
19 R. M. Dagnall, K. C. Thompson and T. S. West, *Talanta*, 14 (1967) 551.

Analytica Chimica Acta
Elsevier Publishing Company, Amsterdam
Printed in The Netherlands

THE DETERMINATION OF TRACE AMOUNTS OF LANTHANUM IN LOW-ALLOY STEELS BY FLAME EMISSION SPECTROPHOTOMETRY

M. E. HOFTON, D. P. HUBBARD AND F. VERNON
Department of Chemistry, Sheffield Polytechnic, Pond Street, Sheffield, S1 1WB (England)

(Received 26th March 1971)

The presence of trace amounts of rare earth elements improves the ductility and impact strengths of heat-treated carbon steels[1,2] and also potentially aids in successful deoxidation and desulphurisation of the steel. Lanthanum is present in certain steels after Mischmetal addition, usually at less than the 0.005% level.

Atomic absorption spectrophotometry does not provide the sensitivity required for the determination of lanthanum at this level of concentration[3-5]. For example, Amos and Willis[5] quote a 1% absorption value of 100 p.p.m. in a nitrous oxide–acetylene flame at the 392.8-nm line. Flame emission spectrophotometry, however, has been employed for the determination of lanthanum. Ishida[6] determined lanthanum in minerals and glasses using the oxide band emission at 440 and 560 nm and an air–acetylene flame. Menis *et al.*[7] studied the flame spectrophotometric determination in an oxygen–acetylene flame. These workers obtained sensitivities for the various oxide bands in aqueous, aqueous methanolic, and 4-methyl-2-pentanone (hexone) solutions and concluded that 743 and 791 nm were suitable wavelengths to use, partly because of the very small background radiation of the flame and partly because interferences were lessened at these wavelengths. They also suggested an extraction at pH 1.5 with 2-thenoyltrifluoroacetone (TTA) before extraction of lanthanum with TTA in hexone from an acetate buffer at pH 5.0 when thorium, uranium, copper and iron are present as major components. A 100-fold increase in sensitivity was obtained when the organic phase was sprayed into the oxygen–acetylene flame compared with when an aqueous solution was sprayed.

It was decided to investigate the possibility of determining lanthanum in steels by flame emission spectrophotometry in an air–acetylene flame. Iron and nickel were found to interfere severely with the lanthanum emission intensity both from aqueous solution and from hexone solution after extraction with TTA. No simple solvent extraction or precipitation procedure could be designed to overcome these interferences and therefore mercury cathode electrolysis was attempted. Traces of iron and nickel remained in solution after electrolysis for 1 h and these still caused interference. However, under the conditions selected for the extraction of lanthanum as the TTA complex into hexone, the residual iron and nickel were extracted only to a small extent. It was therefore possible to make use of a "blank" extraction from solution of pH 2.5 to overcome this slight interference. Manganese, which is not quantitatively deposited in mercury, also interferes but this can be removed by a simple chemical procedure following the electrolysis. The method was applied to the recovery of lanthanum added to B.C.S. steels and to the determination of lanthanum in steels of known lanthanum content.

EXPERIMENTAL

Apparatus

A Unicam SP90 atomic absorption spectrophotometer was used in the emission mode with a Meker burner for air–acetylene.

Electrochemical analyzer (Baird and Tatlock).

Standard instrumental conditions

Wavelength 743 nm
Slit width 0.10 mm
Burner height 15 mm
Air pressure 30 p.s.i.; flow 5 l min^{-1}
Acetylene pressure 5 p.s.i.; flow 0.4 l min^{-1}.

Reagents

All the reagents used were of analytical-reagent grade.

Standard lanthanum solution (100 *p.p.m.*). Dissolve 0.117 g of high-purity lanthanum oxide in the minimum amount of 2 *M* nitric acid and evaporate just to dryness. Dissolve the residue in water and dilute to 1 l. Store in a polythene bottle.

Mixed acid. Mix 3 parts of water, 6 parts of concentrated nitric acid and 1 part of concentrated sulphuric acid.

Analysis of low-alloy steels

Dissolve 1.00 g of the alloy in 40 ml of mixed acid, evaporate to dryness and dissolve the residue in 25 ml of water. Evaporate to dryness and dissolve the residue in 25 ml of 10 % (v/v) sulphuric acid. Cool and dilute to 150 ml with water. Add 50 ml of mercury and electrolyse for 90 min at a current of 5 A. Evaporate the aqueous solution to *ca.* 50 ml, add 5 ml of 0.1 *M* silver nitrate and 10 ml of 10 % (w/v) ammonium persulphate solution, and simmer for 5 min. Cool, add 50 % (w/v) sodium hydroxide solution until alkaline, add a further 2 ml and simmer for 1 min. Cool and filter through No. 541 filter paper. Wash the beaker and filter paper twice with 1 % (w/v) sodium hydroxide solution and several times with water. Finally wash the filter paper with 75 ml of hot 5 % (v/v) nitric acid solution. Add 5 ml of concentrated hydrochloric acid to the filtrate and simmer. Filter through No. 541 filter paper and wash the precipitate twice with 5 % (v/v) hydrochloric acid solution. Evaporate the solution to dryness, cool and redissolve in 5 ml of water.

Add 10 ml of 1 *M* ammonium acetate solution, adjust the pH to 5.0 with 2 *N* nitric acid or 2 *N* ammonia solution and transfer to a separating funnel. Add 10 ml of 0.02 *M* TTA in hexone and shake for 30 sec. Allow the two phases to separate. Transfer the aqueous phase to another separating funnel and adjust the pH to 2.5 by adding a predetermined quantity of 1 *M* hydrochloric acid*. Add 10 ml of 0.02 *M* TTA in hexone and shake for 30 sec. Dry both organic phases over sodium sulphate and spray each into the flame. Subtract the emission reading of the extract of the pH 2.5 solution from the emission reading of the extract of the pH 5.0 solution, and read off the lanthanum content from the calibration graph.

Preparation of calibration graph

Transfer 0, 2, 4, 6 and 8 ml of 10-p.p.m. lanthanum solution (prepared by appropriate dilution of the standard lanthanum solution) into a series of separating

---

* Adjust the pH to 2.5, in the first instance, by dropwise addition of 1 *M* hydrochloric acid from a burette. The amount added can be used for all subsequent additions at this stage.

funnels, add 10 ml of 1 *M* ammonium acetate solution and continue as described above. The calibration curve is linear for 0–8 p.p.m. of lanthanum in the organic layer.

RESULTS AND DISCUSSION

Preliminary investigations in aqueous solution

A preliminary study of the sensitivities of various lanthanum oxide band emissions (442, 544, 562, 585, 743 and 785 nm) in the air–acetylene flame showed that the bands at 442, 544 and 562 nm were the most sensitive but the emission intensity obtained at 743 nm gave the most stable reading. This is in agreement with the results of Menis *et al.*[7] who used oxy–acetylene flames. In view of this and the prospect of less interference, 743 nm was selected for further study. Optimal conditions in aqueous solution were essentially the same as those given in the experimental section except that the optimal acetylene flow was 0.8 $l\ min^{-1}$ and the optimal burner height was 20 mm. Large excesses of chromium and nickel caused severe interference at 743 nm as well as at 445 and 542 nm. It was obvious that, although sufficient sensitivity was obtainable from aqueous solutions, interference from elements commonly found in steels would present many problems.

Extraction of lanthanum with 2-thenoyltrifluoroacetone (TTA) into hexone

Poskanzer and Foreman[8] have summarized the extraction of many metals with TTA from acetate solution into hexone. They found that lanthanum was completely extracted by a solution of 0.1 *M* TTA in hexone from a 1 *M* acetate solution buffered at pH 5. A prior extraction at pH 1.5 was recommended when large amounts of iron were present. In the present work it was found desirable to extract with 0.02 *M* TTA in hexone as, on spraying the more concentrated solution, instability of the emission readings and capillary blockage occurred.

Quantitative extraction of up to 100 μg of lanthanum into 10 ml of 0.02 *M* TTA in hexone was obtained on shaking the 2 phases for 30 sec. A hexone extract containing 5.0 p.p.m. of lanthanum gave an emission intensity reading of 52 divisions on the recorder. This corresponds to a sensitivity of 0.096 p.p.m. of lanthanum per scale division (1 mV) and is an approximately 5-fold increase in sensitivity over that obtainable from aqueous solution.

Interference from chromium, nickel and iron

If a 1-g sample weight is taken, a steel containing 0.01% of lanthanum extracted into 10 ml of hexone gives a solution containing 10 p.p.m. of lanthanum. On addition of chromium, nickel and iron, in amounts corresponding to up to 5, 5 and 60% respectively in steel, to the aqueous solution before extraction, severe interference was found from chromium(III), nickel, iron(II) and iron(III). Chromium(VI) caused no interference. Chromium(III) caused suppression of the lanthanum signal whereas both nickel and iron(II) caused enhancement. Experiment showed that the interference of nickel on lanthanum was purely of a spectral type. In the case of iron(III), the interference followed an unusual pattern. The results indicated that iron(III) inhibited the extraction of lanthanum in addition to interfering spectrally. It was obvious, therefore, that traces of nickel and iron interfered with the proposed procedure and needed to be removed before the extraction of lanthanum.

Removal of interfering elements

Solvent extraction. Nickel and iron are extracted by TTA throughout the acidic pH range but the number of extractions required for complete removal is too great to make a preliminary extraction an attractive proposition. Other systems were investigated, including thiocyanate for iron and dimethylglyoxime for nickel, but either too many extractions were required for complete removal or lanthanum was lost in the process.

Precipitation. Ammonia was used to separate the insoluble lanthanum hydroxide from the soluble nickel tetrammine complex, but some nickel was retained in the hydroxide precipitate even after a double precipitation and caused interference with the lanthanum emission intensity after extraction. Carron *et al.*[9] have described a separation technique based on the precipitation of rare earth oxalates with calcium as carrier. This technique was attempted but met with little success, as enough nickel oxalate was formed to cause interference in the subsequent extraction and determination of lanthanum.

Mercury cathode electrolysis. Mercury cathode electrolysis removes quantitatively several of the elements likely to be found in steels, *e.g.* iron, chromium, nickel, molybdenum[10]. Elements such as aluminium and rare earths are not deposited in the mercury and remain completely in solution. Indeed, this separation technique forms part of the British Standard Method for the determination of aluminium in steels[11]. Electrolysis from dilute sulphuric acid at a current of 5 A, removed almost completely iron, nickel, chromium and molybdenum in the amounts likely to be present in steel from a 1-g sample. However, when the initial amounts of iron and nickel were 1 g and 0.05 g, respectively, 140 μg of iron and 25 μg of nickel were detected in the aqueous solution even after electrolysis for 3 h.

These trace amounts of iron and nickel were not enough to interfere with the determination of lanthanum when each element was present separately. However, the presence of sulphate ion inhibited the extraction of lanthanum as its TTA complex. Manganese was not quantitatively removed from solution by electrolysis and interfered with the lanthanum emission. Aluminium, which is not electrodeposited, also caused interference. After the electrolysis stage, therefore, it was necessary to separate lanthanum from sulphate ions, manganese and aluminium. Manganese was oxidised to permanganate with ammonium persulphate, and lanthanum hydroxide was precipitated with silver as a carrier. The silver was subsequently removed by precipitation as chloride, leaving a solution containing rare earths in addition to minute traces of other metals. Lanthanum was extracted into hexone as its TTA complex after the mercury cathode electrolysis stage and chemical separation. At this point, it was found that although trace amounts of iron and nickel, remaining after electrolysis, did not cause interference when present individually, some kind of cumulative interference was observed when these elements were present together as in a steel sample. This small interference was eliminated by use of a blank extraction.

Blank extraction

Lanthanum is extracted from aqueous solution by TTA into hexone at pH values greater than 3 and quantitatively at pH 5. An extraction at pH 5 extracts all the lanthanum plus small quantities of iron and nickel. Approximately 15% of the nickel and 4% of the iron were found to be extracted by 0.02 *M* TTA into hexone from

TABLE I

RECOVERY OF LANTHANUM ADDED TO STANDARD STEELS

Alloy	*Lanthanum added* (%)	*Lanthanum found* (%)
BCS 255/1	0.0010	0.0009
BCS 329	0.0030	0.0029
BCS 251/1	0.0040	0.0041
BCS 215/2	0.0050	0.0053

aqueous solution of pH 5. The percentage extractions for iron and nickel did not vary much over the whole acid pH range. Although it has been stated above that the interference of iron was rather unusual, certainly at these levels it was completely spectral and was definitely not an inhibiting one. By carrying out a second extraction at pH 2.5, one obtains a hexone extract containing no lanthanum and amounts of iron and nickel approximately equal to the amounts present in the lanthanum extract from the pH 5 solution. The difference in emission from these two solutions when sprayed into the flame is due solely to the lanthanum content of the solution.

Recovery of lanthanum by the proposed method

Lanthanum was added to four British Chemical Standard Steels and the steels were subjected to the proposed method. Table I shows the recoveries of lanthanum obtained. The amounts of lanthanum added and found are shown as equivalent per cent in the steel.

TABLE II

THE DETERMINATION OF LANTHANUM IN LOW-ALLOY STEELS

Alloy	*Lanthanum content* (%)[a]	*Proposed method* (%)
A1	0.0010	0.0013
A2	0.0020	0.0018
A3	0.0015	0.0014
A4[b]	0.0010	0.0008

[a] Values provided by the British Steel Corporation. Total rare earth content was determined by oxalate precipitation, cerium was isolated and determined by oxalate precipitation, and the difference quoted as lanthanum.

[b] High-speed steel.

Application to low-alloy steels

Results for the determination of lanthanum in three low-alloy steels and one high-speed steel by the proposed method are shown in Table II. These results are considered perfectly satisfactory. Although the method involves mercury cathode electrolysis there seems no reason why it should not be acceptable to the steel industry since the currently accepted method for aluminium involves this separation technique. With regard to time of analysis, six samples can be analysed in rather less than a working day.

The authors acknowledge with thanks B.S.C. (Special Steel Products Division) for provision of the steel samples and for a maintenance grant for one of us (M.E.H.).

SUMMARY

A method is described for the determination of 0.001–0.008 % of lanthanum in steels by flame emission spectrophotometry. After sample dissolution the bulk of the interfering elements are removed by mercury cathode electrolysis. A hydroxide precipitation of lanthanum with silver as carrier is followed, after dissolution of the precipitate, by extraction as its 2-thenoyltrifluoroacetone complex into isobutyl methyl ketone from aqueous solution buffered at pH 5. The organic phase is sprayed into an air–acetylene flame and the emission intensity measured at 743 nm. A "blank" extraction from aqueous solution of pH 2.5 is used to eliminate slight interferences from iron and nickel remaining after the electrolysis stage.

RÉSUMÉ

On décrit une méthode pour le dosage du lanthane dans les aciers (0.001 à 0.008%) par spectrophotométrie d'émission de flamme. On élimine les éléments pouvant gêner par électrolyse sur cathode de mercure. On procède ensuite à une précipitation d'hydroxyde de lanthane en présence d'argent, comme entraîneur, dissolution du précipité et extraction sous forme de son complexe avec la 2-thénoyltrifluoroacétone dans l'isobutylméthylcétone, en milieu tampon pH 5. La phase organique est vaporisée dans une flamme air–acétylène; l'intensité de l'émission est mesurée à 743 nm. On effectue une extraction à blanc à pH 2.5 pour éliminer les légères interférences du fer et du nickel restant après électrolyse.

ZUSAMMENFASSUNG

Es wird eine Methode zur Bestimmung von 0.001–0.008% Lanthan in Stählen durch Flammenemissionsspektrophotometrie beschrieben. Nach Auflösung der Probe wird die Hauptmenge der störenden Elemente durch Elektrolyse mit einer Quecksilberkathode entfernt. Das Lanthan wird mit Silber als Träger als Hydroxid gefällt und nach Wiederauflösung des Niederschlages als 2-Thenoyltrifluoraceton-Komplex aus wässriger, auf pH 5 gepufferter Lösung mit Methylisobutylketon extrahiert. Die organische Phase wird in eine Luft–Acetylen-Flamme gesprüht und die Emissionsintensität bei 743 nm gemessen. Durch "Blind"-Extraktion aus wässriger Lösung von pH 2.5 werden geringe Störungen durch Eisen und Nickel, die nach der Elektrolysestufe verblieben sind, eliminiert.

REFERENCES

1 G. A. Lilliequist and C. G. Michelson, *J. Metals*, 4 (1952) 1024.
2 C. D. Berry and A. A. Dorvel, *Amer. Foundryman*, 20 (1951) 45.
3 Perkin-Elmer Corp., *Analytical Methods for Atomic Absorption Spectrophotometry*, 1965.
4 J. W. Anderson, *5th Nat. Meeting, S.A.S., Chicago, 1966.*
5 M. D. Amos and J. B. Willis, *Spectrochim. Acta*, 22 (1966) 1325.
6 R. Ishida, *J. Chem. Soc. Japan, Pure Chem. Sect.*, 76 (1955) 60.
7 O. Menis, T. C. Rains and J. A. Dean, *Anal. Chem.*, 31 (1959) 187.
8 A. M. Poskanzer and B. M. Foreman Jr., *J. Inorg. Nucl. Chem.*, 16 (1961) 323.
9 M. K. Carron, D. L. Skinner and R. E. Stevens, *Anal. Chem.*, 27 (1955) 1058.
10 R. C. Overbeck and D. L. Chase, *Anal. Chem.*, 23 (1951) 1134.
11 *B.S. No. 1121, Part 35*, 1967.

Analytica Chimica Acta
Elsevier Publishing Company, Amsterdam
Printed in The Netherlands

EXCITATION EFFICIENCIES OF DIFFERENT X-RAY TUBE TARGETS FOR SOME LOW-ENERGY X-RAY SPECTRAL LINES*

C. J. TOUSSAINT

Chemistry Division, Euratom C.C.R., Ispra (Italy)

(Received 18th January 1971)

In order to secure the maximum intensity of X-ray fluorescence when demountable X-ray tubes are used, it is necessary to know the intensities of radiation of different wavelengths emitted by X-ray tubes with various targets. This is particularly true in the case of soft X-ray fluorescence analysis, where it is necessary to estimate quantitatively the anode which will give the best fluorescence excitation of the element under consideration.

Moreover, by making use of the results obtained for the demountable tube, suitable materials for the anodes of sealed X-ray tubes, which operate in the long-wavelength (> 4 Å) region of the spectrum can be predicted.

Work previously reported has been concerned with the efficiency of excitation of the Al Kα spectrum from a pure aluminium sample as a function of target material, primary beam filtration and X-ray tube voltage[1], and with the effect of various anode elements and X-ray tube window materials on the excitation of potassium, silicon and aluminium[2]. The effects of varying the X-ray tube target, the target take-off angle, the tube voltage and the tube window thickness on the excitation efficiency of chlorine and magnesium have also been studied[3]. The present paper reports experimental measurements on the excitation efficiency for the Kα spectra of the elements chlorine through magnesium as a function of primary beam filtration, tube voltage and target material.

EXPERIMENTAL

The experimental arrangement was that of the standard C.G.R. cristallobloc 31 fluorescence spectrograph, with a demountable tube[4], vacuum path, flow counter (2 μm mylar window) and standard pulse-discrimination circuits. Figure 1 shows schematically the basic arrangement used. Targets of chromium, iron, cobalt, nickel, copper, molybdenum, silver, tungsten, platinum and gold were used. Intensity measurements of the Kα spectrum for the elements chlorine, sulphur, phosphorus, silicon, aluminium and magnesium were made at the peak and at the background a few degrees θ away from the peak. The general operating conditions are given in Table I.

The excitation voltage of 30 kV (with no filter between target and sample) for the Mg Kα line was chosen after consideration of the results reported by Short and

---

* Presented by G. Vos at the 7ème Colloque d'Analyse par Diffractométrie et Spectrométrie X, Lyon, 1968.

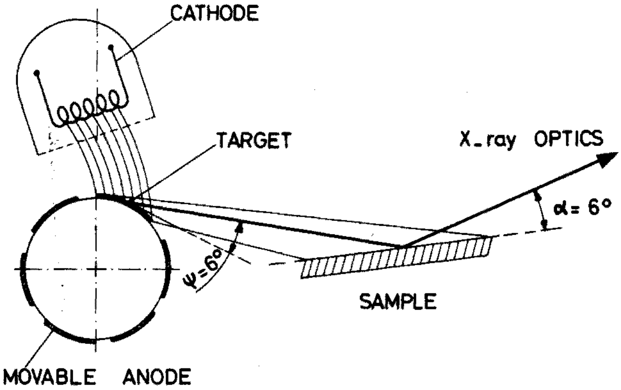

Fig. 1. Schematic diagram of excitation of fluorescence X-rays in the sample.

TABLE I

GENERAL OPERATING CONDITIONS

Element	*Excitation conditions with primary beam filtration*		*Without crystal*[a]		
Mg (pure)	50 kV	15 mA	30 kV	15 mA	KAP
Al (pure)	50 kV	15 mA	15 kV	15 mA	KAP
Si (pure)	50 kV	15 mA	30 kV	15 mA	KAP
P ($NaHPO_4$)	50 kV	15 mA	—		Gypsum
S (pure)	50 kV	15 mA	—		Gypsum
Cl (NaCl)	50 kV	15 mA	—		Gypsum

[a] Curved Johann-type crystal optics.

TABLE II

ABSORPTION EDGES OF THE ELEMENTS CHLORINE THROUGH MAGNESIUM TOGETHER WITH WAVELENGTHS OF SELECTED CHARACTERISTIC RADIATIONS OF THE ANODES USED

Target	*Atomic number*	*Characteristic line and wavelength* (*Å*)				*Element*	*K-absorption edge* (*Å*)
Ag	47	Kα	0.599	$L\alpha_1$	4.154	Na	11.48
Mo	42	Kα	0.709	$L\alpha_1$	5.406	Mg	9.512
Cu	29	Kα	1.540			Al	7.948
Ni	28	Kα	1.657			Si	6.738
Co	27	Kα	1.789	Lα	12	P	5.784
Fe	26	Kα	1.936			S	5.018
Cr	24	Kα	2.289			Cl	4.397
Au	79	$L\alpha_1$	1.277	Mα,	5.840		
Pt	78	$L\alpha_1$	1.313	Mα,	6.047		
W	74	$L\alpha_1$	1.476	Mα,	6.983		

Ruscoe[3], who found an optimal voltage around 20 kV (except for a chromium target), using a target take-off angle of 20°. Since this optimal voltage is dependent on the take-off angle, and increases with decreasing angle, a voltage of 30 kV was chosen in the present experiments (X-ray tube with 6° take-off angle).

Table II lists the absorption edges of the elements magnesium through chlorine, together with the wavelengths of selected characteristic radiations of the anodes used.

Two modes of operation of the X-ray tube were studied. In the first method, the primary beam filtration consisted of a 100 μm thick beryllium window; in the second, no type of filtration was used between target and sample. Some experiments with a 25 μm beryllium window, for the Si Kα spectrum were also done.

In the second method, the efficiency of excitation results in a combination of primary and secondary excitation, since back-scattered electrons are added to the primary radiation from the target. This fraction of electrons back-scattered is essentially independent of voltage in the range from 5 to about 700 kV, but increases with increasing atomic number of the target[5]. Very probably also with a very thin filter between target and samples, at high voltages (> 50 kV) back-scattered electrons will reach the sample.

THEORETICAL CONSIDERATIONS

It is well known that a strong primary characteristic line, close to the critical absorption edge on the short wavelength side of the excited element, together, although to a less extent, with the long-wavelength continuum, are very efficient in exciting the low energy X-ray spectral lines.

The theoretical expression for the energy distribution of this continuum as a function of wavelength is given by Kulenkampf's[6] formula:

$$E_\lambda \mathrm{d}\lambda = CZ\lambda^{-2}(\lambda_0^{-1} - \lambda^{-1})\mathrm{d}\lambda + BZ^2\lambda^{-2}\mathrm{d}\lambda \tag{1}$$

where B and C are constants, Z the atomic number of the target element and λ_0 the short-wave limit of the continuous spectrum. The constant B however is so small that the second term is ordinarily neglected in comparison with the first. Figure 2 shows the calculated energy distribution of the long-wavelength continuum for several targets, bombarded with 50-keV electrons.

Kramers[7] has calculated the continuous spectra from thick targets. His formula gives good agreement with measurements of the integrated energy and the general shape of the continuous spectrum. In terms of ergs in a wavelength interval dλ per bombarding electron the Kramers' formula is:

$$I(\lambda)\mathrm{d}\lambda = 4.5 \cdot 10^{-29} Z(\lambda_0^{-1} - \lambda^{-1}) \cdot \lambda^{-2}\mathrm{d}\lambda \tag{2}$$

where Z is the atomic number of the target and λ_0 the short-wavelength limit of the continuous spectrum given in cm.

For the purpose of excitation of fluorescent X-rays, all photons of wavelength greater than the critical absorption edge λ_c of the specimen element may be neglected. Therefore by taking the corresponding expression for the intensity distribution of the continuous spectrum, in number of photons per wavelength interval dλ:

$$I_{\mathrm{cont}}(\lambda) = 1.8 \cdot 10^{-14}\, mZ\{(\lambda/\lambda_0) - 1\}\lambda^{-2} \tag{3}$$

where m is the number of bombarding electrons per second, and integrating between the limits λ_0 and λ_c

$$\int_{\lambda_0}^{\lambda_c} I_{\mathrm{cont}}(\lambda)\mathrm{d}\lambda = 1.8\cdot 10^{-14} mZ[\lambda_0^{-1}\ln\lambda+\lambda^{-1}]\Big|_{\lambda_0}^{\lambda_c} \tag{4}$$

$$m^{-1}\int_{\lambda_0}^{\lambda_c} I_{\mathrm{cont}}(\lambda)\mathrm{d}\lambda = 0.15\cdot 10^{-14} ZV[\ln(\lambda_c/\lambda_0)+(\lambda_0/\lambda_c)-1] \tag{5}$$

the expression obtained, where V is the X-ray tube voltage in kV, can be used to obtain a quantitative idea about the numbers of photons in the useful continuous spectrum,

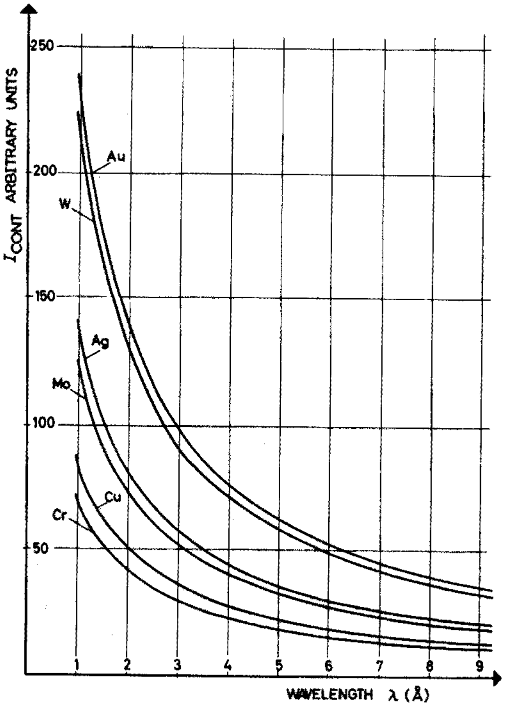

Fig. 2. Calculated intensity distribution of the long-wavelength continuum for several targets, bombarded with 50 keV electrons.

TABLE III

NUMBER OF PHOTONS IN THE CONTINUOUS SPECTRUM FOR SEVERAL TARGETS AT 30 kV, BETWEEN WAVELENGTHS λ_0 AND λ_c FOR MAGNESIUM, ALUMINIUM AND SILICON

Target	*Z*	$m^{-1}\int_{\lambda_0}^{\lambda_c} I_{\mathrm{cont}}(\lambda)\,\mathrm{d}\lambda\cdot 10^6$		
		$\lambda_0-\lambda_c$ Mg	$\lambda_0-\lambda_c$ Al	$\lambda_0-\lambda_c$ Si
Cr	24	235	217	200
Cu	29	284	262	241
Mo	42	412	379	350
Ag	47	461	424	391
W	74	725	668	616
Au	79	774	713	658

for different targets[8]. The results for six anode materials, for an X-ray tube voltage of 30 kV, for the case of the elements silicon, aluminium and magnesium are given in Table III (without self-absorption correction).

It can be seen that the number of photons between a heavy target like gold and a light element target, *e.g.* chromium, differs by a factor of about 3. Between the gold target and the medium element target silver, the difference is only about 1.5. The values of the target self-absorption are not exactly known, but depend on the angle of view of the emitted X-rays, and increase with increasing atomic number. However, if target self-absorption is taken into account, only slight differences can be expected between the excitation efficiencies of the long-wavelength continuum of a heavy and a medium element target.

With regard to the characteristic lines, the dominant factor is the closeness of the line to the absorption edge of the element of interest and the line-intensity. When a filter is used in the primary beam, unfortunately the low-energy portion of the continuous spectrum and the long-wavelength characteristic lines are heavily absorbed. This is shown in Fig. 3, where the calculated transmission of selected radiations through various X-ray tube window thicknesses, are given as a function of wavelength. A wavelength of about 6.6 Å, very effective in exciting the chlorine Kα spectrum, gives a transmission of 60 % for a 25-μm beryllium window and only 15 % transmission for the 100-μm beryllium window. The characteristic lines Ag Lα, Mo Lα, Au Mα and W Mα, are absorbed in the 100-μm beryllium window to the extent of 40 %, 65 %, 70 % and 90%, respectively.

In order to predict the most suitable target for the excitation of a given element, the intensity of the characteristic line (K radiation > L radiation > M radiation) must be taken into account, as well as the closeness of the characteristic wavelength to

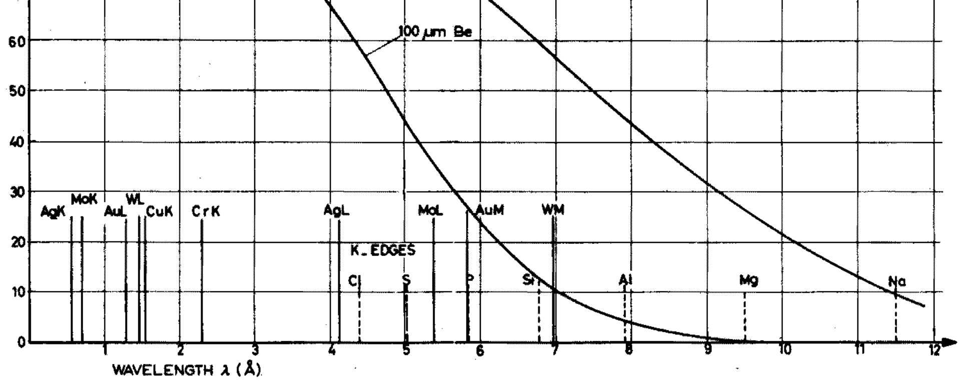

Fig. 3. Calculated X-ray transmission characteristics of X-ray tube windows as a function of wavelength.

the absorption edge of the element under consideration and the transmission of the characteristic line and long-wavelength continuum through the X-ray tube window. By working without a filter between target and sample, the effect of back-scattered electrons, which amount increases with increasing atomic number, has also to be considered.

RESULTS

Relative excitation efficiencies of the elements chlorine through silicon for various targets are given in Tables IV and V. The data have been normalized so that the highest intensity obtained is 100.

Table IV shows that with a 100-μm beryllium window between target and sample, the silver target is the most efficient for exciting the chlorine, sulphur and phosphorus Kα spectra. For chlorine and sulphur, the chromium target is also very

TABLE IV

EXCITATION EFFICIENCIES FOR THE Cl, S AND P Kα LINES AS A FUNCTION OF TARGET MATERIAL
(Primary beam filtration 100 μm beryllium)

Cl Kα		*S Kα*		*P Kα*	
Anode	*Relative excitation efficiency*	*Anode*	*Relative excitation efficiency*	*Anode*	*Relative excitation efficiency*
Ag	100	Ag	100	Ag	100
Cr	90	Cr	99	Mo	89
Co	56	Co	77	Cr	76
Fe	54	Fe	75	Cu	56
Ni	47	Ni	68	Au	42
Cu	41	Cu	63	W	38
W	39	W	61		
Au	36	Au	57		
Pt	34	Pt	41		
Mo	20	Mo	38		

TABLE V

EXCITATION EFFICIENCIES FOR THE Si Kα SPECTRUM

Primary beam filtration 100 μm Be		*Primary beam filtration 25 μm Be*		*No primary beam filtration*	
Anode	*Rel. excitation efficiency*	*Anode*	*Rel. excitation efficiency*	*Anode*	*Rel. excitation efficiency*
Cr	100	Mo	100	Au	100
Ag	99	Au	73	Cr	93
Mo	77	Ag	70	Mo	92
Au	65	Cr	52	Cu	90
W	51	W	32	Ag	85
Cu	46	Cu	27	W	84

effective but for P Kα a greater efficiency is obtained with the molybdenum target. Although the Mo Lα line is heavily absorbed in the X-ray tube window (*ca.* 65%), the closeness to the P K-absorption edge is the most important factor.

The particularly low efficiencies of the molybdenum, platinum and gold targets for exciting chlorine and sulphur Kα lines may be noted. This serves to emphasize the importance of using a primary wavelength that is close to the fluorescence absorption edge. The Mo Lα, Pt Mα and Au Mα lines are situated after the absorption edges of chlorine and sulphur, while the Mo Kα, Pt Lα and Au Lα lines are too far away from the edges to have a considerable effect on the excitation. The relative increase of excitation for all the targets with respect to the silver target for sulphur Kα excitation in comparison with chlorine Kα excitation, can be explained by the position of the silver Lα line relative to the chlorine and sulphur K-absorption edges. Since it can be concluded from Table IV that the targets Co, Fe and Ni (wavelengths between Cu and Cr) and Pt (Au) are not very interesting, they were omitted and the further experiments were carried out with the two light element targets Cr and Cu, the medium element targets Ag and Mo and the heavy targets Au and W. Table V lists the excitation efficiencies obtained for the Si Kα spectrum.

In the case of a 100-μm beryllium window between target and sample, the silver and chromium targets provided the best excitation of Si Kα. Copper and tungsten are

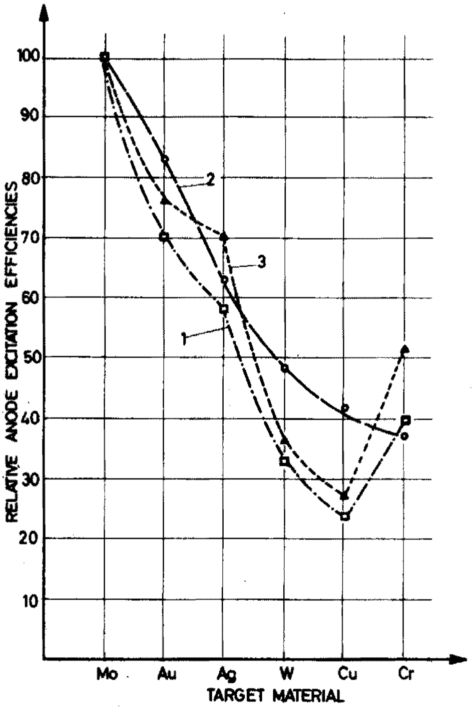

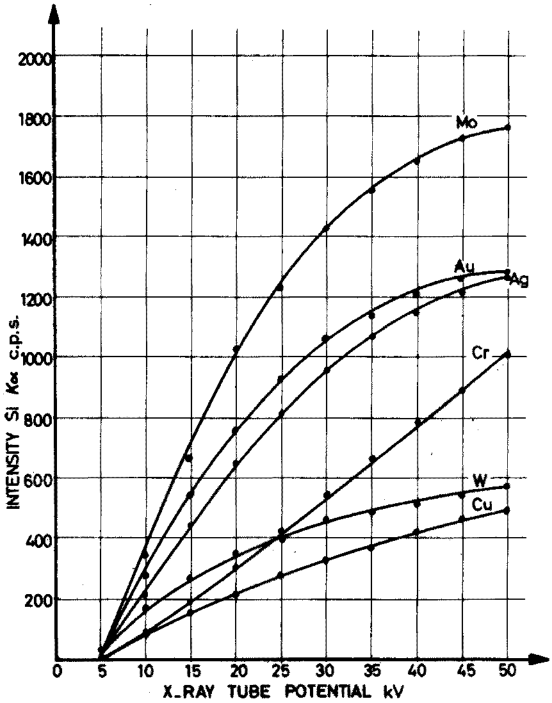

Fig. 4. Anode excitation efficiencies for Si Kα obtained with pure silicon (3, △), 0.6% Si in low-alloy steel (2, ○) and 3.0% Si in aluminium (1, □). Primary beam filtration 100 μm Be.

Fig. 5. Experimental efficiencies for a variety of targets *vs.* kilovoltage obtained for pure silicon. Tube window 100 μm Be. Intensity expressed as counts sec^{-1}.

the least efficient. When the beryllium thickness was decreased to 25 μm, the molybdenum target was more efficient. Although the gold M-series is closer to the silicon K-absorption edge than the molybdenum L-series, the latter are more intense and are also less absorbed by the window. With no filter between target and sample, the gold anode is the most efficient target, but no large differences in efficiency were found between all the targets studied.

A thirty-fold increase in intensity for the silicon Kα line was obtained by decreasing the beryllium tube window thickness from 100 to 25 μm. With no filter at all in the primary beam, a ninety-fold increase in intensity was obtained in comparison with the 100-μm beryllium filter in the primary beam.

Since all excitation efficiency measurements were carried out with pure or major concentrations of the elements which spectra were excited, further studies were made to establish if the results found for a pure silicon sample were also valid for small concentrations of silicon in a heavy matrix and for small concentrations of silicon in a matrix composed of low atomic number elements. The results of this investigation are shown in Fig. 4. The almost identical shapes of the curves for pure silicon and for low concentrations of silicon in a light element matrix are remarkable.

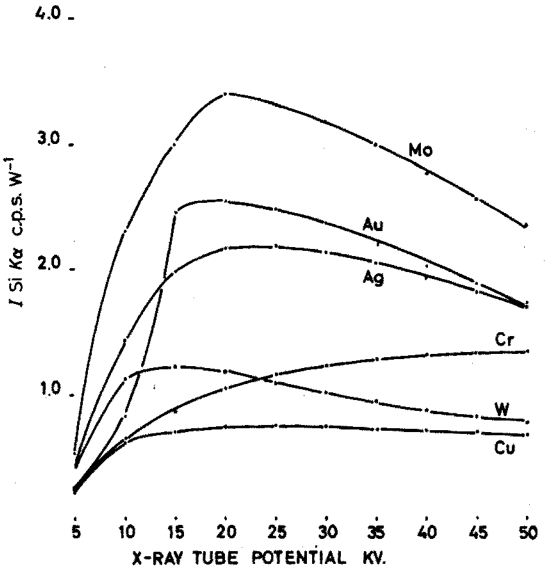

Fig. 6. Experimental efficiencies for a variety of targets *vs.* kilovoltage obtained for pure silicon. Tube window 100 μm Be. Intensity expressed as counts $\sec^{-1}$ W^{-1}.

The intensity of the Si Kα spectrum (pure silicon) as a function of tube voltage for various targets is shown in Figs. 5 and 6. In Fig. 5 the intensity is given in counts per sec and in Fig. 6 in counts per sec per watt. In the first case the optimum voltage for all the targets has not yet been reached; measurements are still increasing at 50 kV. If however the intensity is plotted as in Fig. 6, the optimal tube voltage is between 15 and 25 kV for all targets except for chromium (about 50 kV). These latter optimal voltages are the optimal conditions per power input to the X-ray tube. To investigate whether these optimal voltages are also the voltages which must be applied to obtain the lowest

TABLE VI

Target	*$R\sqrt{B}$ (optimal voltage from Fig. 6)*	*$R\sqrt{B}$ (50 kV all targets Fig. 5)*
Mo	5400	5300
Au	3900	2600
Cr	3600	3600
Ag	2600	2700
W	2600	1000
Cu	1650	1750

limit of sensitivity, the following experiments were carried out. Since the excitation conditions, where the figure of merit, $R\sqrt{B}$, has the greatest value are optimal for the detection of the lowest possible concentration[9], this figure of merit was determined for each target, with the optimal voltages found in Figs. 5 and 6.

The results are given in Table VI. It can be seen that except for gold and tungsten, there are only slight differences between the figure of merit for the two optimal voltages. In this case, an optimal voltage of 50 kV for the targets Mo, Cr, Ag and Cu should be preferred; by using a high excitation voltage, the fluorescent intensity changes rather slowly with voltage, thus there will be a minimum in the rate of change of intensity caused by fluctuations in the voltage. During the experiments it was noted that the background intensity increased in general with both atomic numbers of the target and with tube voltage. According to Thatcher and Campbell[1], the optimal tube voltage is in general inversely related to the mass absorption coefficient of the primary radiation in the target. Consequently one can predict from the values in Table VII that the optimal kilovoltage, for Si Kα excitation, would be lowest for gold and would increase for the other targets in the following order: molybdenum, silver, chromium and so on.

TABLE VII

Spectral lines and wavelength (Å)		*Self-absorption ($\mu m/\rho$)*
Au Mα	5.840	1160
Mo Lα	5.406	630
Ag Lα	4.154	460
Cr Kα	2.289	90
Cu Kα	1.540	54
W Lα	1.476	149

This follows from the argument that the greater the absorption of the anode for its own characteristic line, the lower will be the optimal kilovoltage for the anode, since at higher kilovoltages the electrons penetrate deeper and a greater fraction of the primary characteristic lines are absorbed in the anode.

Except for copper and tungsten the order of decreasing self-absorption was found to be inverse to the order of decreasing optimal kilovoltage, as found in Fig. 6.

Optimal voltages for Au, Mo, Ag and Cr are respectively 18, 21, 34 and 50 kV. The optimum voltages for copper and tungsten are anomalous in this respect, but can be explained by the fact that since the copper and tungsten series are far removed from the Si K edge, the excitation is largely determined by the continuum and thus the optimal voltages found (respectively 27 and 15 kV) are the optimal voltages for the continuous spectrum.

TABLE VIII

RELATIVE EXCITATION EFFICIENCIES FOR Al Kα AND Mg Kα AS A FUNCTION OF TARGET MATERIAL

Al Kα				*Mg Kα*			
Primary beam filtration 100 μm Be		*No primary beam filtration*		*Primary beam filtration 100 μm Be*		*No primary beam filtration*	
Anode	*R.E.E.*[a]	*Anode*	*R.E.E.*	*Anode*	*R.E.E.*	*Anode*	*R.E.E.*
Ag	100	Au	100	Ag	100	Au	100
Cr	88	Mo	93	Mo	94	W	94
Mo	86	Ag	92	Cr	82	Mo	84
Au	66	W	89	Au	70	Ag	78
W	56	Cr	87	W	59	Cr	64
Cu	42	Cu	85	Cu	41	Cu	60

[a] Relative excitation efficiency.

Table VIII gives the excitation efficiencies for the Al Kα and Mg Kα spectra, for a 100-μm beryllium window in the primary beam and with no filter in the primary beam. The most efficient targets for both elements are the silver target with the primary beam filtration and the gold target by removing the filter between target and sample, thus allowing back-scattered electrons to add to the primary radiation. Although the tungsten Mα line is relatively close to the Al K absorption edge, the gold target is slightly superior, probably because of the greater number of back-scattered electrons and the somewhat more intense continuum.

The substantial increase in intensity obtained by simply removing the X-ray tube window is demonstrated by the following example. The output from a pure magnesium sample, with a gold target with the 100-μm beryllium window was 1.3 counts sec^{-1} W^{-1}. By removing the window the output rose to 540 counts sec^{-1} W^{-1}. This is an approximately 400-fold increase in intensity. There was however also an increase in the intensity of the background from 1.0 to 6.0 counts sec^{-1}.

CONCLUSIONS

The experiments described above have shown that when a 100-μm beryllium window is placed between target and sample, the silver target is generally the most efficient for the excitation of the Kα spectrum of the elements chlorine through magnesium. By removing the filter between target and sample, the gold target provided the best excitation of the silicon, aluminium and magnesium Kα lines. Extrapolating these latter results to the excitation of the chlorine, sulphur and phosphorus Kα radiation without primary filtration, it can be predicted that for chlorine and sulphur the silver target, and for phosphorus the molybdenum target must be the most efficient targets. The importance of the transparency of the tube window has been shown. It also has been shown, that a principal K, L or M line becomes the dominant factor when its energy just exceeds the critical absorption energy of the secondary emitter.

The author is very grateful to Mr. G. Maffioli who carried out a part of the experimental work.

SUMMARY

Experimental studies with a demountable X-ray tube vacuum spectrograph have been made of the effects of varying the X-ray tube target and the tube window thickness on the fluorescence excitation of the elements chlorine through magnesium. Cr, Fe, Co, Ni, Cu, Mo, Ag, W, Pt and Au targets have been investigated. It has been found that using a 100-μm thick beryllium window between anode and sample, a silver target provides the best excitation for all the elements investigated. With no primary beam filtration, the gold target is the most efficient in exciting the Kα spectra of silicon, aluminium and magnesium. A 400-fold increase in intensity, the latter expressed in counts sec^{-1} W^{-1}, has been obtained for the Mg Kα spectrum with a gold target for the windowless X-ray tube spectrograph in comparison with the thin-window (100-μm beryllium window) X-ray spectrograph.

RÉSUMÉ

Des études expérimentales sont effectuées à l'aide d'un spectrographe à tube à rayons-X, sur l'influence de la cible et de l'épaisseur de la fenêtre du tube sur la fluorescence du chlore à travers le magnésium. Les cibles Cr, Fe, Co, Ni, Cu, Mo, Ag, W, Pt et Au sont examinées. Une fenêtre de béryllium de 100 μm entre anode et échantillon, a permis d'obtenir, avec cible d'argent, la meilleure excitation pour tous les éléments examinées.

ZUSAMMENFASSUNG

Mit Hilfe eines Vakuum-Röntgenspektrographen mit demontierbarer Röhre wurde der Einfluss des Targets der Röhre und der Dicke des Röhrenfensters auf die Fluoreszenzanregung der Elemente Chlor bis Magnesium untersucht. Es wurden Targets der Elemente Cr, Fe, Co, Ni, Cu, Mo, Ag, W, Pt und Au erprobt. Bei Verwendung eines 100 μm dicken Berylliumfensters zwischen Anode und Probe ergibt ein Silbertarget für alle untersuchten Elemente die beste Anregung. Ohne Primärstrahlfiltration ist das Goldtarget für die Anregung der Kα-Spektren von Silicium, Aluminium und Magnesium am wirksamsten. Der fensterlose Spektrograph erzielt mit einem Goldtarget beim Mg Kα-Spektrum eine um den Faktor 400 höhere Intensität (ausgedrückt in Impulse sec^{-1} W^{-1}) als der Spektrograph mit dünnem Fenster (100 μm Beryllium).

REFERENCES

1 J. W. THATCHER AND W. J. CAMPBELL, *U.S. Bur. Mines, Rept. Invest. 6689*, 1965.
2 N. SPIELBERG, *J. Appl. Phys.*, 33 (1962) 2033.

3 M. A. Short and M. J. H. Ruscoe, *Adv. X-ray Analysis*, Plenum Press, New York, 1967, p. 520.
4 C. J. Toussaint and G. Vos, *Anal. Chem.*, 38 (1966) 711.
5 E. J. Sternglass, *Phys. Rev.*, 95 (1954) 345.
6 H. Kuhlenkampf, *Ann. Phys.*, 69 (1962) 548.
7 H. A. Kramers, *Phil. Mag.*, 46 (1923) 836.
8 N. Spielberg, *Philips Res. Rept.*, 14 (1959) 215.
9 N. Spielberg and M. Bradenstein, *Appl. Spectrosc.*, 17 (1963) 6.

Anal. Chim. Acta, 55 (1971) 373–384

Analytica Chimica Acta
Elsevier Publishing Company, Amsterdam
Printed in The Netherlands

ELECTRODES SPECIFIQUES D'ANIONS A LONGUE CHAINE HYDROCARBONEE

APPLICATION AU DOSAGE POTENTIOMÉTRIQUE DE DÉTERGENTS ANIONIQUES

CLAUDE GAVACH ET CLAIRE BERTRAND
Département de Physico-chimie Colloïdale, C.N.R.S., Boîte postale 1018, 34-Montpellier (France)

(Reçu le 12 mars 1971)

Les nouvelles électrodes à membrane mises au point au cours des dernières années sont des électrodes spécifiques d'espèces ioniques inorganiques. Coetzee et Freiser[1] ont montré qu'il était possible de réaliser, à partir d'électrodes à membrane liquide du commerce, des électrodes qui donnent une réponse sensiblement nernstienne avec certains anions organiques tels que les ions acétate, formate, propionate, benzoate. Par ailleurs, Gavach et Seta ont indiqué une méthode de dosage potentiométrique des ions alkyl-triméthyl-ammonium à longue chaîne hydrocarbonée[2] au moyen d'une électrode à membrane liquide épaisse spécifique de ces ions.

On décrit ici le comportement d'électrodes du même type, spécifiques des ions dodécyl-sulfate (DS^-), tétrapropylènebenzène-sulfonate ($TPBS^-$) et dioctylsulfosuccinate ($DOSS^-$) dont les sels de sodium constituent les détergents anioniques les plus couramment utilisés.

On montre également que ces électrodes permettent de réaliser le dosage potentiométrique de ces détergents anioniques dont les méthodes conventionnelles de dosage comportent une phase d'extraction par un solvant non aqueux[3,4].

PRINCIPE

Le principe de cette électrode à membrane liquide épaisse dérive des résultats de l'étude de certaines piles à phases liquides dont il convient de rappeler les grandes lignes.

On désigne par R^- un des anions étudiés à longue chaîne hydrocarbonée et par S^+ un cation organique tel que l'électrolyte S^+R^- soit pratiquement insoluble dans l'eau et très soluble dans un solvant organique comme le nitrobenzène dans lequel il est fortement dissocié. Dans le cas des électrodes présentées ici, l'ion S^+ est un cation alkylpyridinium à longue chaîne hydrocarbonée.

Lorsqu'on effectue une mesure avec ce type d'électrode spécifique des ions R^-, on constitue la chaîne électrochimique suivante:

E.C.S.	Na^+R^- conc. variable dans H_2O (solution e_1)	R^-S^+ conc. fixe dans nitrobenzène (solution n)	S^+X^- conc. fixe dans H_2O (solution e_2)	Ag–AgX

$$\underbrace{\qquad\qquad\qquad\qquad\qquad\qquad\qquad\qquad\qquad\qquad}_{\text{Electrode spécifique des ions } R^-}$$

(E.C.S. = électrode au calomel saturé; X^- = ion Cl^- ou Br^-)

L'ensemble des deux solutions aqueuses e_1 et e_2 et de la solution organique n forme une pile à membrane liquide épaisse à double distribution[5] dont la f. é.m., c'est-à-dire la d.d.p. de Galvani $\varphi_{e_1}-\varphi_{e_2}$ mesurée entre les deux solutions aqueuses a pour expression:

$$\varphi_{e_1}-\varphi_{e_2}=F^{-1}[\mu^0_{\mathrm{S}^+_{(e)}}+\mu^0_{\mathrm{R}^-_{(e)}}-\mu^0_{\mathrm{S}^+_{(n)}}-\mu^0_{\mathrm{R}^-_{(n)}}]+(RT/F)\ln(a_{\mathrm{R}^-_{(e_1)}}a_{\mathrm{S}^+_{(e_2)}}/a_{\mathrm{R}^-_{(n)}}a_{\mathrm{S}^+_{(n)}}) \quad (1)$$

(a = activité ionique; μ^0 = potentiel chimique standard)

Donc, pour une série de mesures effectuées avec une électrode de composition fixe et une solution e_1 de concentration variable, le potentiel d'électrode E, c'est-à-dire la d.d.p. entre la solution e_1 et l'électrode Ag–AgX, plongée dans la solution e_2 de composition et de concentration constante, varie en fonction de l'activité en ion R^- de la solution e_1 suivant la loi de Nernst.

$$E=\mathrm{const}+(RT/F)\ln a_{\mathrm{R}^-_{(e_1)}} \quad (2)$$

Le détergent anionique NaR est soluble dans l'eau et, à un moindre degré, dans le nitrobenzène. Lorsqu'on amène en contact une solution aqueuse de NaR avec une solution de RS dans le nitrobenzène, il se produit un passage de NaR de la solution aqueuse vers la solution organique; en effet, le système formé par ces deux phases en contact va évoluer vers un état d'équilibre thermodynamique qui peut être atteint au bout d'un certain temps. A cet état d'équilibre correspondent de nouvelles valeurs des activités des ions R^- et Na^+ dans les deux milieux qui satisfont la relation suivante:

$$a_{\mathrm{R}^-_{(n)}}a_{\mathrm{Na}^+_{(n)}}/a_{\mathrm{R}^-_{(e)}}a_{\mathrm{Na}^+_{(e)}}=p^2 \quad (3)$$

Le coefficient de partage limite de NaR entre l'eau et le nitrobenzène (p), est égal au rapport des concentrations de NaR dans l'eau et le nitrobenzène, lorsque cet électrolyte se trouve seul, à très faible concentration, à l'équilibre de distribution entre les deux solvants[6].

C'est pourquoi, lors de l'immersion de l'extrémité inférieure de l'électrode spécifique aux ions R^- dans une solution aqueuse de NaR, les deux solutions vont se trouver presque instantanément à l'équilibre de partage sur une très faible épaisseur de part et d'autre de l'interface. Cependant l'abaissement de concentration en NaR de la solution aqueuse dans la couche en équilibre de distribution avec la solution organique est négligeable, car d'une part l'activité de l'ion R^- de la solution organique, $a_{\mathrm{R}^-_{(n)}}$, est fixée par la composition de l'électrode et d'autre part les valeurs des coefficients de partage des détergents NaR étudiés ici sont comprises entre 3×10^{-2} et 10^{-3}.

Le calcul indique que, dans les cas les plus défavorables, la diminution de la concentration en NaR en solution aqueuse est toujours inférieure à 0.1%. Donc, dans tous les cas, la relation (2) rend pratiquement compte des variations de E en fonction de l'activité de l'anion à longue chaîne R^- dans la solution aqueuse étudiée.

Si l'on ajoute à la solution e_1 une quantité croissante de solution aqueuse de SX de titre connu (X^-: ion halogénure), la formation d'un précipité de RS qui en résulte entraîne une diminution du nombre d'ions R^- libres dans la solution e_1 et, d'après la relation (1), un abaissement du potentiel d'électrode. Lorsque la totalité des ions R^- libres de la solution e_1 aura ainsi disparu, toute nouvelle addition de SX transformera la pile de membrane liquide à double distribution en une pile de membrane liquide à effet de concentration[7,8] dont la d.d.p. a pour nouvelle expression:

$$\varphi_{e_1} - \varphi_{e_2} = (RT/F) \ln \left(a_{\mathrm{S}^+_{(e_2)}} / a_{\mathrm{S}^+_{(e_1)}}\right)$$

Cette brusque variation de la d.d.p. de part et d'autre du point équivalent, due principalement au changement de nature de la pile à membrane liquide, constitue le principe du dosage potentiométrique des ions R^- en solution aqueuse. C'est ce même principe qui était à la base du dosage potentiométrique des détergents cationiques réalisé au moyen d'une électrode de même type[2].

Comme toutes les autres électrodes spécifiques à membrane liquide, ce type d'électrode ne peut être utilisé qu'en milieu aqueux à cause de la miscibilité avec le nitrobenzène de la plupart des solvants organiques.

PARTIE EXPÉRIMENTALE

Le prototype d'électrode[9] utilisé dans cette étude comporte un cylindre de verre terminé dans sa partie inférieure par un tube également en verre, de faible diamètre (2 mm) et ouvert à son extrémité. C'est cette partie qui durant les mesures se trouve immergée dans les solutions étudiées. Cette partie de l'électrode qui contient la phase organique se trouve en communication, d'une part avec un compartiment renfermant la solution aqueuse de référence (solution e_1) en contact avec l'électrode Ag–AgX, et d'autre part avec un réservoir de solution organique.

Les diverses solutions aqueuses de NaTPBS utilisées dans cette étude ont été obtenues par dilution à partir d'une solution standard à 5% (Merck).

Le dioctylsulfosuccinate de sodium est un produit BDH purifié suivant la méthode de Rudenko *et al.*[10] par dissolution dans le méthanol suivie d'une centrifugation et d'une filtration. Les chlorure et bromure d'hexadécylpyridinium (HPyCl et HPyBr) sont des produits Fluka. Le chlorure d'hexadécylpyridinium est de qualité purissimum, et le bromure, de qualité purum, est recristallisé dans l'acétone. Le NaDS a été purifié suivant une méthode déjà décrite[11]. Les dodécyl-sulfate, dioctylsulfosuccinate et tétrapropylènebenzène-sulfonate d'hexadécylpyridinium sont obtenus par précipitation en mélangeant une solution aqueuse de HPyCl avec une solution aqueuse du détergent anionique correspondant. Le dodécyl-sulfate d'hexadécylpyridinium est recristallisé dans l'acétone.

RÉSULTATS

Les variations des potentiels de ces électrodes spécifiques par rapport à une électrode de référence au calomel saturé sont représentées en fonction de la concentration en détergent et non de l'activité moyenne, car, d'une part, les concentrations utilisées sont assez faibles, du moins dans les domaines où la dissociation ionique est totale, et d'autre part toute tentative d'évaluation d'un coefficient d'activité ionique moyen semble hasardeuse en raison du caractère hautement dissymétrique du couple d'ions Na^+R^-.

La Figure 1 représente les variations du potentiel E d'une électrode spécifique des ions DS^- en contact avec une solution aqueuse de concentration variable en NaDS. La courbe (a) est relative au cas où NaDS est seul présent en solution aqueuse, tandis que la courbe (b) est relative au cas où la solution aqueuse de NaDS à concentration variable contient un excès de NaCl (10^{-1} *M*).

Dans la Figure 2, on a représenté les variations du potentiel d'une électrode

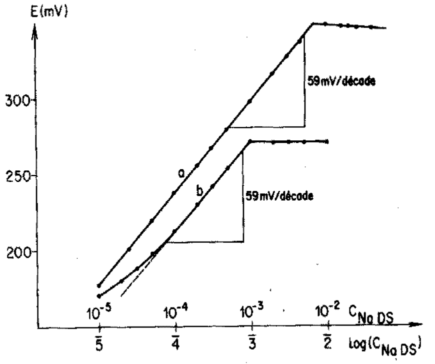

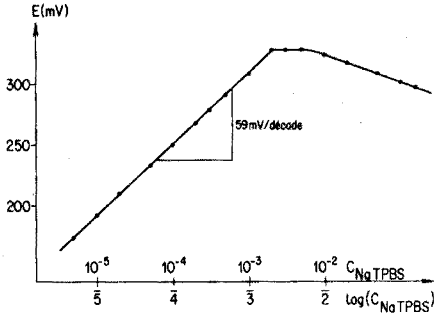

Fig. 1. Potentiels par rapport à l'E.C.S. de l'électrode spécifique des ions DS⁻ avec (a) solution de NaDS, concentration variable; (b) solution aqueuse de NaDS à concentration variable + NaCl 10^{-1} *M*.

Fig. 2. Potentiels par rapport à l'E.C.S. de l'électrode spécifique des ions TPBS⁻ avec une solution de NATPBS à concentration variable.

spécifique des ions TPBS⁻ lorsque cette électrode se trouve en contact avec une solution aqueuse de NaTPBS à des concentrations variables, ce détergent étant le seul soluté présent dans la solution.

La Figure 3 est relative aux d.d.p. obtenues avec une électrode spécifique des ions DOSS⁻, dans le cas où cette électrode se trouve immergée dans une solution aqueuse de NaDOSS à concentration variable.

La Figure 4 représente les réponses de l'électrode spécifique aux ions TPBS⁻ lorsque celle-ci est en contact avec des solutions aqueuses de différentes concentrations d'une part de NaDOSS (courbe a) et d'autre part de NaDS (courbe b).

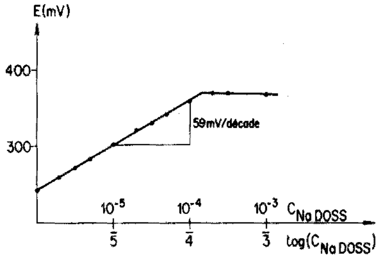

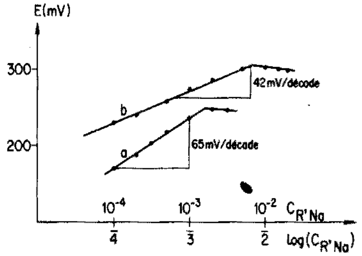

Fig. 3. Potentiels par rapport à l'E.C.S. de l'électrode spécifique des ions DOSS⁻ avec une solution de NADOSS à concentration variable.

Fig. 4. Potentiels par rapport à l'E.C.S. de l'électrode spécifique des ions TPBS⁻ avec des solutions de NaR' à concentration variable. (a) R' = DOSS⁻, (b) R' = DS⁻.

Sur la Figure 5 sont représentées les variations du potentiel d'une électrode spécifique des ions DS⁻ lorsque cette électrode est en contact avec une solution contenant NaDS à la concentration fixe de $5 \cdot 10^{-4}$ *M* et NaCl à des concentrations variables. Sur le même graphique sont représentées (courbe en pointillés) les valeurs calculées du potentiel d'électrode correspondant à la variation du coefficient d'activité de l'ion DS⁻ due à la modification de la force ionique du milieu; on tentera plus loin d'expliquer la divergence entre les deux courbes.

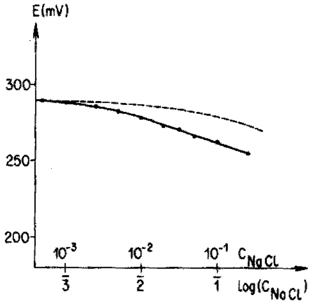

Fig. 5. Potentiels par rapport à l'E.C.S. de l'électrode spécifique des ions DS^- avec une solution de NaDS $5 \cdot 10^{-4}$ M + NaCl à concentration variable. Courbe pointillée: variation du potentiel d'électrode uniquement due au changement du coefficient d'activité ionique.

DISCUSSION

On sait que les détergents ioniques en solution aqueuse, sont pratiquement entièrement dissociés aux faibles concentrations. Mais dans le domaine des fortes concentrations, ces solutions contiennent, outre les ions libres, des micelles formées par l'association d'un certain nombre d'ions à longue chaîne et partiellement neutralisées par des contre-ions. La concentration à partir de laquelle apparaissent les micelles est appelée concentration critique micellaire (c.c.m.).

Toutes les courbes représentant les variations du potentiel d'électrode en fonction du logarithme de la concentration du détergent se composent de deux parties.

Dans le domaine des faibles concentrations, le potentiel d'électrode croît avec la concentration en détergent. La réponse d'une électrode est rigoureusement nernstienne lorsque la solution aqueuse contient le sel de sodium de l'anion pour lequel cette électrode est spécifique, et, dans ce cas, la relation (2) est parfaitement vérifiée. Aux fortes concentrations, c'est-à-dire dans le domaine micellaire, le potentiel d'électrode décroît faiblement lorsque la concentration du détergent augmente.

Il semble qu'on puisse lier cette décroissance au fait que la charge électrique des ions organiques qui constituent une micelle est incomplètement compensée par les ions inorganiques qui se fixent à la surface de la micelle d'une façon stable; la micelle reste chargée, avec le signe de ses ions organiques, et l'excès d'ions inorganiques se répartit en couche diffuse. Ainsi la solution intermicellaire contient un excès d'ions inorganiques du signe opposé à celui des ions à longue chaîne, et sa concentration en ions excédentaires est d'autant plus grande que la concentration en micelles est plus élevée. Il pourrait en résulter une diminution de l'activité de l'ion R^- libre, placé dans une atmosphère diffuse d'ions en majorité de signe opposé.

On remarquera (Fig. 1, courbe b) que cet effet disparait à peu près complètement lorsque la solution aqueuse contient un sel minéral à une concentration beaucoup plus grande que celle du détergent.

Sur chaque courbe représentant les variations du potentiel d'électrode en fonction de la concentration en détergent, l'abscisse du point de cassure correspond à la c.c.m. Donc ce type d'électrode permet de déterminer potentiométriquement la c.c.m. de solutions de détergents dans l'eau pure ou en présence d'un excès de sel minéral. Les valeurs de la c.c.m. ainsi déterminées sont en accord satisfaisant avec les valeurs déterminées par d'autres méthodes (Tableau I).

TABLEAU I

C.C.M. DE DÉTERGENTS ANIONIQUES DÉTERMINÉES POTENTIOMÉTRIQUEMENT (PRÉSENTE ÉTUDE) ET PAR D'AUTRES MÉTHODES

Détergents	*C.c.m. déterminée par électrodes spécifiques*	*C.c.m. déterminée par d'autres méthodes*	*Réf.*
NaDS (dans l'eau pure)	$7 \cdot 10^{-3}$	$6 \cdot 10^{-3}$–$8 \cdot 10^{-3}$	12
NaDS (dans solution de NaCl 10^{-1} *M*)	$1 \cdot 10^{-3}$	$1.4 \cdot 10^{-3}$	12
NaDOSS (dans l'eau pure)	$1.3 \cdot 10^{-3}$	$1.25 \cdot 10^{-3}$	10
NaTPBS (dans l'eau pure)	$2 \cdot 10^{-3}$	$1.3 \cdot 10^{-3}$–$2 \cdot 10^{-3}$	12

La Figure 4 indique que l'électrode spécifique aux ions TPBS$^-$ ne donne pas de réponse nernstienne avec des ions DS$^-$ et DOSS$^-$ en solution.

Néanmoins, dans le domaine submicellaire, le potentiel d'électrode varie encore linéairement avec le logarithme de l'activité de l'ion à longue chaîne, et reste pratiquement constant aux fortes concentrations. L'abscisse du point d'intersection des deux droites obtenues correspond bien à la c.c.m.

La réponse non nernstienne d'une électrode spécifique des ions R$^-$ en contact avec une solution aqueuse de R'Na (R'$^-$ autre anion à longue chaîne hydrocarbonée) est vraisemblement liée à un échange d'ions à longue chaîne entre la membrane liquide et la solution aqueuse suivant la réaction:

$$R^-_{(n)} + R'^-_{(e)} \rightleftharpoons R^-_{(e)} + R'^-_{(n)}$$

Un tel échange d'ions est à l'origine du défaut de sélectivité des électrodes spécifiques à membrane liquide.

Dans le domaine de dissociation complète du détergent, les valeurs du potentiel de l'électrode spécifique des ions DS$^-$ en contact avec une solution contenant simultanément NaDS et NaCl sont inférieures aux potentiels d'électrodes obtenues avec des solutions de NaDS dans l'eau pure (Fig. 1, courbe b, et Fig. 5). L'abaissement du coefficient d'activité de l'ion DS$^-$ évalué de façon approchée par la formule limite de Debye–Hückel, est insuffisant pour rendre compte de cet effet. La différence des potentiels de l'électrode spécifique des ions DS$^-$ en présence et en l'absence de NaCl en solution pourrait être liée à la dimérisation de l'ion dodécyl-sulfate en solution[13,14], l'électrode spécifique n'étant sensible qu'à l'activité de la forme monomère.

DOSAGE POTENTIOMÉTRIQUE DES DÉTERGENTS ANIONIQUES

Les détergents anioniques seront dosés potentiométriquement au moyen de cette électrode spécifique suivant le principe exposé plus haut. La solution titrante est une solution de bromure d'hexadécylpyridinium. L'électrode utilisée est soit une

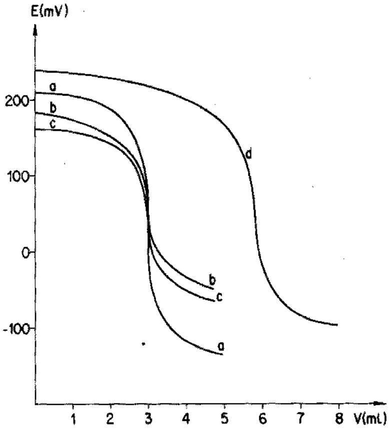

Fig. 6. Courbes de titrages potentiométriques. Solution titrante: bromure d'hexadécylpyridinium $5 \cdot 10^{-4}$ *M*. (a) NaDS 10^{-4} *M* (15 ml), électrode spécifique des ions DS^-; (b) NaDS 10^{-4} *M* + NaCl 10^{-1} *M* (15 ml), électrode spécifique des ions DS^-; (c) NaDS 10^{-4} *M* (15 ml), électrode spécifique des ions $TPBS^-$; (d) mélange de 10 ml de solution de NaDS 10^{-4} *M* + 10 ml de solution de NaDOSS 10^{-4} *M* + 10 ml de solution de NaTPBS 10^{-4} *M*, électrode spécifique des ions $DOSS^-$.

électrode spécifique de l'ion à longue chaîne présent en solution (Fig. 6, courbes a, b), soit une électrode spécifique d'un autre ion à longue chaîne (Fig. 6, courbe c), mais dans ce dernier cas, la limite de dosage est plus faible (Tableau II).

TABLEAU II

LIMITES INFÉRIEURES DES DOSAGES POTENTIOMÉTRIQUES DES DÉTERGENTS DANS L'EAU PURE, SUIVANT L'ÉLECTRODE SPÉCIFIQUE UTILISÉE

Détergent *Electrode spécifique*	*NaDS*	*NaTPBS*	*NaDOSS*
DS^-	$5 \cdot 10^{-6}$ *M*	$5 \cdot 10^{-5}$ *M*	$3 \cdot 10^{-5}$ *M*
$TPBS^-$	10^{-5} *M*	$2 \cdot 10^{-6}$ *M*	$2 \cdot 10^{-5}$ *M*
$DOSS^-$	10^{-5} *M*	$5 \cdot 10^{-5}$ *M*	10^{-6} *M*

TABLEAU III

PRÉCISION DES DOSAGES POTENTIOMÉTRIQUES AVEC L'ÉLECTRODE SPÉCIFIQUE AUX IONS DS^-

Nombre d'ions-grammes d'ions à longue chaîne en solution	*NaDS seul en solution*	*Mélange à égale proportion* {*NaDS* + *NaTPBS* + *NaDOSS*
10^{-3}	±0.1%	±1.5%
$2 \cdot 10^{-4}$	±0.15%	±2%
10^{-4}	±0.2%	±3%
$5 \cdot 10^{-5}$	±0.3%	±5%
10^{-5}	±1%	Dosage impossible
$5 \cdot 10^{-6}$	±1.5%	

Par cette méthode il est également possible de doser les détergents anioniques en présence d'un excès de sel minéral (Fig. 6, courbe b), ou encore de doser globalement un mélange de trois détergents en solution (Fig. 6, courbe d).

Comme il apparaît dans le Tableau III, la précision du dosage diminue lorsque la concentration en détergent décroît, et pour un même nombre d'ions-grammes d'ions à longue chaîne en solution, la précision est meilleure lorsque le détergent est seul présent en solution que dans le cas du mélange de plusieurs détergents.

RÉSUMÉ

On décrit le principe des électrodes à membrane liquide épaisse spécifiques des ions dodécyl-sulfate (DS^-), tétrapropylènebenzène-sulfonate ($TPBS^-$) et dioctylsulfosuccinate ($DOSS^-$) dont les sels de sodium sont des détergents anioniques très répandus. Ces électrodes ont une réponse nernstienne lorsque les solutions aqueuses des détergents sont totalement dissociées. Dans le domaine micellaire, les potentiels d'électrode varient très peu avec la concentration. Ces électrodes peuvent être utilisées pour la détermination de la concentration critique micellaire et pour le dosage potentiométrique des détergents anioniques dans l'eau pure et en présence d'un excès de sel minéral.

SUMMARY

The principle of liquid membrane electrodes which are specific for the ions dodecylsulfate (DS^-), tetrapropylenebenzenesulfonate ($TPBS^-$) and dioctylsulfosuccinate ($DOSS^-$) is described. The sodium salts of these anions are common detergents. These electrodes show a Nernstian response when the detergents are completely dissociated. In the micellar range, the electrode potentials vary little with concentration. These electrodes can be used for the determination of the critical micelle concentration, and for the potentiometric titration of anionic detergents in aqueous solutions and in the presence of inorganic salts.

ZUSAMMENFASSUNG

Es wird das Prinzip dicker Flüssigkeitsmembran-Elektroden beschrieben, die für die Ionen Dodecylsulfat (DS^-), Tetrapropylenbenzolsulfonat ($TPBS^-$) und Dioctylsulfosuccinat ($DOSS^-$) spezifisch sind. Die Natriumsalze dieser Anionen sind sehr gebräuchliche Detergentien. Die Elektroden zeigen bei vollständiger Dissoziation der Detergentien Nernstsches Verhalten. Im Micellarbereich ändert sich das Elektrodenpotential nur wenig mit der Konzentration. Diese Elektroden können verwendet werden für die Bestimmung der kritischen Micellkonzentration und die potentiometrische Titration anionischer Detergentien in wässrigen Lösungen und bei Überschuss anorganischer Salze.

BIBLIOGRAPHIE

1 C. J. Coetzee et H. E. Freiser, *Anal. Chem.*, 40 (1968) 2071.
2 C. Gavach et P. Seta, *Anal. Chim. Acta*, 50 (1970) 407.

3 J. LONGWELL ET W. D. MANIECE, *Analyst*, 80 (1955) 167.
4 D. C. ABBOT, *Analyst*, 87 (1962) 286.
5 C. GAVACH, *J. Chim. Phys.*, 64 (1967) 818.
6 P. SETA, *Thèse de spécialité*, Montpellier, 1968.
7 M. DUPEYRAT, *J. Chim. Phys.*, 61 (1964) 306.
8 O. D. BONNER ET D. C. LUNNEY, *J. Phys. Chem.*, 70 (1966) 1140.
9 J. GUASTALLA ET C. GAVACH, *Brevet ANVAR*, No. 690 1276, 1969.
10 B. RUDENKO, I. AVERBASH, K. SMIRNOV ET D. LEVI, *Kolloidn. Zh.*, 30 (1968) 414.
11 R. WILLIAMS, J. PHILLIPS ET K. MYSELS, *Trans. Faraday Soc.*, 51 (1955) 728.
12 K. SHINODA, *Colloid Surfactants*, Chap. I, Academic Press, New York, 1965.
13 P. MUKERJEE, K. J. MYSELS ET C. A. DULIN, *J. Phys. Chem.*, 62 (1958) 1390.
14 P. MUKERJEE, *J. Phys. Chem.*, 62 (1958) 1397, 1404.

Analytica Chimica Acta
Elsevier Publishing Company, Amsterdam
Printed in The Netherlands

FLUORIMETRIC DETERMINATION OF MICRO AMOUNTS OF ZIRCONIUM WITH QUERCETIN ON FILTER PAPER

S. R. DESAI AND (Miss) K. SUDHALATHA
Analytical Division, Bhabha Atomic Research Centre, Trombay, Bombay 85 (India)

(Received 15th March 1971)

Zirconium fluoresces weakly with quercetin in solution. However, the fluorescence is enhanced when the reaction is developed on a filter paper[1]. The present paper describes a method for the quantitative determination of traces of zirconium by means of this reaction on filter paper, and its application for determining the element in rock and monazite samples. Zirconium is separated from interfering elements by the ring-oven technique.

EXPERIMENTAL

Apparatus

Jarrel-Ash G.M. Fluorimeter Mark V with reflectance attachment.

Aminco-Bowman spectrofluorophotometer (model 4–8202) with solid sample accessory.

Circles of 36.3-mm diameter were cut from Whatman No. 40 filter paper to fit in the slot of the sample slide of the Jarrel-Ash fluorimeter.

A ring oven was constructed according to the specifications given by Weisz[2].

Reagents

Quercetin solution. The reagent (Koch-Light Laboratories) was purified by crystallisation from water–ethanol solution and dissolved in 95% ethanol to give an 0.03% solution.

Standard zirconium solution. A stock solution (10 mg Zr ml^{-1}) was prepared as recommended by Sandell[3]. The working solution (20 μg Zr ml^{-1}) in 4 M hydrochloric acid was prepared by suitable dilution of the stock solution.

The reagent solution and working solution of zirconium should be prepared fresh for each series of determinations.

Procedure

Place a sized filter paper on the ring oven, centre it and hold it in place by the retainer ring. Spot 10 μl of quercetin solution on the centre of the filter paper. After a minute, spot 5 μl of zirconium working solution on it. Allow this to dry and wash the spot four times with 20-μl portions of 0.02 M hydrochloric acid solution. Allow the spot to dry before each wash. After the final wash (when the paper is dry), add 5 μl of 2 M hydrochloric acid on the spot. Remove the paper from the ring oven and dry for

2 min under an infrared lamp. Place the paper on the sample slide of the fluorimeter, and cover it with a black disc. (This is a concentric disc of outer diameter 36.6 mm, central hole diameter 8.5 mm and thickness 3.6 mm, made out of any black nonfluorescent material. This cuts off the background fluorescence of the unspotted region of the filter paper.) Measure the fluorescence after 2 min. Take three readings at three different orientations by rotating the paper through 120° each time and take the mean of these readings. Take another filter paper through the procedure except for the addition of zirconium solution and treat this as a blank. Standardise the instrument with a suitable standard (*e.g.* uranium glass) before taking measurements. Prepare two circles for each solution and take the mean reading of the two measurements. Prepare a calibration curve with 5-μl aliquots from solutions of zirconium in 4 *M* hydrochloric acid containing different concentration of the metal.

Reagent concentration

The strength of the reagent solution was varied from 0.01 to 0.1 %, the volume being kept constant at 10 μl. Maximal fluorescence was obtained for reagent concentrations of 0.02–0.05 %, while lower and higher concentrations of the reagent gave low fluorescence intensities. All further experiments were carried out with 0.03 % reagent solution. It was also found that spotting the reagent first followed by the zirconium solution gave higher fluorescence intensities than when the zirconium was spotted first.

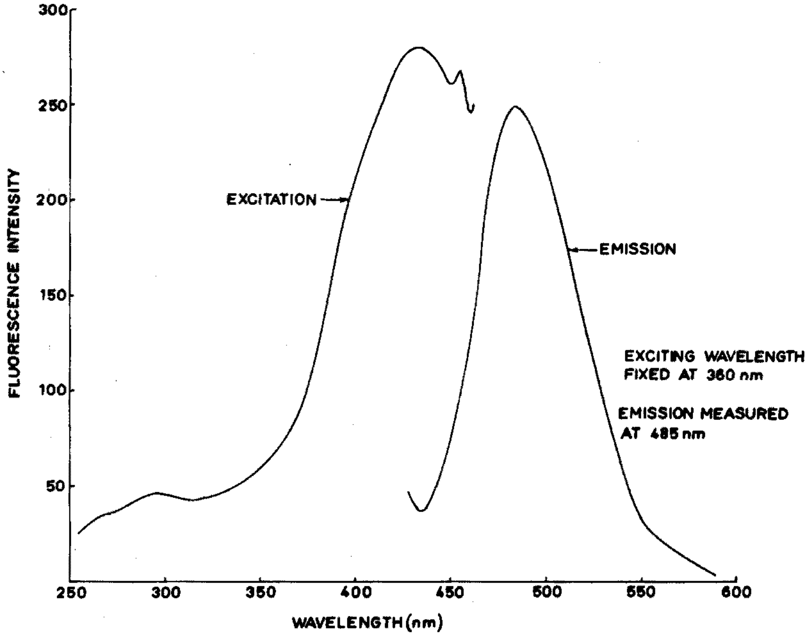

Fig. 1. Excitation and emission spectra (uncorrected) of zirconium–quercetin complex on filter paper. Fluorescence was developed on filter paper by applying 0.03 % alcoholic solution of quercetin followed by 100 μg Zr ml^{-1} solution.

Effect of acidity

The zirconium–quercetin fluorescence on the filter paper was developed with various strengths of the hydrochloric acid used in the final stage of spotting. It was found that the intensity of the fluorescence increased with acidity from 0.1 *M* upto 1.0 *M* and remained steady at higher acidities upto 4.0 *M*. All further experiments were carried out by spotting 2 *M* hydrochloric acid. In addition to hydrochloric acid, perchloric, sulphuric and nitric acid media were also studied. It was found that fluorescence intensity was maximal in hydrochloric acid media, while, as expected, nitric acid completely quenched the fluorescence.

Effect of foreign ions

The effects of various cations and anions in 100-fold amounts compared to 0.1 μg of Zr were studied under the optimal conditions for zirconium fluorescence. Of the elements studied Cr, Fe, Ni, Co, Pb, Sb, Au, Cu, Tl, Mo, V, U, W, Se, Ce, Hg, La, Y, Eu, Bi, Nb, Ti and Mn quenched the fluorescence, while Li, Na, K, Ca, Mg, Sn, Zn, Al, Be, Ga and Th were found to fluoresce. However, the fluorescence of these elements was very weak compared to that of zirconium. Oxalate, tartrate, acetate, phosphate, fluoride and EDTA were found to quench the fluorescence.

Spectral characteristics

The excitation and emission spectra of the zirconium–quercetin complex on the filter paper were obtained on the Aminco-Bowman Spectrofluorophotometer by mounting the filter paper strip on the solid sample accessory. The excitation and emission maxima (uncorrected) occurred at 435 nm and 485 nm, respectively (Fig. 1). The spectra of the reagent could not be obtained owing to rapid fading of the fluorescence.

Separation of zirconium from interfering ions on ring oven

It was found from preliminary experiments on the ring oven that the zirconium–quercetin complex on the filter paper did not move from the spot when washed with 0.02 *M* hydrochloric acid. This was confirmed by measuring the fluorescence of the spot, before and after washing five times with the acid. It was further found that all the interfering elements except Mo, W, V, Nb, and Sb could be washed out of the spot.

Procedure for opening rock samples

Weigh 0.25 g of the sample in a platinum crucible. Add 5 ml of hydrofluoric acid and evaporate to dryness on a waterbath. Repeat the operation twice. Add 2 ml of concentrated sulphuric acid to the crucible, place it on a sandbath and fume strongly, bringing it to dryness. Fuse the contents of the crucible with sodium carbonate and leach the melt with water. Transfer the slurry to a centrifuge tube and centrifuge. Discard the supernate, wash the residue with 25 ml of distilled water, centrifuge, and discard the washings. Repeat this step twice. Take up the residue in 4 *M* hydrochloric acid by warming and make up to 5 ml in a volumetric flask. If there is any turbidity at this stage, filter the solution through Whatman (No. 40) filter paper and use 5 μl of the filtered solution for spotting.

Procedure for opening monazite samples

Weigh 0.25 g of the monazite sample and transfer to a 100-ml beaker. Add 5 ml of concentrated sulphuric acid, place it on a sandbath and heat to copious fumes of the acid for 2 h. Cool the beaker to room temperature and place it in an ice tray. Add 30 ml of chilled water to dissolve the pasty mass. Filter through Whatman (No. 540) filter paper and wash the residue with dilute (1:250, v/v) sulphuric acid. Reject the filtrate, transfer the filter paper with the residue to a nickel crucible, dry and ash it. Fuse the residue with 1 g of sodium hydroxide and a pinch of sodium peroxide. Take up the fused mass in hydrochloric acid and make up to 50 ml in a volumetric flask with 4 *M* hydrochloric acid. From this take 5 μl for spotting.

RESULTS AND DISCUSSION

The high intensity of the zirconium–quercetin fluorescence on filter paper is probably due to the rigidity and planarity offered by the filter paper medium to the chelate. The reagent also shows fluorescence on the paper in chloride medium but it fades within 2 min. In contrast, the fluorescence of the zirconium–quercetin complex is stable for 5 min and then fades slowly. Though the complex shows bright fluorescence on the filter paper, the blue fluorescence of the latter gives a high background. Hence to cut off this radiation the paper is covered with a black disc which allows only a small portion of the developed spot to be viewed by the photocell of the fluorimeter.

The analytical data on the determination of zirconium with quercetin on filter paper presented here were obtained on a Jarrel-Ash G. M. fluorimeter with its usual set up (excitation at 365 nm, emission bandpass 525–580 nm), as proper filters were not available. Though the excitation maximum of the complex is at 435 nm, the shorter wavelength excitation by 365 nm may be preferable in view of closeness of the excitation and emission maxima. On this instrument 0.05 μg of zirconium could be determined (one could probably go to lower limits with proper filters) and the fluorescence intensity was found to be linear from 0.05 to 0.25 μg of zirconium.

For determining zirconium in complex samples, it is necessary to separate it from interfering elements. As can be seen from the studies on ring oven, the technique provides good separation of zirconium from many of the interfering elements. The fluorimetric method combined with the ring oven technique was applied to determine

TABLE I

DETERMINATION OF ZIRCONIUM IN STANDARD SAMPLES

Sample	*Zr found*		*Zr reported (p.p.m.)*
	Zr (p.p.m.)	*ZrO_2 (%)*	
USGS Std. G1	196, 200		210 (recommended value)[4]
USGS Std. G2	252, 273, 242		Range 250–400[5]
USGS Std. GSP 1	332		Range 323–685[5]
Tonalite T1	128, 115, 106		120[6], 187[7]
Standard Monazite B		1.21, 1.24, 1.08, 1.12, 1.04, 1.06, 1.08, 1.20, 1.19, 1.05, 1.30, 1.08, 1.22 Mean = 1.14	1.25% ZrO_2[a]

[a] Independent determination in this laboratory.

zirconium in rock and monazite samples. The results obtained on some standard rock samples and on a monazite sample are shown in Table I.

The relative standard deviation calculated on 13 independent determinations on the monazite sample was found to be 7.5% on the mean value of 1.14% of ZrO_2 obtained by this method.

The authors are grateful to Dr. Ch. Venkateswarlu for his interest and helpful discussions during the course of this work.

SUMMARY

The fluorescence of the zirconium–quercetin complex on filter paper is used for the determination of zirconium. Optimal conditions as regards acidity, reagent, concentration, etc., for maximal fluorescence intensity, and the interference of other ions have been studied. The method is applied to the determination of zirconium in rock and monazite samples. The ring-oven technique is used to separate zirconium from interfering elements.

RÉSUMÉ

Une méthode de dosage du zirconium est proposée; elle est basée sur la fluorescence du complexe zirconium–quercétine, sur papier. On examine les conditions optimales d'acidité, de réactif, de concentration pour obtenir la meilleure intensité de fluorescence ainsi que l'influence d'autres ions. Ce procédé est appliqué au dosage du zirconium dans les roches et les échantillons de monazite. La technique du four à anneau est utilisée pour la séparation du zirconium d'avec des éléments gênants.

ZUSAMMENFASSUNG

Die Fluoreszenz des Zirkonium–Quercetin-Komplexes auf Filterpapier wird für die quantitative Bestimmung von Zirkonium ausgenutzt. Die optimalen Bedingungen (Acidität, Reagenz, Konzentration usw.) für grösste Fluoreszenzintensität sowie die Störungen durch andere Ionen wurden untersucht. Die Methode wird auf die Bestimmung von Zirkonium in Gesteins- und Monazitproben angewendet. Für die Abtrennung des Zirkoniums von störenden Elementen wird die Ringofen-Technik benutzt.

REFERENCES

1 C. E. White, in J. H. Yoe and H. J. Koch, *Trace Analysis*, John Wiley, New York, 1957, p. 215.
2 H. Weisz, *Microanalysis by Ring Ove Technique*, Pergamon Press, Oxford, 1961, p. 15.
3 E. B. Sandell, *Colorimetric Determination of Traces of Metals*, 3rd Edn., Interscience, New York, 1959, p. 978.
4 M. Fleischer and R. E. Steevens, *Geochim. Cosmochim. Acta*, 26 (1962) 525.
5 F. J. Flanagan, *Geochim. Cosmochim. Acta*, 33 (1969) 81.
6 C. O. Ingamells and N. H. Suhr, *Geochim. Cosmochim. Acta*, 27 (1963) 897.
7 M. J. Kaye, *Geochim. Cosmochim. Acta*, 29 (1965) 139.

Analytica Chimica Acta
Elsevier Publishing Company, Amsterdam
Printed in The Netherlands

SPECTROPHOTOMETRIC DETERMINATION OF SMALL AMOUNTS OF SULPHUR DIOXIDE BY MOLECULAR COMPLEX FORMATION WITH *o*-XYLENE

M. K. BHATTY AND A. TOWNSHEND
Chemistry Department, The University, P.O. Box 363, Birmingham B15 2TT (England)

(Received 11th February 1971)

Sulphur dioxide is one of the most harmful air pollutants[1]; it affects both living organisms and inanimate structures. Sulphur dioxide and sulphites are also widely used as reductants and preservatives. The determination of sulphur dioxide, particularly in small amounts, is therefore frequently required.

Sulphur dioxide and sulphite have been determined titrimetrically[2] and colorimetrically[3] over a wide concentration range. These determinations are based on the reducing nature of sulphur dioxide, its acidic character or its easy convertibility into sulphur trioxide. Among the titrimetric methods, iodimetric procedures have usually been applied[2]. These have several sources of errors, principally the atmospheric oxidation of sulphurous acid, and the loss of sulphur dioxide and iodine by volatilization, and they may be further complicated by the co-presence of reductants such as hydrogen sulphide.

Various methods are available for the determination of sulphur dioxide based on its conversion to sulphur trioxide by oxidants such as hydrogen peroxide. However, these methods lack specificity and the results obtained may not be reliable, especially when the samples, whether gases or liquids, also contain hydrogen ions and/or sulphate-generating species. The colorimetric determinations of sulphur dioxide have commonly involved sulphuric acid and a bleached dye, such as fuchsin, first proposed by Steigmann[4]. Atkin[5] and Urone and Boggs[6] modified the reagent for use in air pollution analysis.

In all methods for the determination of sulphur dioxide, but especially for trace determinations, the air-oxidation of sulphite solutions on standing has been a significant difficulty. The above workers decreased this deterioration by adding glycerol, probably because the induced oxidation of the alcohol consumes most of the oxygen available[7]. The most important advance, however, is due to West and Gaeke[8], who achieved a much improved stability by "fixing" sulphur dioxide as disulphitomercurate(II). The sulphur dioxide was later determined spectrophotometrically by means of bleached *p*-rosaniline and hydrochloric acid. In this way, they were able to trap and determine 0.005–0.2 p.p.m. of sulphur dioxide from a 38.2-l air sample (0.6–21 μg of sulphur dioxide). Recently, Humphrey *et al.*[9] have shown that alkaline sulphite solutions can be stabilized by EDTA, and determined the sulphite concentration by measurement of the absorbance of the thiol produced by the reduction of 4,4′-dithiodipyridine or 5,5′-dithio-bis-(2-nitrobenzoic acid) by sulphite. The method is less sensitive than the *p*-rosaniline method, but it is more rapid and the reaction conditions are less stringent.

Scoggins[10] recently described a spectrophotometric method for the determination of 0.01–1% of sulphur dioxide in sulphuric acid, based on its absorbance at 276 nm. Although the method is not sensitive, it is rapid and does not require chromogenic reagents.

The present paper describes a new approach to spectrophotometric determination of sulphur dioxide. Sulphur dioxide and aromatic or olefinic compounds form molecular complexes which have a charge transfer absorption band in the region of 300 nm[11,12]. Dainton *et al.*[12] measured the spectral characteristics of eleven such molecular complexes of sulphur dioxide; molecular absorptivities up to 7140 were found. In the present investigation, optimal conditions for the determination of sulphur dioxide based on molecular complex formation are established. Sulphur dioxide is extracted by the organic donor solvent from acidified sulphite solutions and the absorbance of the molecular complex is measured.

EXPERIMENTAL

Solutions

Tetrachloromercurate(II) solution, 0.1 *M*. Dissolve mercury(II) chloride (27.2 g; G.P.R. grade) and sodium chloride (11.7 g; A.R. grade) in water and dilute to 1 l.

Sulphite solution, 0.033%. Dissolve 0.33 g of anhydrous sodium sulphite (96%; G.P.R. grade) in 10^{-3} *M* EDTA solution or the tetrachloromercurate solution and dilute with the same reagent to 1 l. Prepare weaker sulphite solutions by dilution with the EDTA or tetrachloromercurate solution.

Metabisulphite solution, 0.03%. Dissolve sodium metabisulphite (0.3 g; G.P.R. grade) in 10^{-3} *M* EDTA solution, and dilute with the same reagent to 1 l. Prepare weaker metabisulphite solutions by dilution with the EDTA solution.

Interfering ion solutions. 10^{-3} *M* metal salts in 10^{-3} *M* EDTA and 10^{-2} *M* salts of the anion solutions were used; all salts were A.R. grade.

Standardization procedure

Transfer 0.0–5.0 ml aliquots of 0.033% or 0.0033% sulphite solution to a series of 25-ml volumetric flasks. Add an appropriate volume of the EDTA (or tetrachloromercurate) solution to raise the volume of each solution to 5 ml. Add to each 5 ml of *o*-xylene and 5 ml of 1+4 sulphuric acid (M.A.R. grade), make up to volume with *o*-xylene and stopper the flasks. Shake the flasks for 5 min and allow to stand for 10 min. Filter each *o*-xylene layer through a little anhydrous sodium sulphate (A.R. grade) previously washed with a little *o*-xylene, beginning with the blank solution, and progressing to the strongest solution. For each solution, filter *ca.* 1-ml portions at a time, and use the first four washings to wash out the 1-cm quartz spectrophotometer cell. Finally, fill the cell and stopper it. Measure the absorbance at 296 nm against the blank extract and construct a calibration graph. Unknown sulphite concentrations are measured by following the same procedure.

RESULTS AND DISCUSSION

Choice of donor molecule

Sulphur dioxide forms 1:1 molecular complexes with many aromatic hydrocarbon donor molecules when it is absorbed by a solution of the donor in *n*-hexane[12]. This suggested a method for the spectrophotometric determination of sulphur dioxide, because the complexes have spectral bands at *ca.* 300 nm, quite distinct from those of the donors, with molar absorptivities up to 7000. Generation of sulphur dioxide by the action of acid on a stabilized sodium sulphite solution, and absorption of the gas from a nitrogen stream by a 1+9 solution of *o*-xylene in *n*-hexane, gave absorbances too small to be of use for determining small amounts of sulphur dioxide. The use of undiluted *o*-xylene gave improved absorbances but reproducible results were difficult to obtain with simple apparatus. Moreover, the stability of the complex was insufficient for quantitative removal of sulphur dioxide from the gas stream. Better results (2.5-fold increased absorbance) were obtained by direct extraction of sulphur dioxide from a sulphite solution acidified with 10% sulphuric acid.

Several donors were examined to establish and compare their suitability as extractants for sulphur dioxide from acidified sulphite solutions. The results (Table I) showed that *o*-xylene gave the largest absorbance with the absorbance maximum of the complex at 296 nm, the farthest removed from the peak of *o*-xylene itself at 280 nm. Again, dilution of the *o*-xylene with hexane merely reduced the absorbance of the extracts.

TABLE I

SPECTRAL CHARACTERISTICS OF THE MOLECULAR COMPLEXES OF SULPHUR DIOXIDE WITH VARIOUS DONORS

Donor	*Wavelength of maximum absorbance (nm)*	*Absorbance*[a]
Benzene	290	0.27
Toluene	288	0.40
o-Xylene	296	0.52
m-Xylene	296	0.49
p-Xylene	<290	0.27[b]
p-Cymene	<290	0.05[b]
Cyclohexene	<290	0.05[b]
Cyclohexane	287	0.04

[a] Obtained by extraction of a sulphite solution containing 40 μg of SO_2 stabilized with tetrachloromercurate, by the standard procedure.
[b] Measured at 290 nm; absorbance maximum obscured.

Interfering ions

As has been found in earlier studies by various workers, unstabilized sulphite solutions deteriorated rapidly, but EDTA[9] and tetrachloromercurate(II)[8] stabilized the sulphite solutions, so that only 15% deterioration occurred in a week. West and Gaeke's method[8], which uses tetrachloromercurate(II) as stabilizer, is remarkably free from interferences[1,13,14]. Any interference likely to be met with, other than some metal ions and excessive amounts of nitrogen oxides, is readily eliminated by taking simple precautions.

When tetrachloromercurate(II) was used in the proposed extraction method, high blank absorbances were obtained, but F^-, Cl^-, SO_4^{2-}, SCN^-, PO_4^{3-}, NO_3^- and

TABLE II

EFFECT OF VARIOUS IONS ON THE ABSORBANCE OF THE *o*-XYLENE EXTRACT

Anion[a]	*Absorbance*		*Metal ion*[b]	*Absorbance*
	EDTA-stabilized	*$(HgCl_4)^{2-}$-stabilized*		*EDTA-stabilized*
—	0.50[c]	0.50[d]	—	0.64[e]
F^-	0.49	0.50	Cu^{2+}	0.64
Cl^-	0.50	0.50	Fe^{2+}	0.62
Br^-	0.50	>2.0	Cd^{2+}	0.64
I^-	0.50	>2.0	Hg^{2+}	0.65
SO_4^{2-}	0.50	0.48	Zn^{2+}	0.64
S^{2-}	0.50	0.66	Pb^{2+}	0.62
SCN^-	0.52	0.46	Mn^{2+}	0.67
PO_4^{3-}	0.50	0.50	Ni^{2+}	0.64
NO_3^-	0.51	0.46		
CN^-	0.50	0.49		
NO_2^-	0.25	0.28		
NO_2^-[f]	0.48	—		

[a] 10^{-4} *M* in 10 ml of acidified solution.
[b] $2 \cdot 10^{-3}$ *M* in the final solution.
[c] 34 μg of SO_2 per ml.
[d] 40 μg of SO_2 per ml.
[e] 44 μg of SO_2 per ml.
[f] After addition of sulphamic acid (0.2 g).

CN^- did not interfere (Table II). Sulphide, iodide and bromide gave enhanced absorbances, whereas nitrite reduced the absorbance. The high values caused by bromide and iodide were found to be due to the extraction of mercury complexes of bromide and iodide by the *o*-xylene. The chloro-complex was found to be also extracted, giving strong absorption at 290 nm but its absorbance was balanced by its extraction in the blank; this accounts for the high blanks when tetrachloromercurate(II) was used. It is interesting to note that extracts of sulphur dioxide from tetrachloromercurate solutions slowly shifted their absorbance maxima from 296 to 300 nm over a period of about 1 h. Because of these serious interferences, further investigation of the tetramercurate-stabilized solutions was abandoned. It should be mentioned, however, that at the lower levels of sulphide, bromide, nitrite, etc. often obtaining in practice, the method might be quite acceptable.

Extraction from acidified EDTA-stabilized solutions was a more effective way of reducing interferences. Table II shows that no metal ions, and only nitrite of the anions tested, interfered seriously. Addition of sulphamic acid[13] (0.2 g) to the sulphite solution, eliminated the effect of 0.9 mg of nitrite. It is interesting that, in the absence of any stabilizing agent, sulphide, bromide and iodide caused a drastic reduction in the amount of sulphur dioxide extracted. It is reasonable to assume, therefore, that EDTA binds traces of metal ions, which would otherwise catalyse the oxidation of bromide and iodide, which subsequently oxidize sulphite. The stabilizing effect of EDTA on sulphite solutions can likewise be attributed to the masking of metal ions which catalyse the air-oxidation of sulphite[15].

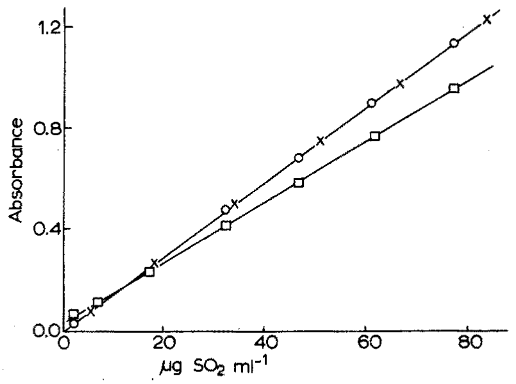

Fig. 1. Variation of absorbance of *o*-xylene extract with concentration of sulphur dioxide in 10 ml of acidified aqueous solution: (□) sulphite stabilized with HgCl$_4^{2-}$; (○) sulphite stabilized with EDTA; (×) metabisulphite stabilized with EDTA.

Calibration curves and reproducibility

Absorbances of sulphur dioxide extracted from acidified sulphite and metabisulphite solutions are given in Fig. 1. Straight-line calibration graphs were obtained for solutions stabilized with EDTA or tetrachloromercurate(II) and sulphur dioxide recoveries from sulphite and metabisulphite were identical. The lower absorbances obtained from the tetrachloromercurate solution could arise from competitive complexing with mercury(II). The absorbances for 20 μg of sulphur dioxide per ml were reproducible within ±0.02 units (*ca.* 1 μg per ml). The absorbance of the organic extract remained unchanged for at least 24 h even when left in contact with the 10% sulphuric acid solution, but loss of sulphur dioxide from the extract occurred slowly in an unstoppered vessel. Filtration through sodium sulphate gave improved reproducibility for absorbances below 0.08 by removing traces of suspended water.

The sulphuric acid concentration in the aqueous layer did not affect the sulphur dioxide recovery, when varied between 5 and 20%. However, 10% acid gave optimal phase separation. Extraction under the recommended conditions removed 82% of the sulphur dioxide from the aqueous phase in a single extraction, the distribution coefficient thus being 3. This indicates that the sensitivity of the procedure can be increased three-fold merely by using a 5-ml acidified aqueous solution, and extracting into 5 ml of *o*-xylene.

Conclusion

The method described provides a simple, selective spectrophotometric method for the determination of sulphur dioxide. The method is rapid, and does not require expensive reagents. It is especially suitable for EDTA-stabilized sulphite solutions, such as would be obtained by absorption of sulphur dioxide from air samples by alkaline solutions[9].

The complex which is responsible for the measured absorbance, forms immediately, and can be completely dissociated by passing nitrogen or air through the *o*-xylene. This means that the system could find application as a continuous monitor for sulphur dioxide in gas streams, for the degree of formation of the molecular complex is dependent on the partial pressure of sulphur dioxide in the gas stream.

The use of molecular complexes of this type for quantitative analytical purposes has received little previous attention. The present system demonstrates their applicability in this field, and subsequent papers will deal with further examples. The instantaneous formation of molecular complexes makes them ideal for use in automatic analysis systems. The reagents used (aromatic hydrocarbons, amines, olefins, etc.) are unusual as spectrophotometric reagents and provide appreciable indifference to the usual interferences.

The authors thank Professor R. Belcher for his help and keen interest. M.K.B. thanks the University of Birmingham for providing the facilities for this research, the Government of Pakistan and the P.C.S.I.R. for leave of absence, and the Nuffield Foundation for the award of a fellowship.

SUMMARY

Sulphur dioxide (0.7–84 μg ml^{-1}) is determined by extraction into *o*-xylene from acidified sulphite solutions stabilized by EDTA. The absorbance of its molecular complex with *o*-xylene is measured at 296 nm. Only nitrite interferes, and this effect is easily eliminated by adding sulphamic acid. The use of tetrachloromercurate(II) to stabilize the sulphite solutions is less satisfactory because of an increased number of interferences, higher blanks and lesser sensitivity.

RÉSUMÉ

L'anhydride sulfureux (0.7–84 μg ml^{-1}) est dosé, par extraction dans l'*o*-xylène, dans des solutions de sulfite, acides, stabilisées par EDTA. L'absorption est mesurée à 296 nm. Seuls les nitrites gênent; son influence est éliminée facilement par addition d'acide sulfamique. L'emploi de tétrachloromercurate(II) pour stabiliser les solutions de sulfite est moins satisfaisant: davantage d'interférences, essais à blancs plus élevés et sensibilité moins bonne.

ZUSAMMENFASSUNG

Schwefeldioxid (0.7–84 μg ml^{-1}) wird durch Extraktion mit *o*-Xylol aus angesäuerten, durch EDTA stabilisierten Sulfitlösungen bestimmt. Die Extinktion des Molekülkomplexes mit *o*-Xylol wird bei 296 nm gemessen. Nur Nitrit stört; dessen Einfluss wird durch Zugabe von Amidoschwefelsäure leicht eliminiert. Die Verwendung von Tetrachloromercurat(II) zur Stabilisierung der Sulfitlösungen ist wegen einer vergrösserten Zahl von Störungen, höherer Blindwerte und geringerer Empfindlichkeit weniger zufriedenstellend.

REFERENCES

1 P. W. West, *Proc. Int. Symp. Anal. Chem., Birmingham, U.K., 1969*, Butterworths, London, 1970, p. 439.
2 I. M. Kolthoff and R. Belcher, *Volumetric Analysis, Vol. III*, Wiley–Interscience, New York, 1957, pp. 293, 425, 462, etc.
3 G. Charlot, *Colorimetric Determination of Elements*, Elsevier, Amsterdam, 1964, pp. 392–3.

4 A. STEIGMANN, *J. Soc. Chem. Ind.*, 61 (1942) 181.
5 S. ATKIN, *Anal. Chem.*, 22 (1950) 947.
6 P. F. URONE AND W. E. BOGGS, *Anal. Chem.*, 23 (1951) 1517.
7 H. N. ALYEA AND H. C. J. BACKSTROM, *J. Amer. Chem. Soc.*, 51 (1929) 90.
8 P. W. WEST AND G. C. GAEKE, *Anal. Chem.*, 28 (1956) 1816.
9 R. E. HUMPHREY, M. H. WARD AND W. HINZE, *Anal. Chem.*, 42 (1970) 698.
10 H. W. SCOGGINS, *Anal. Chem.*, 42 (1970) 1091.
11 L. J. ANDREWS AND R. M. KEEFER, *J. Amer. Chem. Soc.*, 73 (1951) 4169.
12 D. BOOTH, F. S. DAINTON AND K. J. IVIN, *Trans. Faraday Soc.*, 55 (1959) 1293.
13 P. W. WEST AND F. ORDOVEZA, *Anal. Chem.*, 34 (1962) 1324.
14 J. B. PATE, B. E. AMMONS, G. A. SWANSON AND J. P. LODGE, *Anal. Chem.*, 37 (1965) 942.
15 D. D. PERRIN, *Masking and Demasking of Chemical Reactions*, Wiley–Interscience, New York, 1970, p. 171.

Analytica Chimica Acta
Elsevier Publishing Company, Amsterdam
Printed in The Netherlands

SPECTROPHOTOMETRIC DETERMINATION OF RUTHENIUM WITH ACENAPHTHENEQUINONEMONOXIME

S. K. SINDHWANI AND R. P. SINGH
Department of Chemistry, University of Delhi, Delhi-7 (India)

(Received 18th March 1971)

Many organic reagents for the determination of trace amounts of ruthenium have been proposed[1-6]. Recently introduced reagents are oximidobenzotetronic acid[7], 2,3-aminopyridine[8], 2,4,6-tris(2′-pyridyl) 5-triazine[9], and chrome azurol S[10]. None of these procedures permits the determination of ruthenium in the presence of all other platinum metals.

Acenaphthenequinonemonoxime (AQM) reacts with ruthenium(III) in hot aqueous media to give dark blue precipitates which are soluble in chloroform and carbon tetrachloride. The present study deals with spectrophotometric determination of ruthenium(III), based on the formation of the blue complex with AQM.

EXPERIMENTAL

Apparatus

All absorbance measurements were carried out with a Unicam SP 600 spectrophotometer in 10-mm matched glass absorption cells. A Metrohm pH meter, type E-350, was employed for pH measurements.

Reagents and solutions

Standard ruthenium solution (0.002 *M*). Dissolve ruthenium(III) chloride (Johnson-Matthey, London) in 1 *M* hydrochloric acid. Standardise gravimetrically by precipitating ruthenium as the hydrated oxide followed by careful ignition in air and reduction to the metal in hydrogen.

Reagent solution. Prepare a 0.04 *M* solution of acenaphthenequinonemonoxime in ethanol.

Chloroform. Reagent-grade chloroform was distilled before use.

Buffer solutions. Buffer solutions of pH 2.7–8.0 were obtained by mixing 1.0 *M* acetic acid and 1.0 *M* sodium acetate in different proportions. Higher pH values were obtained with sodium hydroxide.

Absorbance curves

The colour was developed by adding 5 ml of the reagent to 1 ml of $5 \cdot 10^{-4}$ *M* ruthenium chloride solution in a 50-ml flask; after adjustment to pH 5.50 with 5 ml of acetate buffer, the mixture was heated on a boiling water bath for 2 h. After cooling, the solution was extracted with 10 ml of chloroform, and the absorbance of the centrifuged chloroform extract was measured. Absorbance curves of the ruthenium

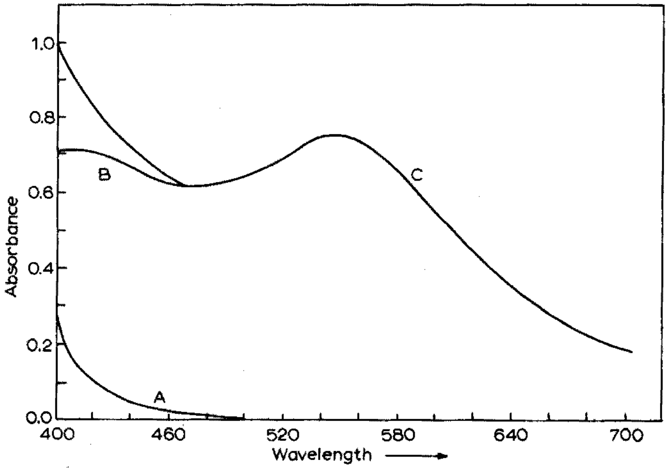

Fig. 1. Absorption spectra of reagent and its ruthenium complex at pH 5.5. (A) Reagent alone *vs.* chloroform, (B) ruthenium complex *vs.* chloroform, (C) reagent + ruthenium *vs.* chloroform. Ruthenium $5 \cdot 10^{-5}$ *M*. Reagent $2 \cdot 10^{-3}$ *M*.

complex and reagent are shown in Fig. 1; the complex shows maximum absorbance at 550 nm and at this wavelength, the absorbance of the reagent is negligible. In subsequent studies a chloroform blank was employed.

Effect of heating time, pH and reagent

The reaction of ruthenium(III) with AQM is slow at room temperature and maximum absorbance is not obtained even after standing for 24 h. The reaction is accelerated by heating on a steam bath; the absorbance gradually increases with increase in the time of heating and becomes constant after about 2.5 h.

The effect of pH on the extractability of the complex was studied. The pH values of the solutions, which contained ruthenium and an excess of the reagent, were adjusted to different levels in the range 3.0–8.0, or higher, and the total volume of the aqueous phase was kept at 10 ml. After heating for 3 h, the ruthenium complex was extracted and measured as described above. A plot of absorbance *vs.* pH showed that constant absorbance was exhibited in the pH range 4.6–6.0. Subsequent studies were therefore carried out at pH 5.5.

The ratio of reagent to metal ion necessary for maximum colour formation was ascertained by adding increasing volumes of reagent solution ($4 \cdot 10^{-3}$ *M*) in ethanol to a constant amount of ruthenium (1.0 ml of $5 \cdot 10^{-4}$ *M*) at pH 5.5. The results showed that at least a seven-fold molar excess of the reagent was required for maximum colour development. In subsequent studies a 10-fold molar excess of the reagent was used.

Adherence to Beer's law and sensitivity of the reaction

Under the optimal conditions described above, Beer's law was obeyed up to 6.57 p.p.m. of ruthenium. Expressed according to Sandell's notation, the sensitivity of the reaction is 0.0065 μg Ru cm^{-2} for $\log I_0/I = 0.001$ at 550 nm. The optimal range for highest precision was determined by means of a Ringbom plot to be 1.50–5.05

p.p.m. The molar absorptivity, calculated from the Beer's law curve, is $1.5 \cdot 10^4$ l mol^{-1} cm^{-1}.

Recommended procedure

Transfer a suitable aliquot containing 15–50 μg of ruthenium to a stoppered bottle and add 4 ml of $4 \cdot 10^{-3}$ *M* reagent solution in ethanol, followed by 5 ml of acetate buffer pH 5.5. Dilute to 10 ml with twice-distilled water and heat on a water bath for nearly 3 h. Remove the bottle from the water bath and allow to stand for 30 min. Add 10 ml of chloroform and shake the contents on a shaking machine for 10 min to obtain equilibration. Separate the organic layer and centrifuge to remove water droplets. Measure the absorbance at 550 nm against a chloroform blank.

Absorbance deviations

Eight separate solutions containing 2.0 p.p.m. of ruthenium(III), gave absorbance readings with an average relative deviation of ±0.88% and a maximum relative deviation of ±1.64% at 550 nm.

Composition of the complex

The molar composition of the complex was determined by Job's[11,12] and mole-ratio methods[13].

The continuous variations method, as adapted by Irving and Pierce for a two-phase system, was employed to establish the composition of the extracted species. The absorbance of the solutions extracted into chloroform was measured at 550 nm. A plot of the absorbance against the mole fraction of AQM is shown in Fig. 2, from which it is seen that maximal absorbance is exhibited when the metal:ligand ratio corresponds to 1:2.

The mole-ratio method (Fig. 3) showed that AQM and ruthenium combine in the ratio 2:1 confirming the results obtained by Job's method.

Stability constant of the complex

The stability constant of the complex was deduced from the conventional

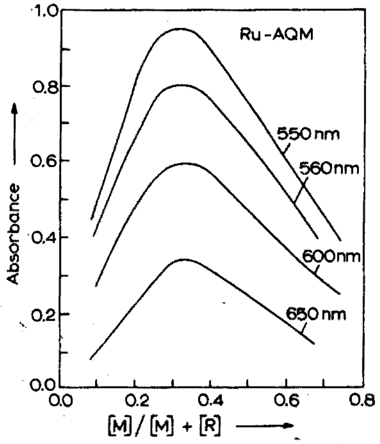

Fig. 2. Composition of ruthenium–AQM complex by Job's method. Total molarity $2.4 \cdot 10^{-4}$ *M*.

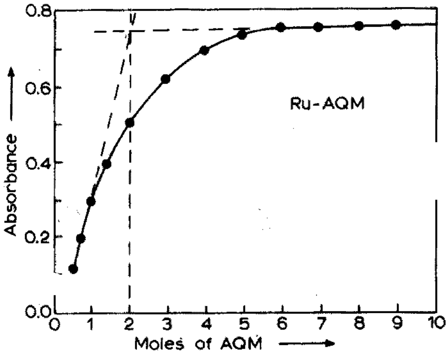

Fig. 3. Composition of ruthenium–AQM complex by the mole-ratio method. Ruthenium $5 \cdot 10^{-5}$ *M*.

relationships[14]. The values of E_m and E_s obtained were 0.750 and 0.510, respectively. The value of α was 0.320 and the stability constant was calculated as $1.9 \cdot 10^8$.

Effect of foreign ions

A series of synthetic samples containing known amounts of ruthenium and foreign ions were prepared and analysed by the recommended procedure. It was found that EDTA, hydroxyammonium chloride and thiourea, if added before the addition of the reagent, completely mask the reaction of ruthenium. Tartrate, citrate and thiocyanate also interfere. The study of interference was mainly confined to the metals of the eighth group of the periodic table and others which are commonly associated with ruthenium. The amounts (in p.p.m.) of ions which do not cause any interference (with 5.05 p.p.m. of ruthenium) are given in parentheses below: Cl^- (400), Br^- (400), I^- (400), F^- (50), $B_2O_3^{2-}$ (30), NO_2^- (40), IO_3^- (20), $C_2O_4^{2-}$ (80), NO_3^- (340), SO_4^{2-} (1000), Rh^{3+} (10), Os(VIII)(10), Pd^{2+} (4), Ir^{3+} (3), Pt(IV)(9), UO_2^{2+} (1000), Cu^{2+} (5), Ag^+ (20), Co^{2+} (10), Ni^{2+} (15), Zn^{2+} (40), Mo(VI)(9), Pb^{2+} (60), Cd^{2+} (60) and Be^{2+} (100).

DISCUSSION

Although various methods are known for the determination of ruthenium, comparatively few are well suited for the purpose. The most sensitive method yet recorded is the catalytic method developed by Surasitic and Sandell[3], for which the recommended range is 0.001–0.100 p.p.m. of ruthenium. Temperature is a critical factor in determining the rate of the reaction.

In the case of 1,10-phenanthroline or its 5-methyl derivative, which have been used for the determination of ruthenium, strong oxidising agents must be absent and interference is caused by silver, manganese and palladium. Acetylacetone[3] and 1,4-diphenylthiosemicarbazide have been used for the determination of ruthenium. Acetylacetone forms an intense pink colour of the composition $Ru(C_9H_7O_2)_3$ with an absorption maximum at 505 nm and a molar absorptivity of 1510. The sensitivity of this method is less than that of the thiourea or *p*-nitrosodimethylaniline reactions. The effect of associated platinum metals has not been recorded. 1,4-Diphenylthiosemicarbazide forms a red-violet complex with maximum absorbance at 560 nm,

TABLE I

COMPARISON OF THE SENSITIVITY OF WELL KNOWN REAGENTS FOR RUTHENIUM

Reagent	*Sensitivity* (μg *Ru cm*$^{-2}$)
Dithiooxamide	0.020/630 nm
1,3,5,7-Naphthylaminetrisulphonic acid	0.010/530 nm
1,10-Phenanthroline	0.0054/448 nm
p-Nitrosodimethylaniline	0.0028/610 nm
Anthranilic acid	0.024/620 nm
2-Nitroso-1-naphthol	0.015/600 nm
Thiocyanate	0.007/590 nm
1,4-Diphenylthiosemicarbazide	0.010/565 nm
2,4,6-Tris(2′-pyridyl) 5-triazine	0.0055/510 nm
Oximidobenzotetronic acid	0.35/520 nm
2,3-Diaminopyridine	0.0084/572 nm
Acetylacetone	2.5/505 nm
Acenaphthenequinonemonoxime (present reagent)	0.0065/550 nm

the sensitivity being 0.010 μg cm^{-2}. However, this method requires prior distillation of tetroxides, although it has the advantage that a 10-fold amount of osmium can be tolerated. Recently, oximidobenzotetronic acid, thiosalicylamide[15], 8-quinolinol, 2,3-diaminopyridine and 2,4,6-tris(2′-pyridyl)-5-triazine have been used for the purpose. Oximidobenzotetronic acid is selective but the sensitivity is very poor. Palladium and some of the base metals interfere in the case of thiosalicylamide. In the 8-quinolinol method, cobalt, chromium, molybdenum, palladium and rhodium interfere. In the 2,3-diaminopyridine method, prior separation of ruthenium as the tetroxide from several other metals is necessary.

In most of the methods including those mentioned above, determination of ruthenium in the presence of Group VIII metals is not possible and consequently, prior separation of these metals is essential. AQM has a high sensitivity and greater selectivity.

A comparison of some of the commonly used sensitive reagents with acenaphthenequinonemonoxime is made in Table I. It can be seen that this reagent ranks amongst the most sensitive reagents for the spectrophotometric determination of ruthenium.

One of the authors (S.K.S.) is grateful to the Council of Scientific and Industrial Research (India) for the award of a Junior Research Fellowship.

SUMMARY

Acenaphthenequinonemonoxime has been found to be a selective and sensitive reagent for the spectrophotometric determination of ruthenium in the pH range 4.6–6.0. The dark blue complex formed shows maximal absorbance at 550 nm. Beer's law is obeyed in the range 0–6.57 p.p.m. of ruthenium, the optimal range for determination being 1.50–5.05 p.p.m. The molar absorptivity is $1.5 \cdot 10^4$ l mol^{-1} cm^{-1}. The complex has the composition 1:2 metal:ligand. The method is shown to be selective and moderate amounts of other platinum metals do not interfere.

RÉSUMÉ

On propose l'acénaphtènequinonemonoxime comme réactif et sensible pour la dosage spectrophotométrique du ruthénium, à un pH de 4.6 à 6.0. Le complexe bleu foncé formé présente une absorption maximum à 550 nm. La loi de Beer s'applique de 0 à 6.57 p.p.m. de ruthénium (concentrations optimales: 1.50–5.05 p.p.m.). Le coefficient d'extinction molaire est de $1.5 \cdot 10^4 \text{mol}^{-1} \text{cm}^{-1}$. La composition du complexe, metal : ligand, est de 1 : 2. L'influence d'autres ions est examinée.

ZUSAMMENFASSUNG

Acenaphthenchinonmonoxim ist ein selektives und empfindliches Reagenz für die spektrophotometrische Bestimmung von Ruthenium im pH-Bereich 4.6–6.0. Die maximale Extinktion des gebildeten dunkelblauen Komplexes liegt bei 550 nm. Das Beersche Gesetz ist im Bereich 0–6.57 p.p.m. Ruthenium erfüllt; für die Bestimmung ist der Bereich 1.50–5.05 p.p.m. optimal. Der molare Extinktionskoeffizient ist $1.5 \cdot 10^4$ 1 mol^{-1} cm^{-1}. Der Komplex hat das Metall–Ligand-Verhältnis 1 : 2. Die Methode ist selektiv; mässige Mengen anderer Metalle stören nicht.

REFERENCES

1 F. E. Beamish and W. A. E. McBryde, *Anal. Chim. Acta*, 9 (1953) 349.
2 F. E. Beamish and W. A. E. McBryde, *Anal. Chim. Acta*, 18 (1958) 551.
3 F. E. Beamish, *Analytical Chemistry of Platinum Metals*, Pergamon Press, London, 1966, p. 366.
4 F. E. Beamish, *Talanta*, 12 (1965) 789.
5 K. Kodama, *Nagoyashi Kogyo Kenkyusho Kenkyu Hokoku*, 38 (1967) 54.
6 E. B. Sandell, *Colorimetric Determination of Traces of Metals*, Interscience, New York, 1959, p. 778.
7 G. S. Manku, A. N. Bhat and B. D. Jain, *Talanta*, 14 (1967) 1229.
8 G. H. Ayres and D. T. Easter, *Anal. Chim. Acta*, 44 (1969) 67.
9 W. A. Embry and G. H. Ayres, *Anal. Chem.*, 40 (1968) 1499.
10 K. K. Saxena and A. K. Dey, *Indian J. Chem.*, 7 (1969) 75.
11 P. Job, *Ann. Chim.*, 9 (1928) 113.
12 H. Irving and T. B. Pierce, *J. Chem. Soc.*, (1959) 2565.
13 J. H. Yoe and A. L. Jones, *Ind. Eng. Chem., Anal. Ed.*, 16 (1944) 111.
14 A. E. Harvey and D. L. Manning, *J. Amer. Chem. Soc.*, 72 (1950) 4488.
15 A. V. Rangnekar and S. M. Khopkar, *Mikrochim. Acta*, 2 (1968) 272.
16 K. Sur and S. C. Shome, *Anal. Chim. Acta*, 48 (1969) 145.

Analytica Chimica Acta
Elsevier Publishing Company, Amsterdam
Printed in The Netherlands

ANALYSE SPECTROPHOTOMETRIQUE DES CHLOROPHYLLES ET DES PHEOPHYTINES a ET b EN MILIEU HYDROACETONIQUE

I. DÉTERMINATION DES EXTINCTIONS MOLAIRES

NOËL DELAPORTE ET DANIELLE LAVAL-MARTIN

Laboratoire P.O.V.A.R., Centre National de la Recherche Scientifique, 4, ter route des Gardes, 92-Meudon (France)

(Reçu le 8 janvier 1971)

Les différentes méthodes de dosage spectrophotométrique des chlorophylles des extraits végétaux, utilisent les coefficients d'absorption spécifique de ces pigments. La détermination de ces coefficients est basée essentiellement sur trois sortes de procédés:

1. mesures pondérales[1-3],
2. dosages du magnésium[4-6]. Dans ce cas, la méthode employée[7] exploite colorimétriquement l'adsorption du déhydro-*p*-toluidinesulfonate de sodium sur l'hydroxyde de magnésium colloïdal,
3. mesures comparatives, par spectrophotométrie, basées sur des coefficients d'absorption déterminés par les auteurs précédents et transposés à un autre milieu[8,9].

Pour un même solvant il n'y a pas accord sur les valeurs des coefficients d'absorption spécifique ni sur la position des maxima caractéristiques des spectres de chlorophylles. Les écarts observés peuvent avoir plusieurs origines: l'existence de formes isomères d'une même chlorophylle, ce qui peut entraîner de légères modifications spectrales[3]; la difficulté des mesures gravimétriques sur un matériel fragile et peu commode à obtenir à l'état cristallisé, et l'imprécision[10] de la méthode colorimétrique utilisée pour doser le magnésium.

Dans ce travail, nous calculons les extinctions molaires des chlorophylles a et b et des phéophytines correspondantes en dosant parallèlement leur magnésium et leur noyau porphyrinique à l'aide de méthodes potentiométriques et spectrophotométriques. Ces extinctions sont données pour les milieux hydroacétoniques, qui sont les plus fréquemment utilisés pour l'extraction et le dosage de ces pigments.

MATÉRIEL ET MÉTHODES

Les chlorophylles pures sont isolées par chromatographies successives sur poudre de cellulose selon une méthode déjà précisée[11].

Les dosages sont effectués à partir de prises d'essai, exactement pesées, contenant environ 1 mg de chlorophylle par ml d'acétone. A partir de la solution initiale, conservée à $-20°$, nous effectuons les mesures des absorptions spectrophotométriques en faisant varier le pourcentage d'eau entre 2.5 et 20% (poids–volume). Nous avons ainsi pu préciser les variations des extinctions molaires, en fonction du taux d'hydratation du milieu.

Chlorophylle a

Formation des phéophytines et séparation du magnésium. Nous ajoutons, à une prise d'essai de chlorophylle, trois volumes d'éther de pétrole 30°–50° et 0.2 ml d'acide chlorhydrique concentré, afin de provoquer la phéophytinisation. Le magnésium libéré est extrait par trois fractions de 5 ml d'acide chlorhydrique 0.1 *M*. La phase éthéropétrolique est rincée à l'eau distillée. L'épiphase éthéropétrolique, contenant la phéophytine, est évaporée sous vide. On reprend par 10 ml d'acide acétique pour le dosage ultérieur du noyau porphyrinique.

Les hypophases hydroacétoniques, contenant le magnésium, sont réunies puis évaporées sous vide. L'extrait sec, additionné de 2.0 ml d'acide nitrique et de 0.2 ml d'acide sulfurique concentré, est chauffé jusqu'à siccité, puis repris par 20 ml d'eau distillée.

Dosage du noyau porphyrinique. Pour doser le noyau porphyrinique des chlorophylles, nous exploitons la propriété, que possèdent les phéophytines, de complexer en milieu anhydre certains ions métalliques, comme le cuivre, le nickel, le cobalt et le cadmium (Berezin *et al.*[12–14]). Ces auteurs montrent que la vitesse de formation des phéophytinates dépend de la nature des cations, ainsi que des solvants. Les réactions observées sont pseudomonomoléculaires en présence d'un excès d'ions métalliques. A partir de ces données, nous avons recherché des conditions favorisant une vitesse de réaction suffisamment rapide, pour permettre un dosage volumétrique des phéophytines par un ion métallique. L'utilisation de l'ion cuivre(II) s'est avérée satisfaisante en milieu acétique et permet un dosage stoechiométrique de la phéophytine a. Au cours de ce dosage, la variation du potentiel du milieu peut être enregistrée. Au point d'équivalence, l'inflexion potentiographique est suffisante pour permettre la détermination de la fin de la réaction. A cet effet, nous utilisons un potentiographe muni d'une électrode au calomel (pont électrolytique d'acide acétique saturé de nitrate de potassium) et d'une électrode de mesure qui peut être en platine. Cependant, ce métal se polarisant rapidement, nous préférons utiliser une électrode de

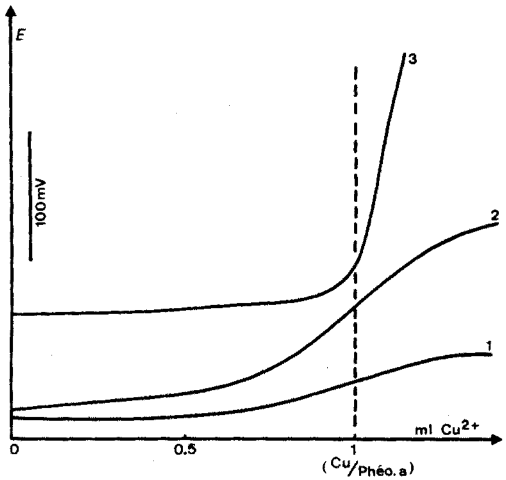

Fig. 1. Dosages électrométriques de la phéophytine a en milieu acétique. (1) Avec électrodes carbone–calomel ; (2) avec électrodes platine–calomel ; (3) avec électrode double de platine (intensité imposée 0.1 μA).

graphite, qui ne se pollue pas si l'on a soin d'éliminer après chaque dosage la partie qui a été immergée (Fig. 1).

La complexation du cuivre modifie le spectre des phéophytines (Fig. 2). Au cours du dosage par le cuivre, en milieu acétique, on peut enregistrer l'évolution de ce spectre à 635 nm, où la différence d'absorption est importante entre la phéophytine et le phéophytinate. La fin de la réaction est caractérisée par un changement dans l'évolution de la densité optique (Fig. 3).

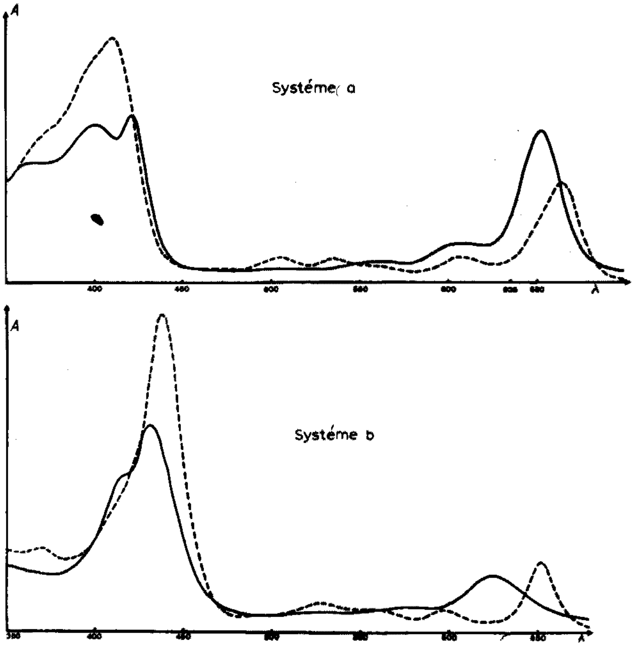

Fig. 2. Spectres des phéophytines et des phéophytinates de cuivre correspondants, dans l'acide acétique. (---) Phéophytine; (——) phéophytinate de cuivre.

Pour déterminer, avec le maximum de précision, la fin des réactions de complexation, nous avons associé les mesures potentiométriques et les mesures spectrophotométriques. Ceci est obtenu en couplant les appareils (Fig. 4) avec une pompe péristaltique qui assure la circulation de la solution acétique de phéophytine entre la cellule potentiométrique et la cellule d'un spectrophotomètre enregistreur à double faisceau (parcours optique 1 mm). Nous dosons en enregistrant simultanément les deux réponses, potentiométrique et spectrophotométrique. La burette automatique couplée au potentiographe distribue une solution d'acétate de cuivre, exactement titrée ($2 \cdot 10^{-2} M$), à une vitesse d'environ 1 ml h^{-1}. Un chronomètre incorporé au potentiographe inscrit un repère de temps qui permet de vérifier la coïncidence des deux enregistrements. Le décalage, dans le temps, des deux réponses indiquant la fin de la titration, dépend à la fois de la vitesse de circulation du liquide et de la vitesse d'admission de la solution titrante; il est négligeable dans nos conditions.

Dosage du magnésium. Pour doser le magnésium, nous employons une méthode classique qui consiste à le complexer, en milieu légèrement alcalin, par l'acide éthylène-

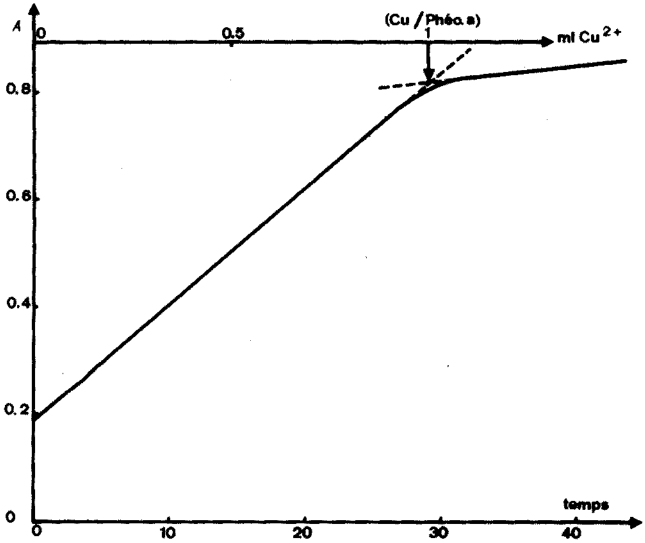

Fig. 3. Evolution de la densité optique, à 635 nm, au cours de la titration de la phéophytine a par le cuivre.

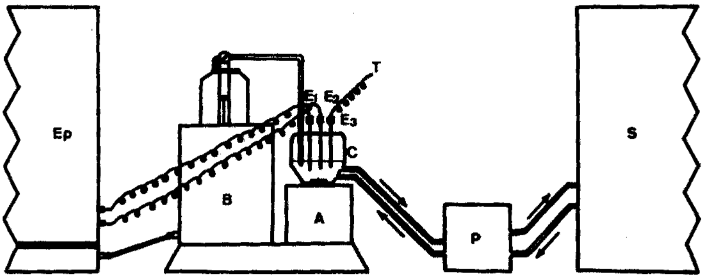

Fig. 4. Schéma du montage assurant la circulation des solutions à titrer entre les cellules potentiométrique et spectrophotométrique. Ep = enregistreur potentiométrique (Metrohm, type E 436), B = burette automatique (1 ml, Metrohm, type E 436 E), A = agitateur magnétique, C = cellule potentiométrique, E1 = électrode de graphite, E2 = électrodes au calomel, E3 = électrode de métal inattaquable, reliée à la terre, P = pompe à circulation, S = spectrophotomètre à double faisceau, enregistreur (Leres, type S 66).

diaminetétraacétique (EDTA). Le magnésium en solution aqueuse est titré par une solution d'EDTA $2.5 \cdot 10^{-2} M$, en présence d'un tampon à base d'éthanolamine, qui maintient un pH de 10.5. La stabilité de ce pH est contrôlé par une électrode combinée verre–calomel. La fin de la réaction de complexation est déterminée par potentiométrie à intensité constante à l'aide d'une électrode double d'argent amalgamée (Fig. 5).

Chlorophylle b

Dosage du noyau porphyrinique. Nous avons observé que dans l'acide acétique, les chlorophylles pouvaient, sans phéophytinisation préalable, complexer les ions cuivriques avec une vitesse inférieure à celle des phéophytines correspondantes. Cette réaction est plus rapide dans le cas de la chlorophylle a que dans le cas de la

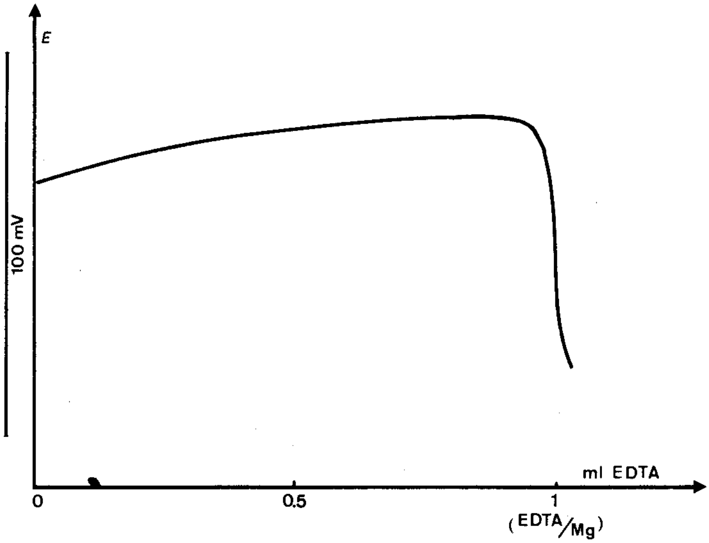

Fig. 5. Dosage voltammétrique du magnésium par l'EDTA (électrode double d'argent amalgamé sous une intensité imposée de 1 μA).

chlorophylle b, mais le terme en est moins net. Ces phénomènes peuvent être dus à un déplacement du magnésium par le cuivre, la constante de stabilité des phéophytinates de cuivre étant supérieure à celle des chlorophylles, mais il peut s'agir aussi d'une forme complexe intermédiaire[15]. Quel que soit le mécanisme mis en jeu, après introduction d'un excès d'ions cuivre(II) dans une solution acétique de chlorophylle, on observe une complexation stoechiométrique. La stabilité de la densité optique à 630 nm indique la fin de la réaction. L'utilisation d'un système d'électrodes platine–calomel, permet un dosage potentiométrique, par l'EDTA, des ions cuivre(II) non complexés, à condition d'ajouter au milieu acétique un demi volume d'acétonitrile. La teneur en noyau porphyrinique est obtenue par différence entre la quantité d'ions cuivriques introduite initialement et celle dosée en retour par l'EDTA.

Dosage du magnésium. La solution ayant servi au dosage du noyau porphyrinique est récupérée quantitativement puis évaporée sous vide. Nous minéralisons jusqu'à siccité avec 2 ml d'acide nitrique et 0.2 ml d'acide sulfurique concentré. Le résidu est solubilisé dans 25 ml d'eau bidistillée. Nous avons alors en solution la quantité de cuivre totale introduite et le magnésium correspondant à la prise d'essai de chlorophylle b. Nous les dosons successivement en utilisant les différences de stabilité que nous avons calculées en fonction du pH, des complexes de ces métaux avec l'EDTA (Fig. 6). Les deux complexes peuvent se former en milieu alcalin, mais celui du magnésium n'est pas stable en milieu acide. Nous dosons donc le cuivre à pH 4.5 puis le magnésium à un pH voisin de 10. Cette titration est suivie potentiométriquement en imposant une intensité constante de 1 μA entre deux électrodes d'argent amalgamé. A pH 4.5 on obtient un premier point d'inflexion correspondant à la complexation des ions cuivriques: on doit retrouver exactement la quantité de cuivre initialement introduite lors du dosage du noyau porphyrinique. Après alcalinisation, on obtient un second point d'inflexion correspondant au dosage du magnésium (Fig. 7): pour une chlorophylle pure la concentration en magnésium doit être équivalente à celle du cuivre complexé précédemment par le noyau porphyrinique.

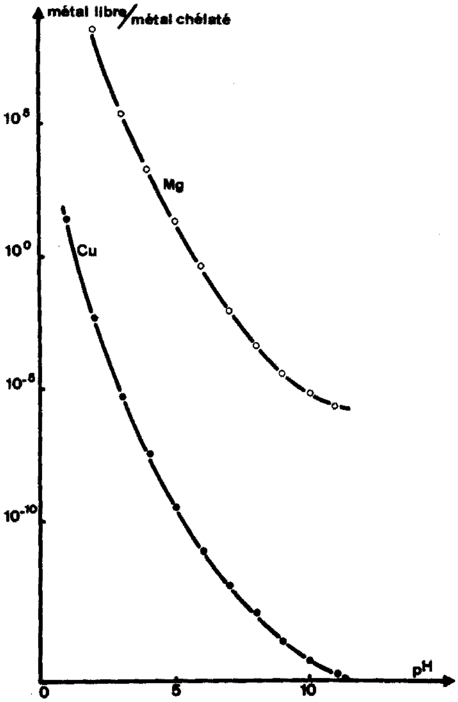

Fig. 6. Rapports, en fonction du pH, des concentrations en ions métalliques libres et en ions métalliques chélatés par l'EDTA (courbes théoriques pour le cuivre et le magnésium, calculées d'après les données de Charlot[16]).

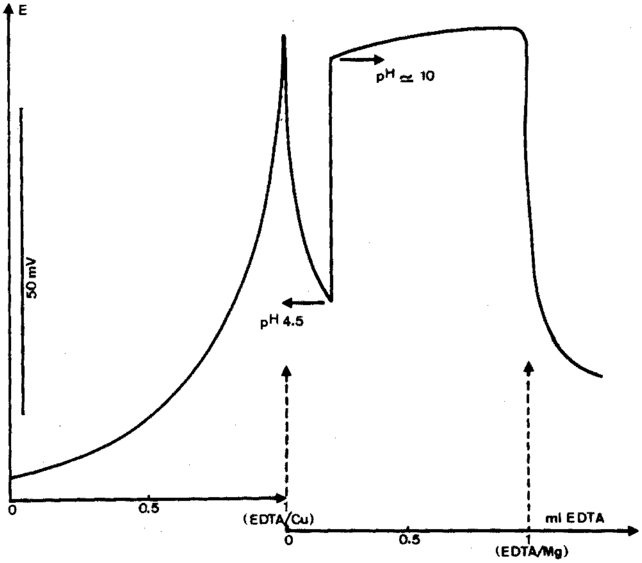

Fig. 7. Dosage voltammétrique du cuivre (pH 4.5) et du magnésium (pH$\simeq$10) par l'EDTA, en milieu aqueux, avec une électrode double d'argent amalgamé (intensité imposée 1 μA).

RÉSULTATS

Chlorophylle a et phéophytine a

Les dosages des noyaux porphyriniques effectués par potentiométrie et par spectrophotométrie sur quinze prises d'essais, donnent deux valeurs moyennes qui diffèrent de 1.2%. Les valeurs déterminées spectrophotométriquement sont plus optimistes que celles obtenues potentiométriquement. Nous avons fait la moyenne de ces deux valeurs et nous l'avons comparée à la moyenne des résultats des dosages de magnésium effectués parallèlement sur les quinze essais. La concentration en noyau porphyrinique est supérieure de 2.1% à la concentration en magnésium. Pour effectuer les calculs des extinctions molaires de la chlorophylle a et de la phéophytine a, dans les différents milieux hydroacétoniques, nous utilisons la demi somme des valeurs obtenues par le dosage du magnésium et par le dosage du noyau porphyrinique. Les extinctions molaires présentées dans le Tableau I sont donc significatives avec une marge d'erreur de ±1.8%.

TABLEAU I

EXTINCTIONS MOLAIRES ε ($\mathrm{l\ mol^{-1}\ cm^{-1}}$) DE LA CHLOROPHYLLE a ET DE LA PHÉOPHYTINE a CALCULÉES POUR DIVERSES LONGUEURS D'ONDE λ (nm) CARACTÉRISTIQUES DE LEURS SPECTRES

	Solvant: acétone–eau (vol–vol)				
	80–20	90–10	95–5	97.5–2.5	100–0
Chlorophylle a	71,200	72,200	73,400	73,800	71,500
	(412)	(411)	(411)	(410)	(410)
	88,000	93,400	98,100	101,000	100,000
	(431)	(430)	(430)	(429)	(428)
	76,600	78,300	80,500	81,400	78,500
	(663)	(662)	(661)	(660)	(659)
Phéophytine a	104,500	107,200	112,000	113,400	
	(409)	(408)	(408)	(408)	
	47,500	46,900	47,700	46,600	
	(663, 664)	(663)	(663)	(663)	
Chlorophylle a et phéophytine a aux points isobestiques	70,000	71,100	71,600	73,300	
	(419)	(419)	(418)	(418)	

Chlorophylle b et phéophytine b

Le calcul des extinctions molaires de la chlorophylle et de la phéophytine b est effectué à partir des résultats de douze dosages. La valeur moyenne des résultats des dosages de magnésium est supérieure de 1% à la valeur moyenne des dosages du noyau porphyrinique. Nous utilisons la demi somme de ces deux moyennes pour définir les extinctions molaires (Tableau II), qui sont significatives à ±1%.

DISCUSSION

Les résultats des dosages du magnésium et du noyau porphyrinique diffèrent de 2.1% pour la chlorophylle a et de 1% pour la chlorophylle b. Pour la première, c'est le chiffre représentant les résultats des dosages du noyau porphyrinique qui est

TABLEAU II

EXTINCTIONS MOLAIRES ε (l mol^{-1} cm^{-1}) DE LA CHLOROPHYLLE b ET DE LA PHÉOPHYTINE b CALCULÉES POUR DIVERSES LONGUEURS D'ONDE λ (nm) CARACTÉRISTIQUES DE LEURS SPECTRES

	Solvant: acétone–eau (vol–vol)				
	80–20	90–10	95–5	97.5–2.5	100–0
Chlorophylle b	51,200	51,000	51,300	51,200	51,000
	(433)	(433)	(433)	(433)	(432)
	123,000	123,600	126,000	128,000	124,000
	(457, 458)	(457)	(456)	(456)	(456)
	44,900	44,700	44,900	45,400	45,000
	(646)	(645)	(645)	(645)	(645)
Phéophytine b	66,200	66,000	67,900	72,300	
	(414)	(413)	(412)	(412)	
	142,800	144,300	147,500	150,000	
	(434)	(434)	(434, 433)	(433)	
	29,000	28,500	28,100	29,700	
	(653)	(653, 652)	(652)	(652)	
Chlorophylle b et phéophytine b aux points isobestiques	72,000	72,300	71,300	72,300	
	(445, 446)	(445, 444)	(444)	(444)	
	27,400	27,900	28,700	29,700	
	(654)	(654)	(653)	(653, 652)	

le plus fort, mais c'est le contraire pour la seconde; ces écarts apparaissent donc inhérents aux manipulations. En effet, dans le cas de la chlorophylle a, la technique de phéophytinisation implique une extraction qui peut être à l'origine du léger déficit en magnésium; nous n'avons pas eu cet inconvénient pour la chlorophylle b. Nous pouvons donc considérer, à ces variabilités près, qu'il y a équivalence entre les valeurs en noyau porphyrinique et en magnésium. A partir des extinctions molaires (Tableaux

TABLEAU III

COMPARAISON DES COEFFICIENTS D'ABSORPTION α (l g^{-1} cm^{-1}) DES CHLOROPHYLLES a ET b ET DES PHÉOPHYTINES a ET b DANS UN MILIEU HYDROACÉTONIQUE 20–80 (vol–vol), À DIVERSES LONGUEURS D'ONDE λ (nm), CARACTÉRISTIQUES DE LEURS SPECTRES

	Chlorophylle a	*Phéophytine a*	*Chlorophylle b*	*Phéophytine b*
Valeurs indiquées par MacKinney[17]	82.04		45.60	
	(663)		(645)	
	90.78		130.3	
	(430)		(460)	
Valeurs indiquées par Vernon[8]	90.8	52.5	52.5	34.8
	(665)	(666, 667)	(648, 649)	(655)
	101.5	127.3	148.0	176.3
	(433)	(409)	(460)	(436)
Valeurs calculées	85.7	54.6	49.5	32.8
	(663)	(663, 664)	(646)	(653)
	98.5	120.0	135.5	161
	(431)	(409)	(457, 458)	(434)

I et II), nous avons calculé les coefficients d'absorption spécifique de façon à pouvoir les comparer avec ceux utilisés pour les milieux hydroacétoniques par MacKinney[17] et par Vernon[8]. L'examen du Tableau III montre que nos coefficients se situent entre les valeurs données par ces deux auteurs.

La conjugaison des méthodes potentiométriques et spectrophotométriques, ainsi que les dosages comparés du magnésium et du noyau porphyrinique permettent donc de titrer les pigments chlorophylliens avec un maximum d'exactitude. La coïncidence des résultats constitue d'autre part un critère de pureté pour les chlorophylles dosées, dont les spectres nous ont servi pour calculer les extinctions molaires.

RÉSUMÉ

Les auteurs ont déterminés les coefficients d'absorption spécifique des chlorophylles a et b, en milieu eau–acétone. Le magnésium est dosé dans chaque chlorophylle à l'aide d'EDTA et détermination du point final par voltamétrie. Le noyau porphyrine est titré par le cuivre(II) dans l'acide acétique anhydre avec détermination du point final, simultanément par spectrophotométrie et par potentiométrie. Des résultats identiques pour ces deux titrages constituent un critère de pureté des chlorophylles examinées. D'autre part, ils permettent une détermination rigoureuse de l'absorption molaire de l'un de ces pigments, pour une longueur d'onde donnée.

SUMMARY

Molar absorptivities of purified chlorophylls a and b were determined in aqueous acetone media. For each chlorophyll, magnesium was titrated with EDTA to a voltammetric end-point, and the porphyrin ring was titrated with copper(II) in anhydrous acetic acid, the end-points being simultaneously determined spectrophotometrically and potentiometrically. The identical results of these two titrations provide a criterion of purity for the studied chlorophylls. Moreover, these results permit the rigorous determination of the molar absorptivity of one of these pigments at selected wavelengths.

ZUSAMMENFASSUNG

Es wurden die molaren Extinktionskoeffizienten der gereinigten Chlorophylle a und b in wässrigen Acetonlösungen bestimmt. Für jedes Chlorophyll wurde das Magnesium mit EDTA bis zu einem voltammetrischen Endpunkt titriert. Der Porphyrinring wurde mit Kupfer(II) in wasserfreier Essigsäure titriert, wobei die Endpunkte simultan spektrophotometrisch und potentiometrisch ermittelt wurden. Die identischen Ergebnisse dieser beiden Titrationen sind ein Kriterium für die Reinheit der untersuchten Chlorophylle. Darüberhinaus erlauben diese Ergebnisse die genaue Bestimmung der molaren Extinktionskoeffizienten eines dieser Pigmente bei charakteristischen Wellenlängen.

BIBLIOGRAPHIE

1 G. MacKinney, *J. Biol. Chem.*, 132 (1940) 91.
2 F. P. Zscheile et C. L. Comar, *Botan. Gaz.*, 102 (1941) 463.
3 H. H. Strain, M. R. Thomas et J. J. Katz, *Biochim. Biophys. Acta*, 75 (1963) 306.
4 V. M. Koski et J. H. C. Smith, *J. Amer. Chem. Soc.*, 70 (1948) 3558.
5 S. L. Granick, *J. Biol. Chem.*, 183 (1950) 713.
6 J. H. C. Smith et A. Benitez, in K. Peach and M. V. Tracey, *Modern Methods of Plant Analysis, Vol. 4*, Springer-Verlag, Berlin–Göttingen–Heidelberg, 1955, p. 142.
7 E. E. Ludwig et C. R. Johnson, *Ind. Eng. Chem., Anal. Ed.*, 14 (1942) 895.
8 L. P. Vernon, *Anal. Chem.*, 32 (1960) 1144.
9 T. Ogawa et K. Shibata, *Photochem. Photobiol.*, 4 (1965) 193.
10 G. Charlot, *Les Méthodes de la Chimie Analytique. Analyse Quantitative Minérale*, Masson, Paris, 1966, p. 784.
11 N. Delaporte et D. Laval-Martin, *Chim. Anal.*, sous presse.
12 B. D. Berezin et N. I. Sosnikova, *Zh. Fiz. Khim.*, 39 (1965) 1348.
13 B. D. Berezin et G. I. Smirnova, *Zh. Fiz. Khim.*, 41 (1967) 1323; 42 (1968) 1952; 43 (1969) 659.
14 B. D. Berezin et A. N. Drobysheva, *Zh. Neorgan. Khim.*, 13 (1968) 2720.
15 L. P. Vernon et G. R. Seely, *The Chlorophylls*, Academic Press, New-York–London, 1966, p. 79.
16 G. Charlot, *L'Analyse Qualitative et les Réactions en Solution*, Masson, Paris, 1963, p. 46.
17 G. MacKinney, *J. Biol. Chem.*, 140 (1941) 315.

Analytica Chimica Acta
Elsevier Publishing Company, Amsterdam
Printed in The Netherlands

ANALYSE SPECTROPHOTOMETRIQUE DES CHLOROPHYLLES ET DES PHEOPHYTINES a ET b EN MILIEU HYDROACETONIQUE

II. MÉTHODE CINÉTIQUE DE DOSAGE

NOËL DELAPORTE ET DANIELLE LAVAL-MARTIN
Laboratoire P.O.V.A.R., Centre National de la Recherche Scientifique, 4, ter route des Gardes, 92-Meudon (France)

(Reçu le 8 janvier 1971)

Certaines méthodes utilisées pour le dosage des chlorophylles sont basées sur l'interprétation de mesures spectrophotométriques effectuées directement sur les extraits[1-7]. Ces méthodes ne sont pas utilisables en présence d'autres substances, comme les phéophytines, qui absorbent dans la région du spectre où sont effectuées les mesures. D'autre part, l'application de ces divers modes de détermination des chlorophylles à un extrait de pigments, donne des résultats dispersés[8-11]. Par contre, l'exploitation des modifications spectrales caractéristiques d'une transformation chimique du corps à doser, peut davantage donner satisfaction. Obéissent notamment à ce principe, les techniques basées sur la phéophytinisation globale des chlorophylles[12-14] et sur la combinaison de la chlorophylle b avec l'hydroxylamine[15]. Ces méthodes utilisent des coefficients d'absorption spécifique précédemment définis[2,5,7] et transposés aux solvants utilisés.

Dans ce travail, en exploitant spectrophotométriquement la différence entre les vitesses de phéophytinisation de la chlorophylle a et de la chlorophylle b, dans les extraits hydroacétoniques de végétaux, nous avons mis au point une méthode de dosage spécifique de chacun de ces deux pigments. Nous présentons aussi un mode de calcul simple, des quantités de phéophytines a et b présentes. Pour le calcul des concentrations, nous avons déterminé les extinctions molaires des pigments dans l'acétone à 10% d'eau.

Conditions du dosage

En milieu hydroacétonique, la température, le taux d'hydratation et la concentration en acide, sont les principaux paramètres qui déterminent les vitesses des phénomènes exponentiels de phéophytinisation des chlorophylles a et b[16]. Une basse température, une forte concentration en acide et une faible teneur en eau permettent d'obtenir une différence importante entre les vitesses de phéophytinisation des deux chlorophylles. Deux de ces paramètres sont difficiles à faire varier: en effet, il est pratique d'effectuer les dosages de chlorophylles à la température ambiante et d'autre part la concentration en acide doit être telle que les vitesses de phéophytinisation soient mesurables aisément. Le seul facteur que l'on peut facilement faire varier reste le taux d'hydratation du milieu, qui doit cependant permettre une extraction commode des pigments à partir du matériel végétal.

Pour provoquer la phéophytinisation des chlorophylles, nous utilisons une concentration en acide chlorhydrique telle, que dans un milieu acétonique à 10% d'eau, la réaction soit terminée en un temps inférieur à 15 min. L'influence des variations de la température ambiante, sur la différence des vitesses de transformation des deux chlorophylles, n'est pas préjudiciable à l'application de la méthode. Dans ces conditions, la chlorophylle b des extraits se phéophytinise à une vitesse 25 à 35 fois inférieure à celle de la chlorophylle a, qui sera donc phéophytinisée en moins d'une minute. Cette fluctuation de la valeur du rapport des vitesses est évidemment liée aux variations de la température, de la concentration de l'acide introduit et du taux d'hydratation du solvant qui peut être plus ou moins voisin de 10%. Dans les extraits végétaux, il y a habituellement deux à trois fois plus de chlorophylle a que de chlorophylle b, la contribution en densité optique de la chlorophylle b est donc relativement faible, son extinction molaire étant en outre inférieure à celle de la chlorophylle a. Il est donc nécessaire d'enregistrer les cinétiques de phéophytinisation à des longueurs d'onde où l'écart est maximum entre l'absorption des chlorophylles et celle des phéophytines résultantes (Fig. 1). Dans la région où les caroténoïdes n'absorbent pas, deux longueurs d'onde sont caractéristiques à cet égard: 663 nm pour la chlorophylle a et 642 nm pour la chlorophylle b. Mais vers 663 nm, la différence de densité optique entre la chlorophylle b et la phéophytine b est si faible qu'elle ne permettrait pas de mesures précises. Par contre aux longueurs d'onde proches de 642 nm, la différence de densité optique entre la chlorophylle a et la phéophytine a est appréciable. Dans cette région du spectre, on peut donc observer facilement la phéophytinisation de chacune des deux chlorophylles. Il suffira pour cela, d'enregistrer une seule cinétique de phéophytinisation, à une longueur d'onde voisine de 642 nm (Fig. 2).

Technique du dosage

Il est nécessaire de connaître approximativement la teneur en eau des tissus végétaux, avant d'en extraire les pigments. En présence de carbonate de magnésium,

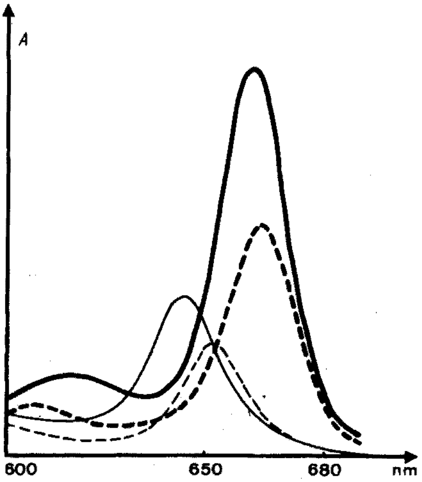

Fig. 1. Spectres, de 600 à 700 nm, des chlorophylles a et b et des phéophytines correspondantes, dans un solvant hydroacétonique 10–90 (vol–vol). (——) C_a; (------) P_a; (——) C_b; (---) P_b.

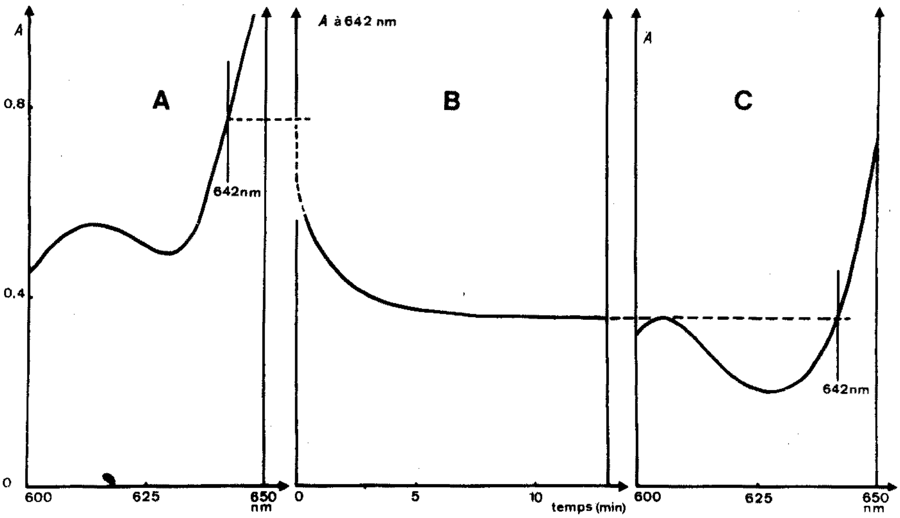

Fig. 2. (A) Spectre d'un extrait hydroacétonique (10–90, vol–vol) de végétal. (B) Enregistrement, à 642 nm, de la cinétique de phéophytinisation des chlorophylles a et b de cet extrait. (C) Spectre de l'extrait, après phéophytinisation complète.

on broie les tissus dans des quantités d'acétone telles, qu'après filtration, la solution finale de volume déterminé renferme 10% d'eau.

Une partie de l'extrait hydroacétonique est alors introduite dans une cellule spectrophotométrique de parcours optique suffisant pour que la modification de densité optique soit mesurable aisément. A l'aide d'un spectrophotomètre à double faisceau, on enregistre l'absorption initiale (A_i) à la longueur d'onde choisie pour les mesures. Ensuite, dans le bouchon de la cellule, prévu à cet effet, on introduit un volume d'acide chlorhydrique, tel que l'effet de dilution soit négligeable. La concentration de l'acide chlorhydrique utilisé dépend de la capacité tampon de l'extrait végétal. Pour obtenir une différence exploitable entre les vitesses de phéophytinisation des deux chlorophylles, il faut que cette concentration permette la phéophytinisation totale de la chlorophylle b dans un temps compris entre 8 et 15 min. Pour nos essais (Fig. 2), effectués à partir d'extraits de haricots verts (*Phaseolus vulgaris*, var. Slander White), nous ajoutons 0.03 ml d'acide chlorhydrique 3 *M*, dans une cellule spectrophotométrique de 5 cm de parcours optique et contenant 15 ml d'extrait acétonique. Le bouchon est fixé puis on agite le contenu de la cellule et on déclenche simultanément l'enregistreur du spectrophotomètre, réglé à une vitesse de 1 cm par minute. La cellule est mise rapidement en place et la cinétique de phéophytinisation est enregistrée (Fig. 2B). Lorsque les chlorophylles sont totalement phéophytinisées, l'absorption devient stable (A_f). On arrête alors l'enregistrement.

Interprétation des cinétiques

Les valeurs des différences $A_x - A_f$ (A_x étant l'absorption à l'instant t) sont mesurées à partir d'une minute (Fig. 3A). Les logarithmes de ces valeurs sont portés en fonction du temps, on obtient une droite uniquement représentative de la cinétique de phéophytinisation de la chlorophylle b. L'ordonnée à l'origine de cette droite ($\log A_b$) permet la détermination de A_b (Fig. 3B).

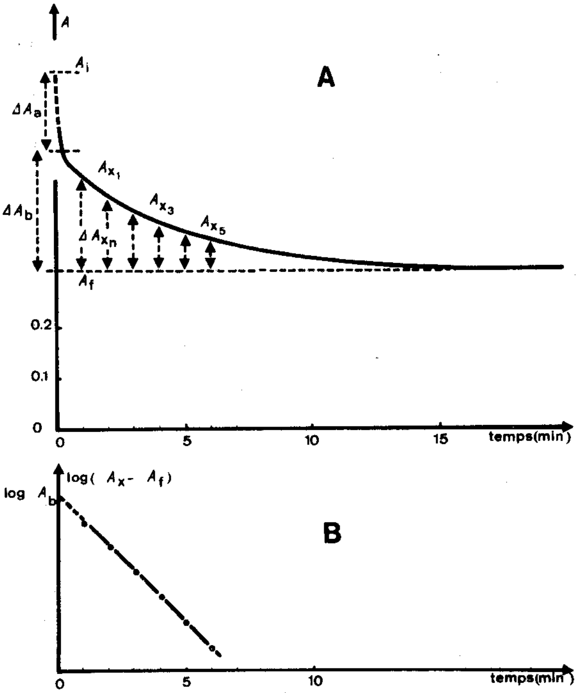

Fig. 3. (A) Enregistrement, à 642 nm, de la cinétique de phéophytinisation des chlorophylles a et b, d'un extrait hydroacétonique de végétal. A_i = densité optique initiale de l'extrait; A_f = densité optique finale de l'extrait, après phéophytinisation; A_{x_n} = densité optique, à n minutes, au cours de la phéophytinisation; ΔA_{x_n} = différence entre la densité optique après n minutes et la densité optique finale; $\Delta A_{\text{a ou b}}$ = différence de densité optique, spécifique de la phéophytinisation totale de la chlorophylle a, ou de la chlorophylle b de l'extrait. (B) Représentation, en coordonnées semi-logarithmiques, de la cinétique de phéophytinisation de la chlorophylle b ($\log A_{x_n} = f(t_n)$).

Il est possible aussi, pour éviter la construction graphique, d'effectuer le calcul rapide de log A_b en déterminant les logarithmes d'un nombre impair $(2n+1)$ de valeurs de $(A_x - A_f)$ (5 ou 7 valeurs suffisent). On calcule la valeur moyenne:

$$\log(A_x - A_f)_{\text{moyen}}$$

et d'autre part on détermine l'écart moyen, E, entre les logarithmes successifs: $\log(A_{x_1} - A_f)$ et $\log(A_{x_2} - A_f)$, $\log(A_{x_2} - A_f)$ et $\log(A_{x_3} - A_f)$, etc. Alors:

$$\log A_b = \log(A_x - A_f)_{\text{moyen}} + (n+1)E$$

Connaissant A_b on effectue:

$$A_b - A_f = \Delta A_b$$

ΔA_b est la différence d'absorption spécifiquement due à la transformation de la chlorophylle b en phéophytine b.

$$A_i - A_b = \Delta A_a$$

ΔA_a représente évidemment la différence d'absorption due à la transformation de la chlorophylle a en phéophytine a.

Détermination des teneurs en chlorophylles

Quelque soit la longueur d'onde choisie pour effectuer les mesures, les différences d'absorption ΔA_a et ΔA_b sont caractéristiques de la transformation de chacune des chlorophylles en la phéophytine correspondante. Pour que ces grandeurs puissent être exprimées en termes de concentrations, il est nécessaire de connaître les extinctions molaires des chlorophylles et des phéophytines dans le solvant choisi. Nous avons déterminé ces extinctions de 614 à 645 nm et aussi à 663 nm, longueur d'onde favorable au seul dosage de la chlorophylle a. Ces déterminations ont été effectuées par titrations parallèles du magnésium et du noyau porphyrinique des chlorophylles a et b, à l'aide de méthodes précisées par ailleurs[17]. Ces coefficients font l'objet du Tableau I.

TABLEAU I

EXTINCTION MOLAIRE DES CHLOROPHYLLES (C_a, C_b) ET DES PHÉOPHYTINES (P_a, P_b)

Longueur d'onde (nm)	ε_{C_a}	ε_{C_b}	ε_{P_a}	ε_{P_b}
614	15900	8600	7600	3600
616	16000	8500	7000	3400
618	15800	8500	6300	3300
620	15400	8600	5800	3200
622	14800	9000	5400	3200
624	14100	9600	5100	3300
626	13300	10900	5000	3400
628	12400	12500	5000	3700
630	11800	14800	5000	4000
632	11200	18100	5200	4700
634	11000	22300	5500	5600
636	11100	27300	5700	6900
638	11600	32700	6200	8700
640	12700	37600	6800	10700
642	14600	41500	7700	13900
645	19600	44700	10100	19600
663	78300		46900	

Calcul des concentrations en chlorophylle a et en chlorophylle b. Si l'on prend pour exemple la chlorophylle a, on peut écrire:

$$\Delta A_a = (\varepsilon_{C_a} - \varepsilon_{P_a}) C_{a_{mol}} \cdot d$$

ou ε_{C_a} et ε_{P_a} sont les extinctions molaires de la chlorophylle a et de la phéophytine a, à la longueur d'onde considérée; $C_{a_{mol}}$ est la concentration molaire de la chlorophylle a phéophytinisée; et d est le parcours optique en centimètres.

Si on tient à exprimer en g l^{-1}, la concentration en chlorophylle a, PM_{C_a} étant le poids moléculaire de la chlorophylle a, on a:

$$C_a = \Delta A_a (\varepsilon_{C_a} - \varepsilon_{P_a})^{-1} \cdot PM_{C_a} \cdot d^{-1} = K_a \cdot \Delta A_a \cdot d^{-1}$$

en définissant:

$$K_a = PM_{C_a} / (\varepsilon_{C_a} - \varepsilon_{P_a})$$

TABLEAU II

COEFFICIENTS K_a ET K_b DE 614 À 645 nm

Longueur d'onde (nm)	$\varepsilon_{C_a} - \varepsilon_{P_a}$	$10^2\ K_a$	$\varepsilon_{C_b} - \varepsilon_{P_b}$	$10^2\ K_b$
614	8300	10.75	5000	18.15
616	9100	9.90	5200	17.55
618	9500	9.45	5200	17.40
620	9700	9.25	5400	16.85
622	9400	9.50	5800	15.75
624	9000	9.95	6300	14.30
626	8300	10.80	7700	11.95
628	7500	12.00	8800	10.35
630	6700	13.30	10800	8.40
632	6000	14.90	13500	6.75
634	5500	16.20	16700	5.45
636	5300	16.75	20400	4.45
638	5500	16.35	24000	3.80
640	5900	15.15	26900	3.40
642	6900	12.95	27600	2.30
645	9500	9.45	25100	3.60

Nous avons calculé les coefficients K_a et K_b pour les longueurs d'onde comprises entre 614 et 645 nm (Tableau II). Ces valeurs permettent, à n'importe laquelle de ces longueurs d'onde, de déterminer les concentrations (g l^{-1}) en chlorophylle a et en chlorophylle b, pour un extrait hydroacétonique de pigments chlorophylliens (10–90, vol–vol), par l'application des formules:

$$C_a = K_a \cdot \Delta A_a \cdot d^{-1}$$

$$C_b = K_b \cdot \Delta A_b \cdot d^{-1}$$

Calcul des teneurs en phéophytines a et b. Dans la plupart des extraits végétaux, les seules substances absorbant dans la région spectrale comprise entre 600 et 700 nm, sont les pigments chlorophylliens et leurs phéophytines. Lorsque les chlorophylles a et b ont été totalement transformées en phéophytines, il est possible de déterminer les concentrations de ces dernières.

Cette détermination peut être effectuée en mesurant, à deux longueurs d'onde distinctes λ_1 et λ_2, les densités optiques A_{λ_1} et A_{λ_2} de l'extrait phéophytinisé.

On peut écrire:

$$A_{\lambda_2}-A_{\lambda_1}=(\varepsilon_{\lambda_2P_a}P_a+\varepsilon_{\lambda_2P_b}P_b)-(\varepsilon_{\lambda_1P_a}P_a+\varepsilon_{\lambda_1P_b}P_b) \tag{1}$$

où $\varepsilon_{\lambda P_{a \text{ ou } b}}$ est l'extinction molaire, à la longueur d'onde λ, de la phéophytine a ou b, et $P_{a \text{ ou } b}$ est la concentration molaire en phéophytine a ou b.

Si l'on choisit λ_1 et λ_2 telles que les extinctions molaires de la phéophytine a, à ces deux longueurs d'onde, soient égales, l'éqn. (1) s'écrira:

$$A_{\lambda_2}-A_{\lambda_1}=(\varepsilon_{\lambda_2P_b}-\varepsilon_{\lambda_1P_b})\cdot P_b$$

et si l'on définit:

$$h=\varepsilon_{\lambda_2P_b}-\varepsilon_{\lambda_1P_b}$$

on a (en mol l^{-1})

$$P_b=(A_{\lambda_2}-A_{\lambda_1})h^{-1}$$

alors:

$$P_a=(A_{\lambda_2}-\varepsilon_{\lambda_2P_b}P_b)\varepsilon^{-1}_{\lambda_2P_a}$$

Nous avons choisi pour λ_1 et λ_2, les longueurs d'onde 608 et 645 nm, où les extinctions molaires de la phéophytine a sont égales ($\varepsilon_{645P_a}=\varepsilon_{608P_a}=10100$), alors que la différence, h, entre les extinctions molaires de la phéophytine b est importante ($h=14500$) puisque $\varepsilon_{645P_b}=19600$ et $\varepsilon_{608P_b}=5100$) (Fig. 4). Nous pouvons donc calculer (en mol l^{-1})

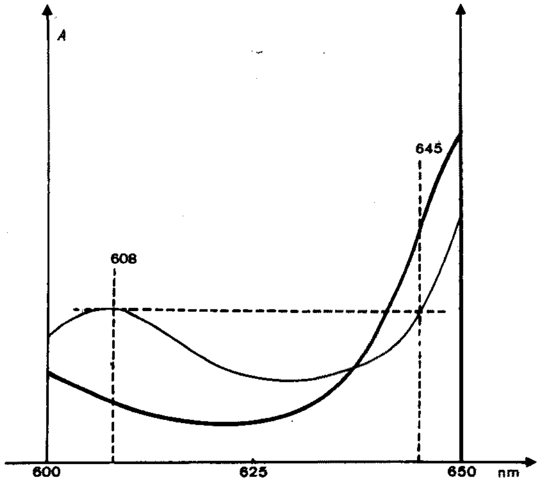

Fig. 4. Spectres de la phéophytine a et de la phéophytine b, montrant l'identité des absorptions de la phéophytine a, à 608 et 645 nm. (——)P_a; (——)P_b.

$$P_b = \frac{1}{14500}(A_{645} - A_{608})$$

$$P_a = \frac{1}{10100}(A_{645} - 19600 P_b)$$

S'il n'y a pas initialement de phéophytine dans l'extrait végétal, les concentrations déterminées doivent correspondre aux concentrations en chlorophylles.

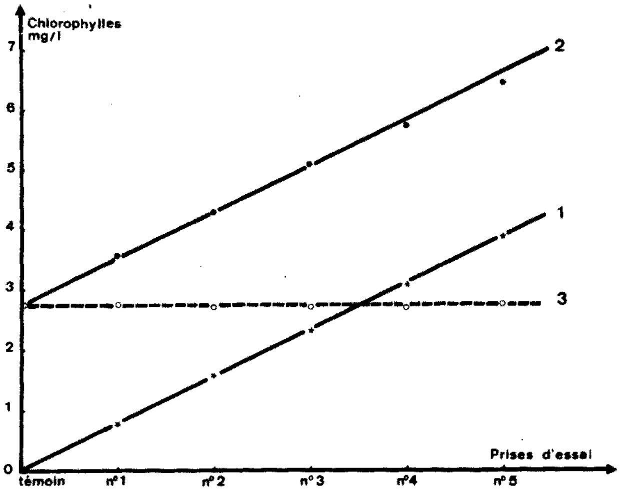

Fig. 5. Courbes représentatives des résultats des essais quantitatifs de détermination des chlorophylles, effectués en enrichissant en chlorophylle a, les différentes prises d'essais d'un extrait végétal. (1) Gamme des quantités de chlorophylle a pure ajoutées. (2) Droite représentative des quantités de chlorophylle a retrouvées, dans les différentes prises d'essais enrichies. (3) Droite représentative des quantités, déterminées par différence, de chlorophylle a initialement présente.

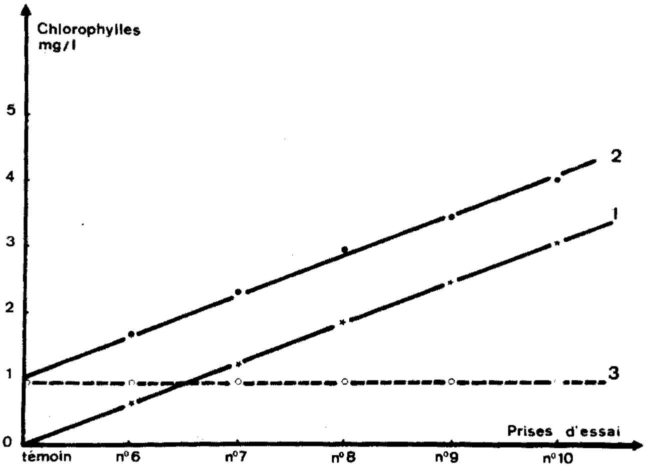

Fig. 6. Courbes représentatives des résultats des essais quantitatifs de détermination des chlorophylles, effectués en enrichissant en chlorophylle b, les différentes prises d'essais d'un extrait végétal. (1) Gamme des quantités de chlorophylle b pure ajoutées. (2) Droite représentative des quantités de chlorophylle b retrouvées, dans les différentes prises d'essais enrichies. (3) Droite représentative des quantités, déterminées par différence, de chlorophylle b initialement présente.

Vérification de la méthode

Quantitativité. Sur un extrait hydroacétonique de haricots verts, nous avons prélevé onze prises d'essais identiques. Dix de ces prises d'essais ont été enrichies avec des quantités connues et croissantes de chlorophylle a ou b pure. La onzième prise d'essai, non enrichie, sert de témoin pour la détermination des quantités de chlorophylles a et b, initialement présentes. Les volumes finaux de ces onze solutions ont été rendus égaux; le solvant étant, dans tous les cas, hydroacétonique 10–90 (vol–vol). Nous avons dosé cinétiquement les chlorophylles a et b de chacune de ces solutions. D'autre part, nous avons tracé les courbes correspondant aux gammes de concentrations, en chlorophylles a et b pures ajoutées (Figs. 5 et 6).

Les dosages effectués sur les mélanges, nous ont permis de retrouver les chlorophylles ajoutées. En effet, l'examen des Figs. 5 et 6 montre que pour chaque série d'essais, la droite représentative des quantités de chlorophylle a ou b déterminées dans les mélanges, est parallèle à la droite correspondante aux quantités de chlorophylle pure de chaque gamme. Le décalage en ordonnée entre ces deux droites parallèles est caractéristique des chlorophylles initialement présentes. Les valeurs en chlorophylles calculées au cours de cette expérience, le sont avec une précision de ±0.7%.

Variabilité. Sur un même extrait hydroacétonique de haricots verts, nous avons effectué sept dosages successifs des chlorophylles. Les résultats obtenus présentent une variation de ±0.8% pour la chlorophylle b et de ±1.8% pour la chlorophylle a. La précision de la méthode sera d'autant meilleure que les écarts d'absorption mesurés seront plus grands.

CONCLUSION

Le dosage cinétique utilisant la différence entre les vitesses de phéophytinisation des chlorophylles a et b offre un certain nombre de caractéristiques intéressantes. L'exploitation de modifications spectrales, dont la vitesse est caractéristique de la nature de chacun des pigments, constitue un critère qualitatif: en effet, la présence éventuelle d'un troisième corps dont le spectre évoluerait sous l'action des acides, perturberait la cinétique apparente des phéophytinisations et serait de ce fait décelable. La quantitativité et la variabilité étudiées montrent que la précision des dosages est satisfaisante; ceci est une conséquence de la spécificité de la méthode. Cette précision est particulièrement intéressante dans le cas de la chlorophylle b, pour laquelle les méthodes habituelles de mesure à deux longueurs d'onde, ne donnent que des résultats approximatifs, qui rendent imprécis les rapports des concentrations des deux chlorophylles. Les extinctions molaires utilisées ont été déterminées pour le solvant qui sert à l'extraction des pigments, et dans lequel sont effectués les dosages. Cette méthode peut être utilisée à diverses longueurs d'ondes ce qui permet de très larges applications. La seule condition à respecter est de travailler sur une différence d'absorption suffisamment grande pour que les mesures soient précises. Ceci peut être obtenu dans tous les cas en utilisant des cuves de grand parcours optique, ou des enregistreurs à expansion d'échelle.

Dans la plupart des extraits végétaux, après acidification, seules les phéophytines absorbent dans la région du spectre où les mesures sont effectuées, ceci permet de calculer les teneurs en phéophytines a et b totales.

RÉSUMÉ

En fixant le taux d'hydratation et la concentration en protons dans les milieux acétoniques, on peut obtenir une différence importante entre les vitesses de phéophytinisation des chlorophylles a et b. Ces propriétés sont utilisées pour doser sélectivement ces pigments par spectrophotométrie, dans les extraits hydroacétoniques de végétaux. Les phénomènes de phéophytinisation obéissent à des lois exponentielles; leurs cinétiques peuvent être enregistrées à une longueur d'onde choisie selon les concentrations relatives des chlorophylles a et b présentes dans l'extrait végétal. Le dosage de la chlorophylle a et de la chlorophylle b est effectué dans des extraits acétoniques à 10% d'eau. Les conditions préconisées permettent une phéophytinisation 25 à 35 fois plus rapide pour la chlorophylle a que pour la chlorophylle b. La durée du dosage n'excède pas 15 min. Les calculs des concentrations en chlorophylles et en phéophytines sont effectués à l'aide des extinctions molaires déterminées pour le solvant utilisé. Les teneurs en pigments sont ainsi obtenues avec une précision supérieure à ±2%, quelles que soient les concentrations relatives en chlorophylles a et b.

SUMMARY

In acetonic solutions, the phaeophytinization velocities of chlorophylls a and b can be very different for certain degrees of hydration and proton concentration of the media. These properties are used for the selective spectrophotometric determination of these plant pigments in an aqueous acetone solution. The phaeophytinization phenomena follow exponential laws; their kinetics can be recorded at a wavelength determined by the relative concentrations of chlorophylls a and b present in the plant extracts. Chlorophyll a and b concentrations are determined in acetone extracts containing 10% water; the phaeophytinization is 25 to 35 times faster for chlorophyll a than for chlorophyll b. Concentrations of chlorophylls and phaeophytins are calculated from the molar absorptivities for the particular solvent used. The procedure requires only 15 min, and a 2% accuracy is obtained, irrespective of the relative concentrations of chlorophyll a and b.

ZUSAMMENFASSUNG

In acetonigen Lösungen können die Phäophytinierungsgeschwindigkeiten der Chlorophylle a und b bei bestimmten Hydratationsgraden und Protonenkonzentrationen des Mediums sehr verschieden sein. Diese Eigenschaften werden für die selektive spektrophotometrische Bestimmung dieser Pflanzenfarbstoffe in wässrigen Acetonlösungen ausgenutzt. Die Phäophytinierungserscheinungen gehorchen Exponentialgesetzen; die Kinetik kann bei einer Wellenlänge aufgezeichnet werden, die durch die relativen Konzentrationen der in den Pflanzenextrakten vorliegenden Chlorophylle a und b bestimmt wird. Die Konzentrationen der Chlorophylle a und b werden in Aceton mit 10% Wasser ermittelt; die Phäophytinierung ist bei Chlorophyll a 25–35 mal schneller als bei Chlorophyll b. Die Konzentrationen der Chlorophylle und Phäophytine werden aus den molaren Extinktionskoeffizienten für das benutzte Lösungsmittel berechnet. Das Verfahren dauert nur 15 min; es wird un-

abhängig von den relativen Konzentrationen der Chlorophylle a und b eine Genauigkeit von 2% erreicht.

BIBLIOGRAPHIE

1 G. MacKinney, *J. Biol. Chem.*, 132 (1940) 90.
2 G. MacKinney, *J. Biol. Chem.*, 140 (1941) 315.
3 H. G. Petering, W. Wolman et R. P. Hibbard, *Ind. Eng. Chem., Anal. Ed.*, 12 (1940) 148.
4 F. P. Zscheile et C. L. Comar, *Botan. Gaz.*, 102 (1941) 463.
5 C. L. Comar et F. P. Zscheile, *Plant Physiol.*, 17 (1942) 198.
6 D. I. Arnon, *Plant Physiol.*, 24 (1949) 1.
7 J. H. C. Smith et A. Benitez, in K. Peach and M. V. Tracey, *Modern Methods of Plant Analysis, Vol. 4*, Springer-Verlag, Berlin–Göttingen–Heidelberg, 1955, p. 142.
8 R. W. van Norman, *Utah Acad. Sci. Proc.*, (1957) 34.
9 Z. S. Sěsták, *Rostl. Vyroba.*, 10 (1964) 1197.
10 D. Laval-Martin, *D.E.A., Physiol. Vég., Appliquée, Fac. Sci. Paris*, 1968.
11 J. F. G. M. Wintermans, *Photosynthetica*, 3 (1969) 112.
12 W. C. Dietrich, *Food Technol.*, 12 (1958) 428.
13 J. P. Sweeney et N. Martin, *Food Res.*, 23 (1958) 635.
14 L. P. Vernon, *Anal. Chem.*, 32 (1960) 1144.
15 T. Ogawa et K. Shibata, *Photochem. Photobiol.*, 4 (1965) 193.
16 N. Delaporte et D. Laval-Martin, *Chim. Anal.*, sous presse.
17 N. Delalorte et D. Laval-Martin, *Anal. Chim. Acta*, 55 (1971) 415.

Analytica Chimica Acta
Elsevier Publishing Company, Amsterdam
Printed in The Netherlands

SHORT COMMUNICATIONS

Determination of calcium, barium and zinc in lubricating oils by atomic absorption spectrophotometry

The determination of metals in used lubricating oils by atomic absorption spectroscopy was first described by Sprague and Slavin[1,2], the samples being diluted with xylene or methyl isobutyl ketone (MIBK) before being sprayed into the flame; a precision of *ca.* 5% was reported for the estimation of iron, nickel, chromium, magnesium, lead, copper and silver. Similarly, used jet-engine oils have been analyzed for silver, chromium, copper, iron, magnesium, nickel and tin[3], and crude petroleum oils for nickel, iron and copper[4]. However, difficulties are encountered in all these methods, because different metal compounds yield different responses, so that the preparation of calibration curves requires samples of the pure additives. Metal-containing additives in lubricating oils are commonly determined by chemical or polarographic methods[5] or emission spectrographic technique[6].

It has recently been shown[7] that the addition of iodine or other halogen-containing compounds, has a remarkable levelling effect on the release of metal atoms from different organometallic compounds containing calcium, barium or zinc. This technique can be applied to the determination of these metals in lubricating oils by atomic absorption spectrophotometry, when the oil is diluted with MIBK before aspiration into a nitrous oxide–acetylene flame. For calibration, only a single standard is needed for each metal.

Experimental

The instrumentation was the same as described previously[7].

Nitrous oxide–acetylene flames were used for all determinations, the oxidant

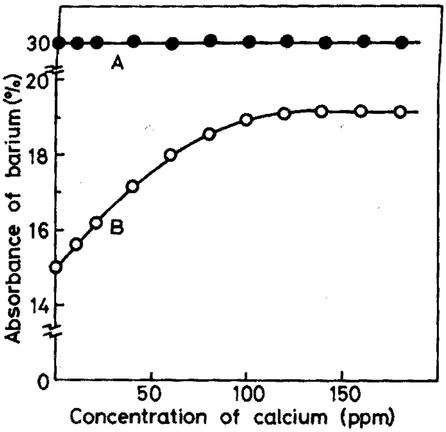

Fig. 1. Effect of calcium on absorbance of the barium line at 553.6 nm. (A) Solution containing 10 p.p.m. of barium and 1.5 mg of lanthanum nitrate per 10 ml. (B) Solution containing only 10 p.p.m. of barium.

flow being 16.7 l min^{-1}, and the acetylene flow 8.8 l min^{-1}, with a burner height of 10 mm. Scale expansion × 1 was used for calcium and zinc, and × 3 for barium; other operating parameters were the same as before.

Standard preparation was carried out as described previously[7].

Interferences. The interferences of phosphorus, calcium, barium and zinc were studied. Phosphorus and zinc did not interfere, but they moderated the interference of calcium on barium. Calcium interfered with barium, but the addition of 1.5 mg of lanthanum nitrate per 10 ml of MIBK to the test solution completely suppressed the interference (Fig. 1).

Calibration curves. The calibration solutions, which contained 1.2 mg of iodine and 1.5 mg of lanthanum nitrate per 10 ml, were prepared for the ranges 2–10 p.p.m. barium, 1–3 p.p.m. calcium and 0.4–2 p.p.m. zinc in lubricating oils. The calibration curves are shown in Fig. 2. The plots of concentration *vs.* absorbance were

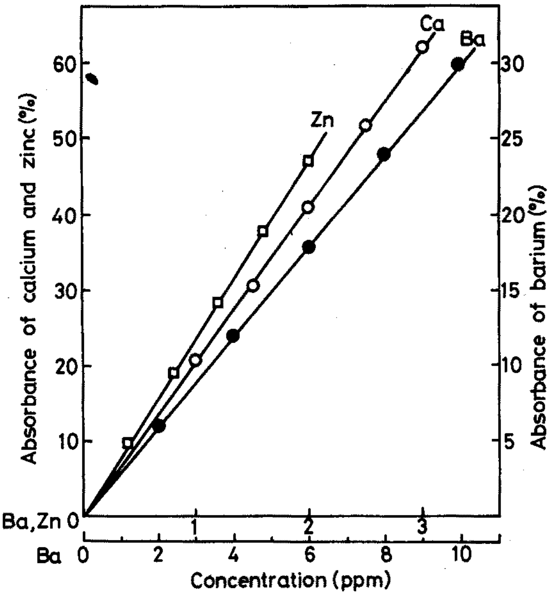

Fig. 2. Calibration curves.

TABLE I

COMPARISON OF RESULTS OF DETERMINATION OF CALCIUM, BARIUM AND ZINC IN LUBRICATING OIL BY THE HALOGEN ADDITION METHOD AND BY CONVENTIONAL ASSAY

Sample no.	*Concentration found* (%)					
	Assay method			*Halogen addition method*		
	Ca	*Ba*	*Zn*	*Ca*	*Ba*	*Zn*
1	0.140	—	0.076	0.138	—	0.077
2	0.301	—	0.097	0.300	—	0.099
3	0.103	0.26	0.080	0.101	0.26	0.081
4	0.090	—	0.078	0.087	—	0.078
5	0.042	0.04	0.095	0.041	0.04	0.096

linear, and were the same for all the additives tested, as well as for mixtures of organometallic and inorganic compounds.

Analysis of oils. A 0.1-g sample was mixed with iodine and lanthanum nitrate as above, and diluted to 50 ml with MIBK before aspiration.

Results and discussion

Table I summarizes the results obtained by the proposed method, compared with the values given by a conventional assay; for the latter, the samples were decomposed with the nitric and hydrochloric acids before atomic absorption spectrophotometry. The differences between the results are well within the usual analytical error.

The atomic absorption method, calibrated with polarographically or chemically analysed lubricating oils, is accurate and precise over the range 0.042–0.301 wt% as calcium, 0.26–0.04 wt% as barium and 0.097–0.076 wt% as zinc. The average analysis time per sample is about 15 min, allowing triplicate readings on samples and reference standards. It should be emphasized, perhaps, that the calcium, barium and zinc contents were measured, assuming lubricating oil or other standards of similar chemical composition.

The authors wish to thank Dr. T. Amemiya and Mr. T. Kozuma, Directors of Maruzen Oil Co., Ltd., for their encouragement and Seigo Yamazoe for valuable experimental assistance.

Maruzen Oil Co., Ltd.,
Research & Development Center,
P.O. Box 1, Satte,
Saitama 340–01 (Japan)

Masayuki Kashiki
Shozo Oshima

1 S. Sprague and W. Slavin, *Perkin-Elmer At. Abs. Newsletter*, 1 (12) (1963) 20.
2 S. Sprague and W. Slavin, *Perkin-Elmer At. Abs. Newsletter*, 4 (10) (1965) 367.
3 E. A. Means and D. Ratcliffe, *Perkin-Elmer At. Abs. Newsletter*, 4 (1) (1965) 174.
4 R. C. Barras, *Jarrell-Ash Newsletter*, June 13, 1962.
5 *IP Standards for Petroleum and its Products*, 25th Edn., 1966.
(a) Calcium: IP 111/49T, Part I, Section I.
(b) Barium: IP 110/60T, Part I, Section I.
(c) Zinc: IP 117/66T, Part I, Section I.
Also, *Polarographic Determination of Zinc in Lube Oils and Additives*, ASTM D1549–64.
6 C. M. Gambrill, A. G. Gassmann and W. R. O'Niell, *Anal. Chem.*, 33 (1951) 1365.
7 M. Kashiki, S. Yamazoe and S. Oshima, *Anal. Chim. Acta*, 55 (1971) 95.

(Received 17th December 1970)

The determination of lead in air by flameless atomic absorption spectrophotometry

The determination of lead contents in atmospheric particulates by means of atomic absorption spectroscopy has been reported by several investigators[1-5]. In the usual sampling technique for such inorganically bound lead, the atmosphere under test is allowed to pass through some sort of filter in order to collect all particles above a certain size. The filter types used comprise glass fibre[4-6], filter paper[7] and millipore filters[1]. After the absorption, the filters can either be treated directly with hydrochloric acid[5] or nitric acid[6] or they can be dry-ashed at 500° [4,7]. These methods have stood the test of experience and are very useful. However, large volumes of air must be aspirated through the filters to obtain enough lead for a determination. This makes the sampling rather time-consuming or requires heavy high-capacity pumps.

When peak values or instantaneous values are of interest, aspiration times of 10–15 min or shorter and much smaller equipment are desirable. The new graphite furnace technique introduced by L'Vov[8] in 1963 and further developed by Massmann[9], West and Williams[10], Donega and Burgess[11] and Welz and Wiedeking[12], has recently been marketed as a commercially available unit. This offers a unique possibility of determining trace elements in extremely small volumes with a high degree of accuracy. Since many samples can be injected into the graphite tube without a prior digestion or preconcentration step, most of the usual contamination encountered in ordinary trace element analysis is avoided.

The present communication describes the use of this technique in a simple, rapid and extremely sensitive method, combined with collection of lead particulates on millipore filters from air volumes down to 10 dm^3.

Equipment and reagents

Air contaminants were collected on 37-mm diameter MF-Millipore filters AA (0.8 μm), made of mixed cellulose esters. These filters were connected to a small portable battery-operated pump (Casella, London), calibrated to 2.7 dm^3 air per min.

A Perkin-Elmer Model 303 Atomic Absorption Spectrophotometer equipped with a Perkin-Elmer (Bodenseewerk) Graphite Cell HGA 70, an automatic recorder readout accessory and a Hitachi–Perkin-Elmer Recorder Model 159 was used. Small sample aliquots were injected into the graphite tube by means of Eppendorf Marburg micropipettes. Flame atomic absorption measurements were carried out on a Perkin-Elmer 403 Atomic Absorption Spectrophotometer with a Boling burner head. A lead Intensitron hollow-cathode lamp was used as light source in all measurements. The only chemical used, nitric acid, was of analytical-reagent grade quality.

Lead solutions. A 1000-p.p.m. stock solution was prepared from 1.000 g of pure lead metal dissolved in 25 ml of nitric acid and diluted to 1 l with distilled water. From this solution 0.1-p.p.m. standard solutions containing 5 ml of nitric acid per 100 ml were prepared daily.

Measurements conditions

Before sample volumes are atomized in the graphite tube, any solvent, organic material or other unwanted components of the matrix must be removed. Smoke signals or false absorption will otherwise occur. Therefore, two separate heat treatment stages, drying and charring ("ashing") must be carried out before the atomization step. For such treatment, the HGA 70 is equipped with seven fixed programmes for easy reproduction of selected temperatures between 60° and 1100° and three clocks for time adjustment. The final atomization temperature is determined by the voltage for the resistance heating of the tube.

Since there is little available information about the settings of the instrument for each type of analysis, the optimal time and temperature of the various stages had to be determined. It was found suitable to dry the sample at 100°, to char at 330° and to atomize at 1900°. Program 4 and a transformer setting of 5 V (2.5 kW) takes care of this automatically. A period of 30 sec for each sequence was found satisfactory.

Procedure

Collect particulate lead samples by aspirating air for 10 min through the millipore filters. Soak the filters in 2.0 ml of 1 + 1 nitric acid in a 50-ml beaker and apply gentle heat. After 5 min, decant into a 10-ml volumetric flask and wash the filters with successive 2-ml portions of warm distilled water. Finally dilute to volume with distilled water.

Inject 5–50 μl of 0.1-p.p.m. lead standard solution into the graphite tube and register the lead absorption peak at program 4 with a 5-V atomization voltage and a 30-sec sequence time. Prepare a blank solution from a new millipore filter treated with nitric acid as described above and register a blank value. Prepare a calibration curve from the peak height measurements after converting percentage absorption to absorbance and subtracting the blank value. (A straight line is obtained up to 2 ng of lead.) Measure small sample volumes in the same way, convert the peak heights to absorbance, subtract the blank value for the same injection volume and evaluate the lead concentration from the calibration graph.

Light scattering

Light scattering, causing too high absorption readings, is well known in flame absorption measurements. Such interference can be corrected for by selecting a non-absorbing line within 10 nm of the analytical line and subtracting the absorption signal from the analytical value. It was found necessary in the present work to examine the peaks for such unspecific absorption. The analytical line used was 217.0 nm and the non-absorbing line was 209.8 nm. In the regular sample and standard solutions, no absorption was recorded at 209.8 nm. In order to establish if the lead particles had been completely dissolved and washed out of the millipore filters, the filters were treated with 1 ml of hot nitric acid; the filters dissolved completely and the solutions were diluted to 10 ml. For the same aliquot sizes (20 μl), the same signals (11%) were recorded at both lines. This was taken as evidence of light scattering and also of complete lead extraction when the millipore filters were leached as recommended in the procedure.

Results and discussion

The proposed method was used in the analysis of a number of air particulate samples collected in Oslo city in November 1970, 1 m above street level. Some of the results obtained are shown in Table I. It is obvious from these data that the sampling and analytical methods used offer satisfactory sensitivity. With 10-min sampling times and 20-μl injection volumes, the sensitivity obtained for 1% absorption is about 0.7

TABLE I

ANALYSIS OF STANDARDS AND SAMPLES OF OSLO CITY AIR
(Scale expansion 1)

Sample	*Air volume (dm^3)*	*Aliquot (μl)*	*Peak height (% abs.)*	*Total amount*[a] *(ng)*	*Concentration in air (μg Pb m^{-3})*
0.1 p.p.m. standard	—	5	14.4	0.5	—
0.1 p.p.m. standard	—	10	24.4	1.0	—
0.1 p.p.m. standard	—	20	41.5	2.0	—
Blank	—	20	1.9	0.07	—
Blank	—	100	9.2	0.35	—
Air sample 1, rush hour	27	20	12.2	0.43	7.9
Air sample 2, rush hour	27	20	17.5	0.66	12.2
Air sample 3, rush hour	27	20	6.5	0.18	3.3
Air sample 4, suburb	54	100	10.1	<0.05	< 0.2

[a] Corrected for blank lead content.

μg of lead per m^3 air. The injected volume can easily be increased to 100 μl. This was done in air sample 4, but the high lead content in the analytical-grade nitric acid, determined to be 3.5 $\mu g\ l^{-1}$ makes it doubtful that a correspondingly better sensitivity can be assumed. For lead concentrations below 1 $\mu g\ m^{-3}$ of air, an increased sampling time or the use of less contaminated acid will give higher sensitivity.

The small sample volumes made it impossible to check the accuracy of the obtained analysis by preconcentration techniques and regular atomic absorption spectrophotometry. However, some sort of comparison was possible since the two solutions with the highest lead concentrations, sample 1 (22 $\mu g\ l^{-1}$) and sample 2 (33 $\mu g\ l^{-1}$) could be measured directly on the Model 403 with maximum scale expansion. The measured values of 26 and 37 μg Pb l^{-1}, respectively, are in acceptable accordance, when the low accuracy of the direct flame method in this concentration range is taken into consideration.

Central Institute for Industrial Research, Sverre H. Omang
Blindern, Oslo 3 (Norway)

1 C. L. Chakrabarti, J. W. Robinson and P. W. West, *Anal. Chim. Acta,* 34 (1966) 269.
2 G. Thilliez, *Anal. Chem.*, 39 (1967) 427.
3 J. Cholak, L. J. Schafer and D. Yeager, *J. Amer. Ind. Hyg. Assoc.*, 29 (1968) 562.
4 C. D. Burnham, C. E. Moore, T. Kowalski and J. Krasniewski, *Appl. Spectrosc.*, 24 (1970) 411.
5 M. Beyer, *Atomic Absorption Newsletter*, 8 (1969) 23.
6 R. Moss and E. V. Browett, *Analyst*, 91 (1966) 428.
7 V. Smolcic, *Arhiv Hig. Rada Toksikol.*, 17 (1966) 309; *Anal. Abstr.*, 14 (1967) 5775.
8 B. V. L'Vov, *Spectrochim. Acta*, 24B (1969) 53.
9 H. Massmann, *Spectrochim. Acta*, 23B (1968) 215.
10 T. S. West and X. K. Williams, *Anal. Chim. Acta*, 45 (1969) 27.
11 H. M. Donega and T. E. Burgess, *Anal. Chem.*, 42 (1970) 1521.
12 B. Welz and E. Wiedeking, *Z. Anal. Chem.*, 252 (1970) 111.

(Received 19th March 1971)

Analytica Chimica Acta
Elsevier Publishing Company, Amsterdam
Printed in The Netherlands

Dosage des traces de bismuth dans les fontes et aciers par spectrométrie de flamme à absorption atomique

Dans un article précédent[1] nous avons cité l'effet nuisible du plomb sur la qualité de la fonte à graphite sphéroïdal. Le bismuth joue également un rôle néfaste d'où l'intérêt de pouvoir contrôler sa teneur, même basse, dans la fonte, et par extension dans les métaux ferreux.

La bibliographie est peu abondante au sujet du dosage de cet élément, et les rares publications offrent des méthodes souvent compliquées et longues. Pour séparer le bismuth (et souvent le plomb) du fer, les auteurs opérent de diverses façons: extraction du fer par acétate d'isobutyle[2], par éther isopropylique[3], par diéthyléther[4], par résine échangeuse d'ions[5] et par des extractions répétées dans divers milieux[6], ou bien séparation du bismuth sous forme de sulfure[7].

La moitié des auteurs[2,5,6] termine le dosage par colorimétrie du complexe $K(BiI_4)$ qui nécessite des traitements divers avant d'être apte à la mesure.

Nos recherches sur le dosage du plomb[1] nous ont conduits à une extraction des dithizonates en milieu cyanuré–ammoniacal. Le pionnier de ces extractions, Fischer[8] a démontré que trois métaux lourds sont extraits ensemble dans le milieu cité: plomb, bismuth et thallium. Tandis que la présence de thallium est hautement improbable dans les fontes et aciers, le plomb et le bismuth s'y trouvent toujours dans des proportions plus ou moins importantes.

La séparation des dithizonates de ces deux éléments exigerait des traitements supplémentaires que l'emploi du procédé à l'absorption atomique rend superflu. Pour la réalisation, il suffisait de trouver les conditions spécifiques au bismuth, car la majeure partie des difficultés a été déjà résolue au cours de la mise au point pour le dosage du plomb. Après avoir expérimenté les raies de 206.2 et 306.8 nm, ce sont les raies de 223.1 et de 222.8 nm qui ont été retenues. Pour éviter la coïncidence entre ces deux raies se trouvant à 0.3 nm près, nous avons d'abord essayé la fente 3 (0.3 mm) qui donne une bande passante de 0.2 nm. Le rapport signal/bruit de fond était élevé mais les lectures étaient trop instables. En utilisant la fente 4 (1 mm), la bande passante s'est élargie à 0.7 nm ce qui signifie que l'absorption sur les deux raies voisines est intégrée. Les lectures sont devenues beaucoup plus stables, nous avons donc adopté les longueurs d'onde 223.1 et 222.8 nm avec la fente 4 de notre appareil.

Pour des raisons expliquées dans l'article précédent[1], nous avons dû choisir la flamme air–acétylène, l'air–propane n'étant pas compatible avec le tétrachlorure de carbone.

Partie expérimentale

Appareil. Spectrophotomètre à absorption atomique Perkin-Elmer AA 303, muni de la lampe à cathode creuse de bismuth, chauffée par un courant de 30 mA.

Conditions de travail. Longueur d'onde: 223.1 et 222.8 nm. Fente: 4. Expansion d'échelle: 5 ou 10 selon la sensibilité. Réponse: 2. Brûleur: Boling; hauteur: 1. Flamme: air comprimé 30 psi et débit 8 div.; acétylène 8 psi et débit 6 div.

Réactifs. Tous les réactifs sont identiques à ceux qui sont donnés dans l'article précédent[1] à l'exception des deux solutions spécifiques au bismuth.

Solutions-mère de bismuth (200 μg *Bi* ml^{-1}). Peser très exactement 0.200 g de bismuth pur, introduire dans un becher de 250 ml. Attaquer par 10 ml d'acide nitrique; après attaque complète, ajouter 20 ml d'acide perchlorique et évaporer aux fumées blanches. Reprendre par de l'eau et transvaser dans une fiole jaugée de 1 l. Compléter, homogénéiser.

Solution étalon de bismuth (5 μg *Bi* ml^{-1}). Prélever 25 ml de la solution-mère, les introduire dans une fiole jaugée de 1 l. Ajouter 20 ml d'acide perchlorique pour empêcher l'hydrolyse, compléter, homogénéiser. Cette solution est à préparer juste avant l'emploi pour éviter l'adsorption des ions de bismuth sur les parois du récipient.

Etablissement de la courbe d'étalonnage. Dans 4 bechers de 250 ml, introduire 0 ... 10 ml de la solution étalon de Bi soit 0 ... 50 μg de Bi, ce qui correspond à 0 ... 100 p.p.m. de Bi dans le cas d'une prise d'essai de 0.5 g. Continuer selon le mode opératoire décrit ci-dessous et tracer la courbe d'étalonnage.

Pour des teneurs supérieures à 100 p.p.m., diminuer la sensibilité de l'appareil par la réduction de l'expansion d'échelle et tracer une courbe d'étalonnage dans les mêmes conditions. Par ailleurs, il est recommandé de vérifier la courbe avec chaque série de dosages.

Mode opératoire. Prise d'essai 0.5 g. L'attaque, le conditionnement de la solution et l'extraction sont identiques aux opérations décrites précédemment[1]. Un rappel bref: attaque chlorhydrique, insolubilisation puis séparation par filtration de la majeure partie du silicium, réduction du fer(III) en fer(II), ajouts du citrate d'ammonium et du cyanure de potassium; extraction du bismuth et du plomb par deux fois 5 ml de dithizone (0.25 g l^{-1} dans CCl_4); nébulisation des extraits réunis et mesure de l'absorption du bismuth par rapport au tetrachlorure de carbone pur.

Résultats

Les échantillons-types avec teneur certifiée en bismuth sont extrêmement rares. Nous nous sommes contentés de tester la méthode sur des solutions synthétiques et nous sommes passés directement au dosage du bismuth dans du fer pur et dans des fontes préparées par notre Division "Métallurgie". Les résultats sont consignés dans le Tableau I.

Dans le cas du fer pur nous avons appliqué la méthode des ajouts dosés.

Conclusion

Le dosage des traces de bismuth dans les fontes et aciers est possible après

TABLEAU I

RÉSULTATS OBTENUS SUR 4 FONTES ET SUR FER PUR

Echantillon	*Bismuth trouvé (p.p.m.)*		
	1	2	3
A	20	25	20
B	52	50	52
C	50	55	52
D	34	37	35
Fer pur	3.5	3.2	3.7

l'extraction du bismuth (et du plomb) sous forme de dithizonate et mesure sélective du bismuth par l'absorption atomique. Une série de 4 à 6 dosages peut être effectuée en une demi-journée par un chimiste entraîné.

Les auteurs remercient la Direction du Centre de Recherches de Pont-à-Mousson pour les avoir autorisés à publier les résultats de leurs travaux.

Centre de Recherches de Pont-à-Mousson,
54 Pont-à-Mousson (France)
G. Kisfaludi
M. Lenhof

1 G. Kisfaludi et M. Lenhof, *Anal. Chim. Acta*, 54 (1971) 83.
2 R. C. Rooney, *Analyst*, 83 (1958) 83.
3 J. C. Margerie et M. Drouzy, *Mem. Sci. Rev. Met.*, LVI (1959) 72.
4 Z. Vevera et B. Bieber, *Hutnicke Listy*, 16 (1961) 667.
5 N. Leontovitch, *Chim. Anal. (Paris)*, 47 (1965) 458.
6 D. Chr. Filipov et I. R. Natchev, *Compt. Rend. Acad. Bulgare Sci.*, 20 (1967) 109.
7 C. G. Carlstrom et W. Palvarinne, *Jernkontorets Ann.*, 146 (1962) 453.
8 H. Fischer, *Angew. Chem.*, 46 (1933) 442.

(Reçu le 18 mars 1971)

Anal. Chim. Acta, 55 (1971) 442–444

Determination of iodine in sea water by an improved Sugawara method

The method of Sugawara *et al.*[1] for the determination of iodine in natural water has been applied to geochemical problems[2]. When the method is used to determine iodine in sea water[3], however, the results for the content of iodine in sea water showed large fluctuation from sample to sample and systematically low values as compared with those of Barkley and Thompson[4].

Recently, Matthews and Riley[5] critically discussed the method and developed a modified procedure. Tsunogai and Sase[6] suggested the mechanism of iodide formation in sea water, in which iodate was proved to be fairly easily reduced to iodide by biological activity. Therefore, it is necessary to analyze or separate iodide from iodate without delay after sea water samples are collected. Miyake and Tsunogai[7], and Tsunogai and Henmi[8] have obtained good results for iodide and iodate in sea water by using the improved Sugawara method, which is reported here.

In the method of Sugawara *et al.*, iodide is coprecipitated with silver chloride from a large volume of water sample. Iodide in the precipitate is oxidized to iodate by acetate solution saturated with bromine at pH 2.8. After the precipitate is filtered off, the iodate in the solution is reduced by sulfite and reoxidized by the bromine solution. The reaction between the iodate and the excess of added iodide renders iodine as triiodide, which is spectrophotometrically determined as the starch–iodine complex. The large errors observed are probably derived from coprecipitation of iodide from sea water, incomplete removal of bromine compounds in higher oxidation states than bromide which are formed in the oxidation treatment.

Coprecipitation of iodide

Matthews and Riley reported that even with vigorous agitation and slow addition of silver nitrate the coprecipitation of iodide never exceeded 90%, even if sufficient silver nitrate was added to precipitate 4% of the chloride present. According to Owen[9], the solubility product of silver iodide is $1.2\cdot10^{-16}$ at 25° and is $2.1\cdot10^{6}$ times smaller than that of silver chloride. If a pure solid phase of silver iodide is made from iodide in sea water, about 20 $\mu g\ l^{-1}$ of iodide remains in the solution on the addition of silver nitrate equivalent to 1% of the chloride present. However, if iodide can freely replace chloride in the solid silver halide, almost all the iodide in sea water precipitates as a eutectic mixture under the condition that a univalent ion in sea water has an activity coefficient of 0.65 and the activity coefficients of halides in the solid are approximately equal to one another.

This situation was experimentally examined by using radioactive ^{131}I as an iodide tracer. To 200 ml of sea water, stirred with a magnetic stirrer, 4 ml of 0.1 *N* silver nitrate solution was added. After stirring for 10 min, it was stored in a dark place. When the silver halide precipitate was filtered within an hour, a considerable fraction of iodide remained in the solution, as shown in Table I. After standing for about one day, however, more than 98% of the iodide was found in the precipitate.

TABLE I

COPRECIPITATION OF IODIDE FROM SEA WATER[a]

Reagents added	*ml*	*Time (h)*	*No. of detns.*	*I^- pptd. (%)*
0.1 *N* $AgNO_3$	4	0.5–1	5	53–80
0.1 *N* $AgNO_3$	4	18–24	8	99±1
0.1 *N* NaBr	2			
Ammonium buffer[b]	16	0.5–1	5	97±2
0.1 *N* $AgNO_3$	8			

[a] Sampled in the western North Pacific; contained 10 μg of I^--iodine and 38 μg of IO_3^--iodine per liter; 200 ml was used.
[b] 1.4 *M* NH_4Cl and 8.0 *M* NH_4OH, pH = 10.2.

Another method for the complete precipitation of iodide is to coprecipitate iodide with silver bromide while chloride remains in solution by the addition of ammonium hydroxide. In this case, the time of analysis is shorter, but the precipitate needs to be separated by centrifuging because the silver bromide precipitate does not easily coagulate.

Interference by bromine compounds

On oxidation of iodide in the precipitate with bromine, some interferences caused serious errors in the analysis. Sugawara *et al.* considered that metallic silver is formed photochemically in the silver halide precipitate and reacts with bromine to produce hypobromous acid. Thus, Sugawara *et al.* reduced it with sulfite and repeated the oxidation treatment with bromine.

It was found, as shown in Table II, that the interferences are completely removed at pH 2.8 when the solution is evaporated to 5–10 ml on a boiling water bath for 2 h and stood for 18 h before the colorimetric determination. The results did not change even though part of the silver in the precipitate was reduced before treatment with bromine.

Besides hypobromous acid, bromate is likely to form in the solution at a higher pH[10]. These ions are more stable in the more alkaline solution and could not be removed by standing at pH 4. On the other hand, below pH 2, free iodine is formed and escapes together with bromine. Therefore, it is necessary to expel bromine from the solution at pH *ca.* 3, but it is not necessary to reduce the solution with sulfite and reoxidize with bromine. It is preferable, if possible, to avoid the photochemical decomposition of silver halide because it consumes bromine and the oxidation of the precipitates requires more time.

TABLE II

INTERFERENCE BY BROMINE IN HIGHER OXIDATION STATES

No. of oxidn. treatments by Br_2	*Time[a] (h)*	*No. of detns.*	*Mean absorbance and std. dev.[c]*
1	0.2–0.5	6	0.441 ± 0.043
2	0.2–0.5	6	0.426 ± 0.034
1	12–18	11	0.370 ± 0.006
2	12–18	6	0.377 ± 0.008
1[b]	12–18	5	0.374 ± 0.007

[a] Time elapsed before the color development.

[b] Before treatment, the precipitate was exposed to sunlight for 2 h.

[c] Total iodine in 250 ml of the same sea water as that in Table I.

Thus, the difficulties in Sugawara's method are easily resolved by letting the solutions stand for a sufficiently long time in both cases in question and the analytical procedure is simplified. The following procedure is recommended.

Procedure

Place a 200–300-ml portion of sea water in a beaker. While stirring with a magnetic stirrer, add 20 ml of 0.1 *N* silver nitrate solution. Allow the solution to stand in the dark more than 20 h. Filter the precipitate through a coarse filter paper (No. 5A, Toyo Filter Paper Co. Ltd.) and reserve the solution for the determination of iodate. Transfer the precipitate to a small beaker with 15 ml of water, add 10 ml of acetate buffer saturated with bromine and let it stand for an hour with occasional stirring. Warm the beaker on a boiling water bath until the solution is colorless. Filter off the precipitate through a fine filter paper (No. 5C) and reduce the filtrate again on a water bath to 5–10 ml. Transfer the solution to a 25-ml graduated flask with 5 ml of acetate buffer and water. After letting it stand for more than 12 h, add 1 ml of 0.5% starch solution and 1 ml of 5% cadmium iodide. Measure the absorbance of the solution at 570 nm after 20 min.

Iodate in the reserved filtrate is determined by the same procedure as mentioned above after the reduction of iodate to iodide by 3 ml of 1% sodium sulfite and 1 ml of 3 *N* sulfuric acid.

Reagents used are the same as those of Sugawara *et al.* Acetate buffer contains 30 ml of acetic acid and 0.50 g of sodium acetate anhydride in 1 l.

Conclusions

The method of Sugawara *et al.* for the determination of iodide in natural water is applied to the determination of iodide in sea water with some simplifications. The error of the method does not exceed $\pm 3\%$ or ± 1 μg I l^{-1} (Table II).

In the actual ocean, the concentration of iodide is often much smaller than that of iodate. Therefore, it is preferable to use more than 500 ml of sea water, to determine the iodide accurately by using the same procedure, but the concentration of iodate is so large that the solution must be diluted twice before the color development.

Matthews and Riley reported that a considerable proportion of iodide in the precipitates of silver halide remained in the precipitate during oxidation by bromine. However, that tendency was not observed unless the precipitate consisted of large aggregates in the solution, which can be easily broken down by the mechanical stirring.

The starch solution greatly influences the sensitivity of this method. High sensitivity can be attained with a starch solution of high amylose content. For this purpose, the commercially available soluble starch reagent is not always appropriate, because the degree of hydrolysis is often too high. We used soluble starch of high amylose content which was obtained by gel filtration[11] or by the following hydrolysis. Wheat starch was immersed in twice the amount of 2 *M* hydrochloric acid at room temperature with occasional stirring. After a week, the starch was washed with water, dried, and used for the analysis.

The author is greatly indebted to Prof. M. Nishimura for his valuable discussions.

Department of Chemistry,
Faculty of Fisheries,
Hokkaido University,
Hakodate (Japan)

Shizuo Tsunogai

1 K. Sugawara, T. Koyama and K. Terada, *Bull. Chem. Soc. Japan*, 28 (1955) 494.
2 K. Terada, *Thesis*, Nagoya University, 1958.
3 K. Sugawara and K. Terada, *J. Earth Sci., Nagoya Univ.*, 5 (1957) 81.
4 R. A. Barkley and T. G. Thompson, *Deep-Sea Res.*, 7 (1960) 24.
5 A. D. Matthews and J. P. Riley, *Anal. Chim. Acta*, 51 (1970) 295.
6 S. Tsunogai and T. Sase, *Deep-Sea Res. Oceanogr. Abstr.*, 16 (1969) 489.
7 Y. Miyake and S. Tsunogai, *La Mer, Bull. Soc. Fr.-jap. Oceanogr.*, 4 (1966) 65.
8 S. Tsunogai and T. Henmi, *Chikyu Kagaku*, 3 (1969) 14.
9 B. B. Owen, *J. Amer. Chem. Soc.*, 60 (1938) 2229.
10 W. M. Latimer, *Oxidation Potentials*, 2nd Edn., Prentice-Hall, 1952, p. 392.
11 N. Handa, personal communication.

(Received 26th January 1971)

Analytica Chimica Acta
Elsevier Publishing Company, Amsterdam
Printed in The Netherlands

A modified spectrophotometric method for the simple rapid determination of phosphate

The phosphate ion is commonly used, in chemistry of biological molecules, as a buffering ion. However, occasions frequently arise where the subsequent removal of the phosphate ion by fractionation is required in order to isolate the compound of interest. In these cases, and where determination of phosphate contents of larger numbers of small samples is necessary, a rapid and simple method is essential.

Of the three main types of colorimetric procedures for phosphate, the molybdenum blue method[1] normally involves a considerable reaction time or a heating stage[2]; in its modified form[3] a solvent extraction is employed. In the molybdovanadophosphoric acid method[4], the acidity of the reaction medium is fairly critical. Attention was therefore turned to the molybdophosphoric acid method[5] which is based on addition of ammonium molybdate solution to an acidified solution of the phosphate, and spectrophotometric determination of the yellow colour produced at 380–420 nm. Whilst this method is basically convenient and simpler than the other two, the volumes employed are inconveniently large and orthophosphate can be determined only in amounts greater than about 0.2 mg. Furthermore, there is a strong tendency for the yellow phosphomolybdate to precipitate within a few minutes of mixing. The molybdophosphoric acid method has therefore been modified to overcome these difficulties, and this modified method is now reported.

Recommended procedure

To samples (total volume 400 μl) containing orthophosphate (0–10 μg), add 50 μl of 2.5 *M* nitric acid (A.R. grade). Mix well, add 50 μl of 10% (w/v) ammonium molybdate solution (A.R. grade; $(NH_4)_6Mo_7O_{24}\cdot 4\,H_2O$) and shake the tubes again. Prepare blanks and standards containing disodium hydrogen orthophosphate similarly. After standing at *ca.* 20° for 6 min, transfer the solutions to micro optical cells (path length 10 mm) and measure the absorbances at 362 nm (a Unicam SP500 spectrophotometer was used). The absorption spectrum of the chromophore and a typical calibration curve are shown in Fig. 1.

Discussion

The phosphate assay in the proposed form is reproducible, reliable and accurate. The scale of working is convenient, not requiring large volume samples. The recommended procedure covers the range 0–10 μg of orthophosphate (Fig. 1), which is equivalent to 0.0–3.3 μg of phosphorus. In the method of Boltz and Mellon[5], absorbances were measured at 380, 400 or 420 nm, probably because of the wavelength range of the then available spectrophotometers. As can be seen from Fig. 1, increased sensitivity is achieved by measuring the absorbance at 362 nm, the maximum of the chromophore absorption curve. Full colour development was found to occur almost instantaneously on addition of the ammonium molybdate reagent, and no precipitation or variation of absorbance was detected during 5 h of monitoring after mixing, indicating the stability of the system.

Interfering ions must be reduced to concentrations within the maximum limits specified[5], but these are not normally encountered in simple applications. A solvent

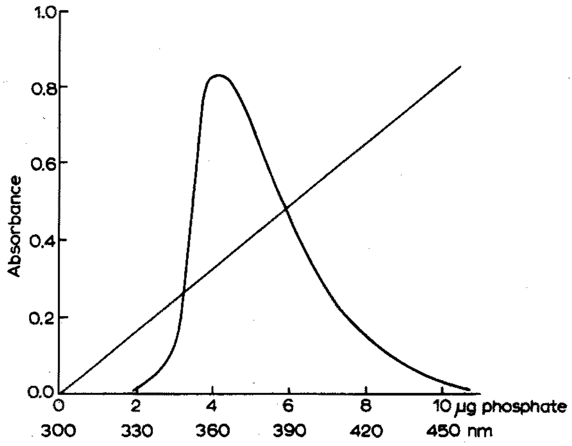

Fig. 1. Absorption spectrum of ammonium molybdophosphate and typical calibration curve for the modified phosphate assay.

extraction along the lines previously described[6] could probably be applied to overcome interference by certain ions, but would of course remove the inherent simplicity of the method.

In its present form, the method is simple, reproducible and rapid. Since the reaction medium is highly acidic, the procedure is suitable for the direct analysis of phosphate after acid hydrolysis. Finally, the method could be easily automated.

Department of Chemistry,
University of Birmingham,
P.O. Box 363,
Birmingham B15 2TT (Great Britain)

J. F. Kennedy
D. A. Weetman

1 S. R. Dickman and R. H. Bray, *Ind. Eng. Chem., Anal. Ed.*, 12 (1940) 665.
2 D. F. Boltz and M. G. Mellon, *Ind. Eng. Chem., Anal. Ed.*, 19 (1947) 873.
3 C. H. Lueck and D. F. Boltz, *Anal. Chem.*, 28 (1956) 1168.
4 R. E. Kitson and M. G. Mellon, *Ind. Eng. Chem., Anal. Ed.*, 16 (1944) 379.
5 D. F. Boltz and M. G. Mellon, *Anal. Chem.*, 20 (1948) 749.
6 C. Wadelin and M. G. Mellon, *Anal. Chem.*, 25 (1953) 1668.

(Received 18th March 1971)

Analytica Chimica Acta
Elsevier Publishing Company, Amsterdam
Printed in The Netherlands

1-(2-Carboxy-4-sulphonatophenyl)-3-hydroxy-3-phenyltriazene as indicator in the EDTA titration of iron(III), and the spectrophotometric determination of oxalate

While molybdenum(VI), vanadium(V), copper(II) and palladium(II) form coloured complexes with 1-(2-carboxy-4-sulphonatophenyl)-3-hydroxy-3-phenyltriazene at a low pH[1,2], nickel(II) forms a complex only at pH 7.8–9.2. The greenish-yellow nickel complex is stable for 4 h, and when 5 ml of reagent solution (0.05% w/v) is used, Beer's law is obeyed in the range 0.0625–1.5 p.p.m. of nickel at 400 nm with an optimal range[3] of 0.25–1.5 p.p.m. The reaction sensitivity[4] for the system is 0.00172 μg cm^{-2} and its molar absorptivity is 34,524.

Iron(III) forms two types of complexes, one of which is bluish violet at a low pH as reported before[1], and the other crimson red at a higher pH, 7.8–8.9. The latter complex shows an absorption peak at 520 nm, for which Beer's law is obeyed from 0.5 to 16 p.p.m. of iron, the optimal range[3] being 2–12 p.p.m. The coloured complex has a reaction sensitivity[4] of 0.0129 μg cm^{-2} and a molar absorptivity of 4428; the absorbance is stable for 3 h when the colour is fully developed with 4 ml of reagent solution (0.5% w/v).

In this paper, the use of the reagent as a metallochromic indicator for the titration of iron with EDTA in presence of a number of cations is discussed. The colour change during the titration is from deep blue to green and finally to yellow. The end-point is clear and becomes still sharper if the titration is carried out in presence of cobalt(II) sulphate; the colour change at the end-point is then from deep blue to pink. If the iron(III) is present in high amounts (above 10 mg), the colour of the reagent–metal complex does not persist for more than 7 min. This may be due to the oxidizing effect of the iron(III) on the reagent, but, in any case, it does not affect the course of a normal titration.

Owing to the large difference in instability constant values between the iron(III)–EDTA complex (10^{-25}) and the indicator complex (10^{-8}), and because of the sharpness of the colour change during the titration (in presence of cobalt sulphate), the reagent is considered to be one of the most promising indicators for the EDTA titration of iron(III).

Fe^{2+}, Cd^{2+}, Sr^{2+}, Be^{2+}, Ca^{2+}, Zn^{2+}, Hg^{2+}, Mn^{2+}, Al^{3+}, Cr^{3+} and Mg^{2+} do not interfere in the direct determination of iron(III). Nickel(II) is tolerated upto 15 mg in 50 ml of solution, but copper(II) interferes.

The bluish violet colour of the iron(III) complex at pH 3.3–4.5 fades on the addition of oxalate or fluoride, the fading being directly proportional to the amount of the iron(III) ion withdrawn from the system by formation of the more stable complex. This can be made the basis of a spectrophotometric determination of oxalate or fluoride, the oxalate method being of greater interest in view of the large number of analogous methods for fluoride.

Reagents

Apparatus and solutions of iron(III) chloride and of diverse ions were the same as reported previously[1]. Twice distilled water was used in all preparations. All the chemicals used were of AnalaR quality.

An aqueous solution of oxalate ion was prepared from oxalic acid, and

TABLE I

TITRATION OF IRON(III) WITH EDTA SOLUTION

Iron(III) taken (mg)	*EDTA required* 0.005 *M* *(ml)*	*Iron(III) found (mg)*	*Iron(III) taken (mg)*	*EDTA required* 0.01 *M* *(ml)*	*Iron(III) found (mg)*
1	3.70	1.02	6	10.8	6.03
2	7.20	2.01	8	14.4	8.04
3	10.80	3.01	10	17.8	9.94
4	14.40	4.02	12	21.4	11.96
5	18.00	5.02	14	25.0	13.96
			16	28.6	15.96
			18	32.7	18.26
			20	37.2	20.77

standardized gravimetrically with a final weighing as calcium carbonate[5]. Aqueous nickel(II) chloride solutions were standardized by the dimethylglyoxime method[5].

Buffer solutions of pH 2.0 or pH 3.6 were prepared by mixing 50 ml of *M* sodium acetate solution with 52 ml or 45 ml, respectively, of *M* hydrochloric acid and diluting to 250 ml with water.

A 0.5% (w/v) reagent solution was used for the spectrophotometric determinations, and a 1.0% (w/v) reagent solution as indicator for the EDTA titration.

Titration of iron(III) with EDTA

Adjust the pH of about 40 ml of iron solution containing 1–17 mg of iron to 1.0–2.5 by adding hydrochloric acid or ammonia solution or with 10 ml of buffer pH 2.0. Add, successively, 40 mg of cobalt(II) sulphate and 10–15 drops of the indicator solution, and titrate with 0.005 *M* or 0.01 *M* EDTA solution, depending on the iron(III) content.

During the titration, the iron–triazene colour gradually disappears and finally at the end-point the colour changes from deep blue to pink. The results of titrations are given in Table I.

The quantity of iron(III) present must not exceed 17 mg per 50 ml of solution. The tolerance limits (in mg) of various foreign ions for the titration of iron (5 mg) are as follows: Ba^{2+} (300), Cd^{2+} (100), Be^{2+} (150), Al^{3+} (75), Ca^{2+} (150), Zn^{2+} (50), Hg^{2+} (150), Sr^{2+} (100), Mn^{2+} (80), Ni^{2+} (15) and Co^{2+} (100). Copper(II) interferes.

Spectrophotometric determination of oxalate

To a standard iron(III) chloride solution (3.5 ml of $1 \cdot 10^{-3}$ *M*), add 4 ml of the reagent solution and adjust the pH to about 3.5 by adding 5 ml of buffer pH 3.6. Transfer the solution to a 25-ml volumetric flask, make up to volume and measure the absorbance at 410 nm against a reagent blank. This gives the absorbance of the iron(III) alone.

Next add different volumes of standard oxalate solutions (in p.p.m.) to a series of solutions of iron(III), as above, and measure the absorbance in the same way.

Figure 1 shows the effect of increasing oxalate ion concentration on the fading of bluish violet colour of the iron complex. The amount of iron(III) withdrawn from

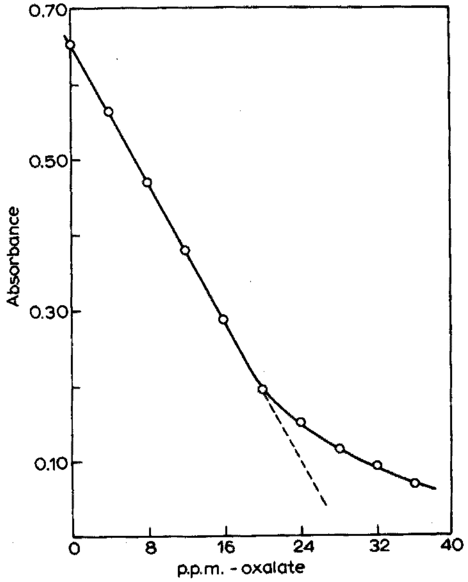

Fig. 1. Calibration curve for the determination of oxalate.

reaction is proportional to the concentration of the oxalate ion in the range 0.5–20.0 p.p.m. Above this concentration the fading of the colour is less than expected.

The same procedure may be followed for the determination of fluoride ion in the range 0.5–36.0 p.p.m.

For both these determinations, the absorbance is independent of time of standing. Common anions such as chloride, sulphate, nitrate and acetate do not interfere, but anions such as phosphate, cyanide, citrate and tartrate interfere.

Department of Inorganic and Analytical Chemistry,
Jadavpur University,
Calcutta-32 (India)

A. K. Majumdar
D. Chakraborti

1 A. K. Majumdar and D. Chakraborti, *Anal. Chim. Acta*, 53 (1971) 127.
2 A. K. Majumdar and D. Chakraborti, *Anal. Chim. Acta*, 53 (1971) 393.
3 A. Ringbom, *Z. Anal. Chem.*, 115 (1938/39) 332.
4 E. B. Sandell, *Colorimetric Determination of Traces of Metals*, 3rd Edn., Interscience, New York, 1959.
5 A. I. Vogel, *A Text Book of Quantitative Inorganic Analysis*, 3rd Edn., Longmans Green, London, 1962.

(Received 29th December 1970)

Analytica Chimica Acta
Elsevier Publishing Company, Amsterdam
Printed in The Netherlands

Important amongst the new range of ion-selective electrodes are those whose basis is a liquid ion-exchanger[1,2]. Salts of some substituted phenanthrolines have been used to make electrodes selective to nitrate[2,3] and perchlorate ions[2,4,5] and long-chain phosphate salts enable electrodes to be made which are selective towards calcium and other divalent ions[5,6]. In the commercial forms of these electrodes[7,8] the exchanger material is dispersed on a small disc of porous material such as cellulose acetate (Millipore filter) or porous glass[9]. The assembly of these commercial electrodes is an operation requiring some practice and attempts have been made to disperse the material in a suitable solid inert matrix[10] or to impregnate it into the surface of porous carbon[11].

Liquid ion-exchange materials are relatively easy to prepare and are not expensive and we have investigated the use of larger quantities of material than are used in the commercial forms.

Design of the titration cell

In principle it is possible to set up a cell with a column of exchanger in a U-

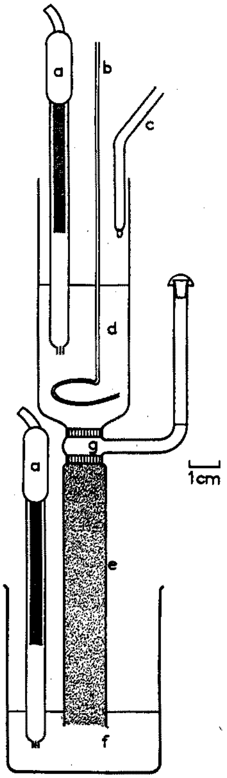

Fig. 1. Titration cell–electrode assembly. (a) Saturated calomel electrodes; (b) glass stirrer; (c) burette; (d) solution for titration; (e) reference solution in agar; (f) bridge solution; (g) liquid ion exchanger between sinters.

tube[6] but for mechanical stability reasons, dispersion in a porous medium is preferable. Impregnation of a single glass sinter disc with liquid ion-exchange material in nitrobenzene solvent was found to be unsatisfactory because globules, though more dense than the aqueous phase above, rose into it. Accordingly the design shown in Fig. 1 was developed where two glass sinters are sealed close together. The side-arm facilitates filling, replacement and replenishment of exchanger. The porosity of sinter used depends on the skill of the glass-blower for some closing of pores occurs on fabrication; grades 1–3 have been used successfully. To avoid gravitational instability the lower aqueous solution, that is the "inner filling" solution of the Orion electrode, was gelled by the addition of 3% agar. The lower sinter was moistened with liquid exchanger and the hot gel solution poured into the inverted device and allowed to set.

Results

To test the system Orion liquid ion-exchange materials were used: $NiL_3(NO_3)_2$ for nitrate and $FeL_3(ClO_4)_2$ for perchlorate, where L is a substituted phenanthroline ligand. Known dilutions of perchlorate gave slopes of less than the theoretical value (*ca.* 43 mV per decade) compared with 55 mV per decade for the Orion electrode, but non-Nernstian behaviour is acceptable for indicator electrodes for titrimetry. Precipitation titrations were carried out with tetraphenylarsonium chloride as titrant for perchlorate[5] and diphenylthallium(III) sulphate for nitrate[12]. Measurements were made with a Solartron Digital Voltmeter (Type LM 1420.2). Steady readings were obtained within 2–3 min of each titrant addition and stirring. Figure 2 shows the titration curve of 0.023 *M* ammonium perchlorate with 0.025 *M* tetraphenylarsonium chloride (K &K Laboratories Inc.) at pH 5 for the Orion electrode and for the titration assembly. For the latter the cell was:

$Hg|Hg_2Cl_2|KCl(sat)|NH_4NO_3(2\ M)|ClO_4^-$ | Liquid ion exchanger | Inner filling solution | $KCl|Hg_2Cl_2|Hg$ (sat)

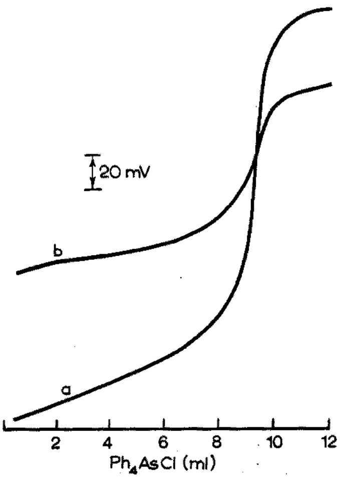

Fig. 2. Titration curves for 0.023 *M* ammonium perchlorate with 0.025 *M* tetraphenylarsonium chloride. (a) Titration cell assembly; (b) Orion electrode.

where the saturated calomel electrode on the right replaces the internal silver–silver chloride element of the Orion body, and the inner filling solution was gelled. Figure 2 shows that the titration cell gave an e.m.f. change (*ca.* 180 mV) greater than that with the Orion electrode (*ca.* 90 mV) but the end-point was the same. Baczuk and Dubois[5] found end-point breaks of 150–200 mV with the Orion electrode, which suggests that our Orion electrode was not functioning properly.

For the nitrate titration the cell used was:

$$\mathrm{Hg|Hg_2SO_4|(NH_4)_2SO_4|NO_3^-}\left|\begin{array}{l}\text{Liquid}\\ \text{ion}\\ \text{exchanger}\end{array}\right|\begin{array}{l}\mathrm{NH_4NO_3}\\ \text{agar}\\ \end{array}\left|\mathrm{(NH_4)_2SO_4|Hg_2SO_4|Hg}\right.$$

The saturated calomel reference electrode was avoided to prevent risk of contamination with chloride. Diphenylthallium chloride (Alfa Inorganics Inc) was converted to sulphate by the method of Goddard and Goddard[13] which involves refluxing an alcoholic potash solution for 8 h. The product is poured into water and the white oxide precipitate is filtered, dried and dissolved in 0.1 *M* sulphuric acid. Sodium sulphate was added to buffer the solution in the range 2–4 pH. The change in e.m.f. in the titration was only 25 mV compared with *ca.* 140 mV observed by DiGregorio and Morris[12] with the Orion electrode. No direct comparison was made in this case. In spite of the small e.m.f. change the end-point was clear.

The titration cell–electrode assembly employing a thick liquid ion-exchange layer, though non-Nernstian, is satisfactory for precipitation titrations of perchlorate and nitrate. Precipitation does not appear to clog the pores of the upper sinter as might have been expected. The device is particularly suitable for student instruction because of its simplicity, and especially if it is combined with preparation of the exchanger materials (see ref. 4 for preparation of phenanthroline salts).

Department of Physical Chemistry,
The University,
Newcastle upon Tyne, NE1 7RU (England)

A. K. Covington
J. M. Thain

1 A. K. Covington, *Chem. in Britain*, 5 (1969) 388.
2 J. W. Ross, in *Ion Selective Electrodes*, N.B.S. Special Publication No. 314, 1969, pp. 57–88.
3 S. Potterton and W. D. Shults, *Anal. Lett.*, 1 (1967) 11.
4 J. W. Ross, *U.S. Patent No. 3,483,112*, 1969.
5 R. J. Baczuk and R. J. Dubois, *Anal. Chem.*, 40 (1968) 685.
6 J. W. Ross, *Science*, 156 (1967) 1378; *U.S. Patent No. 3,429,785*, 1969.
7 Orion Research Inc., *92 Series Electrodes*, Instruction Manual.
8 W. Simon, H.-R. Wuhrmann, M. Vasak, L. A. R. Pioda, R. Dohner and Z. Stefanac, *Angew. Chem.*, 9 (1970) 445.
9 Corning Glass Works, *Calcium Ion Electrode*, Technical Information, No. 476041, 1968.
10 F. A. Schultz, A. J. Petersen, C. A. Mask and R. P. Buck, *Science*, 161 (1968) 267.
11 J. Ruzicka and J. C. Tjell, *Anal. Chim. Acta*, 49 (1970) 346; 51 (1970) 1.
12 J. S. DiGregorio and M. D. Morris, *Anal. Lett.*, 1 (1968) 811; *Anal. Chem.*, 42 (1970) 94.
13 A. E. Goddard and D. Goddard, *J. Chem. Soc.*, (1922) 482.

(Received 31st March 1971)

Analytica Chimica Acta
Elsevier Publishing Company, Amsterdam
Printed in The Netherlands

BOOK REVIEWS

J. M. Cleveland, *The Chemistry of Plutonium*, Gordon and Breach, New York–London, 1970, xxii + 653 pp., price $ 23.40 (£ 9.75).

This is a comprehensive and authoritative treatise of importance to all chemists working with plutonium. The book is divided into four sections. After a short general introduction there is a long section on the solution chemistry of plutonium. This deals with oxidation states, oxidation–reduction reactions, complexes, separations by ion exchange and solvent extraction, and non-aqueous and molten salt chemistry of plutonium. The next section provides a full account of the known compounds of plutonium, and the final section deals with chemical processing and the separation of plutonium from irradiated reactor fuels.

Although there is little mention of the analytical chemistry of plutonium, analytical chemists will find this book very useful for information and references purposes. For instance, there are more than 500 references dealing with the chemistry of the complexes of plutonium in aqueous solution. The appearance of this book is very timely because it fills a need for a complete and up-to-date treatise on plutonium chemistry. Essentially the literature is covered up to and including 1968, and a few references to work published in 1969 are also recorded. The book is well written by an expert in this field of chemistry and it is attractively produced. Analytical chemists working with plutonium-containing materials will undoubtedly find this treatise most helpful.

G. W. C. Milner (Harwell)

Anal. Chim. Acta, 55 (1971) 456

Developments in Applied Spectroscopy, Vol. 7B, Edited by E. L. Grove and A. J. Perkins, Plenum Press, New York and London, 1970, xi + 291 pp., price $ 12.50.

Like the earlier complementary volume (7A), this volume also contains a collection of selected papers presented at the 7th National Meeting of the Society of Applied Spectroscopy, held (in place of the 19th Mid-America Symposium on Spectroscopy) in Chicago in May 1968.

The main chapter headings of Vol. 7B, completing a total coverage of 42 papers in these two volumes, are: Infrared and Raman Spectroscopy, Internal-Reflection Spectroscopy, Nuclear Magnetic Resonance Spectroscopy, and Spectrochemical Applications to Textiles and Fibres.

W. T. Elwell (Birmingham)

Anal. Chim. Acta, 55 (1971) 456

Johannes Flügge, *Grundlagen der Polarimetrie*, Walter de Gruyter and Co., Berlin, 1970, xi + 159 pp., price DM48,—.

This handy booklet appeared in the series *Arbeitsmethoden der Modernen Naturwissenschaften* and is divided into nine chapters. The table of Contents with its clear setting and decimalised paragraph-numbering is followed by the first chapter on the theoretical basis of polarimetry, including an account on natural and non-natural optical activity. The second chapter describes the functions of various parts of polarimeters (polarisers, analysers, sources of radiation, etc.), ending up with a short outline of the construction of the polarimeters themselves. A separate chapter (3) deals with the characteristics of human visual organs (of which the eye itself is only a part) and some special techniques applied in visual polarimetry. The next chapter (4) describes all the theoretical and practical aspects of the polarimetric measurement, followed by a detailed description of commercial polarimeters (5). Chapter 6 entitled "Ellipsometry" enlarges upon the application of circular dichroism in polarimetry. In practice, polarimetry is used primarily for the quantitative determination of sugars. The next chapter (7) is devoted therefore entirely to the practical aspects of "Saccharimetry". Two short chapters follow, the first (8) dealing with magneto-optical activity and related subjects, while the second (9) with errors of polarimetric measurements. A selected list of references and an index concludes the book.

Typing and binding are exceptionally good. One might dispute the particular order in which the chapters follow (an alternative arrangement would be to put theory first, then instrumentation, then applications), but this is a minor criticism of this very useful book which fills a definite gap in the modern literature of instrumental analytical techniques. An English version would be welcome.

G. Svehla (Belfast)

Anal. Chim. Acta, 55 (1971) 457

T. T. Gorsuch, *The Destruction of Organic Matter*, Pergamon Press, Oxford, 1970, viii + 152 pp., price £2.75.

Few books have given me greater pleasure to review than this one, because it has so many commendable features. The determination of one or more of a wide range of "non-organic" elements present at very low levels in an organic matrix is an assignment that must have confronted most analysts at some time, irrespective of their special interests, and a book that deals with such problems, especially by an undisputed expert, is most welcome.

Dr. Gorsuch is well-known from his earlier publications, and this book, probably the first to be published exclusively on the subject, is essentially a collated presentation of both his own pioneering work and the contributions of others. It presents a carefully-chosen account of what the problems are and how to deal with them by conventional procedures.

The monograph is mainly concerned with total-decomposition procedures (as a preliminary stage), though mention is made of others. The author's involvement in the determination of trace constituents in organic media and his experience in radiochemical analysis, provides the simple explanation for his success in combining

Anal. Chim. Acta, 55 (1971) 457–458

the two. It is doubtful if the inherent shortcomings associated with the quantitative recovery of trace elements from an organic environment, an aspect so often unknown and frequently ignored by the analyst, could have been more effectively highlighted than by radiochemical analysis.

It is refreshing to read a book with such potential interest; more especially to be able to give it an unreserved recommendation.

W. T. Elwell (Birmingham)

Anal. Chim. Acta, 55 (1971) 457–458

PUBLICATIONS RECEIVED

Proceedings of the Third Symposium on Coordination Chemistry, Edited by M. T. Beck, Akademiai Kiado, Budapest, 1970, 525 pp., price £ 6.00 (paperback).

This volume contains the contributed papers (48) of the 3rd Symposium on Coordination Chemistry, which was held in Debrecen, Hungary, in 1970. The papers are mainly concerned with the chemistry of mixed-ligand and outer-sphere complexes.

Proceedings of the Third Analytical Chemical Conference, Edited by I. Buzas, Akademiai Kiado, Budapest, 1970, Vol. 1, 318 pp., Vol. 2, 459 pp., price £ 9.00 for two volumes (paperback).

These volumes contain the proceedings of the 3rd Analytical Chemistry Conference, which was held in Budapest in August 1970. Most of the papers in the first volume deal with separation methods, and those in the second volume with organic analysis and thermal analysis.

P. van der Winkel, *De Bepaling van Sporenelementen in Biologisch Materiaal door Neutronenactiverings-analyse*, Kon. Vlaamse Academie voor Wetenschappen, Kunstlaan 43, 1040 Brussel, 189 pp., price 500.— BF.

1. *Internationales Symposium: Aspekte der chemischen und toxikologischen Beschaffenheit der Umwelt*, Georg Thieme Verlag, Stuttgart, 1970, 160 pp., price DM 38.— (paperback).

This volume contains the proceedings, including verbatim discussions, of the symposium on chemical and toxicological aspects of environmental quality which was held in Munich in July, 1969. The 17 papers given cover a very wide field of pollution problems, including analytical techniques. Much of the content is in English. The volume should be of value to all interested in environmental problems.

L. Sachs, *Statistische Methoden. Ein Soforthelfer*, Springer-Verlag, Berlin, 1970, xi + 103 S., Preis Geheftet DM 8.80 (US $ 2.50).

This small book contains descriptions of the most important simple statistical methods. It is plentifully supplied with examples and Tables and provides an excellent introduction or refresher course for those who require to use statistical techniques.

Catalog of Standard Reference Materials, NBS Special Publication 260, U.S. Government Printing Office, Washington, D.C. 20402, July 1970, 84 pp., price 75 cents.

Anal. Chim. Acta, 55 (1971) 458

ANALYTICA CHIMICA ACTA, VOL. 55 (1971)

AUTHOR INDEX

Aggett, J. 349
Akatsu, E. 333
Al-Jarrah, R. H. 135
Aomura, K. 153
Asano, M. 333

Balsenc, L. 253
Beeler, R. 253
Berge, H. 193, 201
Bertrand, C. 385
Bhatty, M. K. 263, 401
Boltz, D. F. 77
Bos, M. 285
Budesinsky, B. W. 115

Campbell, D. E. 265
Chakraborti, D. 450
Chester, J. E. 47
Covington, A. K. 453
Crump-Wiesner, H. J. 29

Dagnall, R. M. 47
Dahmen, E. A. M. F. 285
Delaporte, N. 415, 425
Desai, S. R. 395
Duyckaerts, G. 145

Feltz, H. R. 29
Frei, R. W. 125
Fujii, I. 19
Furukawa, M. 231

Gavach, C. 385
Gee, P. J. 315
Gorgia, A. 247
Guilbault, G. G. 107

Haerdi, W. 253
Hernandez, J. A. 325
Hofton, M. E. 367
Holzbecher, J. 273
Hubbard, D. P. 367
Huber, C. O. 179

Irving, H. M. N. H. 135, 169, 269, 315
Ishiguro, Y. 231
Ishihara, M. 19
Iyer, C. S. P. 89

Jacobsen, E. 293
Jacobsen, T. V. 293
Jamil, M. 145
Jamro, G. H. 125

Kamidate, T. 153
Kashiki, M. 436
Kennedy, J. F. 448
Kies, H. L. 239
Kisfaludi, G. 442
Konieczny, J. M. 83
Koshimura, H. 163
Kunovits, G. 221

Laval-Martin, D. 415, 425
Lenhof, M. 442
Lombard, S. M. 13
Looyenga, R. W. 179
Ludwig, H. 303

Majumdar, A. K. 450
Marlow, K. W. 13
Mawby, A. 269
McGonigle, E. 83
Menis, O. 89
Monnier, D. 247, 253
Muto, H. 19

Navratil, O. 125
Němcová, I. 239
Němec, I. 239
Nicolas, D. J. 59
Norris, J. D. 359
Norton, E. F. 1

Odier, M. 209
Okubo, T. 163
Omang, S. H. 439
Oshima, S. 436

Patti, F. 325
Plichon, V. 209
Plock, C. E. 278
Porthault, M. 341
Pugh, H. 97
Purdy, W. C. 29

Ringstorff, H. 193, 201
Rocca, J. L. 341
Ryan, D. E. 273
Ryan, J. A. 83

Sasaki, S. 231
Shibata, S. 231
Simpson, R. B. 169
Sindhwani, S. K. 409
Singh, R. P. 409
Smith, J. S. 169
Stoenner, R. W. 1
Svec, J. 115
Su, Y.-S. 265
Sudhalatha, K. 395

Takada, K. 19
Tanaka, T. 185
Tanner, J. T. 13
Taylor, M. R. G. 47
Thain, J. M. 453
Toussaint, C. J. 373
Townshend, A. 263, 401
Tsunogai, S. 444

Vasquez, J. 278
Vaughan, A. 107
Vernon, F. 367
Vienney, J. 37

Waterman, W. R. 97
Webb, M. S. W. 67
Webb, R. J. 67
Weetman, D. A. 448
Weiss, K. G. 77
Weisz, H. 303
West, T. S. 349, 359

Yoshimori, T. 185
Yotsuyanagi, T. 153

Zatka, V. 273
zur Nedden, P. 145

ANALYTICA CHIMICA ACTA, VOL. 55 (1971)

SUBJECT INDEX

- Acenaphthenequinonemonoxime,
  - spectrophotometric detn of ruthenium with —— (Sindhwani, Singh) 409
- Acid–base strengths,
  - ——in pyridine (Bos, Dahmen) 285
- Acidimetry,
  - viscometric titrations, a new technique applied to —— (Simpson *et al.*) 169
- Aldehydes,
  - colour reaction of carbohydrates and —— with cysteine and thioglycolic acid in sulphuric acid (Kunovits) 221
- Alkalimetry,
  - viscometric titrations, a new technique applied to —— (Simpson *et al.*) 169
- Aluminum electrolytic baths,
  - detn of oxygen in —— by a fast-neutron activation method (Takada *et al.*) 19
- 1-Amino-3-iminopropenes, heterocyclic N,N-disubstituted,
  - ——as analytical reagents (Zatka *et al.*) 273
- Ammonium hexanitratocerate(IV),
  - kinetic data on the oxidation of 1,1-diphenyl-2-picrylhydrazyl by —— in anhydrous acetonitrile (Němec *et al.*) 239
- Anion-exchange resin,
  - separation of hafnium and scandium on —— (Balsenc *et al.*) 253
- Antimony,
  - detn of —— in soils by a.a.s. (Nicolas) 59
  - detn of —— in standard rocks by instrumental neutron activation analysis (Lombard *et al.*) 13
- Antipyrine method,
  - u.v. spectrophotometric detn of nitrite by —— (Weiss, Boltz) 77
- Atomic absorption spectrophotometry,
  - detn of antimony in soils by —— (Nicolas) 59
- Atomic absorption spectroscopy,
  - detn of different impurities in plutonium by —— (Vienney) 37
  - detn of vanadium in brines by —— (Crump-Wiesner *et al.*) 29
  - —— with a carbon filament atom reservoir (Aggett, West) 349
- Atomic fluorescence spectroscopy,
  - —— with a carbon filament atom reservoir (Aggett, West) 349
- Automatic infrared analysis,
  - —— of meprobamate (Ryan *et al.*) 83
- Barium,
  - detn of —— in lubricating oils by a.a.s. (Kashiki, Oshima) 436
- Bismuth,
  - detn of traces of —— in crude metal and steel by flame a.a.s. (Kisfaludi, Lenhof) 442
- Brines,
  - determination of vanadium in —— by a.a.s. (Crump-Wiesner *et al.*) 29
- *p*-Bromomandelic acid,
  - detn of zirconium in glasses, glass-ceramics and refractories with —— (Su, Campbell) 265

- Cadmium(II),
  - liquid–liquid extrn of zinc(II) and —— by (carboxy-2-ethyl) diphenylphosphine oxide in chloroform (Rocca, Porthault) 341
- Calcium
  - detn of —— in lubricating oils by a.a.s. (Kashaki, Oshima) 436
  - sepn method of —— and strontium applied to the prepn of —— salts with a very low content of strontium (Patti, Hernandez) 325
- Calcium chloride hexahydrate–tri-*n*-butyl phosphate,
  - radiochemical studies on the solvent extr. of several elements in —— systems (Akatsu, Asano) 333
- Carbohydrates,
  - colour reaction of —— and aldehydes with cysteine and thioglycolic acid in sulphuric acid (Kunovits) 221
- Carbon filament atom reservoir,
  - atomic absorption and fluorescence spectroscopy with a —— (Aggett, West) 349
- (Carboxy-2-ethyl) diphenylphosphine oxide,
  - liquid–liquid extrn of zinc(II) and cadmium(II) by —— in chloroform (Rocca, Porthault) 341
- 1-(2-Carboxy-4-sulphonatophenyl)-3-hydroxy-3-phenyltriazene,
  - —— as indicator in the EDTA titration of iron(III) (Majumdar, Chakraborti) 450
- Catalytic reactions,
  - kinetic difference method based on —— (Weisz, Ludwig) 303
- Chlordiazepoxide,
  - electrochemical reduction of —— at mercury electrodes (Jacobsen, Jacobsen) 293

2-Chloro-1,10-phenanthroline,
  steric hindrance to the formation of metal complexes of —— (IRVING, GEE) 315
Chlorophylls a and b,
  spectrophotometric detn of —— and phaeophytins a and b in aq. acetone media (DELAPORTE, LAVAL-MARTÍN) 415, 425
4-[(5-Chloro-2-pyridyl)azo]-1,3-diaminobenzene,
  —— as a new sensitive and selective reagent for cobalt (SHIBATA *et al.*) 231
Chromium(III),
  extrn of —— from aq EDTA by solutions of tetra-*n*-hexylammonium chloride in dichloroethane (IRVING, AL-JARRAH) 135
Cobalt,
  4-[(5-chloro-2-pyridyl)azo]-1,3-diaminobenzene as a new sensitive and selective reagent for —— (SHIBATA *et al.*) 231
  detn of —— and nickel in a separated air–acetylene flame using a dual element electrodeless discharge lamp (NORRIS, WEST) 359
Copper,
  detn of —— in sea water using a.c. polarography (ODIER, PLICHON) 209
  detn of small amounts of sulphur in —— (PUGH, WATERMAN) 97
Copper chelates of alkyl-substituted β-diketones,
  effect of substituents on the distribution coefficients of —— (KOSHIMURA, OKUBO) 163
Copper(II) perchlorate,
  kinetic data on the oxidation of 1,1-diphenyl-2-picrylhydrazyl by —— (NĚMEC *et al.*) 239
Copper(II) solutions,
  solvent extrn of aliphatic sulphides with —— (YOTSUYANAGI *et al.*) 153
Cysteine,
  colour reaction of carbohydrates and aldehydes with —— and thioglycolic acid in sulphuric acid (KUNOVITS) 221

β-Diketones, alkyl-substituted,
  effect of substituents on the distribution coefficients of —— and their copper and iron chelates (KOSHIMURA, OKUBO) 163
1,1-Diphenyl-2-picrylhydrazyl,
  kinetic data on the oxidation of —— by copper(II) and iron(II) perchlorates, and by ammonium hexanitratocerate(IV) in anhydrous acetonitrile (NĚMEC *et al.*) 239
Dithizone,
  detn of mercury(II) by —— (GORGIA, MONNIER) 247

Electrodeless discharge lamp,
  detn of cobalt and nickel in a separated air–acetylene flame using a dual element —— (NORRIS, WEST) 359
Electrodes,
  —— specific for anions with a long hydrocarbon chain (GAVACH, BERTRAND) 385
  titration cell– —— ass mbly for liquid ion-exchange —— (COVINGTON, THAIN) 453
Europium(III)
  extrn of —— by a disphosphonic acid in different organic solvents (JAMIL *et al.*) 145

Flameless atomic absorption spectrophotometry,
  detn of lead in air by —— (OMANG) 439
Flames,
  use of less-common —— in analytical atomic spectrometry (CHESTER *et al.*) 47

Glyoxal dithiosemicarbazone,
  photometric detn of silver and mercury with —— (BUDESINSKY, SVEC) 115
Gold,
  detn of —— by atomic fluorescence and atomic absorption spectroscopy with an unenclosed atom reservoir (AGGETT, WEST) 349

Hafnium,
  separation of —— and scandium on anion-exchange resin (BALSENC *et al.*) 253
Heavy metal chelates of pyridine-2-aldehyde-2-quinolylhydrazone,
  extractive–photometric study of —— (FREI *et al.*) 125
Human serum alkaline phosphatase,
  detn of —— by semi-solid state fluorimetric analysis (GUILBAULT, VAUGHAN) 107

Iodine,
  detn of —— in sea water by an improved Sugawara method (TSUNOGAI) 444
Iron,
  spectrophotometric detn of vanadium and —— with β-isopropyltropolone (MENIS, IYER) 89
Iron(III),
  1-(2-carboxy-4-sulphonatophenyl)-3-hydroxy-3-phenyltriazene as indicator in the EDTA titration of —— (MAJUMDAR, CHAKRABORTI) 450
Iron chelates of alkyl-substituted β-diketones,
  effect of substituents on the distribution coefficients of —— (KOSHIMURA, OKUBO) 163
Iron(II) perchlorate,
  kinetic data on the oxidation of 1,1-diphenyl-2-picrylhydrazyl by —— (NĚMEC *et al.*) 239
β-Isopropyltropolone,
  spectrophotometric detn of vanadium and iron with —— (MENIS, IYER) 89

Kinetic difference method,
  —— based on catalytic reactions (WEISZ,

Ludwig) 303

Lanthanum, detn of trace amounts of —— in low-alloy steels by flame emission spectrometry (Hofton *et al.*) 367
Laser microprobe,
  semi-quantitative analysis by means of —— (Webb, Webb) 67
Lead,
  detn of —— in air by flameless a.a.s. (Omang) 439

Manganese nitrate hexahydrate–tri-*n*-butyl phosphate,
  radiochemical studies on the solvent extrn of several elements in —— systems (Akatsu, Asano) 333
Meprobamate,
  automatic quantitative i.r. analysis of —— . Biphasic method (Ryan *et al.*) 83
Mercury,
  photometric detn of silver and —— with glyoxal dithiosemicarbazone (Budesinsky, Svec) 115
Mercury(II),
  sepn from organomercurial on glass microbeads and detn by dithizone (Gorgia, Monnier) 247
Mercury(II) solutions,
  solvent extrn of aliphatic sulphides with —— (Yotsuyanagi *et al.*) 153
Metal complexes of 2-chloro-1,10-phenanthroline,
  steric hindrance to the formation of —— (Irving, Gee) 315
Metal traces,
  concentration on a mercury surface (Berge, Ringstorff) 193, 201

Neutron activation,
  detn of antimony in standard rocks by —— (Lombard *et al.*) 13
  detn of oxygen in aluminum electrolytic baths by —— (Takada *et al.*) 19
  —— detn of thorium in rocks and minerals using the 22-min ^{233}Th activity (Norton, Stoenner) 1
Nickel,
  detn of cobalt and —— in a separated air–acetylene flame using a dual element electrodeless discharge lamp (Norris, West) 359
Nitrite,
  u.v. spectrophotometric detn of —— by the antipyrine method (Weiss, Boltz) 77

Organodiphosphorus extractants, acidic,
  extrn of europium(III) by a diphosphonic acid in different organic solvents (Jamil *et al.*) 145
Oxalate,
  spectrophotometric determination of —— (Majumdar, Chakraborti) 450
Oxygen,
  detn of —— in aluminum electrolytic baths by a fast-neutron activation method (Takada *et al.*) 19

Perchlorate–fluoride electrolyte,
  detn of zinc in uranium by differential linear sweep oscillographic polarography with a —— (Plock, Vasquez) 278
Phaeophytins a and b
  spectrophotometric detn of chlorophylls and —— in aq. acetone media (Delaporte, Laval-Martin) 415, 425
Phosphatase,
  detn of human serum alkaline —— by semi-solid state fluorimetric analysis (Guilbault, Vaughan) 107
Phosphate,
  modified spectrophotometric method for the simple rapid detn of —— (Kennedy, Weetman) 448
Plutonium,
  detn of different impurities in —— by a.a.s. (Vienney) 37
Polarography, a.c.,
  detn of copper in sea water using (Odier, Plichon) 209
Polarography, linear sweep oscillographic,
  detn of zinc in uranium by —— with a perchlorate–fluoride electrolyte (Plock, Vasques) 278
Potentiometric titration,
  —— of anionic detergents using electrodes specific for anions with a long hydrocarbon chain (Gavach, Bertrand) 385
Primary standard substance,
  coulometric investigation on the use of single crystals of sodium chloride as —— (Yoshimori, Tanaka) 185
Pyridine,
  acid–base strengths in —— (Bos, Dahmen) 285
Pyridine-2-aldehyde-2-quinolylhydrazone,
  extractive–photometric study of bivalent heavy metal chelates of —— (Frei *et al.*) 125

Quercetin,
  fluorimetric detn of micro amounts of zirconium with —— on filter paper (Deai, Sudhalatha) 395

Ruthenium,
  spectrophotometric detn of —— with acenaphthenequinonemonoxime (Sindhwani, Singh) 409

Scandium,
  separation of hafnium and —— on anion-exchange resin (BALSENC *et al.*) 253
Sea water,
  detn of copper in —— using a.c. polarography (ODIER, PLICHON) 209
  detn of iodine in —— by an improved Sugawara method (TSUNOGAI) 444
Silver,
  photometric detn of —— and mercury with glyoxal dithiosemicarbazone (BUDESINSKY, SVEC) 115
Sodium chloride,
  coulometric investigation on the use of single crystals of —— as a primary standard (YOSHIMORI, TANAKA) 185
Spectrophotometry,
  —— of chlorophylls and phaeophytins a and b in aq. acetone media (DELAPORTE, LAVAL-MARTIN) 415, 425
  —— detn of ruthenium with acenaphthenequinonemonoxime (SINDHWANI, SINGH) 409
  —— detn of vanadium and iron with β-isopropyltropolone (MENIS, IYER) 89
  modified —— method for the simple rapid detn of phosphate (KENNEDY, WEETMAN) 448
Strontium,
  sepn method of calcium and —— applied to the prepn of calcium salts with a very low content of —— (PATTI, HERNANDEZ) 325
Sulphate,
  detn of —— by atomic absorption inhibition titration (LOOYENGA, HUBER) 179
Sulphides, aliphatic,
  solvent extrn of —— with copper(II) and mercury(II) solutions (YOTSUYANAGI *et al.*) 153
Sulphur,
  detn of small amounts of —— in copper (PUGH, WATERMAN) 97
Sulphur dioxide,
  improved u.v. spectrophotometric method for the detn of —— (BHATTY, TOWNSHEND) 263
  spectrophotometric detn of small amounts of —— by molecular complex formation with *o*-xylene (BHATTY, TOWNSHEND) 401

Tetra-*n*-hexylammonium chloride in dichloroethane,
  extrn of chromium(III) from aq EDTA by solutions of —— (IRVING, AL-JARRAH) 135
Thioglycolic acid,
  colour reaction of carbohydrates and aldehydes with cysteine and —— in sulphuric acid (KUNOVITS) 221
Thorium,
  neutron activation method for the detn of —— in rocks and minerals using the 22-min ^{233}Th activity (NORTON, STOENNER) 1
Titration cell–electrode assembly
  —— for liquid ion-exchange (COVINGTON, THAIN) 453

Ultraviolet spectrophotometry,
  improved —— method for the detn of sulphur dioxide (BHATTY, TOWNSHEND) 263
Uranium,
  detn of zinc in —— by differential linear sweep oscillographic polarography with a perchlorate-fluoride electrolyte (PLOCK, VASQUES) 278

Vanadium,
  detn of —— in brines by a.a.s. (CRUMP-WIESNER *et al.*) 29
  spectrophotometric detn of —— and iron with β-isopropyltropolone (MENIS, IYER) 89
Viscometric titrations,
  ——, a new technique applied to acidimetry and alkalimetry (SIMPSON *et al.*) 169

X-ray spectral lines,
  excitation efficiencies of different X-ray tube targets for some low-energy —— (TOUSSAINT) 373

Zinc,
  detn of —— in lubricating oils by a.a.s. (KASHIKI, OSHIMA) 436
  detn of —— in uranium by differential linear sweep oscillographic polarography with a perchlorate–fluoride electrolyte (PLOCK, VASQUES) 278
Zinc(II),
  liquid–liquid extrn of —— and cadmium(II) by (carboxy-2-ethyl)diphenylphosphine oxide in chloroform (ROCCA, PORTHAULT) 341
Zinc(II) dithizonate, primary,
  crystal structure of —— and its relevance to the stabilities of its *o*- and *p*-methyl derivatives (MAWBY, IRVING) 269
Zirconium,
  detn of —— in glasses, glass-ceramics and refractories with *p*-bromomandelic acid (SU, CAMPBELL) 265
  fluorimetric detn of micro amounts of —— with quercetin on filter paper (DESAI, SUDHALATHA) 395

Analytica Chimica Acta
Elsevier Publishing Company, Amsterdam
Printed in The Netherlands

Errata

I. Šinko and S. Gomišček, Simultaneous Determination of Copper and Bismuth in High-Purity Lead by Anodic-Stripping Polarography, *Anal. Chim. Acta*, 54 (1971) 253–260.

Page 257, Table III, the last two lines should read

0.010	% Antimony	4.1	1.8
0.10	% Antimony	—[b]	1.9

B. W. Budesinsky and J. Svec, Photometric determination of silver and mercury with glyoxal dithiosemicarbazone, *Anal. Chim. Acta*, 55 (1971) 115–124.

Page 120, formula should read:

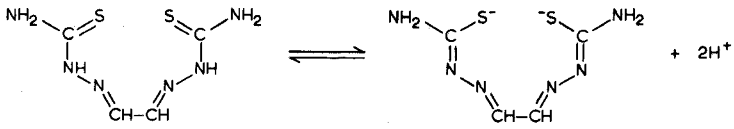

CONTENTS

Acid–base strengths in pyridine. Part II.
M. Bos and E. A. M. F. Dahmen (Enschede, The Netherlands) (Rec'd 19th March 1971) . . . 285

Electrochemical reduction of chlordiazepoxide at mercury electrodes
E. Jacobsen and T. V. Jacobsen (Oslo, Norway) (Rec'd 16th March 1971) 293

Eine kinetische Differenzmethode unter Verwendung katalysierter Reaktionen
H. Weisz und H. Ludwig (Freiburg i. Br., Deutschland) (Eing. den 27. März 1971) . 303

Steric hindrance to the formation of metal complexes of 2-chloro-1,10-phenanthroline
H. M. N. H. Irving and P. J. Gee (Oxford, England) (Rec'd 18th March 1971). . . 315

Nouvelle méthode de séparation calcium–strontium appliquée à la préparation d'un sel de calcium de très faible teneur en strontium
F. Patti et J. A. Hernandez (Fontenay-aux-Roses, France) (Reçu le 12 mars 1971) 325

Radiochemical studies on the solvent extraction of several elements in $Mn(NO_3)_2 \cdot 6H_2O$– and $CaCl_2 \cdot 6H_2O$–tri-*n*-butyl phosphate systems
E. Akatsu and M. Asano (Ibaraki-ken, Japan) (Rec'd 26th January 1971) 333

Etude de l'extaction liquide–liquide du zinc(II) et du cadmium(II) par l'oxyde de (carboxy-2-éthyl)-diphenylphosphine en solution dans le chloroforme
J. L. Rocca et M. Porthault (Villeurbanne, France) (Reçu 11 mars 1971) 341

Atomic absorption and fluorescence spectroscopy with a carbon filament atom reservoir. Part IV. The determination of gold by atomic fluorescence and atomic absorption spectroscopy with an unenclosed atom reservoir
J. Aggett and T. S. West (London, England) (Rec'd 21st January 1971) 349

Multi-element atomic fluorescence spectroscopy. Part IV. The determination of cobalt and nickel in steels by atomic fluorescence spectroscopy in a separated air–acetylene flame with a dual-element electrodeless discharge lamp
J. D. Norris and T. S. West (London, England) (Rec'd 15th March, 1971) 359

The determination of trace amounts of lanthanum in low-alloy steels by flame emission spectrophotometry
M. E. Hoften, D.P. Hubbard and F. Vernon (Sheffield, England) (Rec'd 26th March 1971) . . . 367

Excitation efficiencies of different X-ray tube targets for some low-energy X-ray spectral lines
C. J. Toussaint (Ispra, Italy) (Rec'd 18th January 1971) 373

Electrodes spécifiques d'anions à longue chaîne hydrocarbonée. Application au dosage potentiométrique de détergents anioniques
C. Gavach et C. Bertrand (Montpellier, France) (Reçu le 12 mars 1971) 385

Fluorimetric determination of micro amounts of zirconium with quercetin on filter paper
S. R. Desai and K. Sudhalatha (Bombay, India) (Rec'd 15th March 1971 395

Spectrophotometric determination of small amounts of sulphur dioxide by molecular complex formation with *o*-xylene
M. K. Bhatty and A. Townshend (Birmingham, England) (Rec'd 11th February 1971) . . . 401

Spectrophotometric determination of ruthenium with acenaphthenequinonemonoxime
S. K. Sindhwani and R. P. Singh (Delhi, India) (Rec'd 18th March 1971) 409

Analyse spectrophotométrique des chlorophylles et des phéophytines a et b en milieu hydroacetonique. I. Détermination des extinctions molaires
N. Delaporte et D.Laval-Martin (Meudon, France) (Reçu le 8 janvier 1971) . . . 415

Analyse spectrophotométrique des chlorophylles et des phéophytines a et b en milieu hydroacetonique. II. Méthode cinétique de dosage
N. Delaporte et D. Laval-Martin (Meudon, France) (Reçu le 8 janvier 1971) . . . 425

(continued on page 4 of cover)

Continued from inside page of cover

Short communications

Determination of calcium, barium and zinc in lubricating oils by atomic absorption spectrophotometry
M. Kashiki and S. Oshima (Saitama, Japan) (Rec'd 17th December 1970) 436

The determination of lead in air by flameless atomic absorption spectrophotometry
S. H. Omang (Oslo, Norway) (Rec'd 19th March 1971) 439

Dosage des traces de bismuth dans les fontes et aciers par spectrométrie de flamme à absorption atomique
G. Kisfaludi et M. Lenhof (Pont-à-Mousson, France) (Reçu le 18 mars 1971) . . . 442

Determination of iodine in sea water by an improved Sugawara method
S. Tsunogai (Hakodate, Japan) (Rec'd 26th January 1971) 444

A modified spectrophotometric method for the simple rapid determination of phosphate
J. F. Kennedy and D. A. Weetman (Birmingham, Great Britain) (Rec'd 18th March 1971) 448

1-(2-Carboxy-4-sulphonatophenyl)-3-hydroxy-3-phenyltriazene as indicator in the EDTA titration of iron(III), and the spectrophotometric determination of oxalate
A. K. Majumdar and D. Chakraborti (Calcutta, India) (Rec'd 29th December 1970) 450

A simple titration cell–electrode assembly for liquid ion-exchange selective electrodes
A. K. Covington and J. M. Thain (Newcastle upon Tyne, England) (Rec'd 31st March 1971). 453

Book Reviews 456

Author Index 459

Subject Index 460

Errata 464